AFOSR-TR- 91 0091

(2)

TSI-90-10-10-WB

Nonlinear Dynamics and Control of Flexible Structures

Final Report

Sept. 1, 1987 – Aug. 31, 1990
for AFOSR Contract F49620-87-C-0103

W.H. Bennett, H.G. Kwatny, G.L. Blankenship,
O. Akhrif, C. LaVigna

SYSTEMS ENGINEERING, INC.
a Division of
TECHNO-SCIENCES, INC.
Greenbelt, MD 20770

Submitted to
Air Force Office of Scientific Research
Directorate of Mathematical and Information Sciences
Bolling Air Force Base, DC 20332-6448
Attn: Ltn. Col. James M. Crowley

Date: Oct. 10, 1990

UNCLASSIFIED
SECURITY CLASSIFICATION OF THIS PAGE

REPORT DOCUMENTATION PAGE

1a. REPORT SECURITY CLASSIFICATION UNCLASSIFIED	1b. RESTRICTIVE MARKINGS
2a. SECURITY CLASSIFICATION AUTHORITY	3. DISTRIBUTION / AVAILABILITY OF REPORT Approved for public release, distribution unlimited
2b. DECLASSIFICATION / DOWNGRADING SCHEDULE	
4. PERFORMING ORGANIZATION REPORT NUMBER(S) TSI-90-10-10-WB	5. MONITORING ORGANIZATION REPORT NUMBER(S)
6a. NAME OF PERFORMING ORGANIZATION Techno-Sciences, Inc. — 6b. OFFICE SYMBOL (*If applicable*)	7a. NAME OF MONITORING ORGANIZATION Air Force Office of Scientific Research
6c. ADDRESS (*City, State, and ZIP Code*) 7833 Walker Drive - Suite 620 Greenbelt, MD 20740	7b. ADDRESS (*City, State, and ZIP Code*) Bolling AFB, DC 20332-6448 AFOSR/NA Bolling AFB DC 20332-6448 Bld 410
8a. NAME OF FUNDING / SPONSORING ORGANIZATION SDIO/IST — 8b. OFFICE SYMBOL (*If applicable*) NA	9. PROCUREMENT INSTRUMENT IDENTIFICATION NUMBER F49620-87-C-0103
8c. ADDRESS (*City, State, and ZIP Code*) Bldg. 41Q Bolling AFB, DC 20332-6448 Bld 410	10. SOURCE OF FUNDING NUMBERS PROGRAM ELEMENT NO. 61102F — PROJECT NO. 2312 — TASK NO. K1 — WORK UNIT ACCESSION NO
11. TITLE (*Include Security Classification*) Nonlinear Dynamics and Control of Flexible Structures (U)	
12. PERSONAL AUTHOR(S) W. H. Bennett; H. G. Kwatny; G. L. Blankenship; O. Akhrif	
13a. TYPE OF REPORT FINAL	13b. TIME COVERED FROM 87/9 TO 90/8 — 14. DATE OF REPORT (*Year, Month, Day*) 10/10/90 — 15. PAGE COUNT 140
16. SUPPLEMENTARY NOTATION	

17. COSATI CODES		
FIELD	GROUP	SUB-GROUP

18. SUBJECT TERMS (*Continue on reverse if necessary and identify by block number*)
Multibody systems, flexible space structures, nonlinear control theory, feedback linearizing control, sliding mode control, Lagranian mechanics

19. ABSTRACT (*Continue on reverse if necessary and identify by block number*)

Basic system requirements for space-based directed energy weapons will require unprecendented levels of control system performance to achieve slewing maneuvers for rapid retargeting and precision alignment of structural components supporting optical system components. Rapid, multiaxis slewing maneuvers will excite multibody dynamics involving nonlinear interactions with structural flexure. Advanced methods of modeling multibody systems with structural flexure are described and several issues in modeling slewing and pointing maneuvers for multibody systems are discussed based on Lagrange's method. Advanced methods in nonlinear control system design based on dynamic inversion by *feedback linearization* are then applied to a generic model of a Space Based Laser system. Connections with methods of *sliding mode control* are described along with practical aspects of implementation. Reduced order modeling issues and implementation of feedback linearizing control for robust stabilization are described. Experiments are outlined for validation and demonstration of critical aspects of nonlinear control for rapid, large angle slewing and precision pointing.

20. DISTRIBUTION / AVAILABILITY OF ABSTRACT ☒ UNCLASSIFIED/UNLIMITED ☑ SAME AS RPT. ☑ DTIC USERS	21. ABSTRACT SECURITY CLASSIFICATION UNCLASSIFIED
22a. NAME OF RESPONSIBLE INDIVIDUAL Ltn. Col. J. Crowley	22b. TELEPHONE (*Include Area Code*) (202) 767-5025 — 22c. OFFICE SYMBOL NA

DD FORM 1473, 84 MAR — 83 APR edition may be used until exhausted. All other editions are obsolete.

SECURITY CLASSIFICATION OF THIS PAGE
UNCLASSIFIED

Foreword

This report describes results obtained during a three year research study on nonlinear modeling and control of flexible space structures with application to rapid slewing and precision pointing of space-based, directed energy weapons. The project is funded by SDIO/IST and managed by AFOSR/SDIO (AFSC). Results reported herein are for the period 1 Sept. 1987 – 31 Aug. 1990. The research effort was conducted at Techno-Sciences, Inc. Greenbelt, Maryland office. The project principal investigator was Dr. William H. Bennett, Director of Control Systems Projects at TSI. Coinvestigators included Drs. Gilmer Blankenship and Harry Kwatny. Dr. Kwatny is Vice President and member of Board of Directors at TSI and is Raynes Professor of Mechanical Engineering and Mechanics at Drexel University. Dr. Blankenship is Vice President and member of Board of Directors at TSI and Professor of Electrical Engineering at University of Maryland, College Park, MD. Associate investigator on the project was Dr. Oussima Akhrif, who is currently parttime member of TSI control systems staff and visiting assistant professor at Case Western Reserve University, Cleveland, Ohio.

During the first two years the project was managed by Ltn. Colonel J. Crowley/AFOSR and Dr. A. Amos/AFOSR. We wish to thank both of these individuals for their insight and direction on this project. During the last year the project technical manager was Dr. Alok Das/AFAL.

Contents

List of Figures

List of Tables

1 Research Objectives and Project Summary

This report describes results of a three year project on Nonlinear Dynamics and Control of Flexible Structures whose principal objective was to develop modeling and control design methods for nonlinear, distributed parameter dynamics arising in requirements for rapid slewing and precision pointing of multibody space structures with elastic interactions. The modeling effort centered around the development of a generic class of models for the structural interactions effecting laser system *line-of-sight (LOS)* pointing for a *Space-Based Laser (SBL)* weapon. Control studies focused on the problem of rapid, multiaxis large angle slewing of the generic SBL system with requirements for precision system LOS pointing. One objective for this project was to establish a framework for experimental validation of the class of nonlinear control laws under consideration. To the extent possible, simulation models were based on predicted dynamics and control configurations for the first test article currenlty under construction at the ASTREX facility at Air Force Astronautics Laboratory. Simulation results are included for several possible experiments. A proposed experimental protocol for validation of compensation of nonlinear couplings effecting slewing and precision pointing is briefly described.

Our approach for slewing and pointing control was to develop several practical extensions and applications of the theory of nonlinear control system synthesis based on linearization by feedback transformation. These methods include control laws based on "dynamic inversion" such as the so-called "method of computed torques" popularized in robotics. However, our analysis indicates that certain essential limitations arise in control of distributed parameter dynamics arising in multibody systems with elastic structural interactions. The approach we consider is based on the implementation of a dynamic inverse of the response of certain principal system outputs representing multibody system pointing and alignment to system actuation. As will be discussed in the sequel this concept of input/output linearization (when it can be achieved) involves decoupling certain complementary or "zero dynamics" from the principal system outputs. Since the decoupled dynamics will in general be nonlinear we refer to this class of control laws as *Partial Linearizing Feedback (PLF)*.

Several critical system requirements and control systems can be identified for a prototype SBL system. Precision line-of-sight (LOS) pointing and tracking must be achieved in concert with requirements for rapid slewing of spacecraft primary body and/or articulation of weapon system aperture (see Figure 1.1). Optical beam quality and jitter performance will be limited by extent to which precision multibody alignment of the structure supporting the optical train can be dynamically controlled during and after spacecraft system slewing maneuvers. Thus slewing and pointing control for an SBL system will involve the integration of several critical control systems. An important feature obtained by PLF control is decoupling of control loops for processing slewing and pointing commands. The class of PLF control laws considered in this study for LOS slewing and pointing admits a special structure which permits the required decoupling/linearizing transformations to readiliy implemented with multiple actuators. One way in which this may be used to advantage is in the integration of

SPACE BASED LASER POINTING AND TRACKING

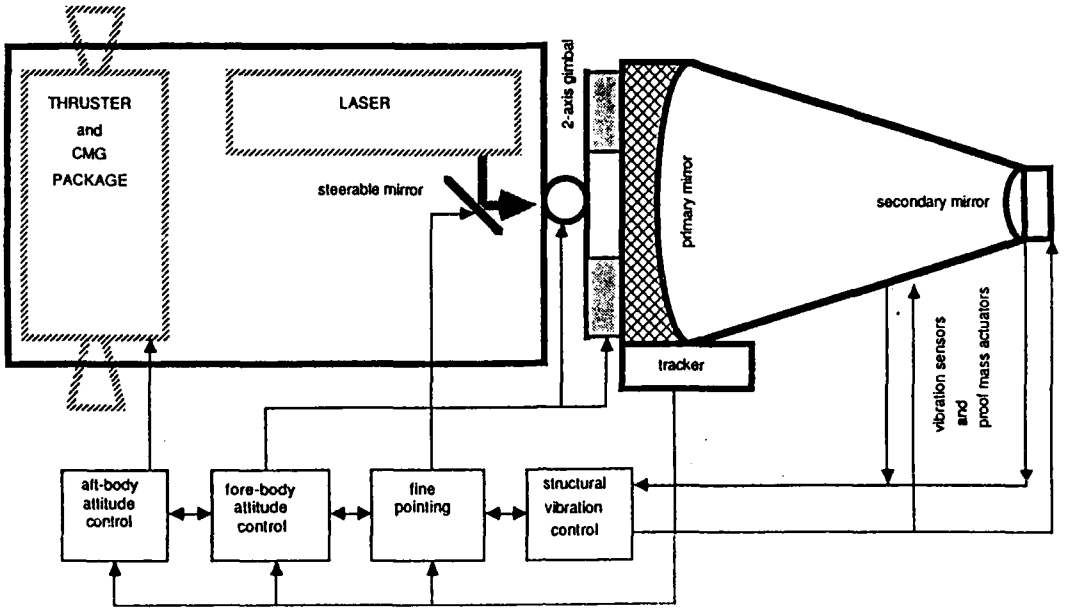

Figure 1.1: Generic Space-Based Laser System with Multiple Control Systems

continuous mode (e.g. reaction wheels, CMG's, etc.) and discontinuous (on/off) actuation (e.g. jets).

Outline of the Project. The first year effort included a survey of the available literature on the dynamic models and control problems for SBL systems. A generic class of SBL models was developed including multibody dynamics of a dual mirror laser beam expander with structural flexure arising in the metering truss which supports the secondary mirror relative to the primary mirror. Initial control studies focused on large angle, but single axis slewing maneuvers and restricted the model to planar motions. Computer simulations were completed demonstrating the slew rates and control requirements for PLF control. During the second year we expanded the computer simulation model to include multiaxis slewing motions and demonstrated several alternative control laws based on PLF compensation which included both continuous and discrete actuation modes. A goal of the effort was to establish a basis for experimental validation of the slewing control laws. Extensive tradeoff studies were performed with simulation models scaled to represent predicted dynamic response for the first test article currently under construction at the ASTREX test facility at Air Force Astronautics Laboratory.

New Results Obtained. A potentially important feature of feedback linearization is the extent to which the idea can be integrated with other standard design methods for multivariable control systems. We have described several alternatives which indicate advantages of

the approach for control of flexible structures. In particular, the integration of active/passive techniques for vibration suppression can be readily incorporated. The idea of *deformation shaping control* has been developed by Dr. T.A.W. Dwyer as part of this project. The method is reported in several papers prepared as part of this project. PLF compensation offers a framework for resolving certain design tradeoffs for the use of active/passive vibration control for rapid slewing and precision pointing of SBL (or other multibody systems).

Robust stabilization and control performance of nonlinear systems is an important issue in many applications. For the current study we are interested in design of control laws whose stability and performance can be predicted and validated in experiments. Several techniques for robust stabilization of nonlinear systems have been developed by Spong and Vidyassagor, Slotine and Sastry, Corless, Gutman, and others. These methods all rely on special structure of the dynamic model uncertainty called "matching conditions". In this research we have developed a new approach which utilizes the framework of adaptive control to provide robust stabilization of nonlinear systems. The approach does not rely on structure matching conditions and represents a significant improvement over available methods.

Overview of the Report for Third Year Activities. In this report we start with a review of the basis for nonlinear PLF control design with emphasis on stabilization. We demonstrate several alternative implementation schemes for PLF control which can arise from several different problems. In particular, we show how PLF compensation can be obtained using switching mode actuation by design of sliding mode control systems. We also indicate how techniques from adaptive control can be used to improve robustness when dynamic models are subject to parametric uncertainty. We next develop a complete framework for modeling multibody systems with elastic structural interactions using Lagrange's equations for continuum mechanical systems. We specialize these systems to the generic SBL models. We then discuss a framework for computation of PLF control laws for Lagrangian systems which focuses attention on the notion of nonlinear system zero dynamics. For practical design of control for large space structures we describe implementation of PLF controls for reduced order models. We specialize the standard model reduction problem for PLF control by considering time scale separation of the system zero dynamics. Finally, we briefly describe a protocol for experiments which can be used to validate PLF control performance predictions. Simulation results are included.

The first [BBKA88] and second [BBKA89] year reports contain additional results on control design and tradeoff studies.

Professional Personnel. The principal investigator for this project is Dr. William H. Bennett and co-principal investigators are Drs. Harry G. Kwatny and Gilmer L. Blankenship from TSI. Dr. Thomas A. W. Dwyer was consultant on the project. We would also like to acknowledge the parttime support from Dr. Oussima Akhrif who graduated in July 1989 with Ph. D. from Electrical Engineering Department of the University of Maryland. Dr.

Akhrif's dissertation developed aspects of feedback linearization for the multibody SBL models developed in this study and some important results are summarized in this report.

Technical Reports/Presentations. As part of the research program we have organized two invited technical sessions, presented several technical papers, and submitted several additional papers for publication as follows.

1. *Nonlinear Dynamics and Control of Aerospace Systems*, invited session at 27th IEEE Cntrl. Dec. Conf., Austin, TX, Dec. 1989.

2. *Robust Control of Uncertain Nonlinear Systems*, invited session at 1989 Amer. Cntrl. Conf., Pittsburgh, PA, June 1989.

Publications/Presentations

1. H.G. Kwatny and W.H. Bennett, "Nonlinear Dynamics and Control Issues for Flexible Space Platforms," *Proc. IEEE Cntrl. Dec. Conf.*, Austin, TX, Dec. 1988.

2. T.A.W. Dwyer, III, "Slew-Induced Deformation Shaping", *Proc. IEEE Cntrl. Dec. Conf.*, Austin, TX, Dec. 1988.

3. O. Akhrif, G. L. Blankenship, and W.H. Bennett, "Robust Control for Rapid Reorientation of Flexible Structures," *Proc. 1989 Amer. Cntrl. Conf.*, Pittsburgh, PA, June 1989.

4. H.G. Kwatny and H. Kim, "Variable Structure Control of Partially Linearizable Dynamics," *Systems & Control Letters*, 15, (1990), pp. 67-80.
(also in) *Proc. 1989 Amer. Cntrl. Conf.*, Pittsburgh, PA, June 1989,

5. W.H. Bennett, "Frequency Response Modeling and Control of Flexible Structures: Computational Methods," *3rd Annual Conf. on Aerospace Computational Control*, Oxnard, CA, Aug.

6. T.A.W. Dwyer, III and F.K. Kim, "Nonlinear robust Variable Structure Control of Pointing and Tracking with Operator Spline Estimation", *Proc. IEEE International Symposium on Circuits and Systems*, Covallis, Oregon, May 9–11, 1989, Paper No. SSP15–5.

7. T.A.W. Dwyer, III and F.K. Kim, "Bilinear Modeling and Estimation of Slew-Induced Deformations," *J. Astro. Sci.* submitted.

8. T.A.W. Dwyer, III, "Slew-Induced Deformation Shaping on Slow Integral Manifolds," *Control Theory and Multibody Dynamics*, Eds. J. Marsden and P.S. Krishnaprasad, (to appear), Amer. Math. Society.

9. T.A.W. Dwyer, III, F. Karray, and W.H. Bennett, "Bilinear Modeling and Nonlinear Estimation", *Proc. Flight Mechanics/Estimation Theory Symposium*, NASA Goddard Space Flight Center, May 1989.

10. T.A.W. Dwyer, III and J. R. Hoyle, Jr., "Elastically Coupled Precision Pointing by Slew-Induced Deformation Shaping," *Proc. 1989 Amer. Cntrl. Conf.*, Pittsburgh, PA, June 21–23, 1989.

11. T.A.W. Dwyer, III and Jinho Kim, "Bandwidth-Limited Robust Nonlinear Sliding Control of Pointing and Tracking Maneuvers," *Proc. 1989 Amer. Cntrl. Conf.*, Pittsburgh, PA, June 21–23, 1989.

12. T.A.W. Dwyer, III , F. Karray and Jinho Kim, "Sliding Control of Pointing and Tracking with Operator Spline Estimation," *3rd Annual Conf. on Aerospace Computational Control*, Oxnard, CA, Aug. 28–30, 1989.

13. W.H. Bennett, O. Akhrif, and T.A.W. Dwyer, "Robust Nonlinear Control of Flexible Space Structures," *Proc. 1990 Amer. Cntrl. Conf.*, San Diego, CA., May, 1990.

14. W. H. Bennett and H. G. Kwatny, "Nonlinear Modeling and Control of Flexible Space Structures", presented at 4th NASA Workshop on Computational Control of Flexible Aerospace Systems, Williamsburg, VA., July 11–13, 1990.

2 Feedback Linearization and Stabilization of Nonlinear Systems

Conventional techniques for stabilization of nonlinear systems via feedback control are still very limited and tend to be tailored to specific situations. Among the most promising new, general approaches utilize linearization (local or possibly global) by *Exact Feedback Linearization (EFL)* [HSM83, KC87]. EFL methods are based on earlier work of Krener [Kre73] and Brockett [Bro78] which demonstrated that a large class of nonlinear dynamical systems can be exactly (i.e. globally linearized) by a combination of nonlinear transformation of the state coordinates with nonlinear state feedback. More recently, the connection between these methods and the idea of input-output (or *Partial) Linearizing Feedback (PLF)* by construction of a *system inverse* [Hir79] has been articulated in a series of papers by Byrnes and Isidori [BI85, BI84]. These connections have engendered a series of design methods with representative results for specific applications by Kravaris and Chung [KC87] and Fernandez and Hedrick [FH87]. In this section we will show how fundamental these construction can become in control system design, discuss alternatives for implementation, and suggest some approaches to integrating the nonlinear design philosophy with more conventional approaches. We focus attention in this section on fundamental concepts culminating in the description of the design approach for multibody systems from the perspective of Lagranian mechanics.

The idea behind feedback linearization is conceptually simple. We start with a nonlinear system model,

$$\dot{x} = f(x) + G(x)u, \tag{2.1}$$

$$y = h(x), \tag{2.2}$$

where $x \in \Re^n$, $u, y \in \Re^m$ with $G = [g_1, \ldots, g_m]$ and assuming the vector fields f, g_i are C^∞ for each $i = 1, \ldots, m$ and $f(0) = 0$. The model structure assumes that the control u enters linearly. The feedback linearization problem is to find a change of basis in the state space, $z = T(x)$, with T diffeomorphic and a feedback law,

$$u = \alpha(x) + \beta(x)v,$$

such that in the new (z, v) coordinates the (closed loop) model has the form,

$$\dot{z} = Az + Bv.$$

We remark that if it possible to find such a control law then the linearization is achieved *through the introduction of active control authority.* An important feature for control system design is that the range of validity of the linearization is given by the transformations, $T(x), \alpha(x), \beta(x)$. The functions may be defined locally or globally.

In contrast, the conventional approach to control design would be based on a linear model obtained by Taylor expansion of the vector fields *about given equilibrium conditions*; x_{eq}, u_{eq}, satisfying,

$$0 = f(x_{eq}) + G(x_{eq})u_{eq}.$$

The conventional linear model used for control design represents perturbation dynamics with respect to the equilibrium conditions and assumes the form,

$$(\dot{\Delta x}) = A\,\Delta x + B\,\Delta u,$$

$$y = C\Delta x$$

where $\Delta x = x - x_{eq}$, $\Delta u = u - u_{eq}$ and

$$A = \left.\frac{\partial f}{\partial x}\right|_{x=x_{eq}}, \quad B = G(x)|_{x=x_{eq}}, \quad C = \left.\frac{\partial h}{\partial x}\right|_{x=x_{eq}}.$$

A major source of model uncertainty in linear control system design arises from assumptions leading to the linear perturbation model. In many cases it may be difficult to estimate the domain of attraction for the equilibria. Indeed, in aerospace applications the control design is often based on a combination of gain scheduling to take into account the dependence of linear perturbation models on operating point conditions which are subject to variation (e.g. trim conditions in aircraft flight control.) For example, the function of a conventional autopilot for aircraft is to compensate for changes in trim conditions and provide stabilization so that the pilot "feels" a standard, linear response to stick commands.

Although the concept of feedback linearization in control system design is potentially revolutionary, its application has many antecedents in applications. The significance for nonlinear control of flexible space structures is the emerging technology for active control and sensing, the dynamics associated with the CSI technology, and the ability of a comprehensive approach to nonlinear dynamic modeling and control design offered by the approaches discussed in this report. Feedback linearization functions in certain applications in a manner similar to gain scheduling [MC80], however, linearization is achieved about a "nominal model" rather than about an operating point. Thus equilibria conditions do not arise explicitly in linearization. One view of such a controller structure is illustrated in block diagram of Figure 2.1. The process linearization which facilitates the design of the linear controller is obtained by the introduction of an *Inverse Force Model (IFM)* for the nonlinear multibody system. The inverse force model transforms commanded accelerations, a_c, into equivalent system generalized forces, f. Thus the linear controller is designed to yield desired system accelerations given the generalized coordinates, q, and their rates, $\dot{q}$.

Precursors to the idea of feedback linearization is pervasive in control applications abound. With the development of the geometric theory of nonlinear systems, computational tools and design methods are becoming available to address control system design on a much larger scope. It is clear that the concept of feedback linearization is pervasive in many fundamental control methods. Our study has focused on the considerations for practical implementation of feedback linearization for rapid slewing and precision pointing of aerospace systems with multibody and elastic interactions. Implementation of feedback linearization definitely requires enhanced control authority and issues related to technology for control actuation will either enable or restrict its application.

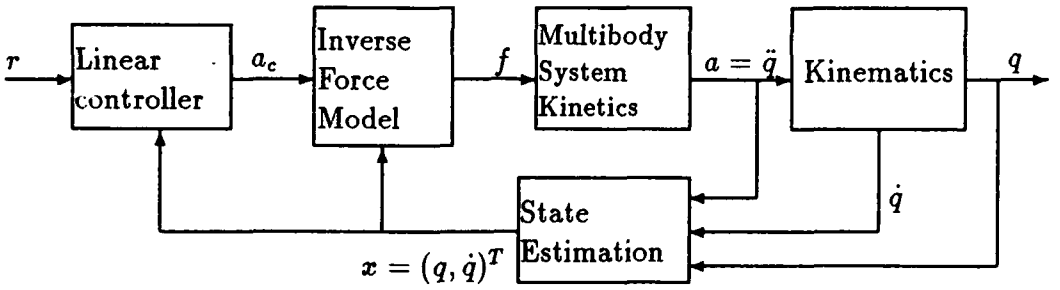

Figure 2.1: Nonlinear Control Concept Using Dynamical System Inverse

It is often suggested that controllers designed based on feedback linearization may be sensitive to model assumptions since the linearization is achieved by cancelation of certain nonlinear terms in the system model. Our study of rapid slewing control of a generic space-based laser model has shown that modeling sensitivity and robustness can be obtained through judicious application of control authority. A central issue in nonlinear control design is the limits of available control authority. For example, actuator saturation contributes to limits on control authority. Discontinuous or saturation mode operation of control actuators can often be desirable but such considerations are often not addressed by linear design methods. We have shown that specific consideration for coordination of discontinuous and continuous modes of control actuation in slewing control methods for multibody systems can be readily found. Finally, it is clear that the cost of feedback linearization, in terms of increased control authority, sensor measurement complexity, or computational burden for online implementation may not always be necessary to achieve system performance objectives. We have also demonstrated that such methods can be readily integrated with standard approaches for linear design once a primary system control objective is identified in terms of a primary system output. As we shall show the role of conventional linearization and control design can be relegated to a subsystem whose dynamics are decoupled (by the action of PLF) from a set of system primary outputs.

2.1 Computation of Partial Linearizing Feedback Compensation

Partial linearization derives directly from the Byrnes-Isidori normal form for nonlinear systems. The essentials of the approach are most easily developed for single-input, single output systems and we will present the approach in that context. The theory for extending these results for multi-input, multi-output problems is now complete and references are included.

Consider a nonlinear dynamical system in the form,

$$\dot{x} = f(x) + g(x)u \tag{2.3}$$

$$y = h(x) \tag{2.4}$$

where f, g are smooth C^∞ vector fields on $\Re^n$ and h is a smooth function mapping $\Re^n \to \Re$. Now if we differentiate (2.4) we obtain

$$\dot{y} = \frac{\partial h}{\partial x}(f(x) + g(x)u). \tag{2.5}$$

In the case that the scalar coefficient of u (viz. $\frac{\partial h}{\partial x}g(x)$) is zero we can differentiate again until a nonzero control coefficient appears. The number of required differentiations is fundamental system invariant which plays a role in constructing a system inverse and therefore in PLF. The Byrnes-Isidori analysis shows that this integer number is analogous to the *relative degree* for a linear system [BI84].

The above construction can be made precise using the notation of differential geometry which has found application in analytical mechanics [Arn78]. We will need only the notion of Lie derivative and Lie bracket. The Lie (directional) derivative of the scalar function h with respect to the vector field f is

$$L_f(h) = \langle dh, f \rangle := \frac{\partial h}{\partial x} f(x). \tag{2.6}$$

Since the above operation results in a scalar function on $\Re^n$, higher order derivatives can be successively defined

$$L_f^k(h) = L_f(L_f^{k-1}(h)) := \langle dL_f^{k-1}(h), f \rangle. \tag{2.7}$$

Then we can write (2.5) as

$$\begin{aligned} \dot{y} &= \langle dh, f \rangle + \langle dh, g \rangle u \\ &= L_f(h) + L_g(h)u. \end{aligned} \tag{2.8}$$

If $L_g(h) = 0$ then we differentiate again to obtain

$$\begin{aligned} \ddot{y} &= \langle dL_f(h), f \rangle + \langle dL_f(h), g \rangle u \\ &= L_f^2(h) + L_g(L_f(h))u. \end{aligned} \tag{2.9}$$

If $L_g(L_f^{k-1}(h)) = 0$ for $k = 1, \ldots, r-1$, but $L_g(L_f^{r-1}(h)) \neq 0$ then the process terminates with

$$\frac{d^r y}{dt^r} = L_f^r(h) + L_g(L_f^{r-1}(h))u. \tag{2.10}$$

The system (2.10) can be effectively inverted by introducing a feedback transformation of the form

$$u = \frac{1}{L_g(L_f^{r-1}(h))}[v - L_f^r(h)] \tag{2.11}$$

which results in an input-output response from $v \to y$ given by

$$\frac{d^r y}{dt^r} = v,$$

a *linear* system.

The integer $r > 0$ can be viewed as a *relative degree* for the nonlinear system (2.3)–(2.4). Note that if we define new state coordinates $z \in \Re^r$ as

$$z_k = L_f^{k-1}(h), \quad k = 1, \ldots, r \tag{2.12}$$

for the r-dimensional nonlinear system (2.10), then the system model can be written in state space form as,

$$\dot{z} = \begin{bmatrix} 0 & 1 & 0 & \cdots & 0 \\ 0 & 0 & 1 & \cdots & 0 \\ 0 & 0 & 0 & \cdots & 1 \\ 0 & 0 & 0 & \cdots & 0 \end{bmatrix} z + \begin{bmatrix} 0 \\ 0 \\ \vdots \\ 0 \\ \alpha(x) + \rho(x)u \end{bmatrix}, \tag{2.13}$$

where

$$\alpha(x) = L_f^r(h), \quad \rho(x) = L_g(L_f^{r-1}(h)). \tag{2.14}$$

More generally, using the new coordinates z (2.12) and introducing a nonlinear feedback control of the form

$$u = \frac{(v - \sigma(x))}{\rho(x)} \tag{2.15}$$

where

$$\sigma(x) = \sum_{k=0}^{r-1} \beta_k L_f^k(h) + L_f^r(h), \tag{2.16}$$

$$\rho(x) = L_g(L_f^{r-1}(h)), \tag{2.17}$$

with β_k for $k = 0, \ldots, r-1$ real positive coefficients then the equations (2.8)–(2.9) can be written in 'reduced' form;

$$\dot{z} = \begin{bmatrix} 0 & 1 & 0 & \cdots & 0 \\ 0 & 0 & 1 & \cdots & 0 \\ 0 & 0 & 0 & \ddots & 0 \\ -\beta_0 & -\beta_1 & -\beta_2 & \ldots & -\beta_{r-1} \end{bmatrix} z + \begin{pmatrix} 0 \\ 0 \\ \vdots \\ 1 \end{pmatrix} v \tag{2.18}$$

$$y = [1, 0, \ldots, 0]\, z. \tag{2.19}$$

2.2 Nonlinear System Transmission Zeros

Note that the process leading to (2.18)–(2.19) provides an equivalent state space realization for the $v \mapsto y$ input-output response of McMillan degree $r \leq n$ (the dimension of the original state space model (2.3)–(2.4)) *by decoupling a portion of the system dynamics from the output response.* This is depicted in Figure 2.3. Thus the new state coordinates z are a 'partial' state for the system. Thus stabilization of (2.18)–(2.19) cannot guarantee stabilization of the full state model (2.3)–(2.4). We remark that in the case that $h(x)$ is such that the relative degree

$r = n$ then the state space transformation (2.12) for $k = 1, \ldots, r$ together with the feedback transformation (2.15) exactly linearizes the full system state model (2.3). The methods described in [HSM83] identify necessary and sufficient conditions for the existence of a C^∞ function $h(x)$ such that $r = n$ and provides a computational approach. The necessary and sufficient conditions for (local) EFL are nongeneric and not likely to be satisfied in general. In the sequel we show how that essential property of involutivity of the f and g vector fields will almost never be satisfied for realistic models of flexible space structures due to the infinite dimensional nature of the state space.

Byrnes and Isidori [BI85] describe the transformation of (2.3)–(2.4) to a *normal form* in which the feasibility of PLF control can be assessed. The main result provides the existence of a diffeomorphic transformation of coordinates $T_h : \Re^n \to \Re^n$ with $(T_h)(x) \mapsto (\xi, z)$, with the state partition in the new coordinates $\xi \in \Re^{n-r}$, $z \in \Re^r$ and inverse, $(\hat{T}_h)(x) \mapsto (\xi, z)$, so that the full state representation in the new coordinates is

$$\dot{\xi} = F(\xi, z), \tag{2.20}$$

$$\dot{z} = \begin{bmatrix} 0 & I_{r-1} \\ 0 & 0 \end{bmatrix} z + \begin{bmatrix} 0 \\ 1 \end{bmatrix} [\mathcal{A}(\xi, z) + \mathcal{B}(\xi, z)u], \tag{2.21}$$

where

$$\mathcal{A}(\xi, z) = \alpha(x)|_{x=\hat{T}(\xi,z)}$$
$$\mathcal{B}(\xi, z) = \rho(x)|_{x=\hat{T}(\xi,z)}.$$

Definition: The *zero dynamics* of the input-output model (2.3)–(2.4) are given by the autonomous system,

$$\dot{\xi} = F(\xi, 0). \tag{2.22}$$

And the system is *locally minimum phase* if the the diffeomorphic transformation T_h is defined on a neighborhood of the origin and (2.22) is asymptotically stable to the origin; $\xi = 0$.

2.3 PLF Computations for Nonlinear MIMO Systems

The nonlinear input/output model is

$$\dot{x} = f(x) + G(x)u \tag{2.23}$$

$$y = h(x) \tag{2.24}$$

where $x \in \Re^n$, $u, y \in \Re^m$ and f, g_i (resp. y_i) for $i = 1, \ldots, m$ are smooth vector fields defined on $\Re^n$ (resp. $\Re^m$). For notational simplicity we write,

$$G(x) = [g_1(x), \ldots, g_m(x)].$$

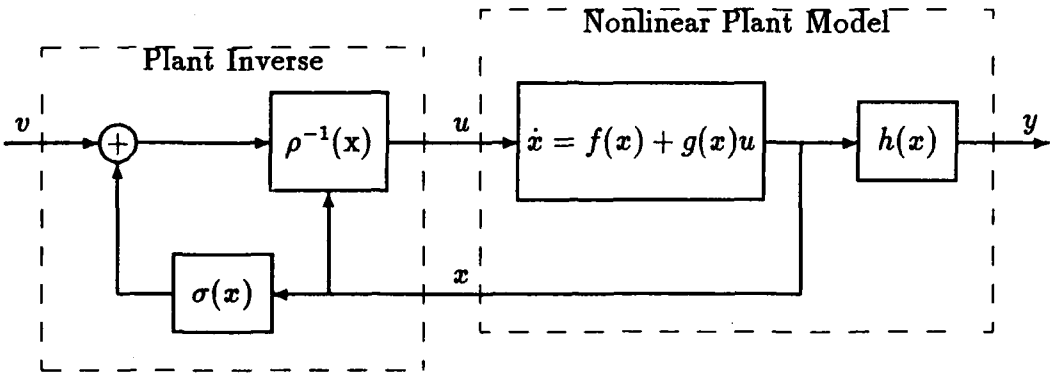

Figure 2.2: Partial Linearizing Feedback via Nonlinear Inverse Model

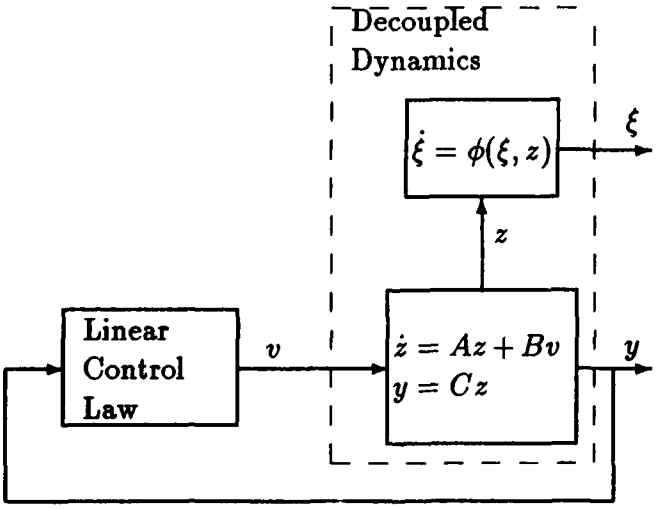

Figure 2.3: Partial Feedback Linearization and Zero Dynamics

In a process similar to the previous section PLF is determined by transformation of the system model (2.23)–(2.24) to a normal form in which we identify a certain $(m \times m)$ *decoupling matrix* which is locally nonsingular.

The process begins with the computation of an appropriate generalization of the MIMO system relative degrees. Let

$$r_i := \min\{k = 1, 2, \ldots : L_{g_j}(L_f^{k-1}(h_i)) \neq 0, \text{ for some } j = 1, \ldots, m\}, \tag{2.25}$$

the i^{th} characteristic number [Fre75]. Each r_i is then the minimal relative degree of the set of m individual output responses y_i obtained from each input u_j for $j = 1, \ldots, m$. Let

$$\mathcal{A}(x) = \begin{bmatrix} \alpha_1(x) \\ \vdots \\ \alpha_m(x) \end{bmatrix}$$

where $\alpha_i(x) = L_f^{r_i}(h_i)$ and

$$\mathcal{B}(x) = \begin{bmatrix} \beta_{11}(x) & \cdots & \beta_m(x) \\ \vdots & \ddots & \\ \beta_{m1}(x) & & \beta_{mm}(x) \end{bmatrix}$$

where $\beta_{ij}(x) = L_{g_j}(L_f^{r_i-1}(h_i))$. Then the desired normal form coordinates are $z \in \Re^r$ where $r = \sum_{i=1}^m r_i$, which are obtained as

$$z = \begin{pmatrix} z_1 \\ z_2 \\ \vdots \\ z_m \end{pmatrix} \tag{2.26}$$

with each $z_i \in \Re^{r_i}$ for $i = 1, \ldots, m$ in the form,

$$z_i = \begin{pmatrix} h_i \\ L_f(h_i) \\ \vdots \\ L_f^{r_i-1}(h_i) \end{pmatrix}. \tag{2.27}$$

Proposition: Given the system (2.23)–(2.24), there exists a diffeomorphic transformation $(T)(x) = (z, \xi)$ to *normal form* coordinates,

$$\dot{z} = Az + E\{\mathcal{A}(z) + \mathcal{B}(z)u\} \tag{2.28}$$

$$\dot{\xi} = F(z, \xi) \tag{2.29}$$

where $A = \text{diag}\{A_1, \ldots, A_m\}$ with

$$A_i = \begin{bmatrix} 0 & I_{r_i-1} \\ 0 & 0 \end{bmatrix}$$

of dimension $r_i \times r_i$ for each $i = 1, \ldots, m$ and E is an $r \times m$ matrix with elements given as,

$$[E]_{ij} = \begin{cases} 1, & \text{if } i = r_i \text{ and } j = i \\ 0, & \text{otherwise} \end{cases}$$

Then the *PLF control*,

$$u = -\mathcal{B}^{-1}(x)\{\mathcal{A}(x) - v\}, \tag{2.30}$$

renders the $v \mapsto y$ input/output response in linear form,

$$\dot{z} = Az + Ev, \tag{2.31}$$

$$y = Cz. \tag{2.32}$$

Definition: The system (2.23)–(2.24) (output constrained) *zero dynamics* are given by

$$\dot{\xi} = F(0, \xi). \tag{2.33}$$

Definition: We say the system is locally *minimum phase* if the zero dynamics are asymptotically stable to the origin $\xi = 0$.

Remark: In general the computation of the normal form with (2.29) independent of u is difficult and not required to establish the minimum phase property. Instead, note that the system *zero dynamics* are just the dynamics of (2.23)–(2.24) constrained to the manifold $\mathcal{M}_h \subseteq \Re^n$ of dimension $n - m$ given by,

$$\mathcal{M}_h = \{x \in \Re^n : h(x) = 0\}.$$

Proposition: The zero dynamics are asymptotically stable if and only if the system,

$$\dot{x} = f(x) - G(x)\mathcal{B}^{-1}(x)\mathcal{A}(x), \quad x(0) \in \mathcal{M}_h$$

is asymptotically stable to origin. We note that $\mathcal{M}_h$ is an *integral manifold* for (2.23)–(2.24).

2.4 Partial Linearization and Variable Structure Control Systems

The theory of Variable Structure (VS) systems addresses the design of control laws which are discontinuous functions of the system state. VS control offers practical solutions for systems employing actuators which can be efficiently operated in bang-bang and other discontinuous modes. Our interest in VS control for rapid slewing of multibody systems arises from the following observations:

1. Design methods for VS control for output regulation have been shown to effect an implicit partial feedback linearization. The implicit partial linearization is achieved through the use of VS control requires only output feedback.

2. Direct implementations of VS control laws can attain a level of robustness to plant model assumptions which is difficult to achieve with smooth control. Moreover, robustness is achieved without overly conservative restrictions on performance. The limitations of robustness for VS designs are clearly related to the minimum phase conditions for PLF design.

3. The use of discontinuous control and the connections between VS and PLF designs suggest several alternatives for integration of various types of actuators, including both switched and continuous modes of operation. Integration of several control actuation systems will be required for implementation of rapid slewing requirements for several candidate large space platforms.

The general theory of VS control design is well known and we will not attempt to present a complete description of its scope. For details see the survey [DZM88]. However, to focus attention on the concepts we seek to exploit we start with a brief description of the basic ideas.

VS control systems utilize high speed switching control to drive the system trajectories toward a specified manifold called the switching surface. Given the nonlinear system (2.23), the VS control laws are of discontinuous type;

$$u_i = \begin{cases} u_i^+(x), & \text{for } s_i(x) > 0 \\ u_i^-(x), & \text{for } s_i(x) < 0 \end{cases} \tag{2.34}$$

with $s_i(x) = 0$ smooth switching surfaces chosen in the state space for each $i = 1, \ldots, m$. The design approach which is preferred is based on the introduction of *sliding modes.*

Definition (sliding modes): A manifold, $\mathcal{M}_s$, consisting of the intersection of $p < m$ switching surfaces, $s_i(x) = 0$, with the property that $s_i \dot{s}_i < 0$ for each $i = 1, \ldots, p$ in the neighborhood of almost every point in $\mathcal{M}_s$ is called a *sliding manifold.* Under these conditions any trajectory of the system which enters $\mathcal{M}_s$ remains confined to the manifold for a finite length of time. We call the motion on $\mathcal{M}_s$ a *sliding mode.*

VS design methods involve a two step process: 1) design the switching surface so that once sliding is achieved the natural sliding mode achieves design objectives such as regulation, stabilization, etc., and 2) design of discontinuous control laws which achieve sliding on desired regions of the switching surfaces. The method of equivalent control is a popular approach for designing the switching surface to achieve desired sliding mode dynamics.

Given the system (2.23) and a manifold, $\mathcal{M}_s = \{x \in \Re^n : s(x) = 0\}$, with $s : \Re^n \to \Re^m$ then sliding is characterized by satisfaction of the constraint equations,

$$s(x) = 0, \quad \dot{s}(x) = 0 \tag{2.35}$$

over the finite time interval, $t_1 > t > t_2$ where $s(x(t_1)) = 0$. Note that a sliding mode is an instance of an integral manifold for the closed loop system. The *equivalent control,* u_{eq}, is

the control required to maintain the system trajectory within the manifold $\mathcal{M}_s$ and is given by the condition,

$$\dot{s} = \nabla s(x)\,\dot{x} = \nabla s(x)\{f(x) + G(x)u_{eq}\} = 0 \tag{2.36}$$

where $\nabla s(x) = \partial s/\partial x$. Under the assumption that $\det\{\nabla s(x)G(x)\} \neq 0$ for $x \in \mathcal{M}_s$ we have,

$$u_{eq} = -[\nabla s(x)G(x)]^{-1}\nabla s(x)f(x), \tag{2.37}$$

and the motion in sliding is given by,

$$\dot{x} = \{I - G(x)[\nabla s(x)G(x)]^{-1}\nabla s(x)\}f(x), \;\; s(x(t_1)) = 0. \tag{2.38}$$

Connections between the design of VS control and feedback linearizing control have received considerable attention [FH87]. The principal focus has been on the problem of synthesis of VS designs for nonlinear systems of the form (2.23) using (exact) feedback linearization. In the sequel we direct attention to the problem of output regulation. The connection we establish with PLF design also illuminates several questions relative to robustness properties of VS designs with sliding modes.

Design objective—Output Regulation. Given the system (2.23)–(2.24) where y indicates a set of regulated outputs, the control problem is to drive the outputs asymptotically to zero.

Since output regulation problem seeks to enforce the set of constraints

$$h_i(x) = 0, \;\; i = 1, \ldots, m,$$

asymptotically it seems reasonable that VS design could be employed. However, the naive choice $s_i(x) = h_i(x)$ leads to the complication that in general—in fact, most often—$[\nabla h(x)G(x)]$ is singular for almost all $x \in \Re^n$. The approach suggested in [KK89] is to design sliding mode via the choice of switching surfaces relative to the normal form coordinates for (2.23)–(2.24) as given by (2.28)–(2.29).

Proposition: Given the system (2.23)–(2.24) obtain the diffeomorphic transformation given by (2.26), (2.27) to the form (2.28)–(2.29). The selection of switching surface,

$$s(z) = Kz \tag{2.39}$$

with K an $m \times m$ constant matrix, solves the output regulation problem if sliding can be achieved. In sliding the equivalent control is,

$$u_{eq} = -\mathcal{B}(x)^{-1}KAz - \mathcal{B}^{-1}(z)\mathcal{A}(z) \tag{2.40}$$

and the sliding dynamics are given by the r linear equations,

$$\dot{z} = [I_r - EK]Az, \quad Kz(0) = 0 \tag{2.41}$$

Proof: The proof is given in detail in [KK89] together with a method for stabilization.

By defintion, the transformation $(T)(x) \mapsto (z, \xi)$ is invertible; $(\hat{T})(z, \xi) \mapsto x$, and the switching surface $s(z) = 0$ can be reflected to the original coordinates $s(x) = 0$. The dynamics in the x coordinates are best understood in terms of the geometry. Define the m-dimensional manifolds $\mathcal{M}_s = \{x \in \Re^n : s(x) = 0\}$ and $\mathcal{M}_h = \{x \in \Re^n : h(x) = 0\}$. The $n - r$ dimensional manifold $\mathcal{M}_z = \{x \in \Re^n : x = \hat{T}(0, \xi)\}$ is contained in both $\mathcal{M}_s$ and $\mathcal{M}_h$.

Assume that in some neighborhood $\mathcal{D} \in \Re^n$ a sliding mode exists on $\mathcal{D}_s = \mathcal{D} \cap \mathcal{M}_s$ which is assumed nonempty. Suppose that $\mathcal{D}_z = \mathcal{D}_s \cap \mathcal{M}_z$ is nonempty. Let α denote a bounded, stable attractor of the zero dynamics contained in $\mathcal{D}_z$. Assume that all trajectories in $\mathcal{D}_z$ converge to α. Then if the initial state is sufficiently close to $\mathcal{D}_s$ the trajectory will eventually reach $\mathcal{D}_s$ and sliding will occur. Clearly the stability of the attractor is critical to the stability of the overall design. In the sequel, we establish conditions for output regulation of multibody systems which guarantee that the zero dynamics have well defined local equilibria so that linear stability analysis of the zero dynamics is appropriate. We remark that the problem of establishing estimates for the domain of attraction in the zero dynamics is an open question.

2.5 Robust Stabilization of Nonlinear Systems

For practical implementation of PLF compensation various researchers have focused attention on conditions which guarantee robust stabilization of the nonlinear system (2.3)–(2.4) with feedback transformation of the form (2.11) by introduction of linear feedback $v = Kz$. A brief survey of the wide range of methods which have been proposed is given in [BBKA88]. In this section we focus attention on a ubiquitous assumption in most of the work on robust stabilization of nonlinear systems based on PLF compensation.

Consider the usual case for engineering design where the open loop system dynamics for (2.23)–(2.24) is given by a nominal model of the form

$$\dot{x} = f^o(x) + G^o(x)u \tag{2.42}$$

$$y = h^o(x), \tag{2.43}$$

where f^o, g_i^o are C^∞ vector fields for $i = 1, \ldots, m$, defined on a manifold $\mathcal{M} \in \Re^n$, with $f^o(0) = 0$. We assume the (true) system response can be modeled via a perturbation of the vector fields;

$$f = f^o + \Delta f, \quad G = G^o + \Delta G$$

with Δf, Δg_i each C^∞ defined on $\mathcal{M}$ and $\Delta f(0) = 0$. In [AB88] a detailed analysis is given leading to sufficient conditions on Δf, ΔG which—together with the assumption that (2.42) is feedback linearizable—guarantees that (2.23) is also linearizable. The conditions given are less restrictive then the usual structure matching conditions [AB87]. The structure matching conditions also play a role in establishing conditions for robust stabilization and we repeat them for convenience.

The structure matching conditions. Under the assumption that the perturbation vector fields satisfy,

$$\Delta f, \Delta g_i \in \Delta \tag{2.44}$$

where $\Delta = Sp\{g_1, \ldots, g_m\}$ then any such model (2.23) is exactly linearizable—in fact, *by the same diffeomorphic transformations.* The above conditions are equivalent to the statement that the perturbations to the vector fields can be factored as:

$$\Delta f(x) = G^o(x) d_f(x), \tag{2.45}$$
$$\Delta G(x) = G^o(x) D_g(x). \tag{2.46}$$

The importance of the structure matching conditions in establishing robust stability is that under these conditions the model uncertainty—after application of PLF compensation—can be equivalently represented by a perturbation (or disturbance) at the compensated system inputs. This facilitates the design of disturbance rejection techniques using either explicitly nonlinear control designs such as Gutman [GL76] or linear control design such as in [Kra87]. To see this we summarize the construction under the assumption that $h(x) = h^o(x)$. Substitute the PLF compensation (2.30) obtained for the nominal model (2.42)–(2.43) into the model for the true system (2.23) to obtain,

$$\begin{aligned} \dot{x} &= f^o + \Delta f + (G^o + \Delta G)\mathcal{B}^{-1}[v - \mathcal{A}] \\ &= f^o + G^o \Delta d_f + G^o(I + D_g)\mathcal{B}^{-1}[v - \mathcal{A}] \\ &= f^0 + G^o \mathcal{B}^{-1}[v - \mathcal{A}] + G^o[d_f + D_g \mathcal{B}(v - \mathcal{A})]. \end{aligned} \tag{2.47}$$

The model after nominal PLF compensation can (by the above assumptions) be transformed to z-coordinates defined in (2.26)–(2.27) to obtain,

$$\dot{z} = Az + E\{v + \eta\} \tag{2.48}$$
$$\dot{\xi} = F(z, \xi), \tag{2.49}$$

where

$$\eta(z, \xi, v) = \left[d_f(x) + D_g(x)\mathcal{B}(x)^{-1}\{v - \mathcal{A}(x)\}\right]\Big|_{x = T^{-1}(z)} \tag{2.50}$$
$$= \left[d_f(x) - D_g(x)\mathcal{B}(x)^{-1}\mathcal{A}(x)\right]\Big|_{x = T^{-1}(z)} + \left[D_g(x)\mathcal{B}(x)^{-1} v\right]\Big|_{x = T^{-1}(z)}. \tag{2.51}$$

Thus it is clear that robust stabilization must address the disturbance rejection of the class of input disturbances $d_v(t)$ which bound the model error; $\|\eta\| \leq \|d_v\|$. An effective design approach, in the case when the nominal model is exactly feedback linearizable, is given by Spong and Vidyasagar [SV87]. There approach utilizes an L_∞ stabilization criterion and obtains a linear, time-invariant feedback control for the v-input.

Remarks: The design methods for robust stabilization of nonlinear systems available in the literature are almost exclusively based on the structure matching conditions. By reflecting the model uncertainty to the system inputs (after nonlinear feedback compensation) they can employ either:

1. linear compensator design which seeks to reduce loop gains consistent with bounded model uncertainty, or

2. nonlinear switching mode compensator design which seeks to over-bound input disturbances by high gain implementations using fast switching control.

Both methods result in essentially conservative designs since the worst case bounds on the input disturbances must be assumed.

In [Akh89] the basis for robust stabilization of nonlinear systems is considered further and new results are obtained for the case of parametric model uncertainty. The new control laws obtained in [Akh89] employ *basic constructions of adaptive control in the context of feedback linearization.* The results show that robust stabilization can be obtained under much less restrictive conditions than the structure matching conditions. Significantly, feedback linearization plays the role of enforcing linearity for subsequent control loop designs. To the extent that this can be achieved in practical applications it can enhance reliability and repeatability thus achieving improved performance prediction—an important feature for space-based systems. Standard constructs in adaptive control can then be applied to enhance the robustness of feedback linearization with model uncertainty. We emphasize that the constructions described below are new and offer stability results for the nonlinear system under very general assumptions. In the next few paragraphs we briefly review some significant aspects of these results.

Robust Stabilization of Nonlinear Systems by Adaptive Methods. Again, starting with the system model in the form (2.23) we assume the model uncertainty can be represented by parametric dependence of the vector fields so that the model has the form,

$$\dot{x} = f(x, \theta) + G(x, \theta)u, \tag{2.52}$$

with θ a p-vector of unknown parameters. We assume that for every $\theta \in B_\theta$, a closed, compact neighborhood of the nominal parameter θ_o, f and g_i, for $i = 1, \ldots, m$, are C^∞ vector fields and $f(0, \theta) = 0$ for $\theta \in B_\theta$. The nominal design model is characterized by the set of nominal parameters and we take $f(x) = f(x, \theta_o)$, $G(x) = G(x, \theta_o)$.

The following assumptions are used in [Akh89] to establish a robust stabilizing controller for the nonlinear system.

Assumption 1: The nominal system is exactly feedback linearizable.[1]

[1]The extension of the results described below to the case of stabilization by PLF is in progress.

It is important to note that assumption 1 is applied only at the nominal plant model with fixed and known parameters θ_o. This is in contrast to the structure matching conditions which are almost universally assumed in the current literature.

Assumption 2: For any $x \in U \subseteq \Re^n$ and $\theta \in B_\theta$,

$$\Delta g_i(x,\theta) \in \text{Sp}\ \{g_1(x,\theta_o),\ldots,g_m(x,\theta_o)\}$$

for $i = 1,\ldots,m$. This assumption implies that there exists an $m \times m$ matrix valued function, $D(x,\theta)$, with smooth elements such that $\Delta G = G^o D$.

Assumption 3: Either there exists an $m \times m$, strictly positive definite matrix, K such that,

$$\forall x \in U,\ \forall \theta \in B_\theta,\quad 0 \leq D(x,\theta) \leq K,$$

or there exist a K, negative definite, such that,

$$\forall x \in U,\ \forall \theta \in B_\theta,\quad K \leq D(x,\theta) \leq 0.$$

This assumption (in various forms) is typical in adaptive control stability analysis and design. It says that the "sign" of this term must be definite and known *a priori.*

The design approach is natural and begins with the transformation

$$z = T(x,\theta_o),$$

to normal form and choice of feedback linearizing compensation (2.30). The v control is chosen in two parts. First, for the nominal design and performance objectives we find $v = Fz$ where $A + EF$ in (2.31) is a stable matrix. In this case, there exists a unique, positive definite, symmetric solution to the Lyapunov equation,

$$(A+EF)^T P + P(A+EF) = -I.$$

The design for the nominal model is now modified by the introduction of adaptation. The control law obtained is described by the following equations;

$$\begin{aligned} u &= -\mathcal{B}^{-1}(x)\{\mathcal{A}(x) - v\}, && (2.53)\\ z &= T(x,\theta_o), && (2.54)\\ v &= Fz + C(z,\hat{\theta})\hat{\theta}, && (2.55)\\ \dot{\hat{\theta}} &= -\Gamma^{-1}C^T(z,\hat{\theta})E^T P z, && (2.56)\\ C(z,\hat{\theta}) &= -\mu\mathcal{B}(z)G^T(z,\theta_o)Pz\hat{\theta}^T. && (2.57) \end{aligned}$$

In these control laws the $p \times p$ matrix $\Gamma > 0$ is the "adaptation gain" which is chosen so that the Lyapunov function,

$$V = z^T P z + \hat{\theta}^T \Gamma \hat{\theta}$$

is positive definite for all $x \in U$ and μ is a positive scalar. The result established in [Akh89] is the following.

Theorem: The adaptive control with feedback linearizing transformation is asymptotically stable to the origin $x = 0$ and $\hat{\theta} \rightarrow \theta$, asymptotically, if for $x \in U$ and $\theta \in B_\theta$ there exists $c_2 > 1$ and

$$2\| T^T(x)P\Psi(x,\theta) - \mu y^T D y \, \|\hat{\theta}\|^2 \, \| \leq c_2 \|T(x)\|^2,$$

where

$$\Psi(x,\theta) = [\Delta f(z,\theta) + \Delta G(z,\theta)\{\mathcal{A}(z) + \mathcal{B}^{-1}Fz\}]$$

and

$$y = G^T(z,\theta_o)P^T z.$$

Proof: [Akh89].

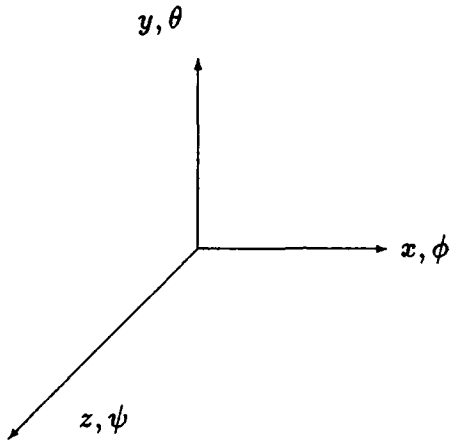

Figure 3.1: Standard Coordinate Frame for Modeling

3 Nonlinear Dynamics of Multibody Systems with Flexible Interactions

In this section we describe the basis for the formal development of a class of evolution models for multibody systems with elastic interactions. We follow the approach suggested by Baillieul and Levi [BL87]. As will be seen, the formulation captures the essential evolution dynamical structure of the system without requiring detailed knowledge of its internal configuration. As such this framework provides a consistent modeling approach for developing a hierarchy of models with increasing internal complexity and fine structure. The main idea is to isolate a "primary body" and to attach a reference frame to it at a convenient location for measuring attitude and displacement dynamics. The motion of all other spacecraft components will then be measured relative to this frame.

Throughout this report we will use the notational conventions given in Table 3.1. Consider a reference frame fixed in the primary body, with origin located by the position vector $R \in \Re^3$ and angular orientation denoted by $L \in SO(3)$, both relative to a fixed inertial frame (see Figure 3.1). L can be parameterized by the Euler angles[2] ψ, θ, ϕ representing sequential rotations about the axes 3,2,1, respectively:

$$L = \begin{bmatrix} \cos\theta\cos\psi & \cos\theta\sin\theta & -\sin\theta \\ \sin\phi\sin\theta\cos\psi - \cos\phi\sin\psi & \sin\phi\sin\theta\sin\psi + \cos\phi\cos\psi & \sin\phi\cos\theta \\ \cos\phi\sin\theta\cos\psi + \sin\phi\sin\psi & \cos\phi\sin\theta\sin\psi - \sin\phi\cos\psi & \cos\phi\cos\theta \end{bmatrix}. \quad (3.1)$$

[2]We use the so-called NASA standard or 321 convention [Gol82].

Notation	Explanation
$x_i,\ i = 1, 2, \ldots$	element of a vector x
x^T	transpose of vector x
$\dot{x} = \frac{dx}{dt}$	time differentiation
$x_z(t,z) = \frac{\partial x}{\partial z}(z,t)$	partial differentiation
$\langle \cdot, \cdot \rangle$	natural (Hilbert space) inner product
$\| \cdot \|$	natural (Hilbert space) norm
δx	differential variation
$x \times y$	vector cross product of x and y

Table 3.1: Standard Notation for Lagrangian Mechanics

A fundamental kinematic relationship is

$$\dot{L}(t) = -\Omega(t)L(t) \tag{3.2}$$

where

$$\Omega = \begin{bmatrix} 0 & -\omega_3 & \omega_2 \\ \omega_3 & 0 & -\omega_1 \\ -\omega_2 & \omega_1 & 0 \end{bmatrix} \tag{3.3}$$

and $\omega = (\omega_1, \omega_2, \omega_3)^T$ is the primary body (inertial) angular velocity as measured in the body coordinates.

Define $\xi \in \Re^3$ as $\xi = (\psi, \theta, \phi)^T$. Then an equivalent relation[3] is

$$\dot{\xi} = \Gamma(\xi)\omega, \quad \Gamma^{-1}(\xi) = \begin{bmatrix} 1 & 0 & -\sin\theta \\ 0 & \cos\psi & \cos\theta\sin\psi \\ 0 & -\sin\psi & \cos\theta\cos\psi \end{bmatrix}. \tag{3.4}$$

The body frame position and orientation can be characterized as a point in the special Euclidian group, $SE(3, \Re)$, each element of which can be represented by a matrix

$$X = \begin{bmatrix} L^T & R \\ 0 & 1 \end{bmatrix}. \tag{3.5}$$

The positions of all other elements of the system are measured relative to the primary body frame. We identify each particle (or element), P, by its "undeformed" position, z, in the primary body frame. Let $u(z,t)$ denote the deformed position of P. Furthermore, we fix a coordinate system in each particle with origin at $u(z,t)$ and aligned—in the undeformed state—with the body axis coordinates. Let $\ell(z,t) \in SO(3)$ denote the orientation of P in the

[3]**Equation (3.4) is essential to the analytic framework for multibody modeling. Alternate parametrisations of $SO(3)$—such as the Cayley-Rodrigues parameters [Dwy84]—can be used to advantage and the general form remains intact.**

deformed state as measured in the primary body coordinates. Note that in the undeformed state

$$\ell_{undeformed} = \begin{bmatrix} 1 & 0 & 0 \\ 0 & 1 & 0 \\ 0 & 0 & 1 \end{bmatrix} \tag{3.6}$$

and for small relative motions[4]

$$\ell_{small} = \begin{bmatrix} 1 & \psi & -\theta \\ -\psi & 1 & \phi \\ \theta & -\phi & 1 \end{bmatrix}. \tag{3.7}$$

The inertial coordinates $U(z,t)$ of a particle P can be obtained from the body coordinates $u(z,t)$ via the relation

$$U(z,t) = L^T u(z,t) + R. \tag{3.8}$$

Note also that

$$\dot{X}(t) = \begin{bmatrix} L^T(t)\Omega(t) & \dot{R}(t) \\ 0 & 0 \end{bmatrix}. \tag{3.9}$$

Also, a direct computation yields

$$\frac{d}{dt}U = L^T(t)[\Omega u + \dot{u}] + \dot{R}(t) \tag{3.10}$$

The kinetic energy of the system can be written in terms of the generalized coordinates $q = (\xi, R, u)$ in the form

$$\begin{aligned} T(q,\dot{q}) &= \tfrac{1}{2}\int_S \|\dot{U}\|^2 dm \;\; = \tfrac{1}{2}\int_S \|L^T[\Omega u + u_t] + \dot{R}\|^2 dm \\ &= \tfrac{1}{2}\int_S \|[\Omega u + u_t]\|^2 + 2\langle \Omega u + u_t, L\dot{R}\rangle + \|\dot{R}\|^2 dm \end{aligned} \tag{3.11}$$

where S denotes that the integral is to be taken over the entire system.

3.1 Lagrange's Equations for Continuum Dynamics

The formalism of Lagrangian dynamics begins with the identification of the configuration space, i.e. the generalized coordinates, associated with the dynamical system of interest. Once the configuration manifold, M, is specified we have the natural definition of velocity at a point $q \in M$ as an vector, $\dot{q}$, in the tangent space to M at q, often denoted T_qM. We then define the state space as the union of all points $q \in M$ along with their tangent spaces, the so-called tangent bundle (c.f. [AM78, Arn78]) T_qM. The evolution of the system in the state space is characterized using Hamilton's principle of least action by the definition

[4]The assumption of small relative motions is useful in the continuum framework to model large displacements. This idea suggests several alternative approximations useful for modeling structural flexure dynamics and is discussed in detail in § 3.3.

of a Lagrangian $L(q,\dot{q}) : M \times T_qM \rightarrow \Re$. Hamilton's principle says that the motion of a dynamical system between times t_1 and t_2 is a "natural" motion if and only if

$$\delta \int_{t_1}^{t_2} L \, dt = 0, \tag{3.12}$$

or—accounting for the presence of external generalized forces, Q—in its generalized form;

$$\int_{t_1}^{t_2} (\delta L + Q^T \delta q) \, dt = 0. \tag{3.13}$$

For *distributed parameter systems (DPS)*, special care is required to properly characterize the configuration space for modeling the system motions. The principal reasons for this fact follow from the application of the models obtained; viz., the study of time evolutions subject to control forces. First, control systems will inevitably involve the implementation of feedback and we are therefore immediately concerned with stability. An appropriate notion of stability is central to the design of feedback control systems. For Lagrangian systems the natural definition of stability is implicit in the structure of the state space which for DPS is a function space and care must be exercised that the construction (and assumptions) of the state space are consistent with the engineering control problem. Second, it is often necessary to define finite dimensional approximations to DPS for a variety of reasons including computer simulation. Again, our primary concern is in approximating the time evolution under the influence of control. As we will make clear in the following section, the formulation of such models in a consistent way is inherently bound to the definition of the configuration space. In this section we confine our discussion to the configuration space for continuous systems with one spatial dimension.

The generalized coordinates are chosen so that all "nonworking" or geometric constraints on the motion are eliminated. This is the key to the utility of the Lagrange formalism for constructing the equations of motion. In the case of DPS any "geometric" boundary conditions (which we will denote $\mathcal{G}$) are therefore included as part of the definition of the configuration space. All other boundary conditions necessary to complete the Euler-Lagrange equations result from the application of Hamilton's Principle, (3.12) or (3.13). These are the "natural" boundary conditions (denoted $\mathcal{N}$).

An essential part of the definition of the configuration space in the infinite dimensional case is the specification of the norm. Although all norms are equivalent in finite dimensions, this is certainly not the case in infinite dimensions. We briefly summarize the main issues. Consider functions $v(z)$ defined on the domain $z \in [0,1]$ and let $D^r v(z)$ denote the r^{th} derivative with respect to z. We denote by H^p the completion of the set of the set of functions with p continuous derivatives and which satisfy

$$\|v\|_p^2 = \int_0^\ell \{|D^p v(z)|^2 + \ldots + |v(z)|^2\} dz < \infty \tag{3.14}$$

These are the *Sobolev spaces* [Lio71]. Equivalently, H^p consists of those functions whose first p derivatives belong to the Hilbert space of square integrable functions. Note that $x \in H^i$ implies $x \in H^{i-1}$ for $i = 1, 2, \ldots$.

Let $H^p_{\mathcal{G}}$ denote the completion of the set of functions satisfying (3.14) as well as a prescribed set of boundary conditions designated $\mathcal{G}$. It is not necessarily true that all of the functions in this new space satisfy the boundary conditions. The reason for this is that an arbitrary sequence of functions, all satisfying the given boundary conditions, may converge to a function which does not satisfy the boundary conditions. However, the following proposition is true. Suppose the boundary conditions $\mathcal{G}$ involve derivatives of order s and none higher. Then all of the functions in $H^p_{\mathcal{G}}$ satisfy the boundary conditions provided $p > s$. Thus, a consistent definition of the configuration space is obtained *if the specified norm is compatible with the geometric boundary conditions.*

Hamilton's principle may be used to derive the Euler-Lagrange equations and the natural boundary conditions. The Euler-Lagrange equations are to be solved along with boundary conditions $\mathcal{B} = \mathcal{G} \cup \mathcal{N}$. In general, the Lagrangian will involve derivatives with respect to z of order p and the Euler-Lagrange equations will involve derivatives of order $2p$. In finding solutions $q(t)$ we seek "weak" (sometimes called generalized or distributional[5]) solutions in $H^p_{\mathcal{G}}$ which satisfy Hamilton's principle or "strong" (pointwise, genuine or classical) solutions in $H^{2p}_{\mathcal{B}}$ which satisfy the Euler-Lagrange equations. The results are equivalent (in $H^p_{\mathcal{G}}$) when both problems have solutions. The Euler-Lagrange equations may be given the interpretation of an evolution equation as we sill describe below.

Finite Dimensional Approximation and Computer Simulation Finite dimensional approximations to the system dynamics may be obtained by seeking an approximate solution to the Euler-Lagrange equations or to Hamilton's principle directly. The latter has the advantage that solutions are to be sought in a larger space of admissible functions which provides a wider choice of approximating functions. Perhaps unexpectedly, this turns out to be of fundamental significance in developing numerical solutions to the required evolution dynamics and for computer simulation. Furthermore, important links to the system physics are retained through this modeling process. These observations appear consistent with many standard engineering methods which introduce approximations to continuous, distributed system dynamics by discretization of the variational problem underlying the Lagrangian dyanmics [Mei67]. Indeed, this is the basis for the Finite Element Method (FEM) for evolution dynamics described in [SF73]. The simulation models developed in this study are based on finite dimensional approximation using *collocation by splines* [Aga84, Sta79, Pre75]. Further details of the method will be given in a later section with examples.

Next we consider some simple continuous systems arising in structural mechanics which will illustrate the evolution modeling setup described above.

[5] There are several approaches to developing the notion weak and strong solutions and many good reasons for doing so. Thus, the proliferation of terminology carries with it sometimes subtle distinctions (c.f. [SF73, RM57, Sta79]).

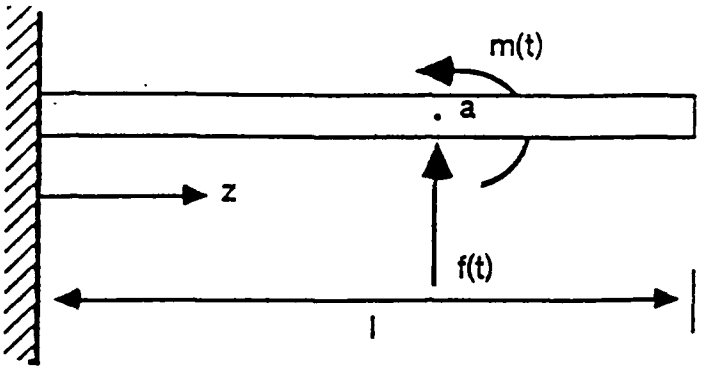

Figure 3.2: Simple Cantilevered Beam

3.1.1 Example: Simple Cantilevered Beam

Consider the cantilevered beam undergoing small transverse motions confined to the plane. The beam is excited by a concentrated force, $f(t)$, and moment, $m(t)$, applied at the point $z = a \in (0,1)$.

Timoshenko Model. Each cross section undergoes a displacement $\eta(z,t)$ and a rotation $\phi(z,t)$. These are the generalized coordinates. The geometric boundary conditions are

$$\mathcal{G}: \ \eta(0,1) = 0 \quad \text{and} \quad \phi(0,1) = 0.$$

Thus, the appropriate configuration space is $H^1_{\mathcal{G}}$. The Lagrangian is

$$L = \int_0^\ell \left[\tfrac{1}{2}\rho A \left(\frac{\partial \eta}{\partial t}\right)^2 + \tfrac{1}{2}\rho I \left(\frac{\partial \phi}{\partial t}\right)^2 \right] - \left[\tfrac{1}{2} EI \left(\frac{\partial \phi}{\partial z}\right)^2 + \tfrac{1}{2}\kappa GA \left(\frac{\partial \eta}{\partial z} - \phi\right)^2 \right] dz$$

and the virtual work $\delta W = Q^T \delta q$ due to the external forces is

$$\delta W = \int_0^\ell \{ f(t)\delta(z-a)\delta\eta + m(t)\delta(z-a)\delta\phi \} dz,$$

where ρ is the mass density, A, the cross section area, I, the moment of inertia, E, the modulus of elasticity, and κG, the effective shear modulus. Upon application of Hamilton's principle, we obtain the partial differential equations

$$\begin{aligned} \rho A \frac{\partial^2 \eta}{\partial t^2} &= \frac{\partial}{\partial z}\left[\kappa GA \left(\frac{\partial \eta}{\partial z} - \phi \right) \right] + f(t)\delta(z-a), \\ \rho I \frac{\partial^2 \phi}{\partial t^2} &= \frac{\partial}{\partial z}\left[EI \left(\frac{\partial \phi}{\partial z} \right) + \kappa GA \left(\frac{\partial \eta}{\partial z} - \phi \right) \right] + m(t)\delta(z-a), \end{aligned}$$

and the natural boundary conditions

$$\mathcal{N}: \ \kappa GA \left(\frac{\partial \eta(\ell,t)}{\partial z} - \phi \right) = 0 \quad \text{and} \quad EI \left(\frac{\partial \phi(\ell,t)}{\partial z} \right) = 0.$$

Thus, we have the evolution equation

$$\begin{bmatrix} \rho A & 0 \\ 0 & \rho I \end{bmatrix} \begin{pmatrix} \ddot{\eta} \\ \ddot{\phi} \end{pmatrix} - \frac{\partial}{\partial z} \begin{bmatrix} \kappa GA \frac{\partial}{\partial z} & -\kappa GA \\ \kappa GA & EI \frac{\partial}{\partial z} \kappa GA \end{bmatrix} \begin{pmatrix} \eta \\ \phi \end{pmatrix} = \begin{pmatrix} f(t) \\ m(t) \end{pmatrix} \delta(z-a)$$

where we interpret $[\eta(\cdot,t), \phi(\cdot,t)]^T$ as an element in H^2_B.

Bernoulli-Euler Model. Suppose that we consider the same situation with the additional Bernoulli-Euler assumptions [BK89]. These are

1. rotational inertia is negligible, $\rho I \to 0$,
2. shear deformation is negligible, $\eta_z - \phi \to 0$.

The deformed beam configuration is completely specified by $\eta(z,t)$. The geometric boundary conditions are

$$\mathcal{G}: \ \eta(0,1) = 0 \quad \text{and} \quad \frac{\partial \eta(0,1)}{\partial z} = 0.$$

Notice that the appropriate configuration space is $H^2_{\mathcal{G}}$. The simplified Lagrangian is

$$L = \int_0^\ell \left[\tfrac{1}{2} \rho A \left(\frac{\partial \eta}{\partial t} \right)^2 - \tfrac{1}{2} EI \left(\frac{\partial^2 \eta}{\partial z^2} \right)^2 \right] dz$$

and the virtual work expression also simplifies to

$$\begin{aligned} \delta W &= \int_0^\ell \left\{ f(t)\delta(z-a)\delta\eta + m(t)\delta(z-a)\delta\left(\frac{\partial \eta}{\partial z}\right) \right\} dz \\ &= \int_0^\ell \left\{ f(t)\delta(z-a) + m(t)\delta^{-1}(z-a) \right\} \delta\eta \, dz. \end{aligned} \tag{3.15}$$

The evolution equation is

$$\rho A \ddot{\eta} + \frac{\partial^2}{\partial z^2} \left[EI \frac{\partial^2 \eta}{\partial z^2} \right] = f(t)\delta(z-a) + m(t)\delta^{-1}(z-a),$$

which is to be interpreted on H^4_B with

$$\mathcal{N}: \ EI \frac{\partial^3 \eta(\ell,t)}{\partial z^3} = 0 \ \text{ and } \ EI \frac{\partial^2 \eta(\ell,t)}{\partial z^2} = 0.$$

3.2 Lagrange's Equations for Multibody Systems with Elastic Interactions

In addition to the kinetic energy, $T(q,\dot{q})$, we assume that a potential energy function $V(q)$ is also available. Then Lagrange's equations take the form

$$\begin{aligned} \frac{d}{dt}\frac{\partial T}{\partial \dot{\xi}} - \frac{\partial T}{\partial \xi} + \frac{\partial V}{\partial \xi} &= Q_\xi, \\ \frac{d}{dt}\frac{\partial T}{\partial \dot{R}} - \frac{\partial T}{\partial R} + \frac{\partial V}{\partial R} &= Q_R, \\ \frac{d}{dt}\frac{\delta T}{\delta \dot{u}} - \frac{\delta T}{\delta u} + \frac{\delta V}{\delta u} &= Q_u, \end{aligned} \tag{3.16}$$

where the generalized forces are defined in terms of the *virtual work expression*;

$$\delta W = Q_\xi^T d\xi + Q_R^T dR + Q_u^T \delta u. \tag{3.17}$$

Now, we define the *system angular momentum* with respect to the origin of the body frame

$$H = \int_S u \times [(\omega \times u + u_t) + L\dot{R}]dm = a + \int_S u \times L\dot{R}\, dm. \tag{3.18}$$

With some calculation[6] these equations reduce to

System Angular Momentum

$$\Gamma^T(\xi)[\dot{a} + \omega \times a] + \int_S u(z,t) \times L\ddot{R}\, dm = Q_\xi - \frac{\partial V}{\partial \xi}, \tag{3.19}$$

System Linear Momentum

$$\int_S [\frac{d}{dt} L^T(u_t + \omega \times u) + \ddot{R}]dm = Q_R - \frac{\partial V}{\partial R}, \tag{3.20}$$

$$u_{tt} + \omega \times (\omega \times u) + \dot{\omega} \times u + 2\omega \times u_t + L\ddot{R} = Q_u - \frac{\delta V}{\delta u}. \tag{3.21}$$

Equivalently we obtain

$$\Gamma^T(\xi)[I\dot{\omega} + \omega \times I\omega] + mc \times L\ddot{R} + \Gamma^T(\xi) D \int_S u \times [\omega \times u + u_t]dm + \int_S u \times L\ddot{R} dm = Q_\xi - \frac{\partial V}{\partial \xi} \tag{3.22}$$

$$m\ddot{R} + mL^T[\omega \times (\omega \times c) + \dot{\omega} \times c] + \int_S L^T[D^2 u + L\ddot{R}]dm = Q_R - \frac{\partial V}{\partial R} \tag{3.23}$$

$$D^2 u + L\ddot{R} = Q_u - \frac{\delta V}{\delta u} \tag{3.24}$$

where the operator D is defined by

$$D(\cdot) := \frac{d}{dt}(\cdot) + \omega \times (\cdot)$$

Note that, in applications, the integrals in (3.19)–(3.21) or (3.22)–(3.21) would not be evaluated directly. Instead, they are to be replaced by momentum expressions in terms of an appropriate choice of generalized coordinates.

[6] Appendix A contains some identities useful for these calculations.

3.3 Geometrically Consistent Reductions and Modeling of Flexible Structures

Recently attention has been drawn to gross qualitative properties of certain dynamic simulation models for multibody aerospace systems with structural flexure which have been obtained by "conventional methods". Such modeling methods, which often employ approximations involving linearization and truncation of position and velocity expressions referenced to body fixed frames, can lead to gross qualitative errors in predicted dynamic responses. Examples include inconsistent or incorrect predictions of dynamic stiffening or softening when the body frame is subject to arbitrary large motion in inertial space. In certain examples dynamic predictions suggest unstable responses inconsistent with physical experiments. Such errors in qualtitative behavior of models can be best understood by a careful analysis of the geometry of the deformations allowed under certain approximations [SVQ86, VQS87, SVQ88, Pos88]. Several computer codes for multibody modeling simulation of Control-Structure Interaction (CSI) effects such as DISCOS, TREETOPS, NBOD2, ALLFLEX, are widely available and used in the aerospace industry. The approximations used implicitly in these codes have been repeatedly called in to question by representatives of both industry and academia [KRB87, BD90].

In this section we briefly describe the geometry of large deformations from the viewpoint of continuum Lagrangian methods. We outline some methods of approximation and reduction of models which are "geometrically consistent". Two issues arise with respect to the geometry of large deformations. the first is the notion of strain and its definition in terms of local material deformations. The second arises when structures exhibit large, transverse global deformations but one chooses to make certain kinematic assumptions which restrain axial deformation.

3.3.1 Definition of Strain

Consider a continuous medium which undergoes a deformation. Let $X \in \Re^3$ denote the coordinates of a particle P lying on a curve C_0 in the undeformed state. Suppose the curve C_0 deforms to the curve C. After deformation the location of the particle P on C is denoted $x \in \Re^3$. If we consider the particles to be infinitesimal rathe than points, then the characteristic length of the curve C_0 (resp. C) is the arc length ds_0 (resp. ds). Similarly, the respective infinitesimal area and volume elements are proportional to ds^2 and ds^3. We may write

$$ds_0^2 = dX_1^2 + dX_2^2 + dX_3^2 \quad \text{and} \quad ds^2 = dx_1^2 + dx_2^2 + dx_3^2.$$

Taking the viewpoint of Lagranian mechanics [Sok56, Fre66] we identify the location of each point P relative to its nominal location in the undeformed state of the structure; i.e., the coordinates are functionally dependent; $x = x(X)$. Then the differential volume element can be given as,

$$ds^2 = \|\frac{\partial x}{\partial X} dX\|^2 = dX^t \left\{ \left[\frac{\partial x}{\partial X}\right]^t \left[\frac{\partial x}{\partial X}\right] \right\} dX. \tag{3.25}$$

We would like to express strain as a measure of deformation per unit area. We thus define strain in terms of the area deformation,

$$ds^2 - ds_0^2 := 2\, dX^t\, E\, dX.$$

where E is the *(Lagrangian) strain tensor*, which satisfies,

$$2E = \left[\frac{\partial x}{\partial X}\right]^t \left[\frac{\partial x}{\partial X}\right] - I_3. \tag{3.26}$$

It is convenient to express the strain in terms of the relative displacement by introducing $u(X)$ which satisfies the relation;

$$x(X) = u(X) + X,$$

so that

$$2E = \left[\frac{\partial u}{\partial X} + I_3\right]^t \left[\frac{\partial u}{\partial X} + I_3\right] - I_3. \tag{3.27}$$

From (3.27) we obtain the components of the strain tensor, ϵ_{ij} for $i, j, k = 1, 2, 3$ as,

$$\epsilon_{ii} = \frac{\partial u_i}{\partial X_i} + \tfrac{1}{2}\left\{[\frac{\partial u_i}{\partial X_i}]^2 + [\frac{\partial u_j}{\partial X_i}]^2 + [\frac{\partial u_k}{\partial X_i}]^2\right\}, \tag{3.28}$$

and for $i \neq j \neq k$,

$$2\epsilon_{ij} = \frac{\partial u_i}{\partial X_j} + \frac{\partial u_j}{\partial X_i} + \left\{\frac{\partial u_i}{\partial X_i}\frac{\partial u_i}{\partial X_j} + \frac{\partial u_j}{\partial X_i}\frac{\partial u_j}{\partial X_j} + \frac{\partial u_k}{\partial X_i}\frac{\partial u_k}{\partial X_j}\right\}. \tag{3.29}$$

When deformations are small—i.e., when $u(X)$ and its partial derivatives are negligible—the second order terms in the strain tensor can be neglected and we recover the infinitesimal strain definitions [Sok56, Fre66],

$$\epsilon_{ii} = \frac{\partial u_i}{\partial X_i}, \tag{3.30}$$

$$\epsilon_{ij} = \frac{\partial u_i}{\partial X_j} + \frac{\partial u_j}{\partial X_i}, \quad \text{for } i \neq j. \tag{3.31}$$

Remarks on Extension: Consider a line segment C_0 which lies in the X_1 axis. At any point P in C_0 an element length is $ds_0 = dX_1$. Thus, using the definition of strain we have,

$$ds^2 - ds_0^2 = 2dX^t\, E\, dX = 2\epsilon_{11} dX_1^2.$$

The extension of this element under deformation is given by,

$$E = (ds - ds_0)/ds_0 \;\Rightarrow\; ds = (1 + E)ds_0.$$

Then

$$ds^2 - ds_0^2 = [(1 + E)^2 - 1]dX_1^2 = 2\epsilon_{11} dX_1^2,$$

which implies that $E = \sqrt{1 + 2\epsilon_{11}} - 1$. For small strain we obtain the usual relation,

$$E = \epsilon_{11}.$$

3.3.2 Global Deformations and Elimination of Axial Dynamics

Consider a one dimensional structural appendage and for simplicity consider it to be modeled as a beam. Recall that each infinitesimal beam element is identified by its location (i.e., the z-coordinate) in the undeformed configuration. Thus, the element configuration variables $\eta(z,t)$ and $\xi(z,t)$ denote the spatial location and rotation at time t of the infinitesimal element located at coordinate z in the undeformed configuration. In many cases, the axial dynamics (i.e., the material motion along the beam centerline) evolves on a substantially shorter time scale than does the transverse or shear dynamics. When this is the case it is often desireable to reduce model complexity by eliminating the axial dynamics from the equations of motion.

One approach to effect this reduction is to enforce additional kinematic constraints on the configuration continuum. The approximation, $\eta_3 \equiv z$ (cf. Fig. 3.3) is a commonly employed approximation and valid for small global deformations. Two undesireable consequences have been observed as resulting from this approximation. The first consequence is the elimination of foreshortening effects in flexible links and has been observed to be of importance in precision robot placement control applications. The second consequence, which may be of significance in large angle attitude motions of flexible space structures, results from the elimination of certain inertial coupling effects. It is important to emphasize that with very large structures that small local deformations (i.e., strains) may result in significantly large global deformations (i.e., displacements).

A variety of alternative approximations can be developed which eliminate axial dynamics while retaining correct geometrical relationships during structural flexure. We explain one such approach by refering to Figure 3.3. The appendage centerline in the undeformed state is coincident with the z axis and has length L. The curve CL shown is the centerline of the deformed beam. Notice that the beam centerline at any time t is parametrically characterized by the map $CL : \Re \rightarrow \Re^3$ given by,

$$\eta_{CL} := \eta(z,t),$$

with $z \in [0, L]$ and t fixed. At any point z, the tangent vector to the curve is

$$v_z = \frac{\partial \eta}{\partial z}.$$

If we insist that the local deformations in the direction of v_z vanish along CL then we must have

$$ds^2 - ds_0^2 = 0 \tag{3.32}$$

which implies

$$\left[\frac{\partial \eta_1}{\partial z}\right]^2 + \left[\frac{\partial \eta_2}{\partial z}\right]^2 + \left[\frac{\partial \eta_3}{\partial z}\right]^2 - 1 = 0. \tag{3.33}$$

Equation (3.33) should be thought of as a partial differential equation in η_3 which is to be solved subject to $\frac{\partial \eta_1}{\partial z}$, $\frac{\partial \eta_2}{\partial z}$, given functions of z. Notice that (3.33) defines a unit sphere in

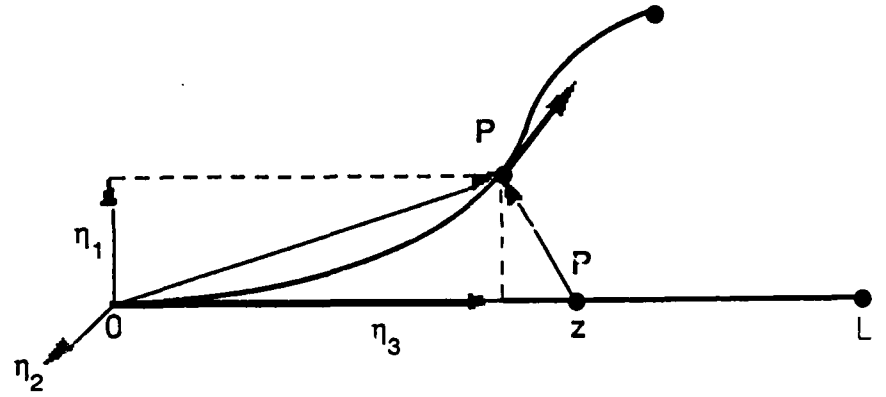

Figure 3.3: Illustrating the geometric considerations in deformation of centerlines of beams

the coordinates, $\frac{\partial \eta_1}{\partial z}$, $\frac{\partial \eta_2}{\partial z}$, and $\frac{\partial \eta_3}{\partial z}$. If $\frac{\partial \eta_3}{\partial z}$ is assumed to be positive, then we may take

$$\frac{\partial \eta_3}{\partial z} = \sqrt{1 - (\frac{\partial \eta_1}{\partial z})^2 - (\frac{\partial \eta_2}{\partial z})^2}, \tag{3.34}$$

and the solution can be obtained by quadrature.

3.4 Generic Models for Slewing and Pointing of Precision Optical Structures

In this section we develop several benchmark generic models for rapid slewing and precision pointing of flexible space structures which are motivated by problems relating to control of precision optical structures subject to elastic interactions. Such problems arise in requirements for rapid retargeting coupled with precision pointing for space-based laser (SBL) systems. The models reflect generic qualitative dynamical properties of such systems. In a subsequent section we develop a simulation model with physical parameters obtained from the benchmark SBL structural model developed in [Le87].

The models developed in this section focus on primary sources of structural interaction with principal body slewing maneuvers affecting system LOS pointing. Modeling assumptions used to characterize generic responses are based on the initial system level tradeoffs described in the R & D Associates report [Le87]. This study indicates that the principal source of structural flexure affecting laser LOS is within the beam expanded optical train—the principal structural component being the metering truss supporting the relative position and orientation of the primary and secondary mirrors. Our initial or first-level model assumes the beam expander primary mirror and support is rigidly attached to the spacecraft body and only the metering truss is subject to flexure. In the second model we include provisions for articulation of the SBL beam expander with respect to the SBL system spacecraft body using a gimbaled joint.

3.4.1 Example: Rigid Body With 1-Dimensional Appendage

We consider a single rigid body attached to a flexible appendage as illustrated in Figure 3.4. The system kinetic energy can be expressed as

$$\begin{aligned} T &= \tfrac{1}{2}\int_{rb} \|\Omega u\|^2 + 2\langle \Omega u, L\dot{R}\rangle + \|R\|^2 dm \\ &\quad + \tfrac{1}{2}\int_{fb} \|\Omega u + u_t\|^2 + 2\langle \Omega u + u_t, L\dot{R}\rangle + \|\dot{R}\|^2 dm \\ &= \tfrac{1}{2}\omega_b^T I_b \omega_b - m_b c^T \Omega_b L\dot{R} + \tfrac{1}{2} m_b \|\dot{R}\|^2 \\ &\quad + \tfrac{1}{2}\int_0^\ell \{\|\Omega_b \eta + \eta_t\|^2 + 2\langle \Omega_b \eta + \eta_t, L\dot{R}\rangle + \|\dot{R}\|^2\}\rho A\, dz \\ &\quad + \tfrac{1}{2}\int_0^\ell \{[\omega_b + \xi_t]^T I[\omega_b + \xi_t]\}\rho\, dz \end{aligned} \tag{3.35}$$

where $c \in \Re^3$ is the location of the rigid body center of mass in the body frame, m_b is the mass of the rigid body, I_b is the inertia tensor of the rigid body in the body frame, and ρ is the mass density of the beam, $\eta(z,t)$ is the position vector of points on the deformed centerline of the beam in the primary body coordinate frame and $\xi(z,t) = [\psi, \theta, \phi]^T(z,t)$ is the beam angular deformation. We have assumed small deformation of the beam so that the angular velocity of the beam section at z is

$$\omega(z,t) = \omega_b + \xi_t(z,t)$$

up to first order in the angular deformation.

The potential energy of the system consists only of the potential energy associated with deformation of the beam. Under Timoshenko beam assumptions [CKEFKPB68] the potential energy function is

$$\begin{aligned} V(\xi,\eta) &= \tfrac{1}{2}\int_0^\ell \Big\{GJ(\psi_z)^2 + EI_2(\theta_z)^2 + EI_3(\phi_z)^2 \\ &\quad + \kappa_1 GA(\eta_{1,z} - \theta)^2 + \kappa_2 GA(\eta_{2,z} + \phi)^2 + \mu EA(\eta_{3,z} - 1)^2\Big\}\, dz \\ &= \tfrac{1}{2}\int_0^\ell \Big\{(\xi_z^T K \xi_z) + (\eta_z - P\xi)^T S(\eta_z - P\xi)\Big\}\, dz \end{aligned} \tag{3.36}$$

where the stiffness matrices are defined as

$$K = \mathrm{diag}(GJ, EI_2, EI_3), \quad S = \mathrm{diag}(\kappa_1 GA, \kappa_2 GA, \mu EA),$$

and

$$P = \begin{bmatrix} 0 & 1 & 0 \\ 0 & 0 & -1 \\ 0 & 0 & 0 \end{bmatrix}.$$

The system angular momentum vector is

$$a = I_b\omega + \int_0^\ell [A\eta \times (\omega_b \times \eta + \dot{\eta}) + I\omega]\rho\, dz$$

so that equations (3.19)–(3.21) reduce to

$$\Gamma^T(\xi)(I_b\dot{\omega}_b + \omega_b \times I_b\omega_b)$$
$$+ \int_0^\ell [\Gamma^T(\xi)A\eta \times (\eta_{tt} + \omega_b \times (\omega_b \times \eta) + \dot{\omega}_b \times \eta + 2\omega_b \times \dot{\eta})$$
$$+ A\eta \times L\ddot{R} + I(\dot{\omega} + \omega_b \times \omega)]\rho\, dz + mc \times L\ddot{R} = Q_{\xi_b}, \tag{3.37}$$
$$m\ddot{R} + mL^T(\omega \times (\omega \times c) + \dot{\omega} \times c) + \int_0^\ell \rho A(L^T D^2\eta + \ddot{R})dz = Q_R, \tag{3.38}$$
$$\rho A(\eta_{tt} + \omega_b \times (\omega_b \times \eta) + \dot{\omega}_b \times \eta + 2\omega_b \times \dot{\eta} + L\ddot{R}) = Q_\eta - S(\eta_{zz} - P\xi_z), \tag{3.39}$$
$$\rho I[\xi_{tt} + \dot{\omega}_b + \omega_b \times (\omega_b + \xi_t)] = Q_\xi - K\xi_{zz} + P^T S(\eta_z - P\xi). \tag{3.40}$$

System Dissipation A simple model of generalized dissipation in the appendage can be obtained by introducing a Rayleigh dissipation function. We formulate such a function based on the assumption that dissipation forces are proportional to beam deformation rates, i.e. generalized coordinate velocities (η_t and ξ_t) and strain rates $((\eta_1)_{tz} - \theta_t, (\eta_2)_{tz} - \phi_t, \xi_{tz})$.

$$R(\eta_t, \xi_t) = \tfrac{1}{2}\int_0^\ell \{\eta_t^T\Xi_1\eta_t + \xi_t^T\Xi_2\xi_t + (\eta_{tz})^T\Xi_3\eta_{tz} + (\xi_{tz})^T\Xi_4(\xi_{tz})\}dz \tag{3.41}$$

where $\Xi_i = \mathrm{diag}(\zeta_{i1}, \zeta_{i2}, \zeta_{i3})$. From $R(\eta_t, \xi_t)$ we obtain the generalized dissipative forces

$$\frac{\delta R}{\delta \eta_t} = \Xi_1\eta_t + \Xi_3(\eta_{tzz} - P\xi_{tz}), \tag{3.42}$$
$$\frac{\delta R}{\delta \xi_t} = \Xi_2\xi_t + \Xi_3(\eta_{tz} - P\xi_t) + \Xi_4\xi_{tzz}. \tag{3.43}$$

3.4.2 Example: Articulated Bodies With Flexible Appendage

We now consider a modification of the previous Example which includes a second body attached to the primary body with a three axis gimbal as illustrated in Figure 2. In addition, the second body carries with it a reaction wheel package. The kinetic energy function is

$$T = \underbrace{\tfrac{1}{2}\omega_p^T I_p\omega_p - m_p c_p^T\Omega_p L\dot{R} + \tfrac{1}{2}m_p\|\dot{R}\|^2}_{\text{primary body}}$$
$$\underbrace{+ \tfrac{1}{2}\omega_s^T I_s\omega_s - m_s c_s^T\Omega_s L_s\{L\dot{R} + \Omega_p c_{gm}\} + \tfrac{1}{2}m_s\|L\dot{R} + \Omega_p c_{gm}\|^2}_{\text{second body (wheels locked)}}$$
$$\underbrace{+ \tfrac{1}{2}\omega_3^T I_3\omega_3 + \omega_s^T I_3\omega_3}_{\text{reaction wheels}}$$
$$+ \tfrac{1}{2}\int_0^\ell \{\|\Omega_p\eta + \eta_t\|^2 + 2\langle\Omega_p\eta + \eta_t, L\dot{R}\rangle + \|\dot{R}\|^2\}\rho A\, dz$$
$$+ \tfrac{1}{2}\int_0^\ell \{(\omega_p + \xi_t)^T I(\omega_p + \xi_t)\}\, \rho dz \tag{3.44}$$

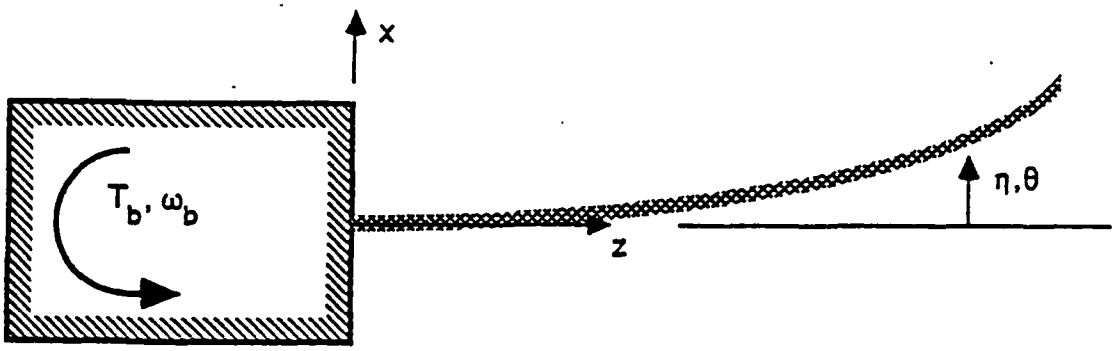

Figure 3.4: Rigid Body with Flexible Appendage

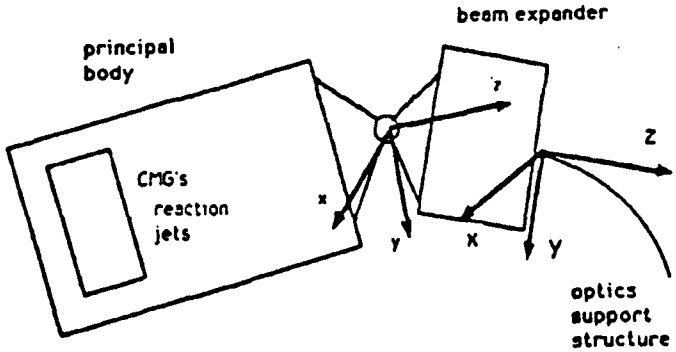

Figure 3.5: Hinged Bodies with Flexible Appendage

Note that c_p and c_s are the locations of the center of gravity of the primary body and second body (including wheels) in their respective body coordinate frames. The vector c_{gm} denotes the location of the three axis gimbal in the primary body frame. The matrix I_1 is the primary body inertia tensor in the primary body frame, I_2 denotes the second body inertia tensor with reaction wheels, and I_3 is the diagonal matrix of wheel inertias.

4 Feedback Linearization of Lagrangian Systems

4.1 Output normal form equations for Lagrangian Systems

Consider the case of a finite dimensional Lagrangian system with Lagrangian,

$$L(q,\dot{q}) : \mathcal{M} \times T_q\mathcal{M} \rightarrow \Re \tag{4.1}$$

and assume that the configuration manifold, $\mathcal{M}$ is locally diffeomorphic to $\Re^n$. Thus the n-vector q has elements which are the generalized coordinates.

For control design we assume there are a finite number of external generalized forces which can be exerted on the system which we collect in the m-vector $f \in \Re^m$. The external forces are introduced by the definition of a differential virtual work expression in terms of the generalized coordinates; $\delta W = \sum_i Q_i^T dq_i$. We assume that the external forces in physical coordinates are such that $m < n$ and for each coordinate, $Q_i = \frac{\partial\, \delta W}{\partial\, dq_i} = G_i f$ and the virtual work takes the form,

$$\delta W = \sum_{i=1}^{n} f^T G_i^T dq_i = f^T G^T dq, \tag{4.2}$$

where $G^T = [G_1^T, \ldots, G_m^T]$.

Assumption 1: The Lagrangian system is regular with respect to external generalized forces; i.e., the operator G is rank m in a neighborhood of every configuration $q \in \mathcal{M}$.

Next we identify a set of system primary outputs, $y \in \Re^n$, given by,

$$y = h(q), \tag{4.3}$$

where $h : \mathcal{M} \rightarrow \Re^m$ is a C^∞ function. We also assume that there exists a C^∞ function, $t(q) \mapsto u$, such that $U(q) = h(q) \oplus t(q)$ is a local diffeomorphism; i.e., there exists an inverse map;

$$q = g(y,u) \tag{4.4}$$

$g : \Re^m \times \mathcal{M}_u \rightarrow \mathcal{M}$.

Proposition 1: Under the above assumptions the Lagrangian system can be decomposed and written in *explicit output coordinates form*[7];

$$\frac{d}{dt}\frac{\partial \hat{L}}{\partial \dot{y}} - \frac{\partial \hat{L}}{\partial y} = D_y(g)^T G f \tag{4.5}$$

$$\frac{d}{dt}\frac{\partial \hat{L}}{\partial \dot{u}} - \frac{\partial \hat{L}}{\partial u} = D_u(g)^T G f \tag{4.6}$$

[7] We use the notation, $D_x(f) := \left[\frac{\partial f}{\partial x}\right]$

where

$$\hat{L}(y,\dot{y},u,\dot{u}) := L(q,\dot{q})|_{q=g(u,y),\dot{q}=\dot{g}(u,y)}, \quad (4.7)$$

$$\dot{g}(u,y) := D_y(g)\dot{y} + D_u(g)\dot{u}. \quad (4.8)$$

Proof of Prop 1: To see this note that (4.8) follows from,

$$\dot{q} = \frac{d}{dt}g(y,u) = \left[\frac{\partial g}{\partial y}\right]\dot{y} + \left[\frac{\partial g}{\partial u}\right]\dot{u}.$$

Also, the virtual work expression is rewritten in the new coordinates as,

$$\delta\hat{W} = f^T G^T \left[\frac{\partial g}{\partial y}\right] dy + f^T G^T \left[\frac{\partial g}{\partial u}\right] du.$$

Then direct application of Lagrange's equations in the (y,u) coordinates gives the desired result.

□

4.2 Structural Assumptions on Lagrangian Systems and PLF Compensation

From the above section we see that under fairly general assumptions a Lagrangian system with n degrees of freedom, m external forces and m outputs defined as in (4.3), that the resulting equations of motion can be obtained by application of Lagrange's equations in the explicit output form (4.5)–(4.6) which we write as,

$$J_y(y,u)\ddot{y} + N(y,u)\ddot{u} + \phi_y(y,\dot{y},u,\dot{u}) = G_y f \quad (4.9)$$

$$J_u(y,u)\ddot{u} + N^T(y,u)\ddot{y} + \phi_u(y,\dot{y},u,\dot{u}) = G_u f. \quad (4.10)$$

Assumption 2: The system inertias; i.e, $J_u, J_y, \begin{bmatrix} J_y & N \\ N^T & J_u \end{bmatrix}$ are symmetric, positive definite operators for $q \in \mathcal{M}$.

Then we have $J_y - NJ_u^{-1}N^T$ is also positive definite on $\mathcal{M}$.

Definition 1: We say that the above m-input by m-output system has *local relative degree 2* for the configuration (y_0,u_0) if and only if the $m \times m$ matrix, $[G_y - NJ_u^{-1}G_u](y,u)$ is invertible everywhere in a neighborhood of (y_0,u_0).

A *Partial Linearizing Feedback (PLF) Compensation* is a nonlinear feedback transformation of the form,

$$f = \mathcal{K}_y(y,\dot{y},u,\dot{u}) + \mathcal{K}_\alpha(y,\dot{y},u,\dot{u})\alpha$$

with $\mathcal{K}_y, \mathcal{K}_\alpha : \mathcal{M} \times T_q\mathcal{M} \to \Re^m$, which renders the compensated response in y linear and time invariant in α, and decouples the remaining (zero) dynamics $(u,\dot{u})$.

Proposition 2: Assume the Lagrangian system has local relative degree 2 for every configuration $q \in \mathcal{A} \subset M$ where $\mathcal{A}$ is an open dense subset of $\mathcal{M}$. Then a *Partial Linearizing Feedback (PLF)* compensation is a feedback of the form,

$$f = -[G_y - NJ_u^{-1}G_u]^{-1}\left\{\phi_y - NJ_u^{-1}\phi_u + [J_y - NJ_u^{-1}N^T]\alpha\right\} \tag{4.11}$$

transforms the closed loop system to input/output linearized and decoupled form;

$$\ddot{y} = \alpha, \tag{4.12}$$

$$J_u(y,u)\ddot{u} + N(y,u)^T\ddot{u} + \phi_u^y(y,\dot{y},u,\dot{u}) = G_u^y\alpha \tag{4.13}$$

where

$$\phi_u^y := \phi_u + G_u[G_y - NJ_u^{-1}G_u]^{-1}(\phi_y - NJ_u^{-1}\phi_u), \tag{4.14}$$

$$G_u^y := G_u[G_y - NJ_u^{-1}G_u]^{-1}[NJ_u^{-1}N^T - J_y], \tag{4.15}$$

where $\alpha \in \Re^m$ represents the control inputs in "acceleration coordinates".

The system primary outputs y given by (4.3) induce a decomposition of the system configuration space as $\mathcal{M} = \mathcal{M}_y \times \mathcal{M}_u$ where $\dim \mathcal{M}_y = m$ and $\mathcal{M}_u = \{q \in \mathcal{M} : h(q) = 0\}$. The PLF compensation (4.11) decomposes the trajectories of (4.9)–(4.10) into controlled responses on $\mathcal{M}_y \times T_y\mathcal{M}_y$ and output constrained or *zero dynamics* on $\mathcal{M}_u \times T_u\mathcal{M}_u$. Then following Byrnes and Isidori [BI85] we say that the system (4.9)–(4.10) is *locally minimum phase* if the output constrained dynamics are asymptotically stable to the origin $(u,\dot{u}) = (0,0)$.

Proposition 3: The system (4.9)–(4.10) is locally minimum phase if and only if the system,

$$J_u^0(u)\ddot{u} + \phi_u^0(u,\dot{u}) = 0 \tag{4.16}$$

is asymptotically stable to the origin, $(u,\dot{u}) = (0,0)$, where

$$\phi_u^0 := \phi_u(y,\dot{y},u,\dot{u})|_{y=0,\dot{y}=0} - \left[G_u[G_y - NJ_u^{-1}G_u]^{-1}(\phi_y - NJ_u^{-1}\phi_u)\right]\Big|_{y=0,\dot{y}=0}, \tag{4.17}$$

$$J_u^0(u) := J_u(y,u)|_{y=0,\dot{y}=0}. \tag{4.18}$$

Proof of Prop's 2 & 3: To see this result we first solve for the accelerations in the pair of equations (4.9)–(4.10) to obtain,

$$\begin{pmatrix}\ddot{y}\\ \ddot{u}\end{pmatrix} = \begin{bmatrix} J_y & N \\ N^T & J_u \end{bmatrix}^{-1}\left\{\begin{pmatrix}\phi_y\\ \phi_u\end{pmatrix} + \begin{pmatrix}G_y\\ G_u\end{pmatrix} f\right\}$$

$$= \begin{pmatrix}\Sigma_y\\ \Sigma_u\end{pmatrix} + \begin{pmatrix}\Gamma_y\\ \Gamma_u\end{pmatrix} f \tag{4.19}$$

where we have assumed that the system inertia is symmetric, positive definite everywhere in $(y,u) \in \mathcal{M}_y \times \mathcal{M}_u$. The desired decoupling and linearizing control is then given as,

$$f = \Gamma_y^{-1}(-\Sigma_y + \alpha) \tag{4.20}$$

Now recall that under the assumption on the system inertias we have,

$$\begin{bmatrix} J_y & N \\ N^T & J_u \end{bmatrix}^{-1} = \begin{bmatrix} \Delta^{-1} & -\Delta^{-1}NJ_u^{-1} \\ -J_u^{-1}N^T\Delta^{-1} & J_u^{-1} + J_u^{-1}N^T\Delta^{-1}NJ_u^{-1} \end{bmatrix}, \tag{4.21}$$

where $\Delta = J_y - NJ_u^{-1}N^T$. Thus we find

$$\Sigma_y = \Delta^{-1}\phi_y - \Delta^{-1}NJ_u^{-1}\phi_u, \tag{4.22}$$

$$\Gamma_y = \Delta^{-1}G_y - \Delta^{-1}NJ_u^{-1}G_u. \tag{4.23}$$

Furthermore, since we have

$$\begin{aligned} \Gamma_y^{-1}\Sigma_y &= [\Delta^{-1}G_y - \Delta^{-1}NJ_u^{-1}G_u]^{-1}[\Delta^{-1}\phi_y - \Delta^{-1}NJ_u^{-1}\phi_u] \\ &= [G_y - NJ_u^{-1}G_u]^{-1}(\phi_y - NJ_u^{-1}\phi_u), \end{aligned} \tag{4.24}$$

then (4.11) follows from (4.20).

To show (4.12)–(4.15) substitute (4.11) into (4.10). Likewise, (4.16)–(4.18) follow from (4.12)–(4.15) by setting $\alpha = 0$ which from (4.12) implies that $y = \dot{y} = 0$.

□

Remarks: The objective of PLF compensation (4.11) is to obtain input/output linearization of $\alpha \mapsto y$ by decoupling of the u dynamics from the outputs, y. We assert that for the Lagrangian systems considered, under the assumptions 1 and 2, and assuming that for the given f and y variables that the system is locally minimum phase, then the response of the PLF compensated system consists of α–controlled motions on $\mathcal{M}_y$ and stable transient motion converging asymptotically to the origin on $\mathcal{M}_u$. For regulation of the primary outputs to zero the dynamic response is decomposed to asymptotic motions toward the manifold $\mathcal{M}_y$ described by (4.12) and motions on $\mathcal{M}_y$ given by (4.16).

Design of the α control is of course simplified by the linear dynamics given by (4.12). As most flexible structure systems are Lagrangian systems with local relative degree two, the design in *acceleration coordinates* is particularly attractive feature of the method. The PLF compensation (4.11) implements an online *Inverse Force Model* (IFM) which effects the transformation to acceleration coordinates. In the sequel we show that the stable implementation of the IFM may be sensitive to parasitics in the decoupled dynamics (4.13).

5 Reduced Order Models and PFL Control of Flexible Structures

Models obtained by finite dimensional approximation of the Euler-Lagrange equations or of the system Hamiltonian as outlined above will typically obtain a large order finite element model in the form,

$$M(q)\ddot{q} + B(q,\dot{q})\dot{q} + K(q,\dot{q})q = Gf, \tag{5.1}$$

where we assume the system inertia, $M(q) : \mathcal{M} \to \Re^{n\times n}$ is symmetric, positive definite on $\mathcal{M}$, reduced configuration space with dimension n and stiffness $K(q,\dot{q}) : \mathcal{M} \times T_q\mathcal{M} \to \Re^{n\times n}$ is symmetric, positive semidefinite stiffness, and $B(q,\dot{q}) : \mathcal{M} \times T_q\mathcal{M} \to \Re^{n\times n}$ models system dissipation on $\mathcal{M} \times T_q\mathcal{M}$.

Our interest in model order reduction arises from consideration for robust implementation of PLF compensation for flexible structures. In general, the dynamics are nonlinear and we base reduction on time scale decomposition with respect to a minimum energy state of the mechanical structure model. For space structure applications there are typically cyclic coordinates involving attitude rotations which do not appear explicitly in the system Lagrangian [Gol82]. These coordinates can be translated to the origin. Thus we focus attention on the linear perturbation model about the origin in $\mathcal{M} \times T_q\mathcal{M}$ to obtain time scale decomposition.

Fact: Under the above assumptions there exists a nonsingular $n \times n$ matrix, P, such that

$$P^T M_0 P = I_n, \quad P^T K_0 P = K_d = \mathrm{diag}\{\omega_1^2, \ldots, \omega_n^2\}$$

with $\omega_1 \leq \cdots \leq \omega_n$, where $M_0 = M(0)$, $K_0 = K(0,0)$.

Assumption 3: Given P as above, let $B_0 = B(0,0)$ and assume that[8]

$$P^T B_0 P = B_d = \mathrm{diag}\{2\zeta_1\omega_1, \ldots, 2\zeta_n\omega_n\}.$$

The transformation $q = Px$ obtains the linear perturbation model in *decoupled* "modal" coordinates [Bal78],

$$\ddot{x} + B_d\dot{x} + K_d x = \bar{G}f, \tag{5.2}$$

where $\bar{G} = P^T G$, whereas, the original nonlinear equations (5.1), written in modal coordinates:

$$\bar{M}(x)\ddot{x} + \bar{B}(x,\dot{x})\dot{x} + \bar{K}(x,\dot{x})x = \bar{G}f, \tag{5.3}$$

[8]The assumption of "modal damping" is—although typical in modeling flexible space structure dynamics—an assertion which may require careful validation in practice. Among other limitations this assumption implies that gyroscopic effects are negligible.

where

$$\bar{M}(x) = P^T \left[M(q)|_{q=Px} \right] P, \tag{5.4}$$

$$\bar{K}(x,\dot{x}) = P^T \left[K(q,\dot{q})|_{q=Px,\dot{q}=P\dot{x}} \right] P, \tag{5.5}$$

$$\bar{B}(x,\dot{x}) = P^T \left[B(q,\dot{q})|_{q=Px,\dot{q}=P\dot{x}} \right] P, \tag{5.6}$$

may be highly coupled in a neighborhood of the origin.

The standard approach to model order reduction for linear models of flexible structures is to retain the first p modes and neglect the $n-p$ residual states. Such an approximation assumes that the system modal coordinates are decomposed as $x = [(x^0)^T, (x^1)^T]^T$ where x^1 is a fast transient (or parasitic) in the time scale of x^0. Thus we seek to approximate the system potential energy by the decomposition of the stiffness in (local) modal coordinates model (5.2);

$$K_d = \begin{bmatrix} K_d^0 & 0 \\ 0 & K_d^1 \end{bmatrix}.$$

To transform the model (5.2) into the standard form for singular perturbation analysis we must identify an appropriate scaling of the stiffness. One natural choice of scaling is to let, $K_d^1 = \frac{1}{\epsilon^2} K_d^{10}$, and the residual coordinates, $x^1 = \epsilon^2 z$, such that $z \sim O(1)$ in ϵ^2. For example, we may take,

$$\epsilon(p) = \frac{1}{\omega_{p+1}} \tag{5.7}$$

for which we see that $\epsilon \to 0$ as p is increased. Then by assumption 3 we have, $B_d^1 = \frac{1}{\epsilon} B_d^{10}$, where $B_d = \begin{bmatrix} B_d^0 & 0 \\ 0 & B_d^1 \end{bmatrix}$; a fact which will become useful in the sequel.

Then (5.2) is decomposed into p-dimensional retained coordinates, x^0 and $(n-p)$-dimensional residual coordinates, x^1,

$$q = [P_0, P_1] \begin{pmatrix} x^0 \\ x^1 \end{pmatrix}, \tag{5.8}$$

where $P_0 : \Re^p \to \Re^n$, $P_1 : \Re^{n-p} \to \Re^n$, such that

$$\ddot{x}^0 + B_d^0 \dot{x}^0 + K_d^0 x^0 = \bar{G}_0 f, \tag{5.9}$$

$$\ddot{x}^1 + B_d^1 \dot{x}^1 + K_d^1 x^1 = \bar{G}_1 f, \tag{5.10}$$

which after scaling becomes singularly perturbed [ABB89] as,

$$\ddot{x}^0 + B_d^0 \dot{x}^0 + K_d^0 x^0 = \bar{G}_0 f, \tag{5.11}$$

$$\epsilon^2 [\ddot{z} + B_d^1 \dot{z}] + K_d^{10} z = \bar{G}_1 f. \tag{5.12}$$

After decomposition and scaling the FEM model (5.3) is also singularly perturbed,

$$\bar{M}_{00}\ddot{x}^0 + \epsilon^2 \bar{M}_{01}\ddot{z} + \bar{B}_{00}\dot{x}^0 + \epsilon^2 \bar{B}_{01}\dot{z} + \bar{K}_{00}x^0 + \epsilon^2 \bar{K}_{01} z = \bar{G}_0 f \tag{5.13}$$

$$\bar{M}_{01}^T \ddot{x}^0 + \epsilon^2 \bar{M}_{11}\ddot{z} + \bar{B}_{10}\dot{x}^0 + \epsilon \bar{B}_{11}^{10}\dot{z} + \bar{K}_{01}^T x^0 + \bar{K}_{11}^{10} z = \bar{G}_1 f. \tag{5.14}$$

The reduced order model is obtained as the quasi-steady state or slow time system by letting $\epsilon = 0$;

$$\bar{M}^0_{00}\ddot{x}^0 + \bar{B}^0_{00}\dot{x}^0 + \bar{K}^0_{00}x^0 = \bar{G}_0 f, \tag{5.15}$$

$$[\bar{M}^0_{01}]^T\ddot{x}^0 + \bar{B}^0_{10}\dot{x}^0 + [\bar{K}^0_{01}]^T x^0 + \bar{K}^{10}_{11}\bar{z} = \bar{G}_1 f, \tag{5.16}$$

where

$$\bar{M}^0_{00}(x^0) = P_0^T M(q)P_0\Big|_{q=P_0x^0}, \tag{5.17}$$

$$\bar{B}^0_{00}(x^0,\dot{x}^0) = P_0^T B(q,\dot{q})P_0,\Big|_{q=P_0x^0,\dot{q}=P_0\dot{x}^0}, \tag{5.18}$$

$$\bar{K}^0_{00}(x^0,\dot{x}^0) = P_0^T K(q,\dot{q})P_0\Big|_{q=P_0x^0,\dot{q}=P_0\dot{x}^0}, \tag{5.19}$$

$$\bar{G}_0 = P_0^T G, \tag{5.20}$$

where (5.15) is the *reduced model* [Kok87]. By assumption, K^{10}_{11} is invertible and we can solve explicitly for the slow time, or quasi-steady state component of z;

$$\bar{z} = [\bar{K}^{10}_{11}]^{-1}\{\tilde{G}f - \tilde{B}\dot{x}^0 - \tilde{K}x^0\}, \tag{5.21}$$

where

$$\tilde{B} = \bar{B}_{10} - \bar{M}^T_{01}\bar{M}^{-1}_{00}\bar{B}_{00}, \tag{5.22}$$

$$\tilde{K} = \bar{K}^T_{01} - \bar{M}^T_{01}\bar{M}^{-1}_{00}\bar{K}_{00}, \tag{5.23}$$

$$\tilde{G} = \bar{G}_1 - \bar{M}^T_{01}\bar{M}^{-1}_{00}\bar{G}_0. \tag{5.24}$$

The boundary layer correction; $z = \bar{z} + \eta$ is obtained in the fast (stretched) time scale, $\tau = t/\epsilon$ where, $\frac{dx}{dt} = \frac{1}{\epsilon}\frac{dx}{d\tau}$ and letting $\epsilon = 0$ after substitution in (5.13)–(5.14). Introducing the notation, $x' := \frac{dx}{d\tau}$ we can write the fast time scale system as,

$$\bar{M}_{11}\eta'' + \bar{B}^{10}_{11}\eta' + \bar{K}^{10}_{11}\eta = \bar{G}_1 f. \tag{5.25}$$

A standard result in singular perturbation theory is that the reduced model (5.15) is $O(1)$ approximation for $\epsilon \ll 1$ if the fast time scale system (5.25) is asymptotically stable [KKO86]. Then the time scale decomposition suggests that trajectories of (5.1) consist of fast transients of (5.25) which converge to the manifold $\mathcal{E}_0 = \{(x,\dot{x}) \in \mathcal{M}^p_0 \times T_x\mathcal{M}^p_0 : z = \bar{z}, \dot{z} = 0\}$, where $\dim \mathcal{M}^p_0 = p$ and trajectories of (5.15) on $\mathcal{E}_0$.

Remarks: For flexible space structures we typically assume that the stability of the fast time scale model is due to inherent damping of the structure rather than the introduction of rapid control. One issue of practical concern is the controllability of (5.25), which for the case of flexible structures depends on the choice of p and slowly maturing technology for wide band vibration control. When the fast time scale system is only *weakly controllable* (i.e.,

controllable only through the slow time system) the contribution of these modes is clearly "parasitic" and neglecting these dynamics will contribute to the robustness of the control design [Kok87]. Model order reduction in flexible space structure control design is typically a multistep process. We recommend that weak controllability issues related to actuation technology be considered as part of any initial reductions. Model order reduction for control design for flexible structures is thus effected by the technology available for actuation and sensing. Structural input/output properties which also effect choice of model order reduction methods include weak vs. strong controllability and/or observability of the reduced models. These and many other issues can effect the choice of time scaling and model reduction.

5.1 PLF Compensation for Reduced Models

Reduced order models of varying dimension can be obtained by the time scale analysis of the previous section where the approximate system dynamics evolve on the reduced manifold $\mathcal{E}_0 \subset \mathcal{M}_0 \times T_q\mathcal{M}_0$. In the next few paragraphs we summarize the transformation of the reduced model to output normal form and the construction of PLF compensation based on the reduced model. Our objective is to demonstrate how considerations for robust implementation of PLF compensation for flexible structures will drive the choice of model reduction.

We focus attention on an m-vector of system outputs (4.3) for the Lagrangian system to the form (4.5)–(4.6). The output map is given in reduced model coordinates by[9],

$$y = h^0(x) := h(q)|_{q=P_0 x}.$$

Then the inverse map for the reduced order model is from (4.4),

$$x = [P_0^T P_0]^{-1} P_0^T g(y,u) =: g^0(y,u).$$

Under smoothness assumptions, we can write,

$$g^0(y,u) = g_y^0(y,u)y + g_u^0(y,u)u, \tag{5.26}$$

and following the procedure of § 5 we identify the reduced model (5.15) in the form (4.9)–(4.10) where,

$$J_y = [g_y^0]^T \bar{M} g_y^0, \quad J_u = [g_u^0]^T \bar{M} g_u^0, \quad N = [g_y^0]^T \bar{M} g_u^0, \tag{5.27}$$

$$G_y = [g_y^0]^T \bar{G}, \quad G_u = [g_u^0]^T \bar{G}, \tag{5.28}$$

$$\begin{pmatrix} \phi_y \\ \phi_u \end{pmatrix} = \begin{bmatrix} \tilde{B}_{yy} & \tilde{B}_{yu} \\ \tilde{B}_{uy} & \tilde{B}_{uu} \end{bmatrix} \begin{pmatrix} \dot{y} \\ \dot{u} \end{pmatrix} + \begin{bmatrix} \tilde{K}_{yy} & \tilde{K}_{yu} \\ \tilde{K}_{uy} & \tilde{K}_{uu} \end{bmatrix} \begin{pmatrix} y \\ u \end{pmatrix} \tag{5.29}$$

[9] In this section we replace the slow time state $x^0 \in \Re^p$ with x for notational convenience.

and

$$\begin{bmatrix} \tilde{B}_{yy} & \tilde{B}_{yu} \\ \tilde{B}_{uy} & \tilde{B}_{uu} \end{bmatrix}(y,\dot{y},u,\dot{u}) = \begin{bmatrix} [g_y^0]^T \\ [g_u^0]^T \end{bmatrix} \bar{B}[g_y^0, g_u^0], \tag{5.30}$$

$$\begin{bmatrix} \tilde{K}_{yy} & \tilde{K}_{yu} \\ \tilde{K}_{uy} & \tilde{K}_{uu} \end{bmatrix}(y,\dot{y},u,\dot{u}) = \begin{bmatrix} [g_y^0]^T \\ [g_u^0]^T \end{bmatrix} \bar{K}[g_y^0, g_u^0]. \tag{5.31}$$

The PLF control on $\mathcal{M}_0 \times T_x\mathcal{M}_0$ is given by (4.11) with (5.29). The analysis of section 2.2 carries over directly to the decomposition of the reduced manifold, $\mathcal{E}_0$.

Let $\mathcal{M}_0^p \subseteq \mathcal{M}$ be the p-dimensional reduced configuration space obtained by retaining the p-dimensional slow time modes according to the scaling $\epsilon(p)$ as in (5.7). Then given a sequence of integers, p_k, such that, $n \geq p_1 > \cdots > p_k \geq m$ the reduced system manifold satisfy, $\mathcal{M} \subset \mathcal{M}_0^{p_k} \subseteq \mathcal{M}_0^m$ and $\mathcal{M}_0^{p_k} = \mathcal{M}_y^{p_k} \oplus \mathcal{M}_u^{p_k}$ where $\dim \mathcal{M}_y^{p_k} = m$ and $\dim \mathcal{M}_u^{p_k} = p_k - m$. In this sense we understand that when $p = m$ we have the case usually considered in robotics [SV87] where the nominal (reduced) model is exactly feedback linearizable by nonlinear transformation of the system state together with feedback. For these cases a variety of control design techniques have been devised to assure robust stabilization subject to bounded model uncertainty of the nominal plant model described by a regular perturbation [Spo87]. Unlike the robotic problems, flexible structure control problems are characterized by high dimensional reduced order models where $m < n$ typically. The IFM implemented by PLF compensation obtains linearization through transformation of the design model to acceleration coordinates. A critical feature for practical implementation of PLF control for flexible structures is the tradeoff between the fidelity of the online IFM vs. the model sensitivity. We will highlight these issues by reference to the case when the zero dynamics of the high order design model are singularly perturbed.

5.2 Model Reduction for Robust Implementation of PLF Control

One way that nonminimum phase responses can arise in flexible structure systems is due to noncollocation of localized point forces and localized position outputs. It is apparent that model order reduction can in some cases reduce a nonminimum phase system to one of reduced order which is minimum phase. This is significant for robust control design. Often instabilities of the zero dynamics are associated with fast time scale effects which may be safely neglected. Indeed, as shown by Sastry et al [SHK89] regular perturbations of the system model for both linear and smooth nonlinear systems, affine in control can induce singular perturbations of their zero dynamics. Thus to determine whether the fast time transients of the zero dynamics for a given reduced model are stable or not may require highly accurate system models. It is clear then that good engineering practice and robust design principals will suggest that fast time transients of the zero dynamics for a given reduced order model should be reduced from the system model before PLF implementation. *Thus we recommend that the system model be further reduced when the zero dynamics exhibit time scale separation.*

The zero dynamics (4.16) can be time scaled if there exists a transformation on $\mathcal{M}_u$ of the form $(\xi_1, \xi_2) = t(u)$ such that the model is decomposed,

$$J^0_{u,11}\ddot{\xi}_1 + J^0_{u,12}\ddot{\xi}_2 + \phi^0_{u,1} = 0, \tag{5.32}$$

$$[J^0_{u,12}]^T\ddot{\xi}_1 + J^0_{u,22}\ddot{\xi}_2 + \phi^0_{u,2} = 0, \tag{5.33}$$

and can be scaled, $\xi_2 = \epsilon z$ so that z is the fast time state and the model is singularly perturbed:

$$J^0_{u,11}\ddot{\xi}_1 + \epsilon J^0_{u,12}\ddot{z} + \bar{\phi}^0_{u,1} + \epsilon\hat{\phi}^0_{u,1} = 0, \tag{5.34}$$

$$[J^0_{u,12}]^T\ddot{\xi}_1 + \epsilon J^0_{u,22}\ddot{z} + \bar{\phi}^0_{u,2} + \epsilon\hat{\phi}^0_{u,2} = 0. \tag{5.35}$$

This decomposes the zero dynamics manifold as $\mathcal{M}_u = \mathcal{M}_{\xi_1} \oplus \mathcal{M}_{\xi_2}$ where $\dim \mathcal{M}_{\xi_1} = p - m$, $\dim \mathcal{M}_{\xi_2} = n - p$.

The implication for reduced order PLF control is now considered. Reduced order PLF compensation can now be designed for the reduced model obtained from the decomposition of the configuration manifold, $\mathcal{M} = \mathcal{M}_y \oplus \mathcal{M}_{\xi_1} \oplus \mathcal{M}_{\xi_2}$ and projection onto the reduced space, $\mathcal{M} = \mathcal{M}_y \oplus \mathcal{M}_{\xi_1}$. The principal question which arises is under what conditions can the time scaling of the zero dynamics lead to time scale decomposition of the Lagranian system in which the fast time scale system can be neglected.

Following the ideas in [Bl85] we assert that there exists a coordinate transformation on $\mathcal{M}_u$ such that the explicit output coordinates expression (4.9)–(4.10) is in *output normal form* and under the previous assertion the dynamics on $\mathcal{M}_u$ can be decomposed so that we can write the system dynamics in the form,

$$J_y(y,\xi)\ddot{y} + \phi_y(y,\dot{y},\xi,\dot{\xi}) = G_y f, \tag{5.36}$$

$$J_{u,11}(y,\xi)\ddot{\xi}_1 + J_{u,12}(y,\xi)\ddot{\xi}_2 + \phi_{u,1}(y,\dot{y},\xi,\dot{\xi}) = 0, \tag{5.37}$$

$$[J_{u,12}(y,\xi)]^T\ddot{\xi}_1 + J_{u,22}(y,\xi)\ddot{\xi}_2 + \phi_{u,2}(y,\dot{y},\xi,\dot{\xi}) = 0. \tag{5.38}$$

We assert that the above normal form equations are also singularly perturbed and the reduced model, obtained by projection onto the configuration space $\mathcal{M}^p_0 = \mathcal{M}_y \times \mathcal{M}_{\xi_1}$, is a valid slow time scale approximation as $\epsilon \to 0$ if the boundary layer system is asymptotically stable. Note that the boundary layer system for the normal form equations will have different stability properties in general from the boundary layer system for the perturbed zero dynamics (5.34)–(5.35). Indeed, even if the zero dynamics have fast time responses which are unstable then we assert that PLF control is implementable for the reduced order model obtained by projection of the system dynamics onto $\mathcal{M}_y \times \mathcal{M}_{\xi_1}$ if the fast time scale part of (5.36)–(5.38) is asymptotically stable.

Remark: The model order reduction obtained by time scale decomposition of the zero dynamics when applied to the system normal form equations obtains a p DOF reduced

model which matches the p slow time modes of the zero dynamics. Thus the system relative degree assumptions will be unchanged under this form of model reduction. The reduced PLF control will implement a slow time scale approximation of the IFM.

6 Experiments in Slewing and Pointing of Multibody Systems

Our studies during the course of this project have investigated some of the potential benefits that can accrue from implementation of dynamic inversion by PLF for control of flexible structures. On the surface, achievable performance of PLF compensation depends on the accuracy of models used to predict the nonlinear couplings. However, during the course of this project we have focused attention on the pragmatic issues of control design with model uncertainty. In this section we describe the assumptions used to obtain reduced models for multiaxis slewing and pointing control of an SBL system. We describe several simulation experiments which can provide a basis for design of laboratory experiments to validate the predicted performance of PLF compensation for slewing and pointing. We have included available data on the ASTREX facility and the first test article in our modeling, control design, and simulation studies in an effort to determine initial feasibility of conducting experiments to validate nonlinear control laws on this facility. In the following paragraphs we describe a series of experiments which could be run on ASTREX and used to validate SBL slewing and pointing control with PLF methods used to compensate for dominant system nonlinear couplings.

6.1 Multibody System Model for Multiaxis Slewing and Precision Alignment

The modeling method of Lagrange's equations, as described in the report [BBKA88], along with spatial discretization via collocation by splines to develop a finite dimensional model suitable for simulation of large angle, multiaxis motion of a generic, two-body model of a SBL system beam expander is described in this section. Beginning with the generic flexible spacecraft model [BBKA88, sec 4] the following model assumptions are made:

1. axial appendage deformations are negligible[10], $\eta_3 \approx z$,
2. translation velocity of the system primary body is negligible, $\dot{R} \approx 0$,
3. torsional appendage deformations are negligible, $\psi(z) \approx 0$.

Thus, following the DPS modeling approach discussed in [BBKA88, sec 3], the configuration space for the distributed parameter model is $SO(3) \times H_{\mathcal{G}}^1$, where $H_{\mathcal{G}}^1$ is the set of continuously differentiable functions, $\chi(z) = [\eta_1, \eta_2, \theta, \phi]^T \in H_{\mathcal{G}}^1$ defined on the interval $z \in [0, \ell]$, and which satisfy the geometric boundary conditions :

$$\mathcal{G}: \quad \eta_1(z) = 0,\ \eta_2(z) = 0,\ \theta(z) = 0,\ \phi(z) = 0, \ \text{ at } z = 0.$$

With the notational conventions in [BBKA88], the model will be described by the appendage lateral deformation, $\eta(t, z) = [\eta_1, \eta_2]^T$, along the body-fixed x and y axes, respectively, and

[10] See § 3.3 for a discussion of this assumption.

appendage angular deformation, $\xi(z,t) = [\theta(z), \phi(z)]^T$. The attitude angular rates referenced to the body fixed frame are denoted, ω_b.

The potential functions for the variational analysis leading to the dynamic equations of motion reduce in this case to:

$$\begin{aligned} T &= \tfrac{1}{2}\omega_b^T I_b \omega_b \\ &\quad + \tfrac{1}{2}\int_0^\ell \|\Omega_b \eta(z) + \eta_t(z)\|^2 \rho A \, dz \\ &\quad + \tfrac{1}{2}\int_0^\ell [\omega_b + P\xi_t(z)]^T I [\omega_b + P\xi_t(z)] \rho \, dz, \end{aligned} \tag{6.1}$$

$$\begin{aligned} V(\eta,\xi) &= \tfrac{1}{2}\int_0^\ell \{EI_\theta \theta_z^2(z) + EI_\phi \phi_z^2(z) \\ &\quad + \kappa_1 GA[(\eta_1(z))_z - \theta(z)]^2 + \kappa_2 GA[(\eta_2(z))_z - \phi(z)]^2\} \, dz, \end{aligned} \tag{6.2}$$

$$R(\dot\eta, \dot\xi) = \tfrac{1}{2}\int_0^\ell \{\eta_t^T \Xi_1 \eta_t + \xi_t^T \Xi_2 \xi_t + (\eta_{tz})^T \Xi_3 \eta_{tz} + (\xi_{tz})^T \Xi_4 (\xi_{tz})\} dz, \tag{6.3}$$

where

$$P = \begin{bmatrix} 0 & 0 & 1 \\ 0 & 1 & 0 \\ 1 & 0 & 0 \end{bmatrix},$$

T is the kinetic energy, V the potential energy, and R the Rayleigh dissipation function. The notation used is standard in continuum mechanics of beams and is summarized in Table 6.1. The area moment tensor is assumed to have the form[11],

$$I(z) = \begin{bmatrix} I_{xx} & 0 & 0 \\ 0 & I_{yy} & 0 \\ 0 & 0 & I_{zz} \end{bmatrix}.$$

For simulation studies contained in this report we utilize a simple damping model given by the assumption that the matrix coefficients in the dissipation function are of the form,

$$\Xi_i = \begin{bmatrix} \zeta_{1,i} & 0 \\ 0 & \zeta_{2,i} \end{bmatrix}.$$

Note that Ξ_1, Ξ_2 model *external dissipation* while Ξ_3, Ξ_4 model *internal dissipation* [BK89]. The control forces acting on the system primary body are modeled as external torques and enter the variational setup through a virtual work expression of the form,

$$\delta W = \tau_b^T \delta \xi_b. \tag{6.4}$$

[11]We use the so-called NASA standard or 321 convention [Gol82].

Notation	Explanation
ρ	mass density
A	cross section area
E	elasticity
κG	effective shear modulus
I	area moment of inertia
$\dot{x} = \frac{dx}{dt}$	time differentiation
$x_z(t,z) = \frac{\partial x}{\partial z}(z,t)$	partial differentiation

Table 6.1: Standard Notation for Lagrangian Mechanics

In the sequel, we refer to the kinetic energy expression in terms of three components;

$$T_{\text{rigid body}} = \tfrac{1}{2}\omega_b^T I_b \omega_b, \tag{6.5}$$

$$T_{\text{flex}_1} = \tfrac{1}{2}\int_0^\ell \|\Omega_b \eta(z) + \eta_t(z)\|^2 \rho A \, dz, \tag{6.6}$$

$$T_{\text{flex}_2} = \tfrac{1}{2}\int_0^\ell [\omega_b + P\xi_t(z)]^T I [\omega_b + P\xi_t(z)]\rho \, dz. \tag{6.7}$$

6.1.1 FEM: Collocation by Splines

A model based on the Finite Element Method (FEM) is obtained by spatial discretization via collocation by splines. The use of splines for such purposes is described in [BBKA88]. Given the geometric boundary conditions described above the discrete approximations of the scalar valued functions, $\eta_1(z), \eta_2(z), \theta(z), \phi(z)$, are decoupled and reduce to approximation of a single scalar function, say $\gamma(z)$, on the interval $z \in [0, \ell]$ with boundary condition, $\gamma(0,t) = 0$. Dividing the interval $[0,\ell]$ into N uniform subintervals and using first-order B-splines we obtain the approximation:

$$\gamma(z,t) \approx \sum_{i=0}^{N} \hat{\gamma}_i(t) B_{i-1}^1(z) \tag{6.8}$$

with the boundary condition,

$$\sum_{i=0}^{N} \hat{\gamma}_i(t) B_{i-1}^1(0) = 0.$$

Then following the reduction procedure described in [BBKA88, §4.4.2] we obtain the FEM approximations with $\Phi(z)$ as given in [BBKA88, Eqn. (4.47)],

$$\eta_1(z,t) \approx \Phi^T(z)\bar{\eta}_1(t) \tag{6.9}$$

$$\eta_2(z,t) \approx \Phi^T(z)\bar{\eta}_2(t) \tag{6.10}$$

$$\theta(z,t) \approx \Phi^T(z)\bar{\theta}(t) \tag{6.11}$$

$$\phi(z,t) \approx \Phi^T(z)\bar{\phi}(t). \tag{6.12}$$

6.1.2 Reduction of the Kinetic Energy Function

Using the FEM approximations of order N we obtain the spatial discretization of the kinetic energy terms,

$$T_{\text{flex}_1} \approx \tfrac{1}{2}\{\omega_b^T I_{\omega\omega}(\bar{\eta})\omega_b + 2\omega_b^T I_{\omega\eta}(\bar{\eta})\dot{\bar{\eta}} + \dot{\bar{\eta}}^T I_{\eta\eta}\dot{\bar{\eta}}\} \tag{6.13}$$

$$T_{\text{flex}_2} \approx \tfrac{1}{2}\{\omega_b^T J_{\omega\omega}\omega_b + 2\omega_b^T J_{\omega\xi}\dot{\bar{\xi}} + \dot{\bar{\xi}}^T J_{\xi\xi}\dot{\bar{\xi}}\} \tag{6.14}$$

where

$$I_{\omega\omega}(\bar{\eta}) = \begin{bmatrix} \bar{\eta}_2^T N_{\eta\eta}\bar{\eta}_2 + \sigma & -\bar{\eta}_1^T N_{\eta\eta}\bar{\eta}_2 & -\bar{\eta}_1^T N_\eta \\ -\bar{\eta}_1^T N_{\eta\eta}\bar{\eta}_2 & \bar{\eta}_1^T N_{\eta\eta}\bar{\eta}_1 + \sigma & -\bar{\eta}_2^T N_\eta \\ -\bar{\eta}_1^T N_\eta & -\bar{\eta}_2^T N_\eta & \bar{\eta}_2^T N_{\eta\eta}\bar{\eta}_2 + \bar{\eta}_1^T N_{\eta\eta}\bar{\eta}_1 \end{bmatrix}, \tag{6.15}$$

$$N_{\eta\eta} = \int_0^\ell \rho A \Phi(z)\Phi^T(z)\, dz, \tag{6.16}$$

$$N_\eta^T = \int_0^\ell \rho A z \Phi^T(z)\, dz, \tag{6.17}$$

$$\sigma = \int_0^\ell \rho A z^2\, dz = \frac{\rho A \ell^3}{3}, \tag{6.18}$$

$$I_{\omega\eta} = \begin{bmatrix} 0 & -N_\eta^T \\ N_\eta^T & 0 \\ -\bar{\eta}_2^T N_{\eta\eta} & \bar{\eta}_1^T N_{\eta\eta} \end{bmatrix}, \tag{6.19}$$

$$I_{\eta\eta} = \begin{bmatrix} N_{\eta\eta} & 0 \\ 0 & N_{\eta\eta} \end{bmatrix}, \tag{6.20}$$

$$J_{\omega\omega} = \int_0^\ell \rho I(z)\, dz, \tag{6.21}$$

$$J_{\omega\xi} = \begin{bmatrix} 0 & N_\phi^T \\ N_\theta^T & 0 \\ 0 & 0 \end{bmatrix}, \tag{6.22}$$

and

$$J_{\xi\xi} = \begin{bmatrix} N_{\theta\theta} & 0 \\ 0 & N_{\phi\phi} \end{bmatrix}. \tag{6.23}$$

The following terms are used in the above expressions,

$$N_\psi^T = \int_0^\ell \rho I_{zz}\Phi^T(z)\, dz, \tag{6.24}$$

$$N_\theta^T = \int_0^\ell \rho I_{yy}\Phi^T(z)\, dz, \tag{6.25}$$

$$N_\phi^T = \int_0^\ell \rho I_{xx}\Phi^T(z)\, dz, \tag{6.26}$$

$$N_{\phi\phi} = \int_0^\ell \rho I_{xx} \Phi(z) \Phi^T(z)\, dz, \tag{6.27}$$

$$N_{\theta\theta} = \int_0^\ell \rho I_{yy} \Phi(z) \Phi^T(z)\, dz. \tag{6.28}$$

Note that the total kinetic energy can be written in the standard form,

$$T \approx \tfrac{1}{2}[\omega_b^T, \dot{\bar{\eta}}^T, \dot{\bar{\xi}}^T] M(\xi_b, \bar{\eta}, \bar{\xi}) \begin{pmatrix} \omega_b \\ \dot{\bar{\eta}} \\ \dot{\bar{\xi}} \end{pmatrix} \tag{6.29}$$

where

$$M(\xi_b, \bar{\eta}, \bar{\xi}) = \begin{bmatrix} I_b + I_{\omega\omega}(\bar{\eta}) + J_{\omega\omega} & I_{\omega\eta}(\bar{\eta}) & J_{\omega\xi} \\ I_{\omega\eta}^T(\bar{\eta}) & I_{\eta\eta} & 0 \\ J_{\omega\xi}^T & 0 & J_{\xi\xi} \end{bmatrix}. \tag{6.30}$$

6.1.3 Reduction of the Potential Energy and Dissipation Functions

As above, the potential energy and dissipation functions are reduced by substitution of the FEM approximations. For the potential energy we obtain,

$$V = \tfrac{1}{2}\{\bar{\theta}^T K_\theta \bar{\theta} + \bar{\phi}^T K_\phi \bar{\phi} + \bar{\eta}_1^T K_{\eta_1} \bar{\eta}_1 + \bar{\eta}_2^T K_{\eta_2} \bar{\eta}_2 + 2\bar{\theta}^T K_{\theta\eta_1} \bar{\eta}_1 + 2\bar{\phi}^T K_{\phi\eta_2} \bar{\eta}_2\}, \tag{6.31}$$

where

$$K_\theta = \int_0^\ell \{EI_{yy} \Phi_z(z) \Phi_z^T(z) + \kappa_1 GA \Phi(z) \Phi^T(z)\} dz \tag{6.32}$$

$$K_\phi = \int_0^\ell \{EI_{xx} \Phi_z(z) \Phi_z^T(z) + \kappa_2 GA \Phi(z) \Phi^T(z)\} dz \tag{6.33}$$

$$K_{\eta_1} = \int_0^\ell \{\kappa_1 GA \Phi_z(z) \Phi_z^T(z)\} dz \tag{6.34}$$

$$K_{\eta_2} = \int_0^\ell \{\kappa_2 GA \Phi_z(z) \Phi_z^T(z)\} dz \tag{6.35}$$

$$K_{\theta\eta_1} = -\tfrac{1}{2} \int_0^\ell \{\kappa_1 GA \Phi_(z) \Phi_z^T(z)\} dz \tag{6.36}$$

$$K_{\phi\eta_2} = -\tfrac{1}{2} \int_0^\ell \{\kappa_2 GA \Phi_(z) \Phi_z^T(z)\} dz. \tag{6.37}$$

Similarly, the dissipation function reduces to the form,

$$R = \tfrac{1}{2}\{\dot{\bar{\eta}}_1^T B_{\eta_1} \dot{\bar{\eta}}_1 + \dot{\bar{\eta}}_2^T B_{\eta_2} \dot{\bar{\eta}}_2 + \dot{\bar{\theta}}^T B_\theta \dot{\bar{\theta}} + \dot{\bar{\phi}}^T B_\phi \dot{\bar{\phi}} + 2\dot{\bar{\theta}}^T B_{\theta\eta_1} \dot{\bar{\eta}}_1 + 2\dot{\bar{\phi}}^T B_{\phi\eta_2} \dot{\bar{\eta}}_2\}, \tag{6.38}$$

where given the expressions,

$$R_0 := \int_0^\ell \Phi(z) \Phi^T(z)\, dz, \tag{6.39}$$

$$R_0' := \int_0^\ell \Phi_z(z) \Phi^T(z)\, dz, \tag{6.40}$$

$$R_0'' := \int_0^\ell \Phi_z(z) \Phi_z^T(z)\, dz, \tag{6.41}$$

we find it convenient to express the individual matrix coefficients in R (arising from the FEM approximation) as:

$$B_{\eta_i} = \zeta_{i1}R_0 + \zeta_{i3}R_0'' \quad \text{for } i = 1,2, \tag{6.42}$$

$$B_\theta = (\zeta_{12} + \zeta_{13})R_0 + \zeta_{14}R_0', \tag{6.43}$$

$$B_\phi = (\zeta_{22} + \zeta_{23})R_0 + \zeta_{24}R_0', \tag{6.44}$$

$$B_{\eta_1\theta} = -\zeta_{13}R_0', \tag{6.45}$$

$$B_{\eta_2\phi} = -\zeta_{23}R_0'. \tag{6.46}$$

Finally, we summarize the model stiffness and damping using the expressions,

$$K_\eta = \begin{bmatrix} K_{\eta_1} & 0 \\ 0 & K_{\eta_2} \end{bmatrix}, \quad K_{\eta\xi} = \begin{bmatrix} K_{\theta\eta_1} & 0 \\ 0 & K_{\phi\eta_2} \end{bmatrix}, \quad K_\xi = \begin{bmatrix} K_\theta & 0 \\ 0 & K_\phi \end{bmatrix},$$

$$B_\eta = \begin{bmatrix} B_{\eta_1} & 0 \\ 0 & B_{\eta_2} \end{bmatrix}, \quad B_{\eta\xi} = \begin{bmatrix} B_{\theta\eta_1} & 0 \\ 0 & B_{\phi\eta_2} \end{bmatrix}, \quad B_\xi = \begin{bmatrix} B_\theta & 0 \\ 0 & B_\phi \end{bmatrix}.$$

6.1.4 Lagrange's Equations

Finally, we compute the equations of motion using Lagrange's equations in the form:

$$\dot{q} = \tilde{\Gamma}(q)p \tag{6.47}$$

$$M(q)\dot{p} + \left[\frac{\partial M(q)p}{\partial q}\right]p - \frac{1}{2}\left[\frac{\partial M(q)p}{\partial q}\right]^T p + \frac{\delta V}{\delta q} = -\frac{\delta R}{\delta p} + Q_q \tag{6.48}$$

with generalized coordinates $q = \{\xi_b, \bar{\eta}, \bar{\xi}\}$, and velocities, $p = \{\omega_b, \dot{\bar{\eta}}, \dot{\bar{\xi}}\}$.

Equations of Motion for Multiaxis Slewing: Applying Lagrange's equation results (after some simplification) in the equations of motion with kinematics of the system attitude expressed in terms of the Gibbs vector, γ;

$$\dot{\gamma} = \Gamma(\gamma)\omega_b, \tag{6.49}$$

and kinetics,

$$[I_b + I_{\omega\omega} + J_{\omega\omega}]\dot{\omega}_b + I_{\omega\eta}\ddot{\bar{\eta}} + J_{\omega\xi}\ddot{\bar{\xi}} + \Omega_b\{[I_b + I_{\omega\omega} + J_{\omega\omega}]\omega_b + I_{\omega\eta}\dot{\bar{\eta}} + J_{\omega\xi}\dot{\bar{\xi}}\} + H\dot{\bar{\eta}} = \tau_b \tag{6.50}$$

$$I_{\omega\eta}^T\dot{\omega}_b + I_{\eta\eta}\ddot{\bar{\eta}} - \tfrac{1}{2}H^T\omega_b + R\dot{\bar{\eta}} + K_\eta\bar{\eta} + K_{\eta\xi}\bar{\xi} + B_\eta\dot{\bar{\eta}} + B_{\eta\xi}\dot{\bar{\xi}} = 0 \tag{6.51}$$

$$J_{\omega\xi}^T\dot{\omega}_b + J_{\xi\xi}\ddot{\bar{\xi}} + K_\xi\bar{\xi} + K_{\eta\xi}^T\bar{\eta} + B_\xi\dot{\bar{\xi}} + B_{\eta\xi}^T\dot{\bar{\eta}} = 0 \tag{6.52}$$

where

$$H(\bar{\eta}, \omega_b, \dot{\bar{\eta}}) = \begin{bmatrix} -\omega_2\bar{\eta}_2^T N_{\eta\eta}^T - \omega_3 N_\eta^T & 2\bar{\eta}_2^T N_{\eta\eta}\omega_1 \\ -\omega_1\bar{\eta}_2^T N_{\eta\eta}^T + 2\omega_2\bar{\eta}_1^T N_{\eta\eta} & -\omega_1\bar{\eta}_1^T N_{\eta\eta}^T - 2\omega_3 N_\eta^T \\ -\omega_1 N_\eta^T + \omega_3 2\bar{\eta}_1^T N_{\eta\eta} + \dot{\bar{\eta}}_1^T N_{\eta\eta} & -\omega_2 N_\eta^T + \omega_3 2\bar{\eta}_2^T N_{\eta\eta} + \dot{\bar{\eta}}_2^T N_{\eta\eta} \end{bmatrix}, \tag{6.53}$$

$$R(\omega_b) = \begin{bmatrix} 0 & \omega_3 N_{\eta\eta} \\ \omega_3 N_{\eta\eta} & 0 \end{bmatrix}. \tag{6.54}$$

6.2 Simulation Model for SBL Slewing and Pointing Control Experiments

A computer simulation model was developed and coded based on the above FEM model for attitude slewing of a flexible space craft (6.49)–(6.52). The model parameters and geometry was chosen to represent the dynamics of a SBL system beam expander with structural flexure arising from the flexure response of the metering truss. A goal of the second year effort was to develop concepts for experimental testing of nonlinear control concepts for flexible space structures. A suitable facility for testing large angle, multiaxis slewing and precision pointing is currently under construction at the Astronautics Laboratory. The ASTREX facility with include 3 axis slewing and the initial test article is a scaled model of a SBL beam expander. We have adapted our nonlinear slewing control simulation model to represent available parameters and geometry of the ASTREX test article. Details of the modeling assumptions and geometry are given below.

6.2.1 Simulation model geometry assumptions and parameters

The objective of the simulation model design was to generate a simplified model that would duplicate, as closely as possible, the geometry and dynamics of the ASTREX test article. Information describing the test article was sparse, therefore, the following assumptions were required to develop a working simulation model:

1. The basic configuration of the model consisted of a rigid body, representing the main mirror assembly and associated structure, and an attached tripod structure, representing the flexible metering truss with secondary mirror, see Figure 6.1.

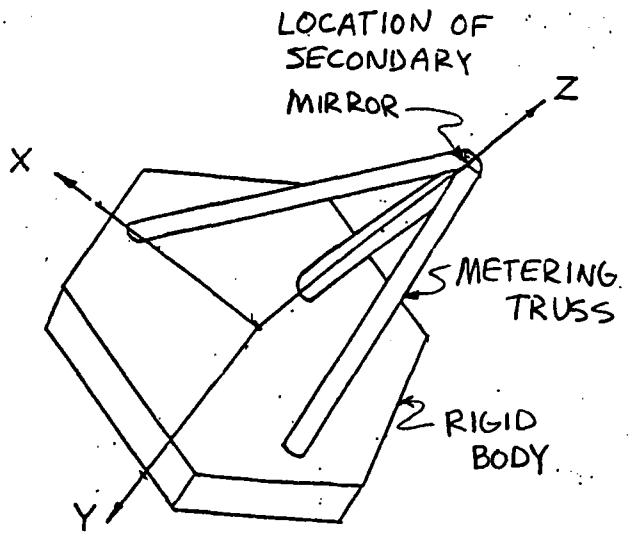

Figure 6.1: Simulation model.

2. The metering truss geometry consisted of a tripod of tubes located at the corners of an equilateral triangular base. The generic model discussed above was readily adapted to represent this geometry by including spatial variation of the area moments $I_{xx}(z)$ and $I_{yy}(z)$ based on this geometry. Details of the computation of the area moments and the resulting FEM model approximations are given in Appendix A.

3. The dimensions of the metering truss model were as follows:

Length, l	-	5.0 m
Base width, b	-	3.8 m
Tube inner dia.	-	8.0 cm
Tube outer dia.	-	12.7 cm
Mass of secondary mirror	-	190 kg (5 % of total sys. mass)

4. The overall system characteristics were as follows:

Mass moments of inertia	I_{xx}	=	16640 kg m^2
	I_{yy}	=	16590 kg m^2
	I_{zz}	=	11660 kg m^2
System mass	m	=	3810 kg
First modal freq. of metering truss		=	12.2 Hz

5. The dynamics of the secondary mirror were neglected and it was modeled as a point mass at the end of the truss.

6. The modulus of elasticity of the truss material was chosen so that its first modal frequency matched that of the ASTREX test article.

6.3 Design Example: Slewing and pointing control with passive vibration suppression

The design methods of PLF have been discussed with application to slewing and pointing of a multibody system. In this example we consider the significance of input-output structure of the PLF control for slewing and pointing of the system primary body axis for use of passive vibration components. The essential idea is that the use of passive vibration absorbers requires tuning for predictable structural resonances. Available technology for *Control Structure Interaction* (CSI) includes devices which interact with the structure through inertially generated forces and torques to provide vibration absorbtion. Such devices include Proof Mass Actuators (PMA's).

Miller and Crawley describe and compare several alternatives for tuning stiffness and damping properties of PMA's for application as passive vibration damping of simple flexible structure models. Their analysis extends the classical analysis and highlights the highly tuned, narrow band behavior of such devices used either as passive vibration absorbers or as active control actuators. Thus damping effectiveness will depend critically on assumed

vibration modes. For nonlinear dynamics of multibody systems such passive tuning is problematical. In the following we consider the importance of PLF and the tuning of PMA's as passive dampers for application to the problem of rapid, large angle slewing and precision pointing.

The slewing and pointing control design based on PLF compensation focuses attention on stability enhancement of the decoupled or zero dynamics. Vibration damping should provide enhanced stabilization in the sense of transient response of the structural elastic responses which have been decoupled from the primary regulated variables by the PLF compensation. Thus PMA tuning should be optimized for the system zero dynamics. A simple example serves to illustrate the point. Consider the case of slewing and pointing of the inertial attitude of the system primary body using external torques applied to the primary body. In this case the dynamic response of the zero dynamics can be described by the (linear) *cantilevered* vibration modes.

A common problem in design of structural vibration control using low authority control actuators is to decouple the rigid body modes from the vibration control loops so that low authority structural actuators are not saturated by interaction with rigid body dynamics. This is typically accomplished by processing paired control loops from symmetrically placed, collocated (torque) actuators and sensors [Jos89]. This approach may be sensitive to system symmetries. An advantage of the PLF compensation scheme for primary body slewing as described above is that the rigid body motion is decoupled from the multibody alignment control.

System Model for Passive Damping by PMA The simplest technology for vibration absorbtion is based on vibration damping by inertial interactions. The Lagrangian approach to system modeling indicates how the former system model can be modified to include the dynamic interaction between the PMA's and the structure.

Consider the model illustrated in Figure 6.2 where two PMA's with single, linear degree of freedom are located at the position $z = \ell$ on the elastic appendage. The pair of PMA's are assumed to have axes of motion aligned with the local coordinate frame. The motion of the moving mass for PMA aligned with the x-axis (resp. y-axis) is given by the coordinate x_a (resp. y_a) defined with respect to a zero energy at rest configuration.

The modified system Kinetic Energy has the form,

$$T = T_{\text{rigid body}} + T_{\text{flex}} + T_{PMA}.$$

The inertial velocity of the appendage at a point z is:

$$v(z) := \eta(z) + \Omega_b \begin{pmatrix} \eta_1(z) \\ \eta_2(z) \\ \eta_3(z) + z \end{pmatrix}.$$

Neglecting axial deformation, $\eta_3 \approx 0$, we obtain the additional kinetic energy in the form,

$$T_{PMA} = \tfrac{1}{2} m_a (\dot{x}_a - v_1(z))^2 + \tfrac{1}{2} m_a (\dot{y}_a - v_2(z))^2 \qquad (6.55)$$

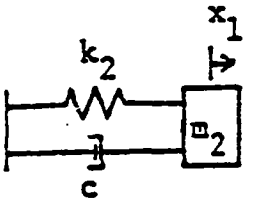

Figure 6.2: SBL model with passive damping by PMA's.

$$= \tfrac{1}{2}m_a[\dot{x}_a - \dot{\eta}_1(z) - \omega_2 z + \omega_3\eta_2(z)]^2 + \tfrac{1}{2}m_a[\dot{y}_a - \dot{\eta}_2(z) + \omega_1 z - \omega_3\eta_1(z)]^2.$$

Assuming the devices are identical and decoupled we take the system potential energy in the form,

$$V = V_{\text{flex}} + V_{PMA},$$

where,

$$V_{PMA} = \tfrac{1}{2}k_a {x_a}^2 + \tfrac{1}{2}k_a {y_a}^2.$$

Applying Lagrange's equations to the PMA terms,

$$\frac{d}{dt}\left(\frac{\partial T_{PMA}}{\partial \dot{q}_i}\right) - \frac{\partial}{\partial q_i}(T_{PMA} - V_{PMA}) = Q_i,$$

with respect to the expanded set of reduced generalized coordinates obtained by retaining N finite elements,

$$q_i \in \{\gamma_b, \bar{\eta}_1, \bar{\eta}_2, \bar{\theta}, \bar{\phi}, x_a, y_a\},$$

one obtains the modified equations of motion in the standard form:

$$\dot{q} = \tilde{\Gamma}(q)p \tag{6.56}$$

$$M_{sys}\dot{p} + B_{sys}p + K_{sys}q = G_{sys}\tau_b \tag{6.57}$$

where

$$q = [\gamma_b^T, \bar{\eta}^T, \bar{\xi}^T, \bar{x}^T]^T,$$

$$p = [\omega_b^T, \dot{\bar{\eta}}^T, \dot{\bar{\xi}}^T, \dot{\bar{x}}^T]^T,$$

and $\bar{x} = [x_a, y_a]^T$. Denoting terms arising from the interaction with the PMA's by superscript 'a' we can write the modified $N_s \times N_s$ system matrices (with $N_s = 2N + 5$) in the form,

$$M_{sys} = \left[\begin{array}{ccc|c} I_b + I_{\omega\omega} + J_{\omega\omega} + M^a_{\omega\omega} & I_{\omega\eta} + M^a_{\omega\eta} & J_{\omega\xi} & M^a_{\omega x} \\ I^T_{\omega\eta} + [M^a_{\omega\eta}]^T & I_{\eta\eta} + M^a_{\eta\eta} & 0 & M^a_{\eta x} \\ J^T_{\omega\xi} & 0 & J_{\xi\xi} & 0 \\ \hline [M^a_{\omega x}]^T & [M^a_{\eta x}]^T & 0 & M_a \end{array}\right],$$

$$B_{sys} = \left[\begin{array}{ccc|c} \Omega_b\{I_b + I_{\omega\omega} + J_{\omega\omega} + M^a_{\omega\omega}\} & \Omega_b\{I_{\omega\eta} + M^a_{\omega\eta}\} + H & \Omega_b J_{\omega\xi} & B^a_{\omega x} \\ I^T_{\omega\eta} + B^a_{\omega\eta} & R + B_\eta + B^a_{\eta\eta} & B_{\eta\xi} & 0 \\ J^T_{\omega\xi} & B^T_{\eta\xi} & B_\xi & \\ \hline [B^a_{\omega x}]^T & 0 & 0 & B^a_{pma} \end{array}\right],$$

$$K_{sys} = \left[\begin{array}{ccc|c} 0 & & & \\ & K_\eta & K_{\eta\xi} & 0 \\ & K^T_{\eta\xi} & K_\xi & \\ \hline 0 & & & K_{pma} \end{array}\right], \quad \text{and} \quad G_{sys} = \begin{bmatrix} I_3 \\ 0 \\ 0 \\ 0 \end{bmatrix}.$$

Letting both PMA's be located at the end of the appendage; $z = \ell$, then the new terms take the form,

$$M^a_{\omega\omega} = \begin{bmatrix} m_a\ell^2 & 0 & -m_a\ell\eta_1(\ell) \\ 0 & m_a\ell^2 & -m_a\ell\eta_2(\ell) \\ -m_a\ell\eta_1(\ell) & -m_a\ell\eta_2(\ell) & m_a(\eta_1^2(\ell) + \eta_2^2(\ell)) \end{bmatrix} \quad (3\times 3) \tag{6.58}$$

$$M^a_{\omega\eta} = \left[\begin{array}{cc|cc} 0\cdots 0 & 0 & 0\cdots 0 & -m_a\ell \\ 0\cdots 0 & m_a\ell & 0\cdots 0 & 0 \\ 0\cdots 0 & -m_a\eta_2(\ell) & 0\cdots 0 & -m_a\eta_1(\ell) \end{array}\right] \quad (3\times 2N) \tag{6.59}$$

$$M^a_{\omega x} = -\left[\begin{array}{c|c} 0 & -m_a\ell \\ m_a\ell & 0 \\ -m_a\eta_2(\ell) & -m_a\eta_1(\ell) \end{array}\right] \quad (3\times 2) \tag{6.60}$$

$$M^a_{\eta x} = \left[\begin{array}{c|c} 0 & \\ \vdots & 0 \\ 0 & \\ -m_a & \\ \hline & 0 \\ 0 & \vdots \\ & 0 \\ & -m_a \end{array}\right] \quad (2N\times 2) \tag{6.61}$$

$$M^a_{\eta\eta} = \text{diag}\{0,\ldots,0,m_a,0,\ldots,0,m_a\} \quad (2N\times 2N) \tag{6.62}$$

$$M_a = m_a I_2, \quad K_a = k_a I_2 \tag{6.63}$$

$$B^a_{\eta\eta} = \left[\begin{array}{c|c} 0 & B^a_{12} \\ \hline -B^a_{12} & 0 \end{array}\right] \quad (2N\times 2N) \tag{6.64}$$

$$B^a_{12} = \left[\begin{array}{cc|c} & & 0 \\ & \bigcirc & \vdots \\ & & 0 \\ \hline 0 & \cdots\ 0 & -2m_a\omega_3 \end{array}\right] \quad (N\times N) \tag{6.65}$$

$$B^a_{\eta\omega} = \left[\begin{array}{c|c|c} 0 & & 0 \\ \vdots & \circ & \vdots \\ 0 & & 0 \\ \ell m_a \omega_3 & & -m_a\omega_3\eta_1(\ell) \\ \hline & 0 & 0 \\ \circ & \vdots & \vdots \\ & 0 & 0 \\ & \ell m_a\omega_3 & -m_a\omega_3\eta_1(\ell) \end{array}\right] \quad (2N \times 3) \tag{6.66}$$

PMA Tuning for Slewing and Pointing Control Such devices provide dissipation by coupling kinetic vibration energy into the moving mass of the PMA where it can be dissipated by localized damping. Since the effectiveness of the energy coupling depends on inertial interactions the mass of the device is a limiting factor in its effectiveness. Nevertheless, the effectiveness of the passive damping depends on tuning the PMA stiffness and damping to the critical vibration mode.

Miller and Crawley review classical and modern approaches to tuning PMA's as vibration absorbers. They discuss tuning with respect to the simple linear model of a PMA interacting with a single degree-of-freedom system as shown in Figure 6.3 where m_1 and k_1 are the structure mass and stiffness respectively, and where m_2, k_2, and c are the absorber mass, spring stiffness, and damper constant respectively. We focus attention on tuning for optimal transient response characteristics as follows. Given the non-dimensional parameters:

$$\delta = \sqrt{\frac{(k_2/m_2)}{(k_1/m_1)}} \quad \text{absorber - structure frequency ratio}$$

$$\beta = \frac{m_2}{m_1} \quad \text{absorber - structure mass ratio}$$

$$\mu = \frac{c}{2m_2\sqrt{k_1/m_1}} \quad \text{non-dimensional damping}$$

choose the PMA stiffness k_a and damping c for a fixed mass ratio such that the maximum modal time constant is minimized. The tradeoff is illustrated in Figure 6.4 which displays a root locus as μ is varied (for a mass ration $\beta = 0.02$). The frequency ratio, δ, for optimal transient response is the value for which the root loci intersect at point A, and is given by,

$$\delta_{TR} = \frac{1}{1+\beta}. \tag{6.67}$$

Application of this approach to flexible structures is of course limited by the interaction between multiple vibration modes.

For the problem of slewing and pointing as discussed in the previous reports we let the primary outputs be the inertial attitude parameters, γ_b, of the primary body frame and

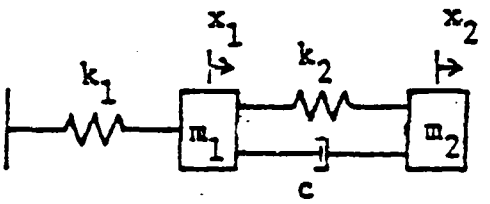

Figure 6.3: Model used by Crawley and Miller for tuning passive absorber to a one DOF system

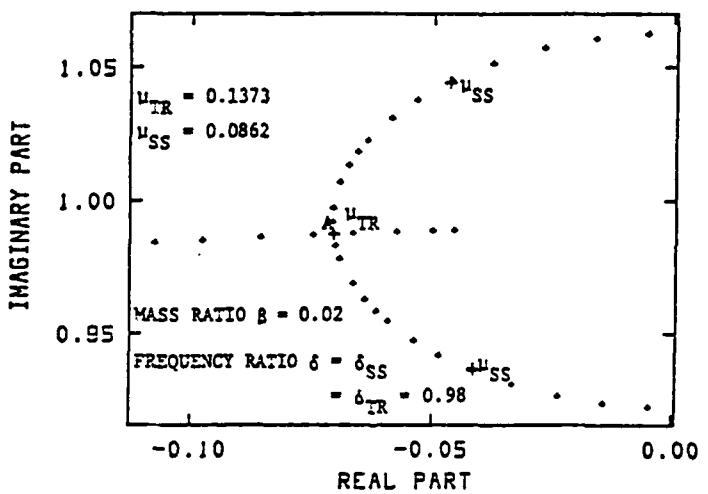

Figure 6.4: Root locus of poles for Miller and Crawley's one DOF system as a function of increasing damper value

Mode	Frequency	
1	12.07	Hz
2	12.07	
3	70.73	
4	70.73	
5	103.19	
6	103.19	
7	271.33	
8	271.33	

Table 6.2: Truss modal frequencies for cantilevered boundary conditions

apply external torques, τ_b, to the primary body. In this case the decoupled dynamics are given by the linear dynamics of the metering truss with cantilevered boundary conditions replacing the interaction with the rigid body. (To see this simply constrain the primary regulated outputs, $y = \gamma_b$ and their rates $\dot{y}$ to the origin and substitute $\gamma_b = 0$, $\omega_b = 0$ in the equations of motion to obtain the zero dynamics.) To tune the PMA's for optimal transient response of the first pair flexible modes of the zero dynamics we apply the strategy of Miller and Crawley to the cantilevered appendage model.

Utilizing the results of Miller and Crawley, we chose an absorber mass to truss mass ratio of .05 for each device and performed a root locus analysis with δ_{TR} given in (6.67). The root locus appears in Figure 6.5 showing the poles of the passive absorber and lowest modal frequency of the truss for different values of absorber damping. Maximum structural damping occurred at the intersection of the root trajectories, with optimal values of absorber damping and spring stiffness of 370 kg/s and 3.9 $\times 10^4 N/m$. As expected, the optimal frequency ratio suggested in (6.67) offered a crude approximation and further refinement was necessary to obtain transient response tuning even for the simple finite element model used in our simulations. The resulting tuned values of PMA parameters were then used in simulations of PLF slewing and pointing (refer to model **MODA**).

Summary of Simulation Results Computer simulations of the finite element model **MODA** were performed comparing the effect the passive PMA absorber on slew times and torque requirements. A standard three axis slew maneuver was defined by initial offset from the desired inertial attitude given by the Gibbs vector,

$$\gamma_b = [0.08, 0.09, 0.036]$$

or in Euler angles,

$$[\psi, \theta, \phi] = [5.^\circ, 10.^\circ, 10^\circ]$$

and results are summarized in tables 6.3 and 6.4. Slew time is computed as the elapsed time for the absolute value of each Gibbs component of the rigid body attitude, γ_b, to become

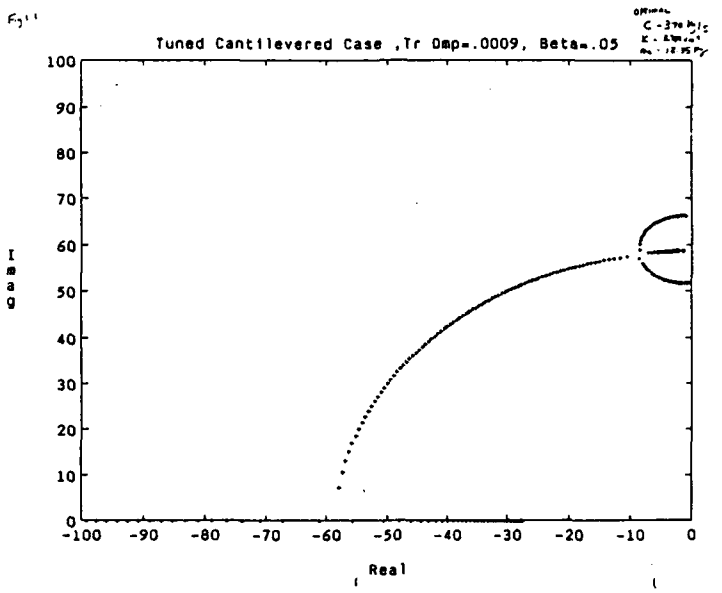

Figure 6.5: Root locus showing interaction between absorber poles and lowest frequency truss poles as a function of absorber damping

less than 0.0002. Peak torque requirements are computed relative to a fixed torque level, τ_0, equivalent to angular acceleration of 10 deg/sec/sec for an equivalent rigid body with inertia moment equal to the total undeformed ASTREX system inertia. The peak torque is computed as

$$\tau_{peak} = \max\{t > 0 : \frac{|\tau(t)| - |\tau_0|}{|\tau_0|}\}.$$

The tables also include performance tradeoffs for implementation of PLF for various reduced order models with r retained degrees of freedom in the SBL system model. Results indicate that slew times were improved with PMA tuned for the dominant elastic mode of the cantilevered truss for various reduced order PLF implementations. This confirms the theoretical predictions of the PLF compensation and stability of the zero dynamics. However, peak torque requirements remained relatively unchanged. (Note that in Tables 6.3 and 6.4, **MODA** r=6 and r=7, correspond to **MODB**, r=4 and r=5, since **MODA** r=4 and r=5 are the modes associated with the absorber dynamics which are not included in **MODB**.). This follows by observing the additional mass of the PMA offset their benefit in stabilization with reference to slewing torque requirements. Figures 6.6 and 6.7 show time responses for slewing simulations comparing **SIMA5**, a reduced order model with absorber which retains the absorber modes and first two truss modes, and **SIMC2**, a reduced order model without absorber which retains first two truss modes. The dotted traces correspond to simulation **SIMA5** and illustrate the dramatic increase in truss damping generated by the tuned absorber as compared with the solid traces of simulation **SIMC2**. (See also Section 6.3 for summary of simulation results.)

Peak Torque $\Delta T_{pk}(r)/T_{pk}(3)$ Relative to rigid body case						
simulation	PLF Model DOF					
model $r =$	3	4	5	6	7	13
MODA	0	0.01	0.01	0.48	0.89	0.89
MODB	0	0.60	0.86			0.90

Table 6.3: Relative Peak Torque Increase with PLF Compensation DOF

Slew Times (sec) to $\|\gamma_i\| < .0002$						
	PLF Model DOF					
$r =$	3	4	5	6	7	13
	Model **MODA**					
Axis 1	1.518	1.472	1.471	1.420	1.419	1.408
2	1.643	1.640	1.629	1.627	1.483	1.476
3	0.940	0.939	0.938	0.940	0.940	0.940
	Model **MODB**					
Axis 1	1.500	1.420	1.420			1.412
2	1.638	1.638	1.482			1.469
3	0.940	0.940	0.941			0.940

Table 6.4: Slewing Times for Standard 3-axis Maneuver

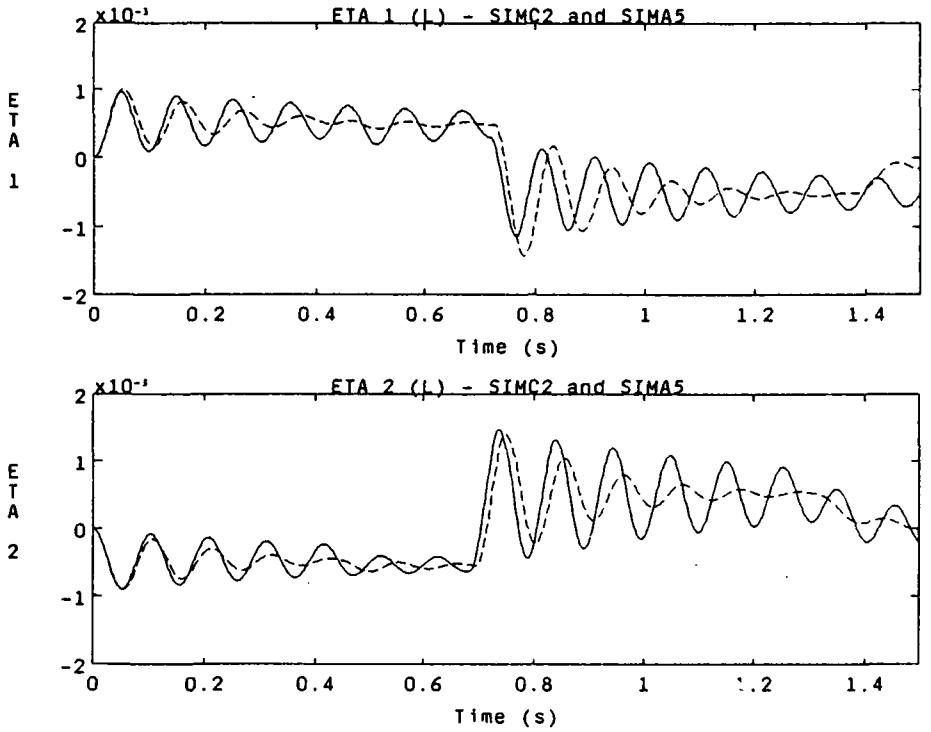

Figure 6.6: Time responses comparing $\eta_1(\ell)$ and $\eta_2(\ell)$ for the models with and without tuned absorber

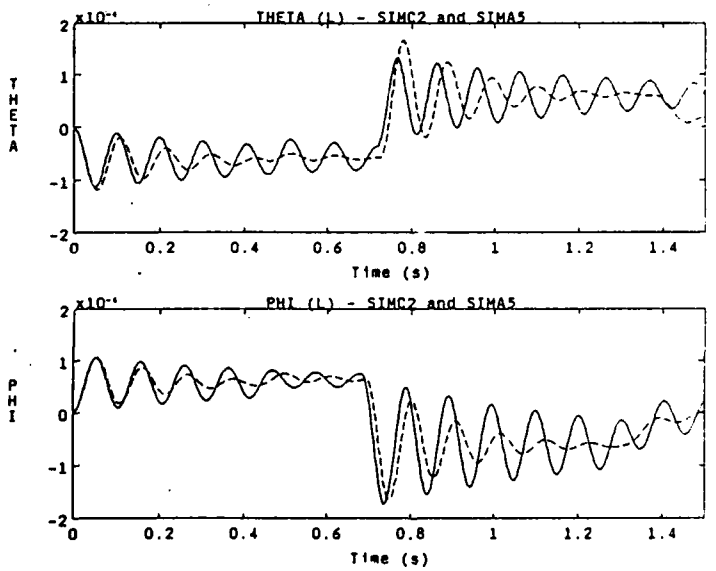

Figure 6.7: Time responses comparing $\theta(\ell)$ and $\phi(\ell)$ for the models with and without tuned absorber

6.4 Design Example: LOS Slewing and Multibody Alignment

The application of slewing and pointing control to SBL as well as other space-based optical systems will require the coordination of multiple actuators for system slewing and multibody alignment. The effective optical LOS for a multiple mirror system will involve relative motion of the mirrors as well as the primary body inertial attitude. Detailed analysis of the optical train of a candidate SBL system is beyond the scope of this study. We will consider a simplified problem which highlights a significant aspect of the application of PLF compensation for multibody alignment when the available controls and/or the choice of regulated outputs leads to system zero dynamics which are unstable in some sense. Of course, the sense in which instability of the zero dynamics may limit application of PLF compensation depends on the application. The available theory suggests that PLF compensation is not feasible for nonminimum phase systems.

Clearly, the limitation of applying PLF compensation to a nonminimum phase system arises from the fact that PLF compensation seeks to implement an online system inverse which is by definition unstable if the system model is nonminimum phase. For the class of Lagrangian systems arising from control of flexible structures the PLF compensation includes an Inverse Force Model. In this section we illustrate some tradeoffs in the implementation of an online IFM for a nonminimum phase system.

System Model for Multibody Alignment Control: The method of Lagrange's equations offers a systematic approach to develop equations of motion for systems with external forces described by a virtual work function. We consider the two body system described previously where we have assumed the multibody configuration rotates about the point $z = 0$ at which the appendage is attached to the primary body. We now assume that the following external forces are applied to the two-body system:

1. torques, τ_b, applied to the primary body,
2. distributed torque function applied to the flexible appendage, $\tau(z) = \sum_k \tau_k \delta(z - \zeta_k)$,
3. distributed force function applied to the flexible appendage, $f(z) = \sum_j f_j \delta(z - \zeta_j)$.

The virtual work function can then be derived as follows. The power flow into the system is given as,

$$\begin{aligned} P = \; & \tau_b^T \omega_b && \text{rigid body torque} \\ & + \int_0^\ell \tau^T(z)[\omega_b + \dot{\xi}(z)]\, dz && \text{distributed torque} \\ & + \int_0^\ell f^T(z)[\omega_b \times \bar{z} + \dot{\eta}(z)]\, dz && \text{distributed force} \end{aligned}$$

where $\bar{z} = [0, 0, z]^T$. Note that

$$\omega_b \times \bar{z} = -\bar{z} \times \omega_b = -\begin{bmatrix} 0 & -z & 0 \\ z & 0 & 0 \\ 0 & 0 & 0 \end{bmatrix} \omega_b = -Z\omega_b,$$

and since $\omega_b = \Gamma(\xi_b)\dot{\xi}_b$ we can write

$$P = \tau_b^T \Gamma(\xi_b)\dot{\xi}_b + \int_0^\ell \{\tau^T(z)\Gamma(\xi_b)\dot{\xi}_b + \tau^T(z)\dot{\xi}(z)\}\, dz + \int_0^\ell \{-f^T(z)Z\Gamma(\xi_b)\dot{\xi}_b + f^T(z)\dot{\eta}(z)\}\, dz. \tag{6.68}$$

The virtual work in (6.4) is replaced with,

$$\delta W = \left\{\tau_b^T \Gamma(\xi_b) + \int_0^\ell \tau^T(z)\Gamma(\xi_b)\, dz - \int_0^\ell f^T(z)Z\Gamma(\xi_b)\, dz\right\} \delta\xi_b + \left\{\int_0^\ell \sum_k \tau_k^T \delta(z-\zeta_k)\, \delta\xi\, dz\right\} + \left\{\int_0^\ell \sum_j f_j^T \delta(z-\zeta_k)\, \delta\eta\, dz\right\}. \tag{6.69}$$

Defining the vector of external forces,

$$\bar{f}_s = [f_1, \ldots, f_j, \ldots]^T, \tag{6.70}$$

and torques,

$$\bar{\tau}_s = [\tau_1, \ldots, \tau_k, \ldots]^T, \tag{6.71}$$

and applying Lagrange's equations gives the system equations of motion in the form,

$$[I_b + I_{\omega\omega} + J_{\omega\omega}]\dot{\omega}_b + I_{\omega\eta}\ddot{\bar{\eta}} + J_{\omega\xi}\ddot{\bar{\xi}} + \Omega_b\{[I_b + I_{\omega\omega} + J_{\omega\omega}]\omega_b + I_{\omega\eta}\dot{\bar{\eta}} + J_{\omega\xi}\dot{\bar{\xi}}\} + H\dot{\bar{\eta}} = \tau_b + \sum_k \tau_k + \sum_j Z_j f_j \tag{6.72}$$

$$I_{\omega\eta}^T\dot{\omega}_b + I_{\eta\eta}\ddot{\bar{\eta}} - \tfrac{1}{2}H^T\omega_b + R\dot{\bar{\eta}} + K_\eta\bar{\eta} + K_{\eta\xi}\bar{\xi} + B_\eta\dot{\bar{\eta}} + B_{\eta\xi}\dot{\bar{\xi}} = G_\eta\bar{f}_s \tag{6.73}$$

$$J_{\omega\xi}^T\dot{\omega}_b + J_{\xi\xi}\ddot{\bar{\xi}} + K_\xi\bar{\xi} + K_{\eta\xi}^T\bar{\eta} + B_\xi\dot{\bar{\xi}} + B_{\eta\xi}^T\dot{\bar{\eta}} = G_\xi\tau_s \tag{6.74}$$

where H, and $\Re$ are given by (6.53)–(6.54) and

$$Z_j = \begin{bmatrix} 0 & -\zeta_j \\ \zeta_j & 0 \\ 0 & 0 \end{bmatrix}. \tag{6.75}$$

Then letting

$$\bar{I} = \left[\begin{array}{cc|c|cc|c} 1 & 0 & & 1 & 0 & \\ 0 & 1 & \cdots & 0 & 1 & \cdots \\ 0 & 0 & & 0 & 0 & \end{array}\right]$$

$$Z = [Z_1, Z_2, \ldots, Z_j, \ldots]$$

we can express the equations of motion in the standard form (6.56)–(6.57) with

$$G = \begin{bmatrix} I_3 & \bar{I} & Z \\ 0 & 0 & G_\eta \\ 0 & G_\xi & 0 \end{bmatrix}.$$

A Control Configuration for System Slewing and LOS Pointing Slewing and pointing control of the optical LOS of a typical beam expander for a SBL system will require system slewing and alignment of the primary and secondary mirrors of the optical system. Such requirements are typical of various large aperture optical systems. With reference to our two-body SBL model the primary body inertial attitude—given by, ξ_b, in Euler angles, (or γ_b, in Gibbs parameters)—represents the system pointing of the primary mirror. Optical misalignments contributing to LOS pointing errors can be described by *misalignment variables*;

$$y_4 = \theta(\ell) + s_1\eta_1(\ell) \tag{6.76}$$

$$y_5 = \phi(\ell) - s_1\eta_2(\ell) \tag{6.77}$$

where s_1 is a sensitivity parameter which depends on the optical components. Then slewing of the system LOS can be viewed as a problem of slewing the primary body attitude while regulating the misalignment variables to zero.

Nonminimum Phase Characteristics and Actuation We assume that control is implemented by three independent external torques applied to the primary system body together with two independent control forces applied at the secondary body. To implement PLF control for the resulting 5-input/5-output problem we first identify stability characteristics of the zero dynamics. Since our concern is with regulation of the primary system outputs consisting of the system outputs ξ_b and the misalignment variables and stability of the elastic structure with respect to its undeformed state we focus attention on the stability properties of the linear perturbation model for the flexible structure as $\xi_b = 0$ and $y_4 = y_5 = 0$. In this case, the local stability of the zero dynamics in a neighborhood of the undeformed state can be determined from the zeros of the transfer function describing dynamics of the linear perturbation model.

The sensitivity parameter which defines the misalignments contributes to the stability properties as shown Figure 6.8. The zero locus shows a nonminimum phase condition occurs for s_1 small enough. The parameter s_1 can be seen as a sensitivity factor that proportions the importance of the linear deformations relative to the angular deformations in the outputs and indicates that it is difficult to control angles using forces instead of torques.

Practical Aspects of Implementing PLF Compensation for Nonminimum Phase Systems The above simple model indicates how parametric sensitivities can change the nature of the nonlinear control problem considered. Available theory for PLF compensation is predicated on the assumption that the system is nonminimum phase. At this point in our study we were interested in considering practical situations which might be encountered in experiments which violated the assumptions which might limit application of PLF control. We wanted to investigate several questions: To what extent model order reduction in the design of PLF compensation is effected by nonminimum phase characteristics? Systems with

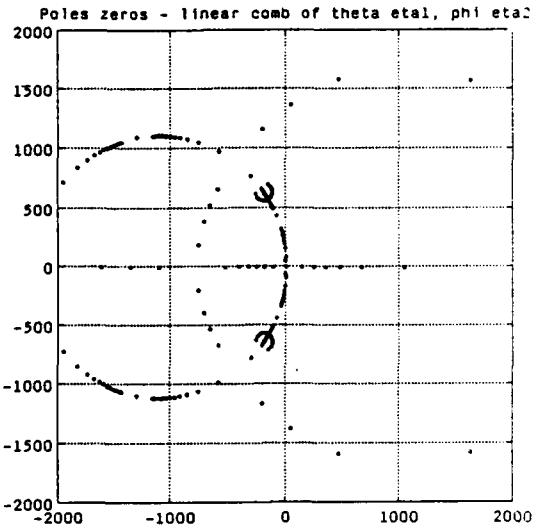

Figure 6.8: Locus of zeros for model **MODE** as s_1 is increased

very fast unstable zero dynamics modes will be characterized by linear models with right half plane zeros which are far from the imaginary axis. Can model reduction schemes be adapted to remove such characteristics from the nominal design model? If PLF compensation is then designed for the reduced and minimum phase model, can it be applied reliably to the full order system?

For implementation and robustness evaluation of PLF control we chose a value of s_1 which gives nonminimum phase behavior. We first applied modal truncation to the open loop system model retaining various order models to determine if a nonminimum phase model could be found. The poles and zeros of various reduced order models using modal truncation appear in Tables 6.5 and 6.6. The number of retained dynamic degrees of freedom is indicated as r. For $r = 6$ the linear perturbation model has no right half plane zeros. However, for $r = 7$ a right half plane zero appears indicating a nonminimum phase condition. Simulation studies were performed to test the behavior of the nonlinear system response with PLF compensation implemented based on the reduced order system model. Cases with $5 < r < 7$ revealed stable responses.

6.5 Design Example: Slewing Control with Noncollocation of Control and Primary outputs

In the ASTREX test article configuration, the rigid body torques are to be generated by cold gas thrusters located a distance from the center of mass of the system, which is the location of the attitude sensors. To simulate the effects of this non-colocation configuration, simulations model **MODD** and **MODF** were designed so that forces F_x and F_y at the end of the truss are to be used to control γ_b. The torque produced by these forces was limited to the

Reduced order model poles	
r = 11	r = 7
(3) 0.00e+00 ± 0.00e+00i	(3) 0.00e+00 ± 0.00e+00i
-2.59e+00 ± 7.58e+01i	-2.59e+00 ± 7.58e+01i
-3.54e+00 ± 8.86e+01i	-3.54e+00 ± 8.86e+01i
-8.89e+01 ± 4.35e+02i	-8.89e+01 ± 4.35e+02i
-9.13e+01 ± 4.41e+02i	-9.13e+01 ± 4.41e+02i
(2) -1.89e+02 ± 6.20e+02i	
(2) -1.31e+03 ± 1.09e+03i	
r = 6	r = 5
(3) 0.00e+00 ± 0.00e+00i	(3) 0.00e+00 ± 0.00e+00
-2.59e+00 ± 7.58e+01i	-2.59e+00 ± 7.58e+01i
-3.54e+00 ± 8.86e+01i	-3.54e+00 ± 8.86e+01
-8.89e+01 ± 4.35e+02i	

Table 6.5: Poles of reduced order model by modal truncation

Reduced order model zeros			
r = 11	r = 7	r = 6	r = 5
-2.64e+03 + 2.60e-12i	-2.04e+03 ± 6.04e+02i	-2.05e+03 ± 5.95e+02i	No Finite Zeros
-1.92e+03 - 2.81e-12i	-2.50e+02 - 5.49e-13i		
-6.71e+02 ± 5.15e+02i	3.23e+02 + 5.75e-13i		
-2.59e+02 + 1.43e-12i			
-2.03e+02 ± 6.40e+02i			
-1.94e+02 ± 6.28e+02i			
7.34e+01 ± 1.39e+03i			
3.38e+02 - 1.01e-13i			

Table 6.6: Zeros of reduced order model by modal truncation

maximum torque avaliable on ASTREX for attitude control. These maximum torque values were determined from the thruster specifications and the moment arms measured relative to the x, y, and z axes. The thruster locations are shown in Figure 6.9, and each produces a maximum thrust of 889.6 N. This configuration yields the following maximum body torques which were used for all simulations except those of model `MODD`:

$$\begin{aligned} \tau_{max_x} &= 8600\ Nm \\ \tau_{max_y} &= 4964\ Nm \\ \tau_{max_z} &= 4964\ Nm \end{aligned}$$

The equivalent maximum forces used for F_x and F_y in simulations `SIMD1-SIMD5` appear below.

$$\begin{aligned} F_{x_{max}} &= 992.8\ N \\ F_{y_{max}} &= 1720.0\ N \end{aligned}$$

A pole–zero plot of the linear perturbation model of this system appears in Figure 6.10 and shows a stable and nonminimum phase response. Simulations for various reduced order models for a maneuver of

$$\gamma_b = [0.05, 0.05, 0]$$

(or in Euler angles,

$$[\psi, \theta, \phi] = [0.3°, 5.7°, 5.7°])$$

appear in Appendix A. Various model order reductions were tested for implementation of PLF compensation for slewing of the primary body attitude and regulation of the misalignments.

Rapid Slewing with multiple modes of actuation. As discussed in the report [Benn89] the use of combined continuous and discontinuous modes of actuation can be incorporated in the rapid slewing and precision pointing problem. Focusing attention on the physical limitations of the ASTREX facility we performed simulation studies of primary body slewing as above but operating the applied forces at the end of the appendage in discontinuous mode. In a physical system the applied forces might be obtained using reaction jets. A critical technology being developed for the ASTREX facility involves throttleable cold gas jets. In our model we have assumed the jets can be modeled as providing pure external forces which can change subject to slew rate limiting.

6.6 Summary of Simulation Results for Rapid Slewing and Precision Pointing

A computer simulation of the SBL two-body model was developed in PC-MATLAB to evaluate slewing and LOS pointing performance. The simulation model parameters shown in Table 6.7 are taken roughly from available data on the ASTREX test article.

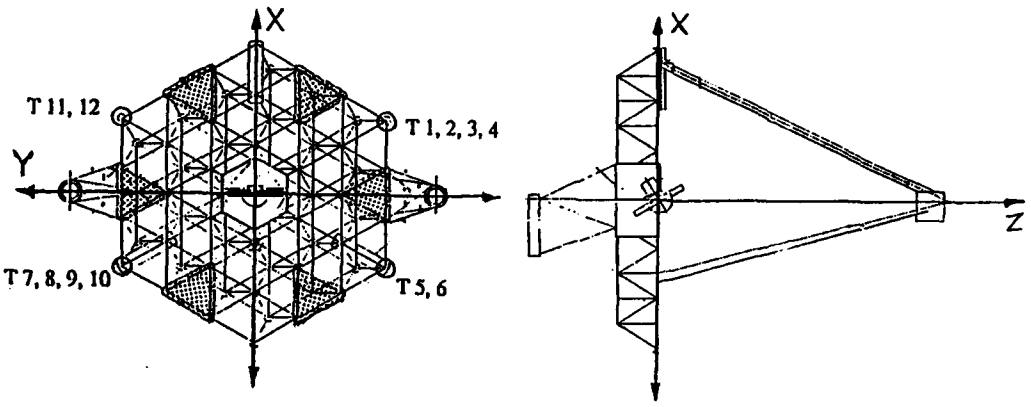

Figure 6.9: Thruster locations - ASTREX test article

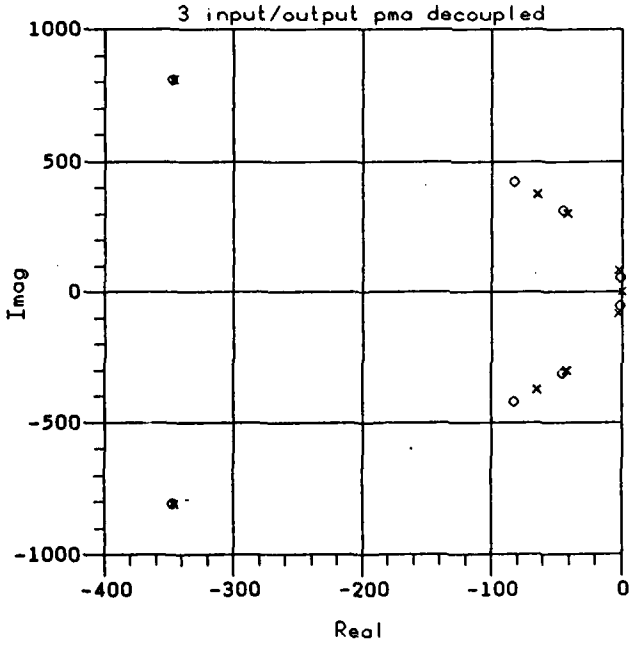

Figure 6.10: Poles and zeros of models **MODD**

As can be seen from the table, five simulation models with three input/output configurations were developed. The purpose of models **MODA**, **MODB**, and **MODC** was to examine how slewing performance was affected when passive absorbers were added to the end of the truss. These models were configured with the control inputs as rigid body torques, τ_b, at each axis and measured outputs as the rigid body attitude, γ_b, in Gibbs vector form. Figure 6.11 illustrates the input output configuration for these models. Also, two passive absorber devices, described in detail above, are located at the end of the truss for vibration damping. The three models differed only in the values of the parameters chosen for the spring and damper constants. In Model **MODA**, the parameters were tuned for optimal transient response as described above. In model **MODB**, the passive damper was tuned to twice the highest **MODAl** frequency to put it in a de-tuned configuration, and model **MODC** the passive damper was decoupled from the truss by making both the spring and damper constant equal to zero. Tradeoff studies comparing simulation results of these models were performed.

The purpose of model **MODD** was to examine how non-colocated sensing and actuation affects slewing performance. This is important because the ASTREX test article is configured such that body torques are generated by thrusters that are not located at the center of mass of the body which is the location of the attitude sensors. In order to simulate this non-colocated condition, model **MODD**, shown in Figure 6.12 was set up with control inputs as two force actuators, F_x and F_y, at the end of the truss and a torque τ_3, about axis three and measured outputs as the rigid body attitude ,γ_b, in Gibbs vector form. Although this configuration is not an exact representation of the thruster placement on ASTREX, it provided us with an approximate model to study this non-colocated condition.

Finally, the purpose of model **MODE** was to examine slewing performance and stability of the SBL with additional force actuators added at the end of the truss to control its vibration. Model **MODE**, shown in Figure 6.13 was set up with the control inputs as two force actuators, F_x and F_y, at the end of the truss and rigid body torques, τ_b, at each axis and measured outputs as the rigid body attitude, γ_b, in Gibbs vector form and two additional outputs relating to the line of sight error.

Table 6.8 identifies the simulations performed for each model along with the corresponding control law. Each simulation is summarized in Appendix A by plots illustrating responses of position, γ_b, attitude rate, $\dot{\gamma}_b$, primary body torques, τ_b, any external forces, F_x, F_y , etc., any other outputs, and deflections at the end of the truss, $\eta(\ell), \xi(\ell)$.

6.7 Experimental Protocol for Validation of PLF: Mode Locking Experiments

A principal objective of the proposed experiments is to verify the effectiveness of PLF compensation by validating the extent to which distinctly nonlinear behavior, observable in the system principal input-output responses for attitude slewing and pointing, can be compensated. Our view is that the occurrence of *mode locking* (sometimes called *phase locking* or entrainment [GH83]) offers a framework for observing nonlinear response of pointing and tracking control loops in experiments. Such nonlinear behavior can always occur when

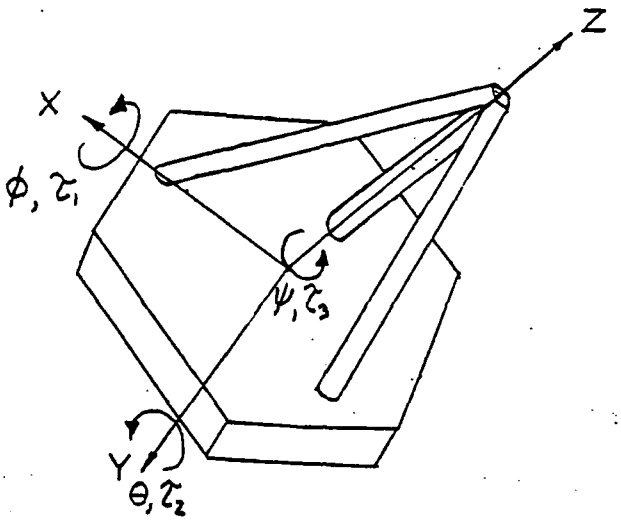

Figure 6.11: **MODA**, **MODB**, **MODC** input/output configuration

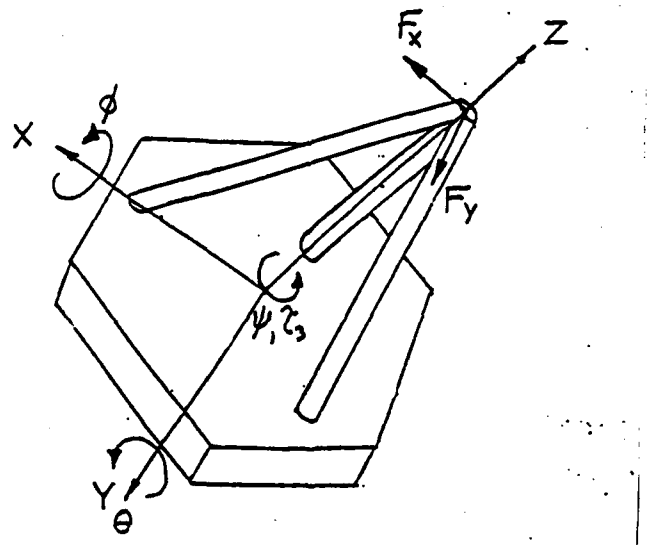

Figure 6.12: **MODD** input/output configuration

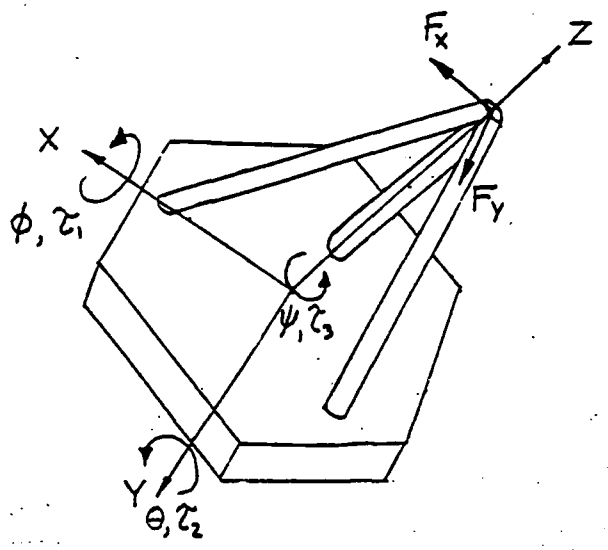

Figure 6.13: MODE input/output configuration

Parameter	Simulation Model				
	MODA	MODB	MODC	MODD	MODE
	SBL beam expander model parameters				
ρ - mass density	1520	-	-	-	-
E - elasticity	1.6E9	1.6E9	1.6E9	4E8	1.6E9
N - # finite elements	2	-	-	-	-
ϵ damping factor	.0009	-	-	-	-
m_ℓ/m_{tot}	0.05	0.05	0.05	0.0	0.05
	Control/Actuator parameters				
outputs	γ_b	γ_b	γ_b	γ_b	γ_b ,LOS
inputs	τ_b	τ_b	τ_b	τ_3, F_x, F_y	τ_b, F_x, F_y
α_{max} [rad/sec^2]	.1745	-	-	-	-
T_{max} Peak Torque	ASTREX	-	-	-	-
g_1 - control gain	5.E9	5.E9	5.E9	5.E9	5.E9
g_2 - control gain	0.0374	-	-	-	-
	Passive absorber parameters				
K - spring constant	3.9E4	5.9E7	0	0	0
B - damping constant	370	0	0	0	0

Table 6.7: Matrix of Simulation Models Considered

Models	Control Laws								
	Continuous PLF/Slewing							Discontinuous PLF/Slewing	
	$r=3$	$r=4$	$r=5$	$r=6$	$r=7$	$r=11$	$r=13$	Slew rate limited torque	Discontinuous torque
	Multiaxis Slew								
MODA	SIMA1	SIMA2	SIMA3	SIMA4	SIMA5		SIMA6		SIMA7
MODB	SIMB1	SIMB2	SIMB3				SIMB4		
MODC	SIMC1		SIMC2		SIMC3				
MODD	SIMD1		SIMD2		SIMD3	SIMD4		SIMD5	
MODE			SIME1	SIME2					

Table 6.8: Matrix of PLF/Slewing Control Implementations

conventional linear attitude control design is applied for multiaxis attitude control implementation, but can be removed by the use of PLF compensation. Mode locking is only one of several types of nonlinear phenomenon which might be considered for experimental demonstration. We propose to focus experiments on demonstration of mode locking for several reasons: mode locking is easy to observe in experiments, is repeatable, and a distinctly nonlinear phenomenon. Mode locking is also of fundamental significance to achievable accuracy of precision pointing control laws for space craft attitude both with and without flexible, multibody interactions.

Mode locking can be readily demonstrated in attitude slewing and pointing experiments with the ASTREX facility and initial test article since it requires relatively small angle motions and can (in principal) be demonstrated in various frequency bands. The experiments require periodic excitation of the system attitude which permits focusing attention on the frequency response and its dependence on elastic interactions at higher frequencies. This is significant for the experimental protocol we have planned in which we emphasize the relationship between control law precision and closed loop bandwidth. Multibody interactions and structural flexure will complicate the types of mode locking possible but its demonstration in experiments should still be easy to observe.

Moreover, mode locking is a relevant factor in control system performance. It is well known that certain nonlinear affects can significantly degrade feedback system performance such as accuracy of tracking. Mode locking will contribute to a degradation of closed loop tracking. From the perspective of nonlinear dynamics it is well known that mode locking is often a precursor to chaotic behavior [BBJ84] which, in the case of closed loop tracking, would imply a complete loss of tracking effectiveness.

In principle, PLF can be used to compensate for the nonlinear interactions which cause mode locking, as well as other, more complicated, dynamical behavior. Thus, feedback linearization should be viewed as a means for introducing nonlinear compensation in the design of feedback loops for achieving *robust precision tracking* as well as executing large

angle, multi-axis slewing.

Mode Locking Experimental Protocol. We next describe in general terms the protocol for experimental demonstration of mode locking in the context of attitude control and compensation by PLF.

Mode locking is a phenomenon associated with nonlinear dynamics involving interactions of periodic motions with at least two distinct frequencies. The underlying periodic behavior may be self induced or associated with external excitation as in active control loops. The simplest and most common example of a system exhibiting mode locking is the periodically forced Van der Pol oscillator [Sto50, GH83, TS86]. In this case, the system exhibits a self excited oscillation (limit cycle). Many other periodically forced and/or interconnected oscillators have been studied using both analytical and experimental demonstrations of mode locking [Sto50, GH83, TS86, BBJ84].

One experiment would involve the design and testing of multiaxis attitude tracking control. The experiment would involve driving the attitude control loops with two independent periodic command signals. To demonstrate small signal tracking response of the attitude control loops one could use command signals as,

$$\phi_c(t) = A_1 \sin \omega_1 t, \quad \theta_c(t) = A_2 \sin \omega_2 t,$$

whereas, to demonstrate slewing response the commands would be replaced with their square wave equivalent. In either case, we anticipate mode locking to be observed in the following way. First, assume that A_2, ω_2 are fixed and A_1, ω_1 are adjustable parameters. As $A_1 \to 0$ we expect to observe a periodic oscillation in the system attitude response of frequency ω_2. Clearly, if A_2 is small the system response is near that of a linear system which can be confirmed in the experiment as follows. Define the ratio, $\Omega := \frac{\omega_2}{\omega_1}$ and choose integers, p, q with $q > p$, then the frequencies are said to be commensurable if they satisfy the relation,

$$p\omega_1 - q\omega_2 = 0$$

and $\Omega = p/q$ is a rational number. For sufficiently small driving amplitude A_1, the system attitude response will be periodic with frequency ω_2 and q is a subharmonic number associated with this periodic motion. For linear systems, if Ω is not rational then the attitude motions are not periodic.

For the nonlinear system, if Ω is not rational and A_1 is small, the motion will not be periodic (as in the linear case). However, if the driving amplitude A_1 is increased then—after a transient—the motion will again become periodic. This, of course, is distinctly nonlinear behavior. The periodic motions are called *mode locked* (or simply *locked*). The aperiodic motions are referred to as *drifting* behavior. Such behavior is typical of nonlinear systems and can be readily demonstrated in experiments. It is common to display mode locking responses as regions of locked and drift behavior in a (A, Ω) parameter space diagram as shown in Figure 6.14. Periodic (locked) and aperiodic (drift) can be readily identified in measured attitude responses observed in experiments.

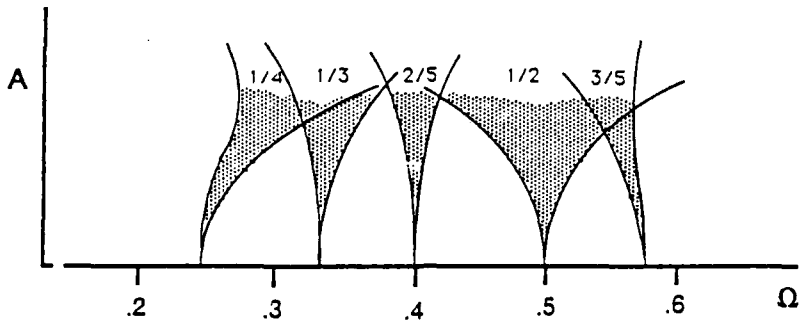

Figure 6.14: Typical parameter space diagram showing regions of locked (shaded) and drift behavior.

We expect that mode locking will be observable when a conventional attitude controller is used because the nonlinear kinematic and dynamic couplings are *not* explicitly compensated by the closed loop control law. The extent to which online implementation of PLF compensation can reduce nonlinear coupling will be clearly evident by comparing the closed loop responses of multiaxis attitude control loops with and without PLF compensation. The goal is to provide distinct qualitative changes in dynamic response representing nonlinear coupling. Since mode locking is demonstrated by driving the system with periodic signals and observing periodic responses one can focus the experiment on tracking behavior in specific frequency bands. This permits considerable flexibility in investigating the interaction with internal nonlinear resonances due to multibody and flexible mode interactions. We anticipate that this flexibility will be extremely important the interaction between the choice of reduced models for structural flexure and the design of multiloop tracking systems.

7 Conclusions and Directions

The principal conclusions from the three year study are that feedback linearization offers a comprehensive approach to the design and implementation of precision control laws for rapid slewing and precision pointing of multibody systems with structural flexure. The methodology for design and implementation of control laws for nonlinear systems offers a fundamental approach which can be readily employed for a wide variety of system designs. Specific concept designs were completed and simulation studies revealed that robust control performance can be obtained with reduced order models. Parametric uncertainty in models can affect performance of PLF compensation. In this study adaptive control techniques have been described which can correct for parameter uncertainty. We have shown that certain standard parameter adaptive methods which have been developed for linear systems (e.g. model reference schemes) may be inadequate or awkward for adaptive PLF compensation. For such problems we have shown an alternate adaptive control method which achieves asymptotic stability under much less restrictive assumptions on the structure of the nonlinearities.

It is our recomendation that validation of achievable levels of performance with PLF compensation can best be established from laboratory experiment employing actuators characteristic of space applications. Providing for multiaxis, large angle motions in the experiment can demonstrate significant nonlinear couplings. We have outlined a protocol for validating the significance of these nonlinear couplings and the extent to which they can be compensated using PLF. The protocol is involves observing steady state controlled motions with periodic reference signals as inputs to the control system.

References

[AB87] O. Akhrif and G.L. Blankenship. Using computer algebra in the design of nonlinear control systems. Proc. ACC, 1987.

[AB88] O. Akhrif and G. L. Blankenship. Robust stabilization of feedback linearizable systems. In *Proc. 27th IEEE Cont. Dec. Conf.*, 1988.

[ABB89] O. Akhrif, G.L. Blankenship, and W.H. Bennett. Robust control for rapid reorientation of flexible structures. In *Proc. 1989 ACC*, pages 1142–1147, 1989.

[Aga84] A. S. Agarwala. *Modeling and Simulation of Hyperbolic Distributed Systems Arising in Process Dynamics.* PhD thesis, Drexel Univ., June 1984.

[Akh89] O. Akhrif. *Nonlinear Adaptive Control with Application to Flexible Structures.* PhD thesis, University of Maryland, College Park, MD, 1989.

[AM78] R. Abraham and J. E. Marsden. *Foundations of Mechanics.* Benjamin/Cummings, Reading, MA, 1978.

[Arn78] V.I. Arnold. *Mathematical Methods of Classical Mechanics.* Springer-Verlag, New York, 1978.

[Bal78] M.J. Balas. Modal control of certain flexible dynamic systems. *SIAM J. Control*, 16:450–462, 1978.

[BBJ84] P. Bak, T. Bohr, and M.H. Jensen. Mode-locking and the transition to chaos in dissipative systems. *Phys. Sci.*, T9:50–58, 1984.

[BBKA88] W. H. Bennett, G. L. Blankenship, H. G. Kwatny, and O. Akhrif. Nonlinear dynamics and control of flexible structures. Technical Report SEI-88-11-15-WB, SEI, November 1988. AFOSR/AFSC contract F49620-87-C-0103.

[BBKA89] W. H. Bennett, G. L. Blankenship, H. G. Kwatny, and O. Akhrif. Nonlinear dynamics and control of flexible structures. Technical Report TSI-89-11-15-WB, TSI, November 1989. AFOSR/AFSC contract F49620-87-C-0103.

[BD90] A. K. Banerjee and J. M. Dickens. Dynamics of an arbitrary flexible body in large rotation and translation. *AIAA J. Guid. Cntrl.*, 13(2):221–227, 1990.

[BI84] C.I. Byrnes and A. Isidori. A frequency domain philosophy for nonlinear systems, with application to stabilization and adaptive control. In *Proc. IEEE CDC*, Las Vegas, NV, 1984.

[BI85] C. I. Byrnes and A. Isidori. Global feedback stabilization of nonlinear systems. In *Proc. 24th IEEE CDC*, pages 1031–1037, Dec. 1985.

[BK89] W.H. Bennett and H.G. Kwatny. Continuum modeling of flexible structures with application to vibration control. *AIAA J.*, 27(9):1264–1273, September 1989.

[BL87] J. Baillieul and M. Levi. Rotational elastic dynamics. *Physica 27D*, 27:43–62, 1987.

[Bro78] R.W. Brockett. Feedback invariants for nonlinear systems. In *Proc. 6th IFAC World Congress*, pages 1115–1120, Helsinki, 1978.

[CKEFKPB68] S. H. Crandall, D. C. Karnopp, Jr. E. F. Kurtz, and D. C. Pridmore-Brown. *Dynamics of Mechanical and Electromechanical Systems.* McGraw-Hill Book Co., New York, 1968.

[Dwy84] T. A. W. Dwyer. Exact nonlinear control of large angle rotational maneuvers. *IEEE Trans. on Auto. Control*, AC–29(9):769–774, 1984.

[DZM88] R. A. DeCarlo, S. H. Zak, and G.P. Matthews. Variable structure control of nonlinear multivariable systems: A tutorial. *Proc. IEEE*, 76(3):212–232, 1988.

[FH87] R. B. Fernandez and J. K. Hedrick. Control of multivariable nonlinear systems by the sliding mode method. *Int. J. Control*, 46(3):1019–1040, 1987.

[Fre66] A. M. Freudenthal. *Introduction to the Mechanics of Solids.* J. Wiley and Sons, New York, 1966.

[Fre75] E. Freund. The structure of decoupled nonlinear systems. *Int. J. Control*, 21(3):443–450, 1975.

[GH83] Guckenheimer and P. Holmes. *Nonlinear Oscillations, Dynamical Systems, and Bifurcations of Vector Fields.* Springer-Verlag, 1983.

[GL76] S. Gutman and G. Leitman. Stabilizing control for linear systems with bounded parameter and input uncertainty. In *Proc. 7th IFIP Conf. on Optimization Techniques*, page 729. Springer-Verlag, 1976.

[Gol82] H. Goldstein. *Classical Mechanics.* Addison-Wesley, Reading, MA, 1982.

[Hir79] R. M. Hirschorn. Invertibility of nonlinear control systems. *SIAM J. Optim. and Control*, 17(2):289–297, 1979.

[HSM83] R. Hunt, R. Su, and G. Meyer. Global transformation of nonlinear systems. *IEEE Trans. Automatic Control*, AC-28:24–31, 1983.

[Jos89] S. M. Joshi. *Control of Large Flexible Space Structures.* Springer-Verlag, 1989.

[KC87] C. Kravaris and C-B Chung. Nonlinear state feedback synthesis by global input/output linearization. *AIChE Journal*, 33(4):592–603, April 1987.

[KK89] H.G. Kwatny and H. Kim. Variable structure control of partially linearizable dynamics. In *Proc. 1989 ACC*, pages 1148–1153, 1989.

[KKO86] P.V. Kokotovic, H. Khalil, and J. O'Reilly. *Sinular Perturbation Methods in Control: Analysis and Design.* Academic Press, New York, 1986.

[Kok87] P. V. Kokotovic. *Singular Perturbations and Asymptotic Analysis in Control Systems*, volume 90, chapter 1. Springer-Verlag '87.

[Kra87] C. Kravaris. On the internal stability and robust design of globally linearizing control systems. In *Proc. ACC*, pages 270–279, 1987.

[KRB87] T. R. Kane, R. R. Ryan, and A. K. Banerjee. Dynamics of a cantilever beam attached to a moving base. *AIAA J. Guid. Cntrl.*, 10(2):139–151, 1987.

[Kre73] A. J. Krener. On the equivalence of control systems and linearization of nonlinear systems. *SIAM J. Cont. and Optim.*, 11:670, 1973.

[Le87] M. Lock and et al. Structural dynamic response of a space based laser system. Technical Report AD-B109 212, February 1987.

[Lio71] J.L. Lions. *Optimal Control of Systems Governed by Partial Differential Equations.* Springer-Verlag, New York, 1971.

[MC80] G. Meyer and L. Cicolani. Applications of nonlinear system inverses to automatic flight control design–systems concepts and flight evaluations. In P. Kent, editor, *Theory and Applications of Optimal Control in Aerospace Systems*, pages 10–1–29. NATO AGARD, 1980. AGARDograph 251.

[Mei67] L. Meirovich. *Analytical Methods in Vibrations.* McMillan, New York, 1967.

[Pos88] T.A. Posbergh. *Modeling and Control of Mixed and Flexible Structures.* PhD thesis, University of MD, 1988.

[Pre75] P. M. Prenter. *Splines and Variational Analysis.* Wiley-Interscience, New York, 1975.

[RM57] R. D. Richtmeyer and K.W. Morton. *Difference Methods for Initial-Value Problems.* Wiler: Interscience, New York, 1957.

[SF73] G. Strang and G. J. Fix. *An Analysis of the Finite Element Method.* Prentice-Hall, Englewood Cliffs, NJ, 1973.

[SHK89] S. Sastry, J. Hauser, and P Kokotovic. Zero dynamics of regularly perturbed systems are singularly perturbed. Technical Report Memo. No. UCB/ERL M89/54, Elect. Res. Lab., Univ. Calif., Berkeley, May 1989.

[Sok56] I. S. Sokolnikoff. *Mathematical Theory of Elasticity.* McGraw-Hill, New York, 1956.

[Spo87] M. W. Spong. Modeling and control of elastic joint robots. *J. Dynamic Sys., Meas. Cntrl.*, 109:310–319, 1987.

[Sta79] I. Stakgold. *Green's Functions and Boundary Value Problems.* John Wiley and Sons Inc., NY, 1979.

[Sto50] J.J. Stoker. *Nonlinear Vibrations.* Wiley Interscience, 1950.

[SV87] M. W. Spong and M. Vidyasagar. Robust linear compensator design for nonlinear robotic control. *IEEE J. Robotics Auto.*, RA-3(4):345–351, 1987.

[SVQ86] J. C. Simo and L. Vu-Quoc. On the dynamics of flexible bodies under large overall motions—the planar case: Parts I & II. *J. Applied Mech.*, 53:849–863, 1986.

[SVQ88] J. Simo and L. Vu-Quoc. The role of nonlinear theories in transient dynamic analysis of flexible structures. *J. Sound & Vibration*, 119:487–508, 1988.

[TS86] J. M. T. Thompson and H. B. Stewart. *Nonlinear Dynamics and Chaos.* J. Wiley and Sons, 1986.

[VQS87] L. Vu-Quoc and J. C. Simo. Dynamics of earth-orbiting sateliites with multibody components. *J. Guid. Cntrl. Dyn.*, 10:549–558, 1987.

A Simulated Slewing Response for Several Control Laws

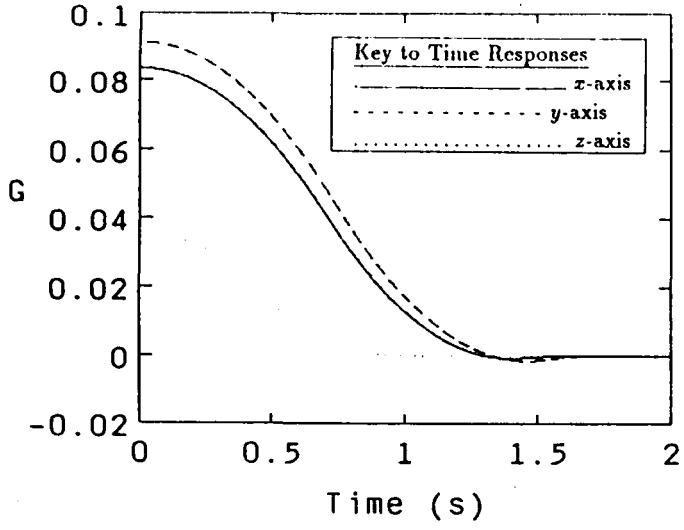
Key to Time Responses
x-axis
y-axis
z-axis
G
0.1
0.08
0.06
0.04
0.02
0
-0.02
0
0.5
1
1.5
2
Time (s)

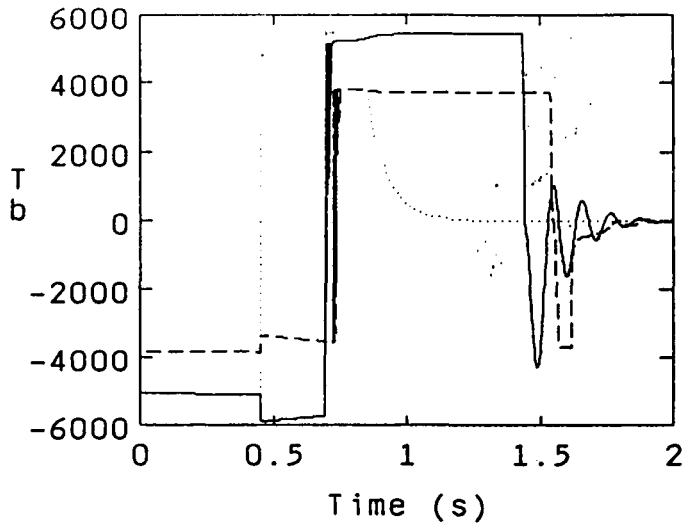
T
b
6000
4000
2000
0
-2000
-4000
-6000
0
0.5
1
1.5
2
Time (s)

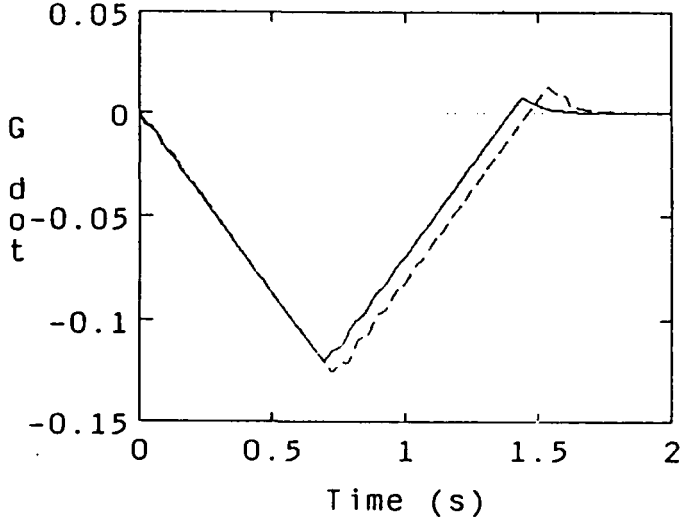
G
d
o
t
0.05
0
-0.05
-0.1
-0.15
0
0.5
1
1.5
2
Time (s)

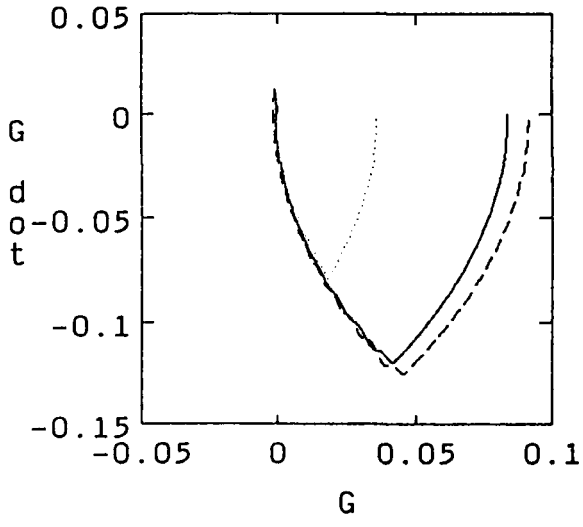
G
d
o
t
0.05
0
-0.05
-0.1
-0.15
-0.05
0
0.05
0.1
G

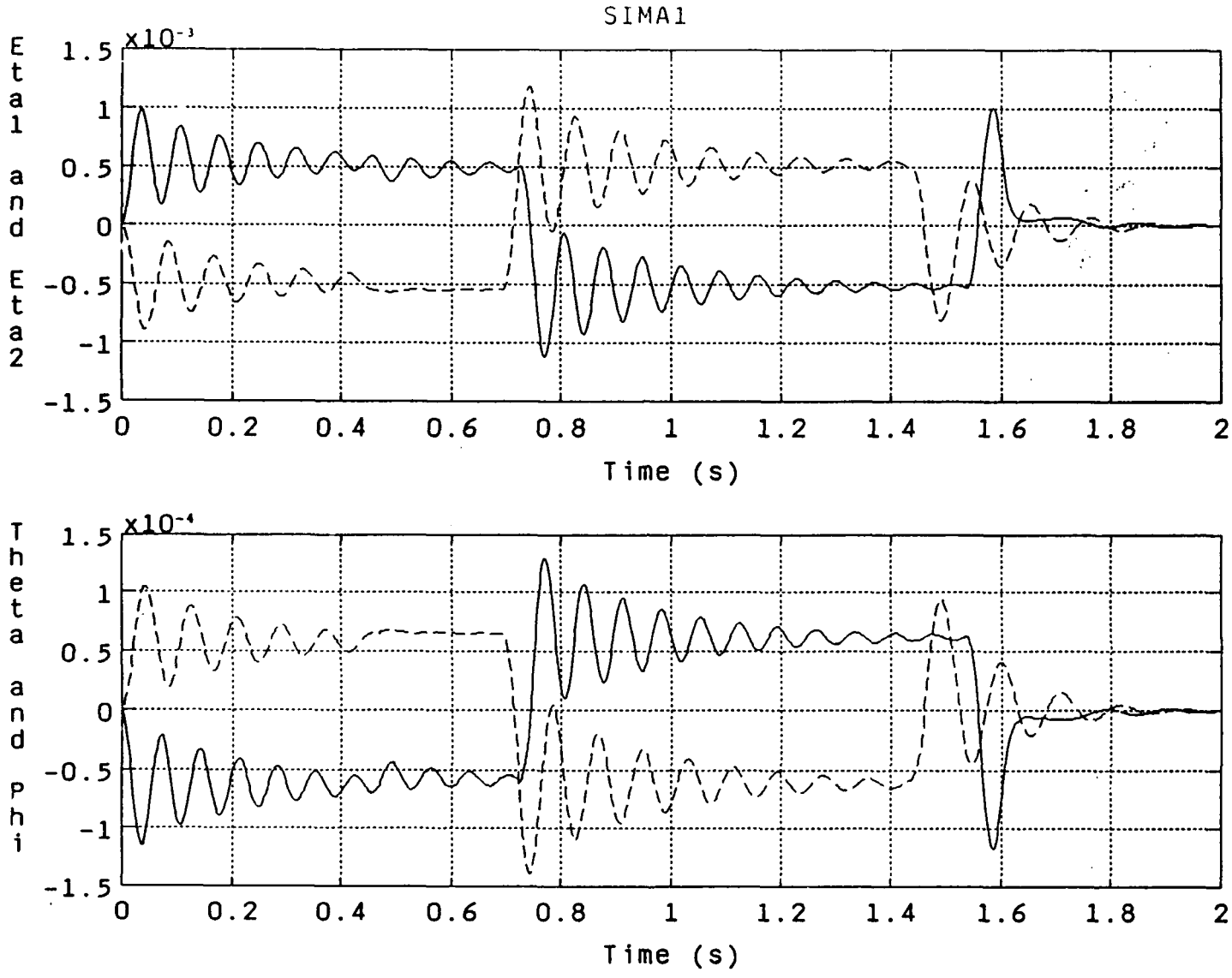
SIMA1
x10⁻³
Eta1 and Eta2
1.5
1
0.5
0
-0.5
-1
-1.5
0
0.2
0.4
0.6
0.8
1
1.2
1.4
1.6
1.8
2
Time (s)
x10⁻⁴
Theta and phi
1.5
1
0.5
0
-0.5
-1
-1.5
0
0.2
0.4
0.6
0.8
1
1.2
1.4
1.6
1.8
2
Time (s)

SIMA2

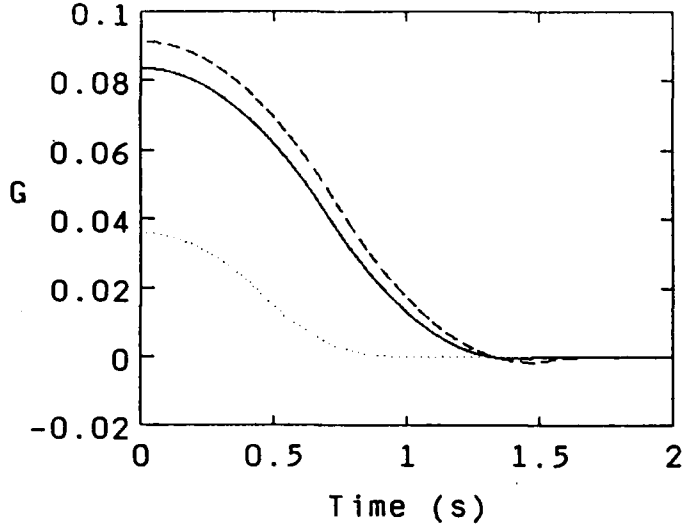
0.1
0.08
0.06
G
0.04
0.02
0
-0.02
0
0.5
1
1.5
2
Time (s)

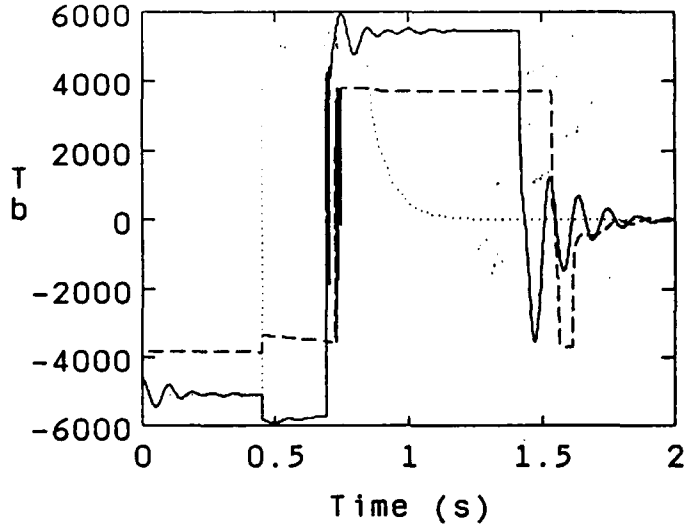
6000
4000
2000
T
b
0
-2000
-4000
-6000
0
0.5
1
1.5
2
Time (s)

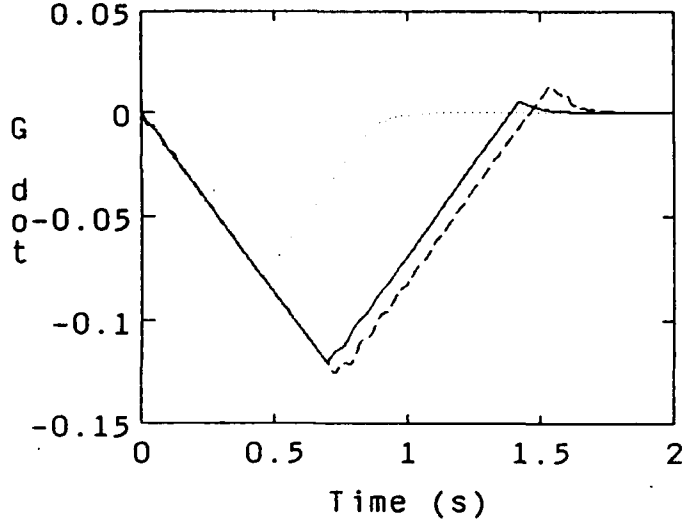
0.05
0
G
d
o-0.05
t
-0.1
-0.15
0
0.5
1
1.5
2
Time (s)

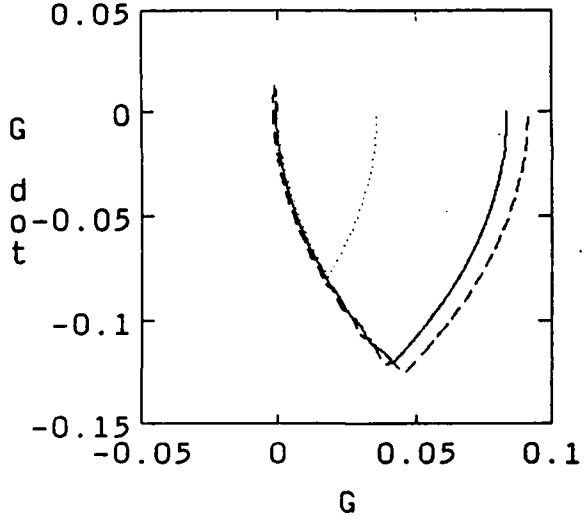
0.05
0
G
d
o-0.05
t
-0.1
-0.15
-0.05
0
0.05
0.1
G

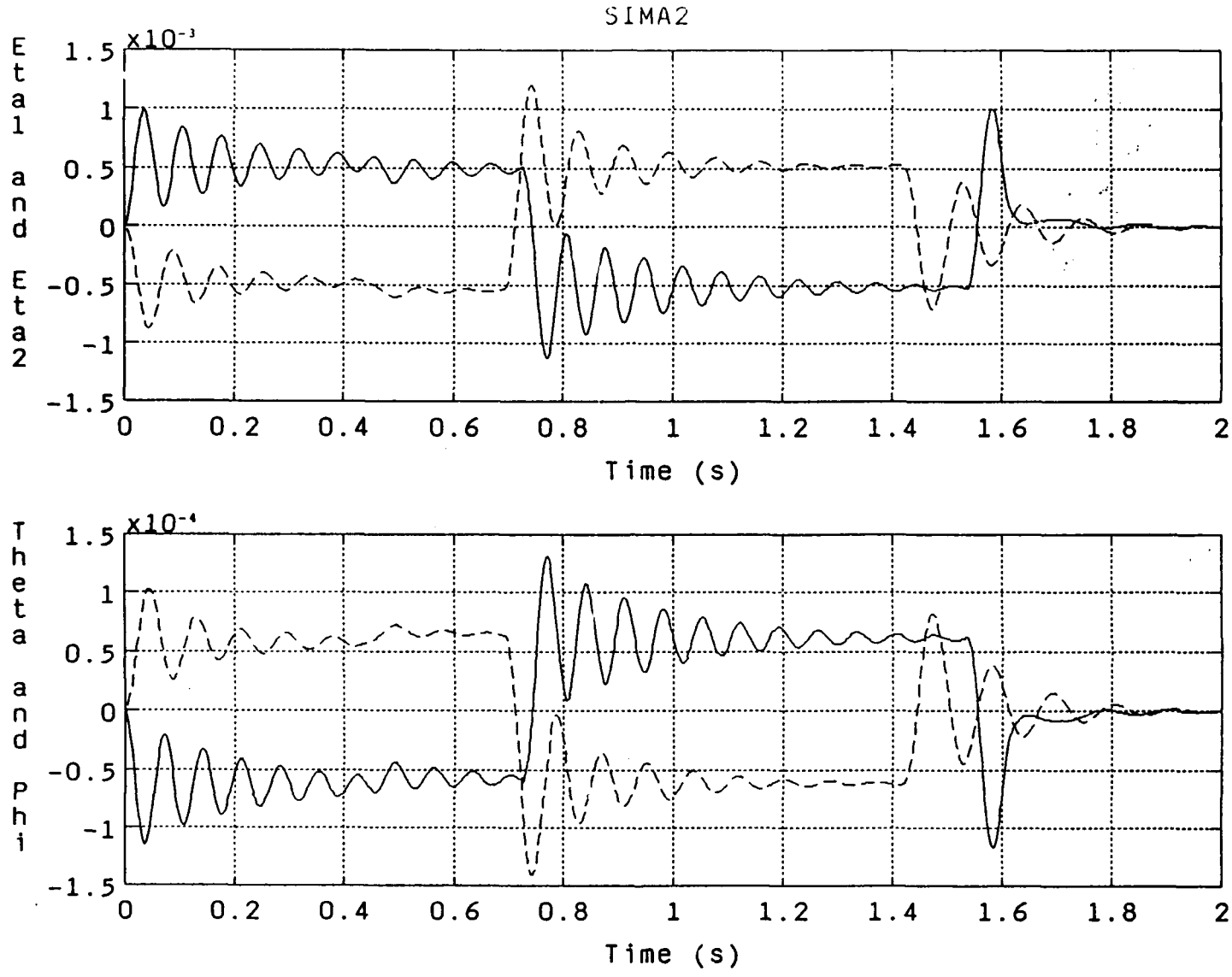
SIMA2
x10⁻³
Eta1 and Eta2
1.5
1
0.5
0
-0.5
-1
-1.5
0
0.2
0.4
0.6
0.8
1
1.2
1.4
1.6
1.8
2
Time (s)
x10⁻⁴
Theta and Phi
1.5
1
0.5
0
-0.5
-1
-1.5
0
0.2
0.4
0.6
0.8
1
1.2
1.4
1.6
1.8
2
Time (s)

SIMA3

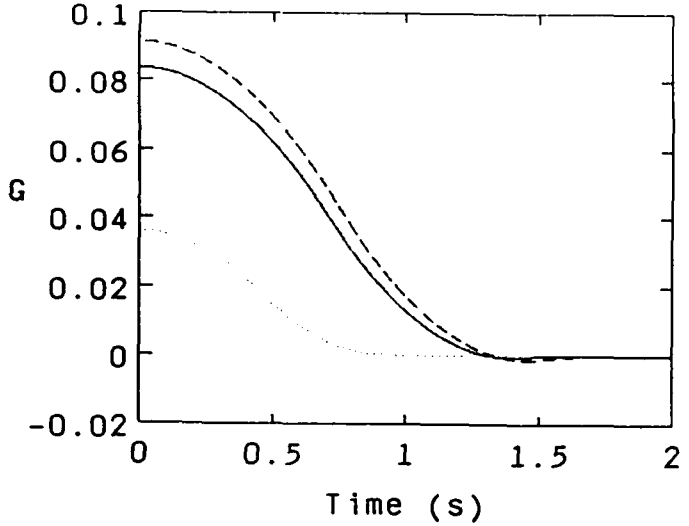
0.1
0.08
0.06
0.04
0.02
0
-0.02
G
0
0.5
1
1.5
2
Time (s)

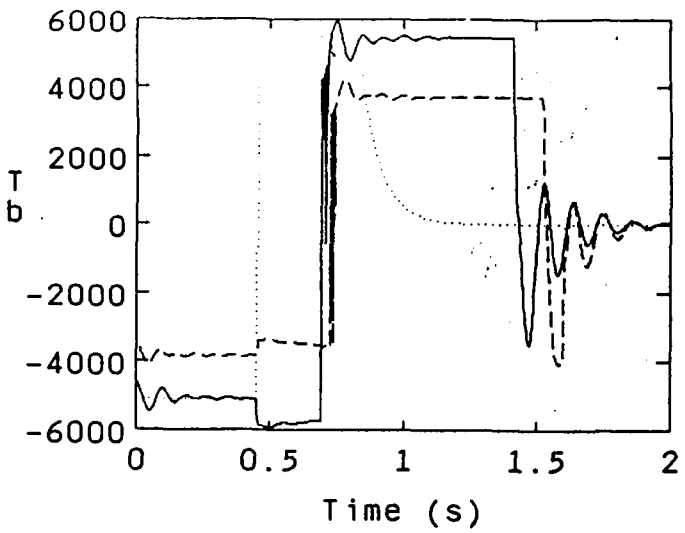
6000
4000
2000
0
-2000
-4000
-6000
T
b
0
0.5
1
1.5
2
Time (s)

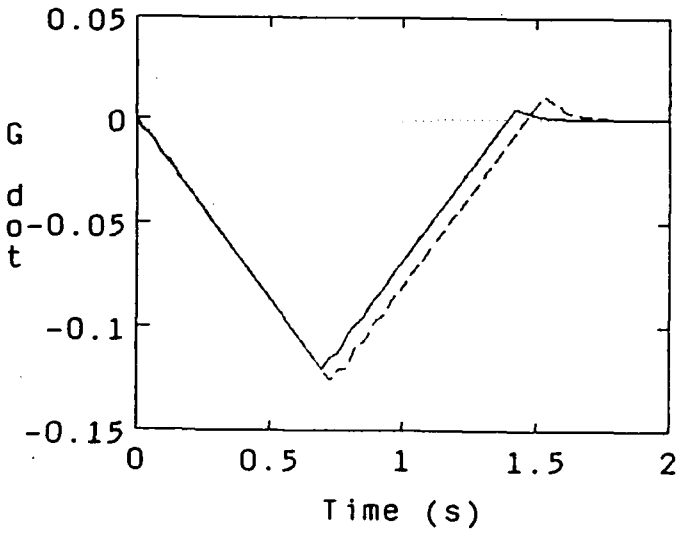
0.05
0
-0.05
-0.1
-0.15
G
d
o
t
0
0.5
1
1.5
2
Time (s)

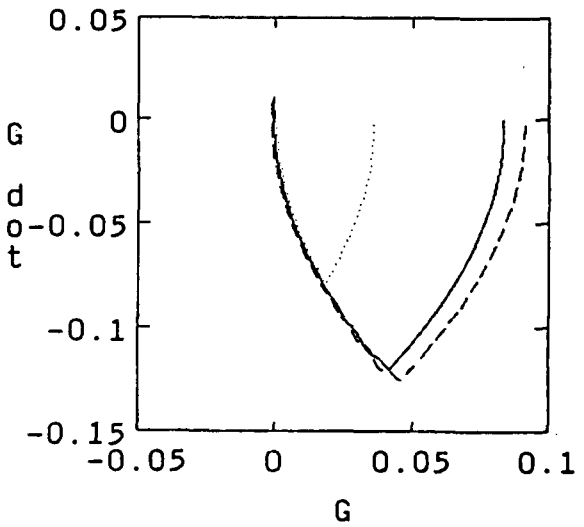
0.05
0
-0.05
-0.1
-0.15
G
d
o
t
-0.05
0
0.05
0.1
G

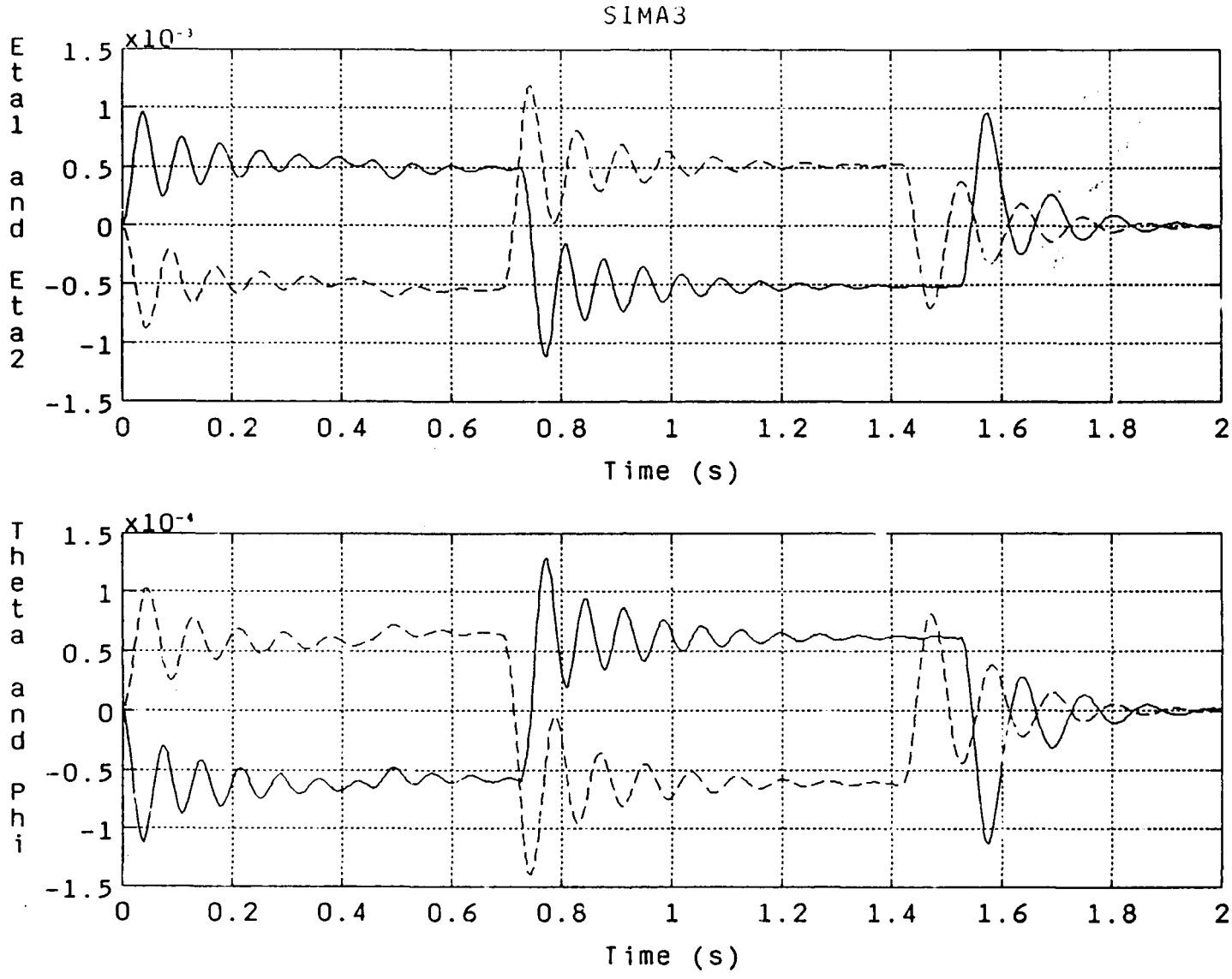
SIMA3
x10⁻³
Eta1 and Eta2
1.5
1
0.5
0
-0.5
-1
-1.5
0
0.2
0.4
0.6
0.8
1
1.2
1.4
1.6
1.8
2
Time (s)
x10⁻⁴
Theta and Phi
1.5
1
0.5
0
-0.5
-1
-1.5
0
0.2
0.4
0.6
0.8
1
1.2
1.4
1.6
1.8
2
Time (s)

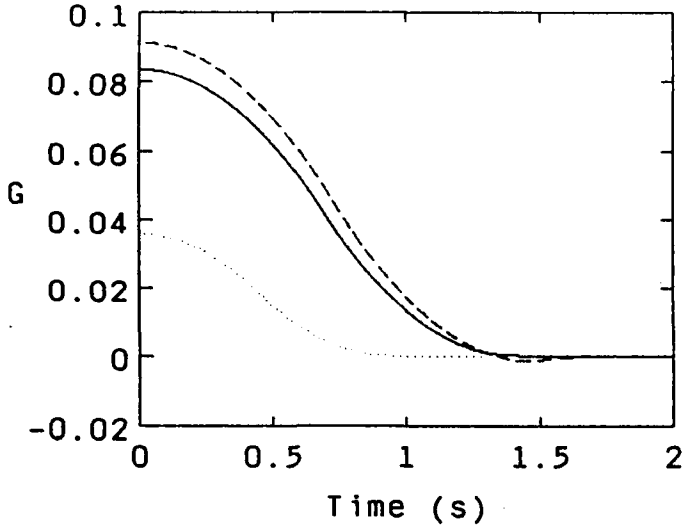
0.1
0.08
0.06
G
0.04
0.02
0
-0.02
0
0.5
1
1.5
2
Time (s)

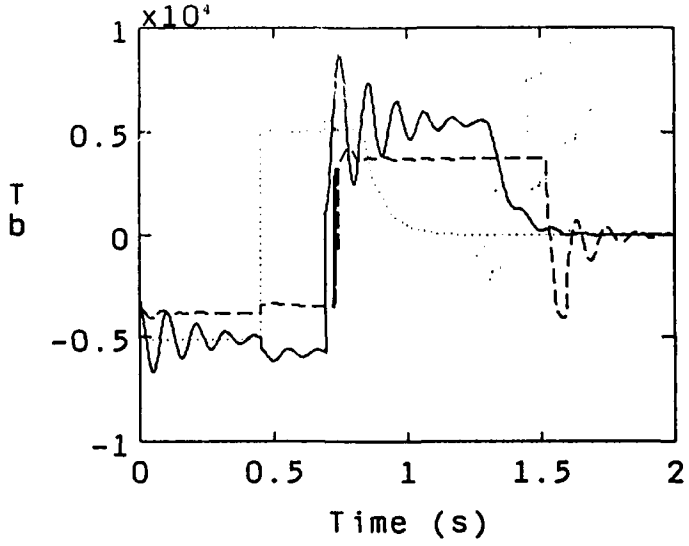
x10⁴
1
0.5
T
b
0
-0.5
-1
0
0.5
1
1.5
2
Time (s)

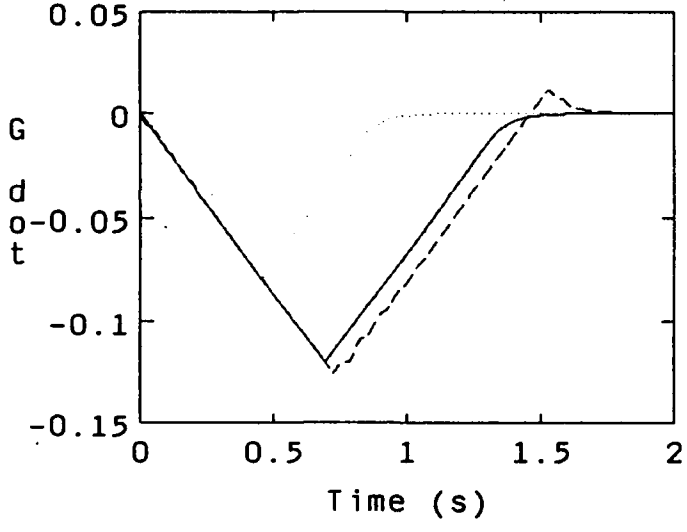
0.05
0
G
d
o-0.05
t
-0.1
-0.15
0
0.5
1
1.5
2
Time (s)

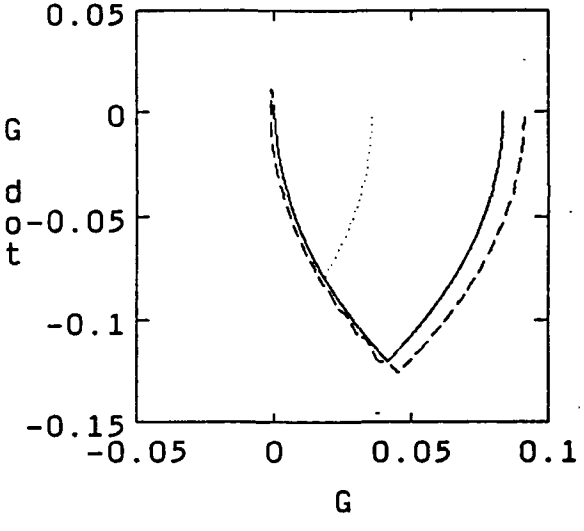
0.05
0
G
d
o-0.05
t
-0.1
-0.15
-0.05
0
0.05
0.1
G

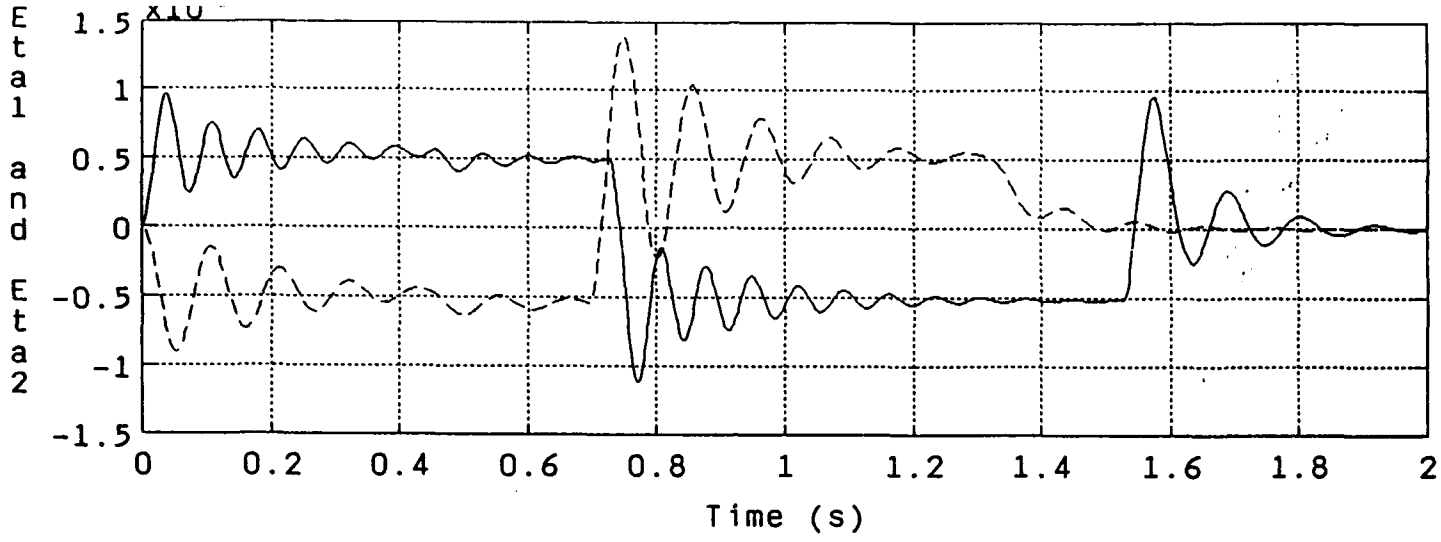
x10
Eta1 and Eta2
1.5
1
0.5
0
-0.5
-1
-1.5
0
0.2
0.4
0.6
0.8
1
1.2
1.4
1.6
1.8
2
Time (s)

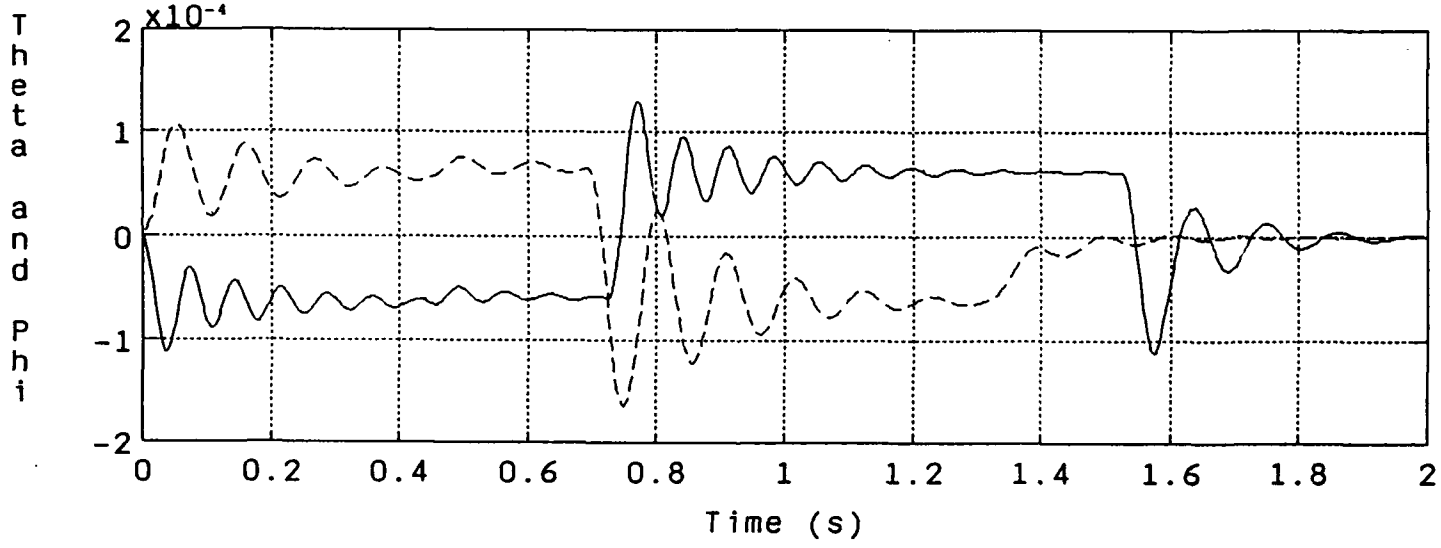
x10⁻⁴
Theta and Phi
2
1
0
-1
-2
0
0.2
0.4
0.6
0.8
1
1.2
1.4
1.6
1.8
2
Time (s)

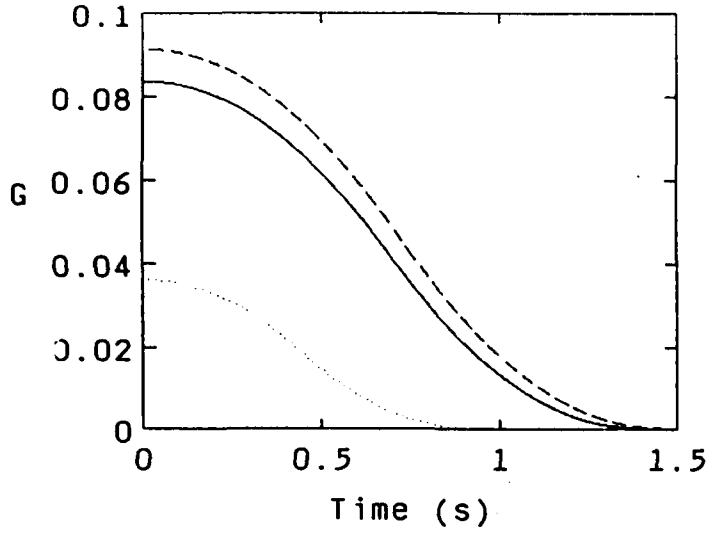
0.1
0.08
0.06
0.04
0.02
0
G
0
0.5
1
1.5
Time (s)

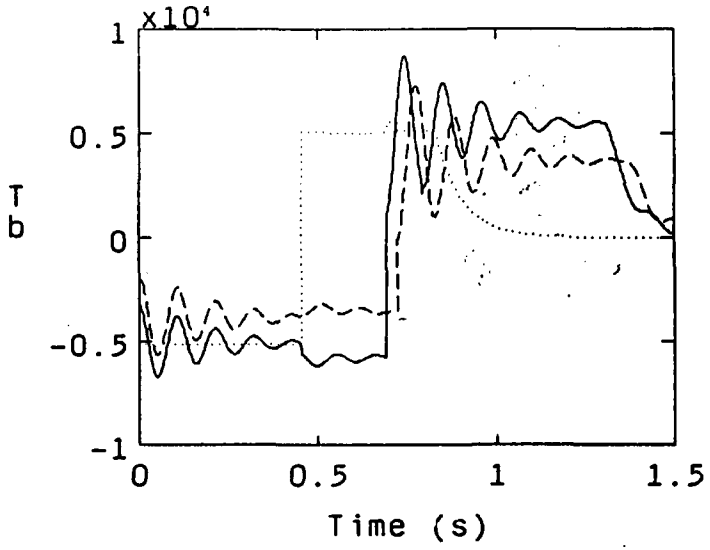
x10⁴
1
0.5
0
-0.5
-1
T
b
0
0.5
1
1.5
Time (s)

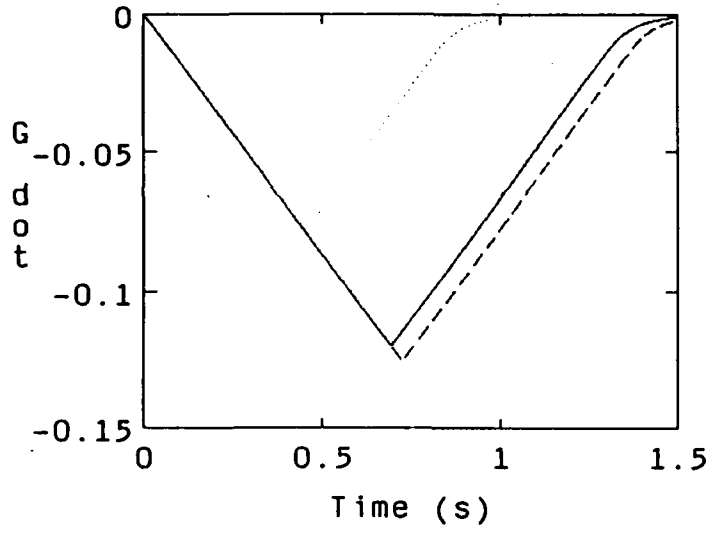
0
-0.05
-0.1
-0.15
G
d
o
t
0
0.5
1
1.5
Time (s)

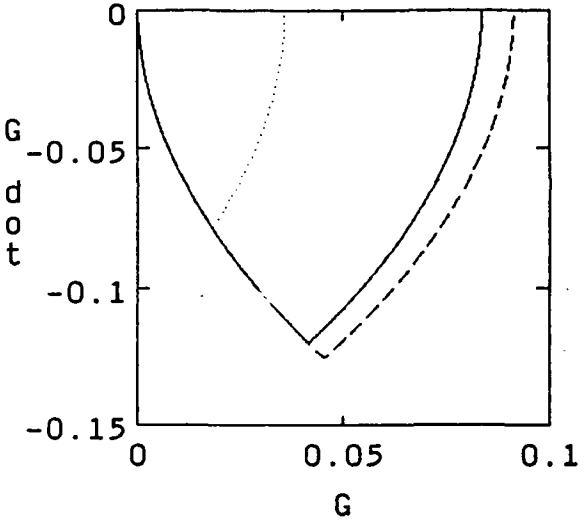
0
-0.05
-0.1
-0.15
G
d
o
t
0
0.05
0.1
G

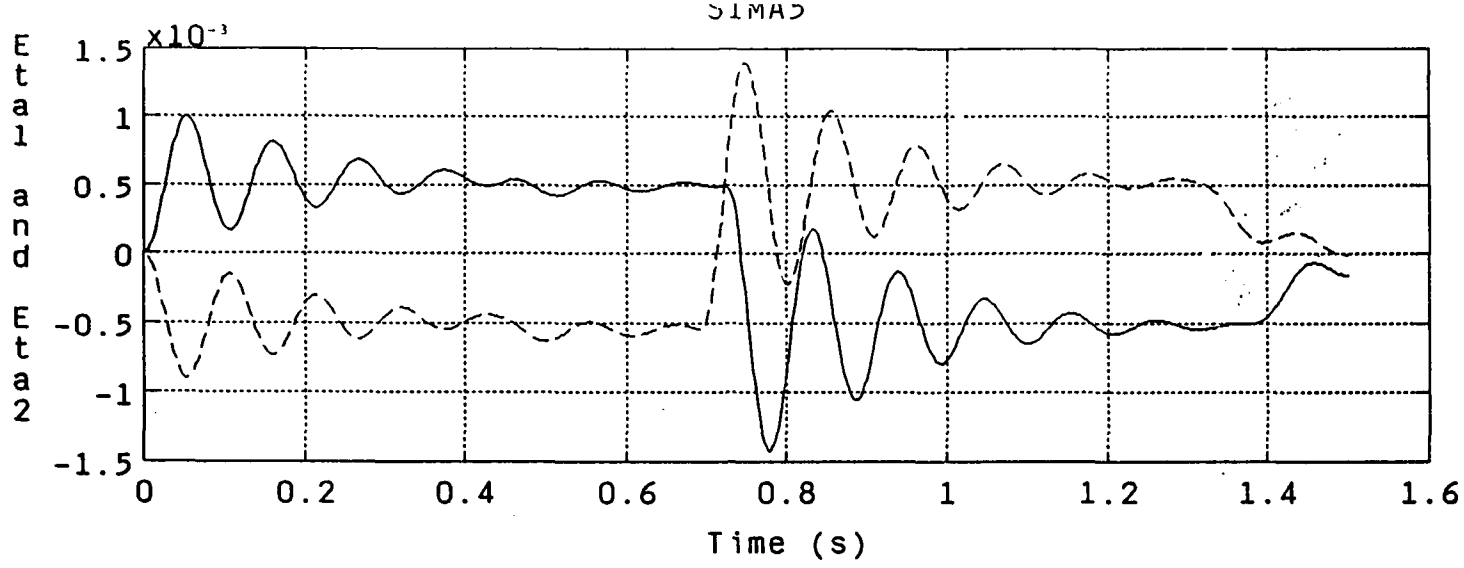
x10^-3
Eta1 and Eta2
1.5
1
0.5
0
-0.5
-1
-1.5
0
0.2
0.4
0.6
0.8
1
1.2
1.4
1.6
Time (s)

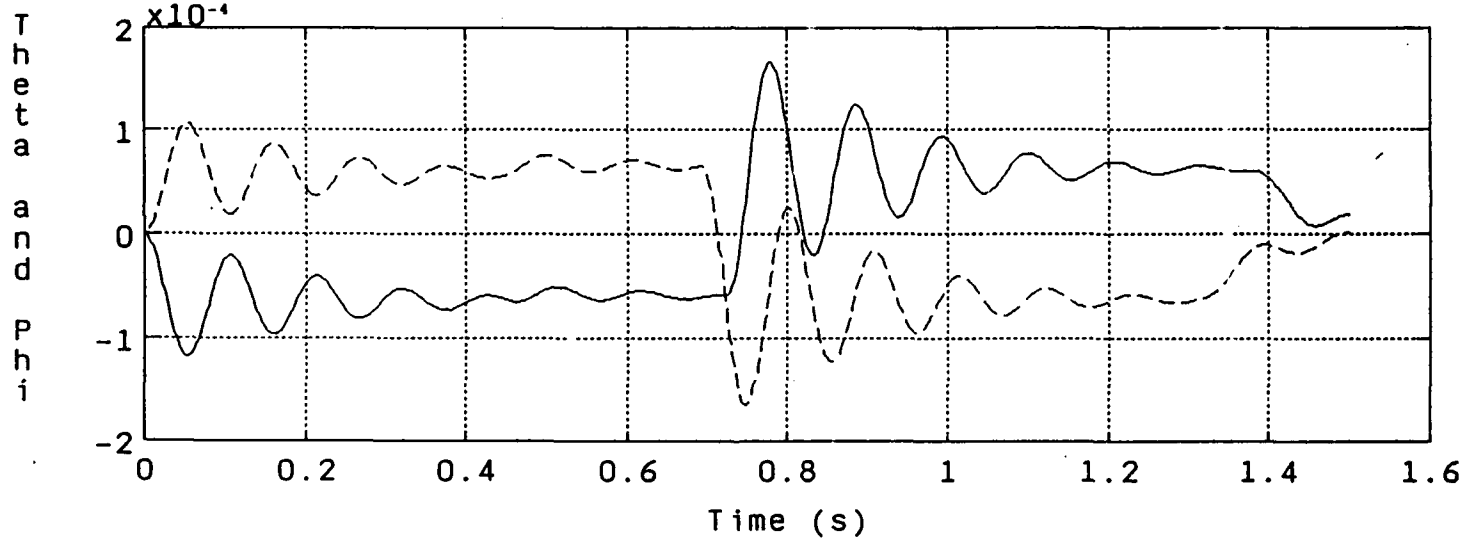
x10^-4
Theta and Phi
2
1
0
-1
-2
0
0.2
0.4
0.6
0.8
1
1.2
1.4
1.6
Time (s)

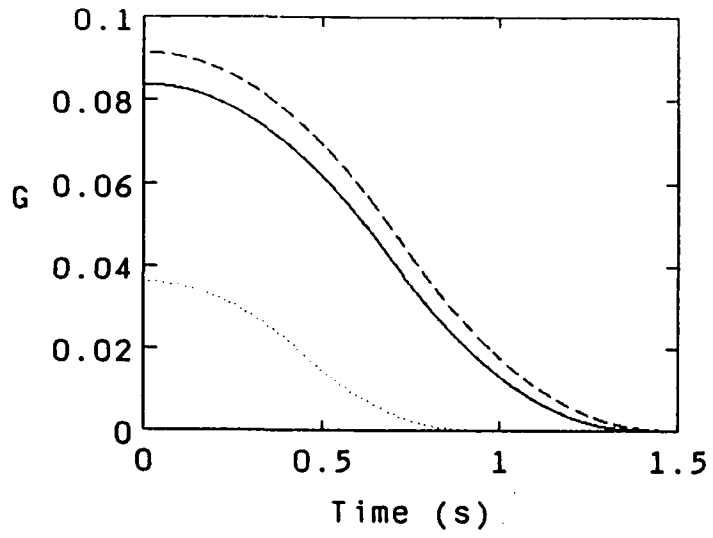
0.1
0.08
0.06
0.04
0.02
0
G
0
0.5
1
1.5
Time (s)

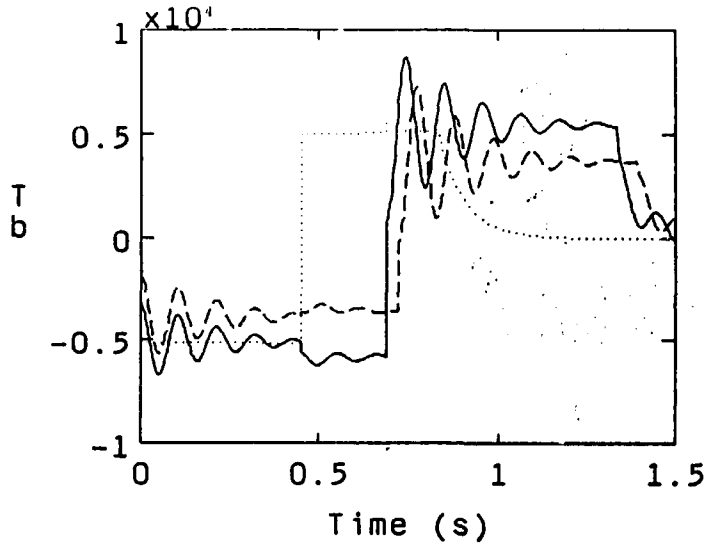
x10⁴
1
0.5
0
-0.5
-1
T
b
0
0.5
1
1.5
Time (s)

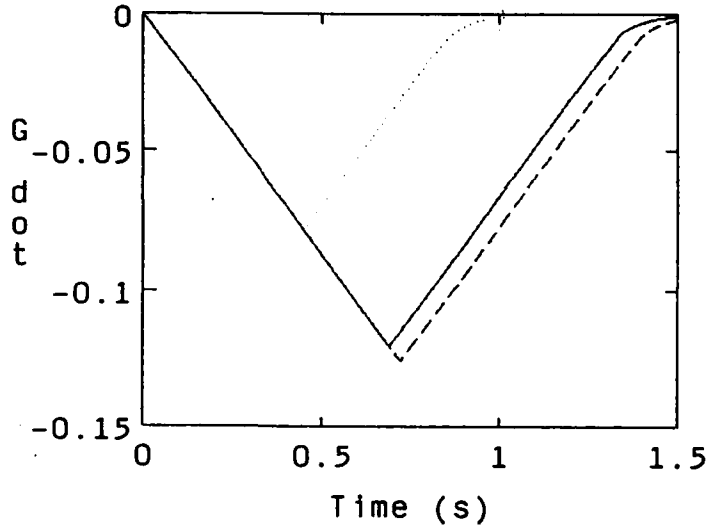
0
-0.05
-0.1
-0.15
G
d
o
t
0
0.5
1
1.5
Time (s)

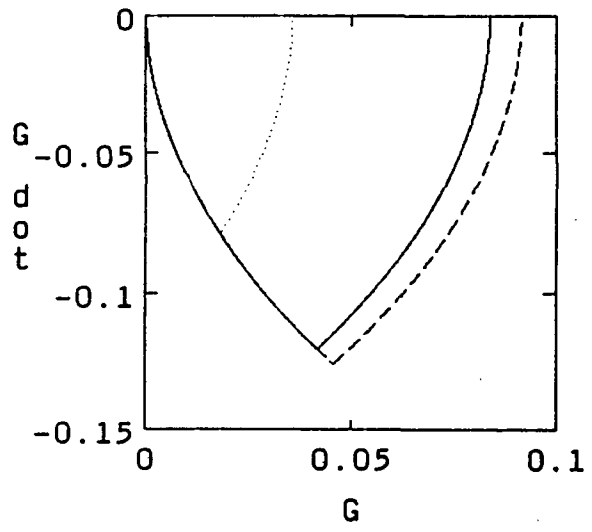
0
-0.05
-0.1
-0.15
G
d
o
t
0
0.05
0.1
G

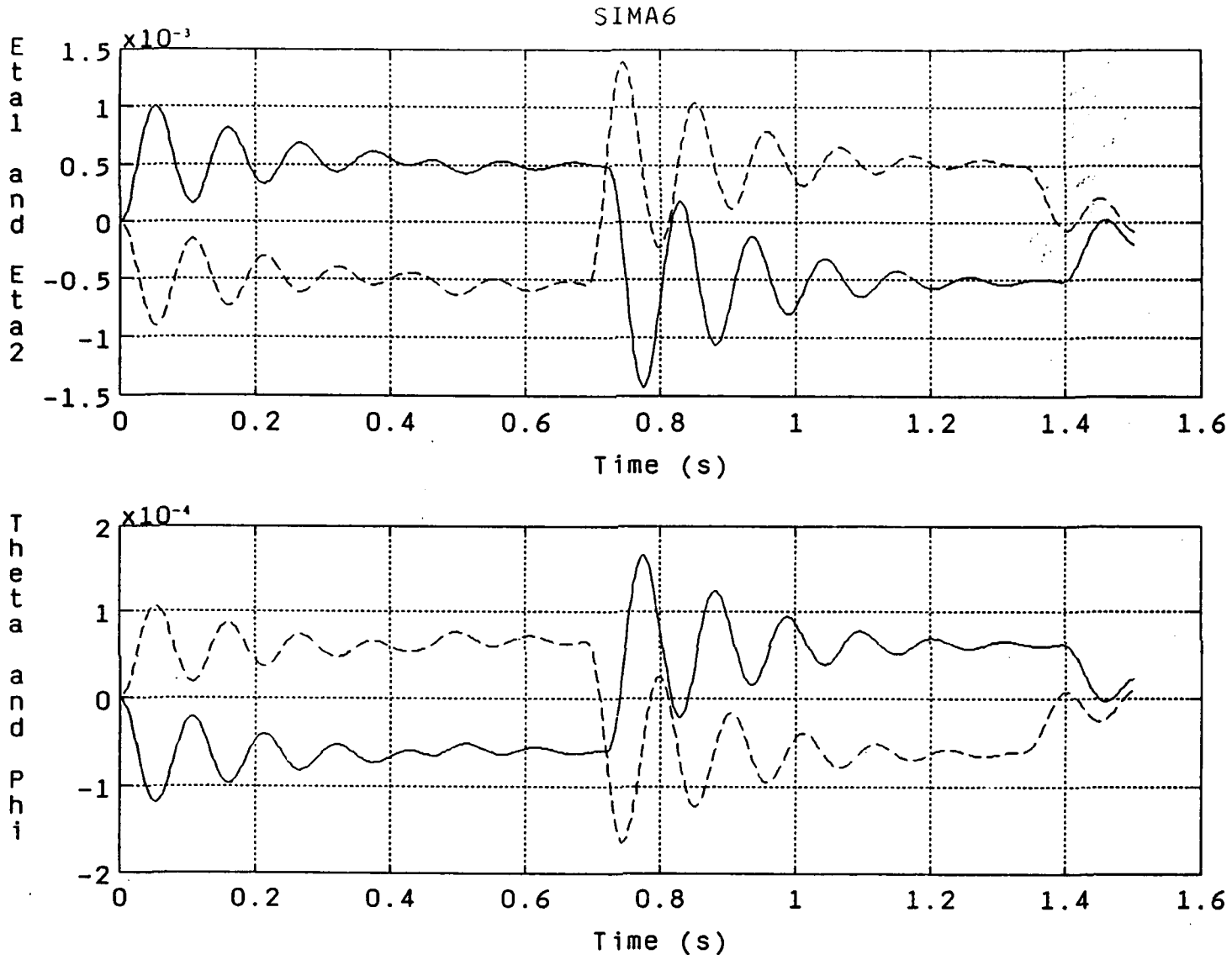
SIMA6
x10⁻³
Eta1 and Eta2
1.5
1
0.5
0
-0.5
-1
-1.5
0
0.2
0.4
0.6
0.8
1
1.2
1.4
1.6
Time (s)
x10⁻⁴
Theta and Phi
2
1
0
-1
-2
0
0.2
0.4
0.6
0.8
1
1.2
1.4
1.6
Time (s)

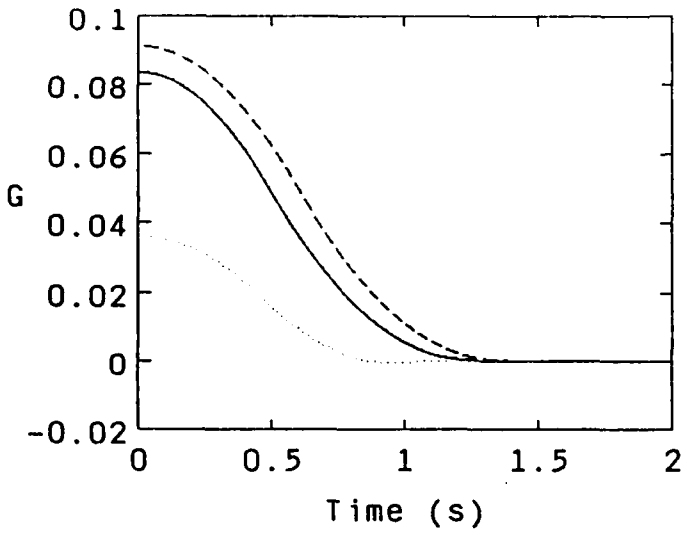
0.1
0.08
0.06
0.04
0.02
0
-0.02
G
0
0.5
1
1.5
2
Time (s)

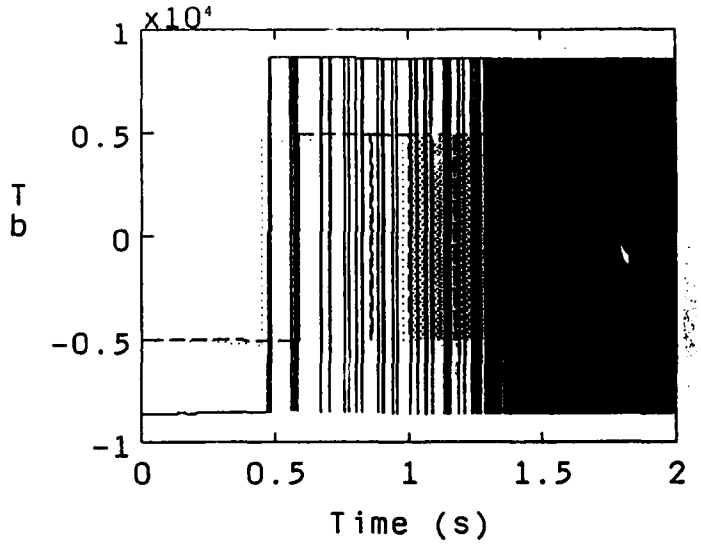
x10⁴
1
0.5
0
-0.5
-1
T
b
0
0.5
1
1.5
2
Time (s)

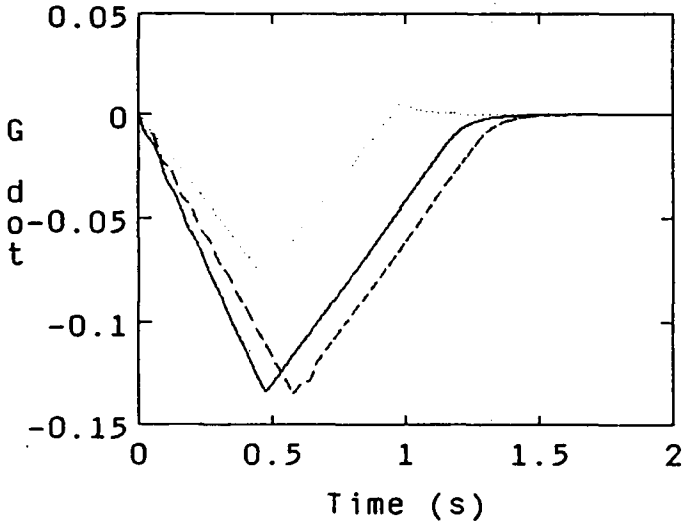
0.05
0
-0.05
-0.1
-0.15
G
d
o
t
0
0.5
1
1.5
2
Time (s)

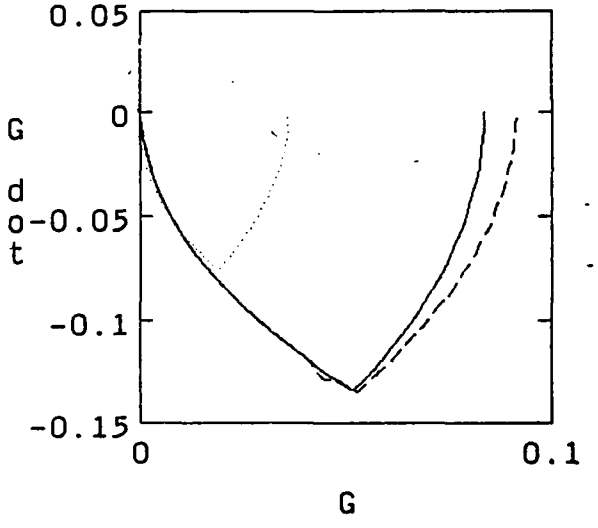
0.05
0
-0.05
-0.1
-0.15
G
d
o
t
0
0.1
G

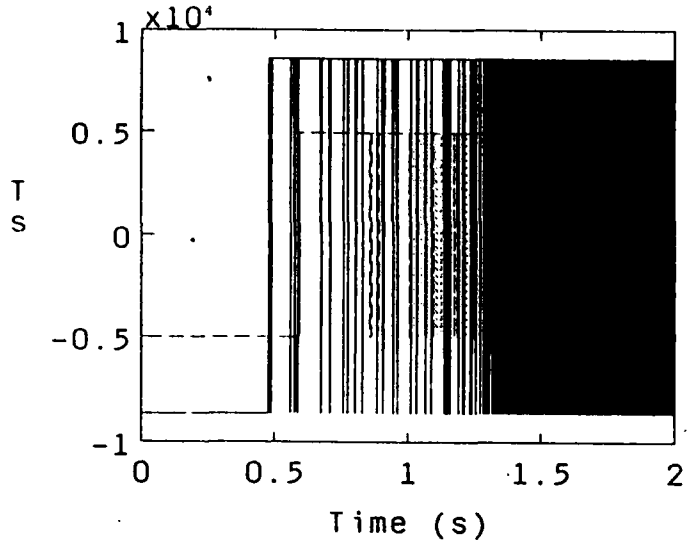
x10⁴
1
0.5
0
-0.5
-1
T
s
0
0.5
1
1.5
2
Time (s)

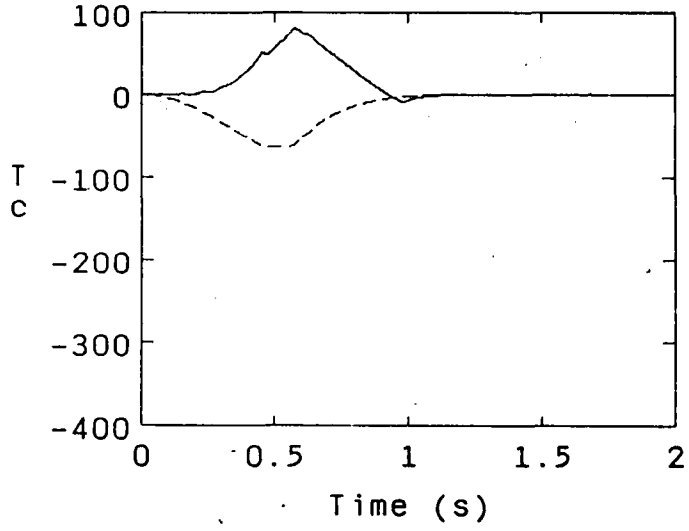
100
0
-100
-200
-300
-400
T
c
0
0.5
1
1.5
2
Time (s)

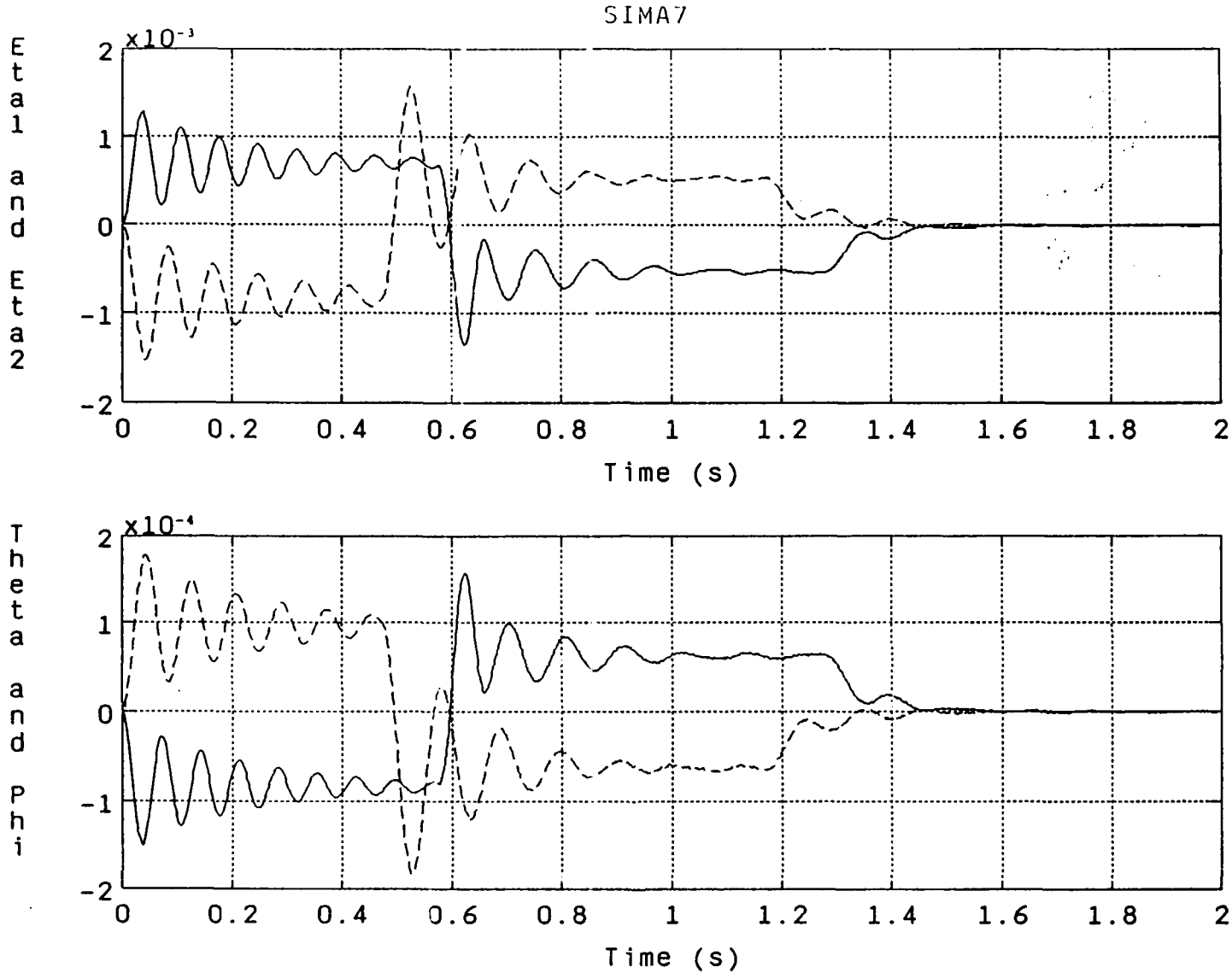
SIMA7
x10⁻³
Eta1 and Eta2
2
1
0
-1
-2
0
0.2
0.4
0.6
0.8
1
1.2
1.4
1.6
1.8
2
Time (s)
x10⁻⁴
Theta and Phi
2
1
0
-1
-2
0
0.2
0.4
0.6
0.8
1
1.2
1.4
1.6
1.8
2
Time (s)

SIMB1

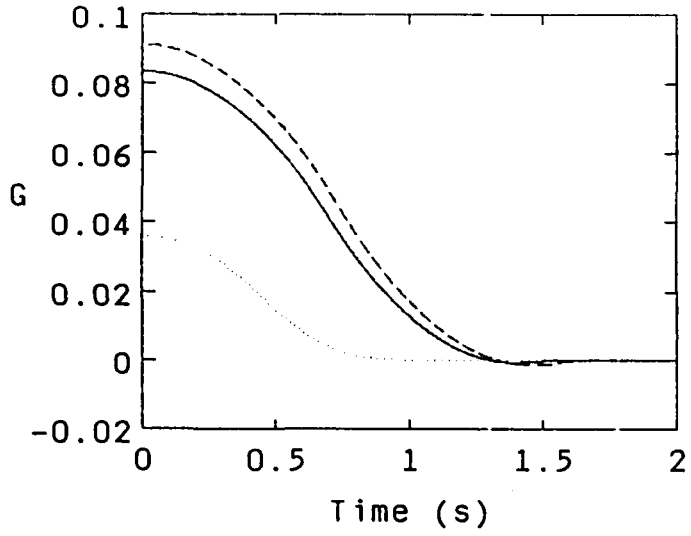
0.1
0.08
0.06
0.04
0.02
0
-0.02
G
0
0.5
1
1.5
2
Time (s)

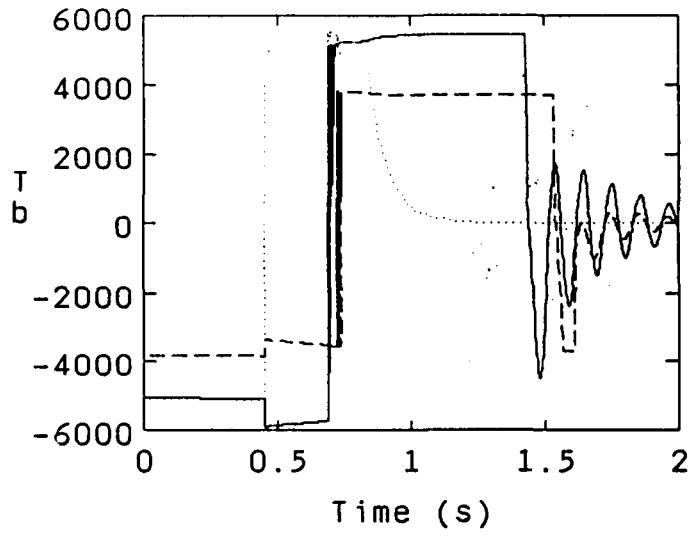
6000
4000
2000
0
-2000
-4000
-6000
T
b
0
0.5
1
1.5
2
Time (s)

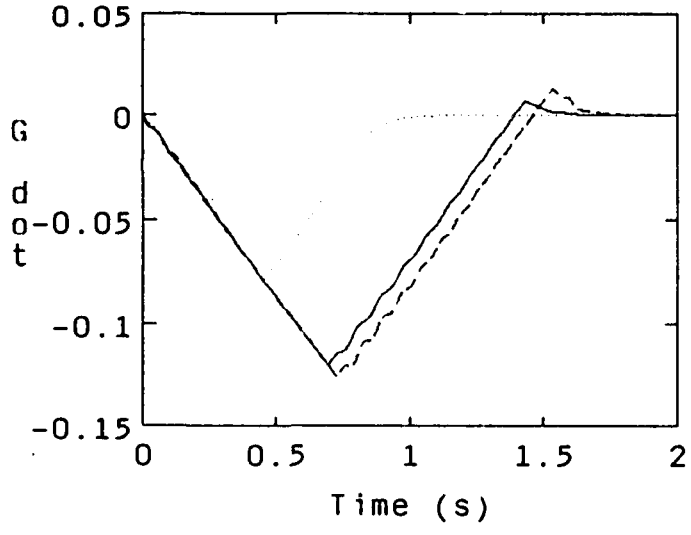
0.05
0
-0.05
-0.1
-0.15
G
d
o
t
0
0.5
1
1.5
2
Time (s)

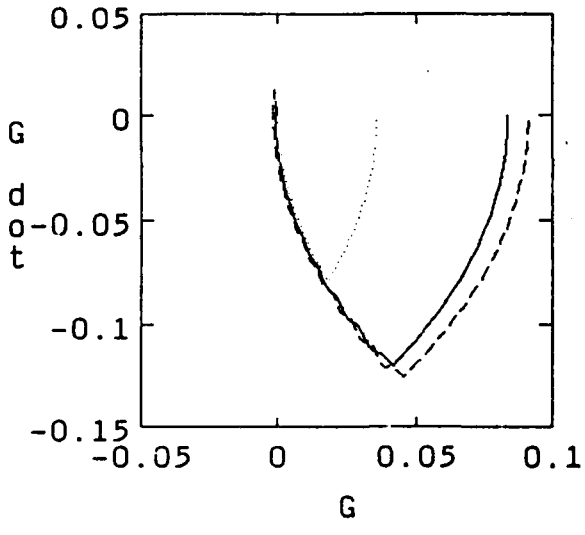
0.05
0
-0.05
-0.1
-0.15
G
d
o
t
-0.05
0
0.05
0.1
G

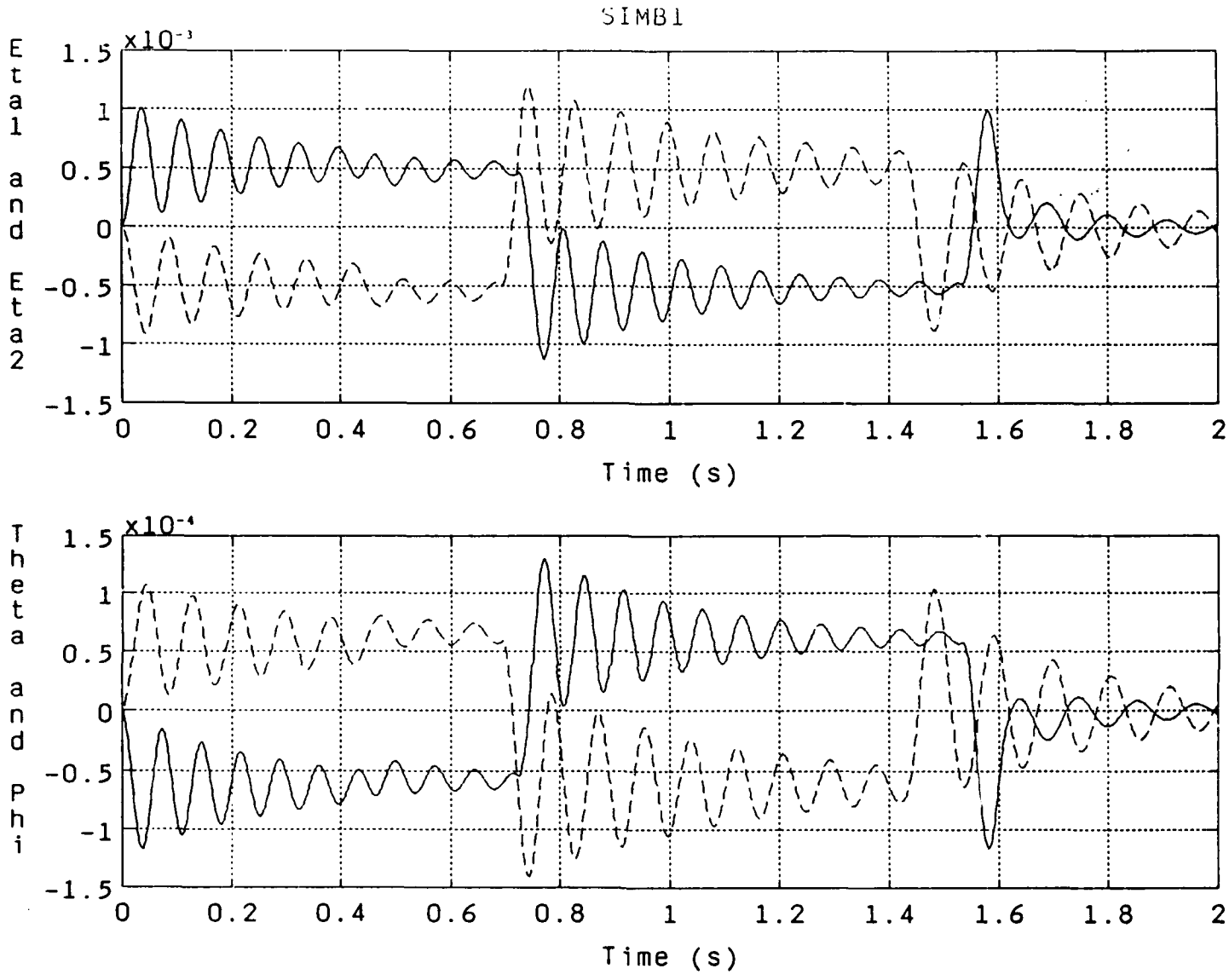
SIMB1
x10⁻³
Eta1 and Eta2
1.5
1
0.5
0
-0.5
-1
-1.5
0
0.2
0.4
0.6
0.8
1
1.2
1.4
1.6
1.8
2
Time (s)
x10⁻⁴
Theta and Phi
1.5
1
0.5
0
-0.5
-1
-1.5
0
0.2
0.4
0.6
0.8
1
1.2
1.4
1.6
1.8
2
Time (s)

SIMB2

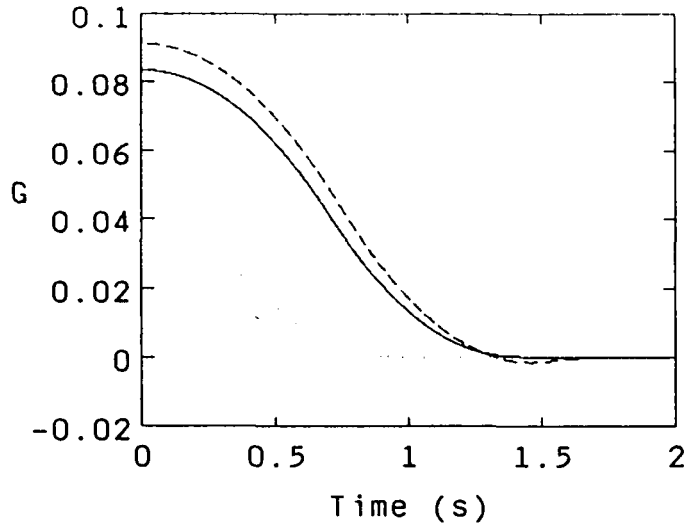
0.1
0.08
0.06
0.04
0.02
0
-0.02
G
0
0.5
1
1.5
2
Time (s)

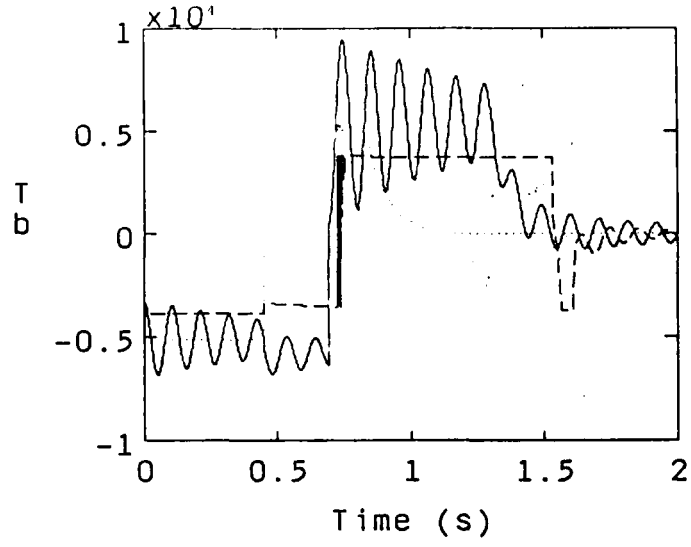
x10⁴
1
0.5
0
-0.5
-1
T
b
0
0.5
1
1.5
2
Time (s)

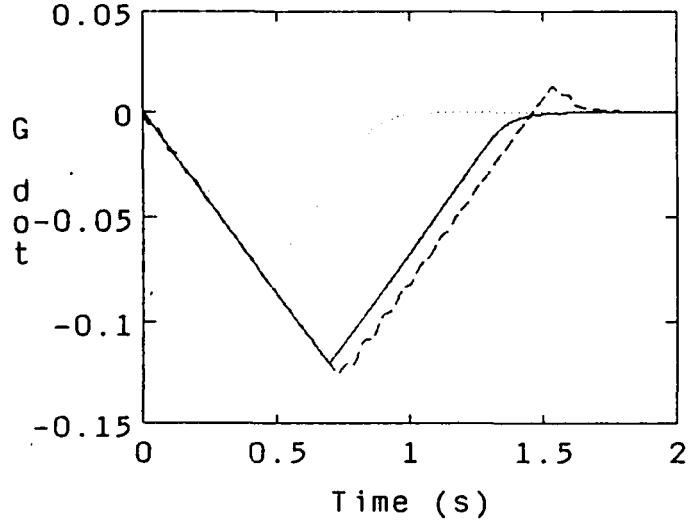
0.05
0
-0.05
-0.1
-0.15
G
d
o
t
0
0.5
1
1.5
2
Time (s)

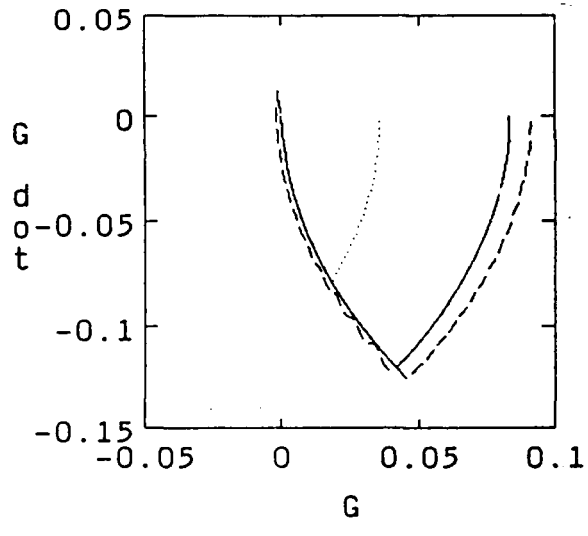
0.05
0
-0.05
-0.1
-0.15
G
d
o
t
-0.05
0
0.05
0.1
G

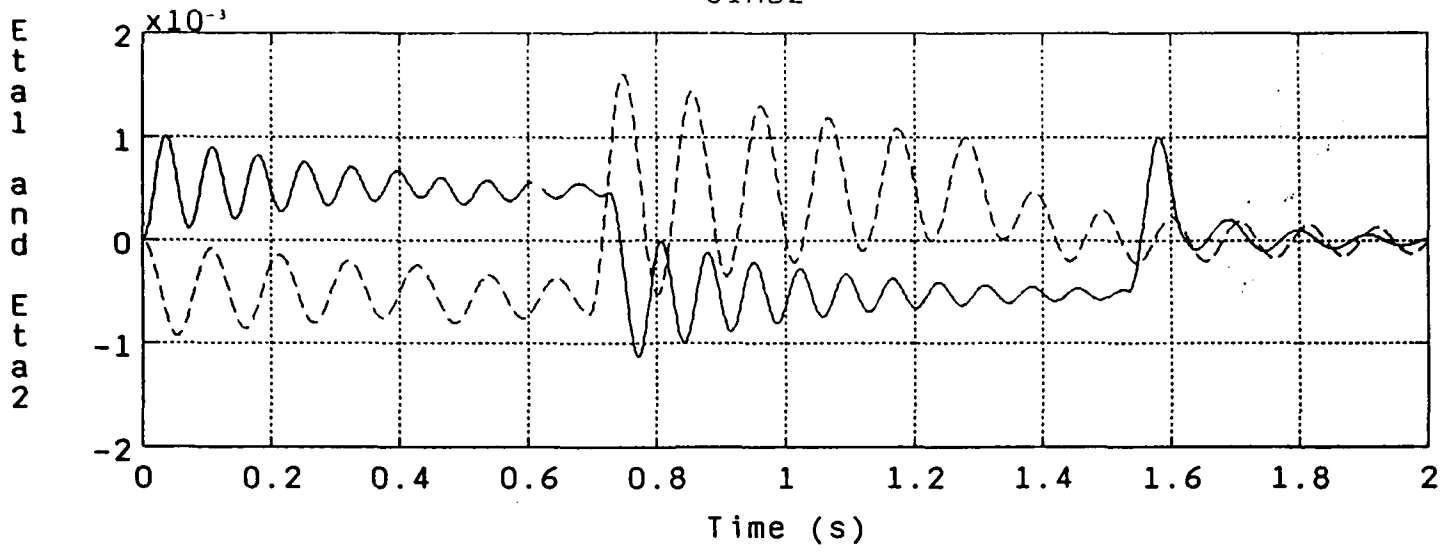
x10⁻³
Eta1 and Eta2
2
1
0
-1
-2
0
0.2
0.4
0.6
0.8
1
1.2
1.4
1.6
1.8
2
Time (s)

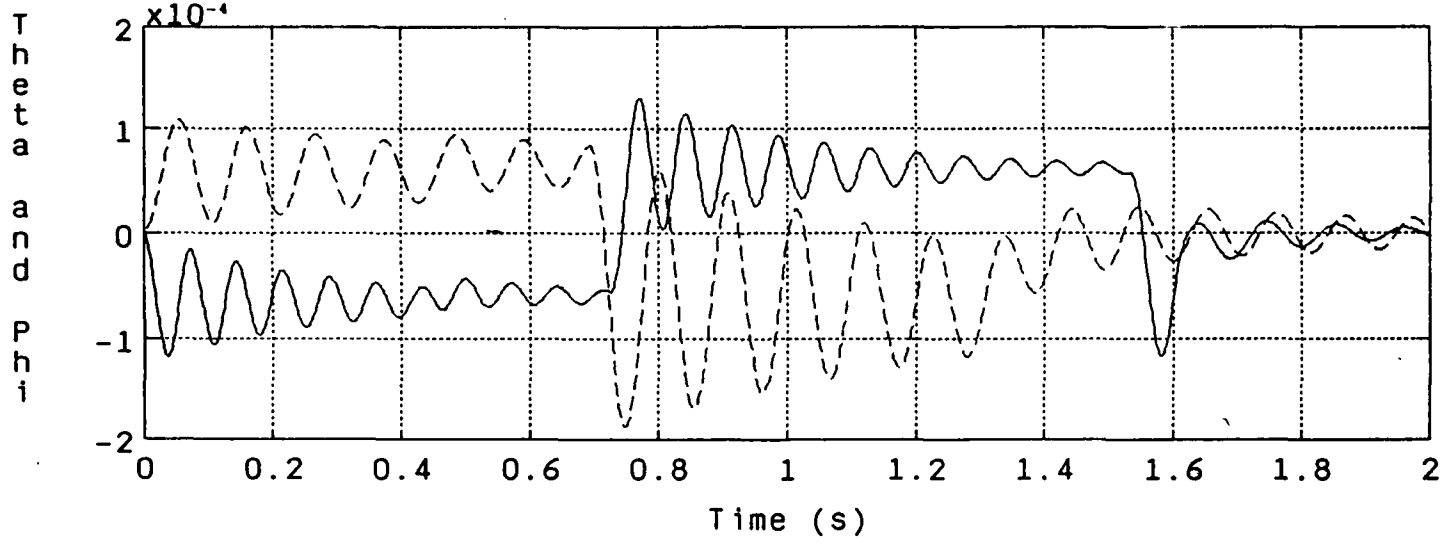
x10⁻⁴
Theta and Phi
2
1
0
-1
-2
0
0.2
0.4
0.6
0.8
1
1.2
1.4
1.6
1.8
2
Time (s)

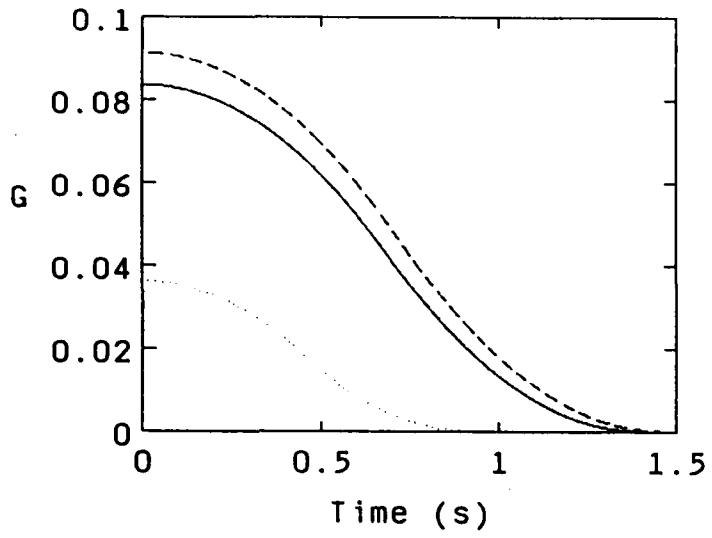
0.1
0.08
0.06
0.04
0.02
0
G
0
0.5
1
1.5
Time (s)

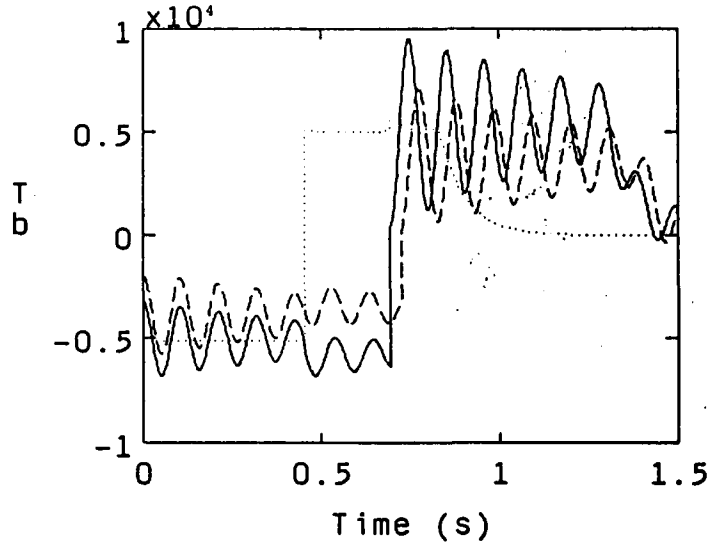
x10⁴
1
0.5
0
-0.5
-1
T
b
0
0.5
1
1.5
Time (s)

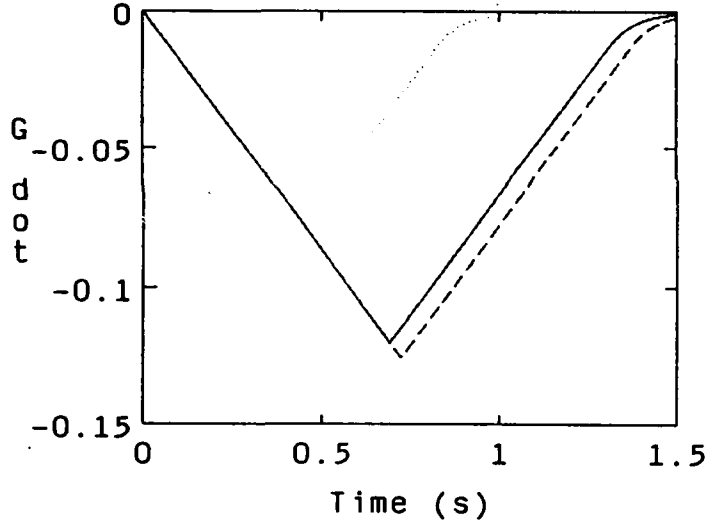
0
-0.05
-0.1
-0.15
G
d
o
t
0
0.5
1
1.5
Time (s)

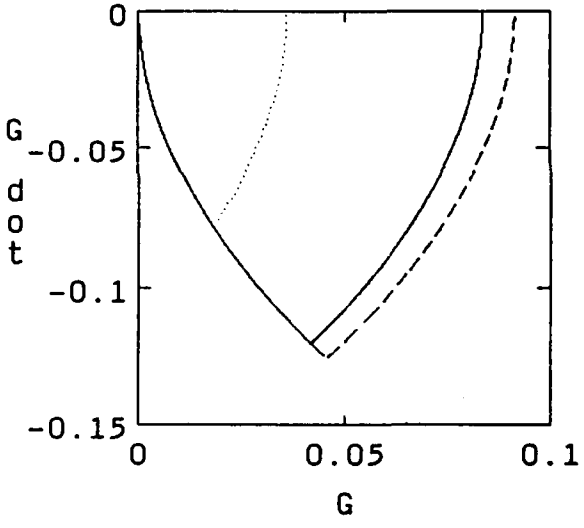
0
-0.05
-0.1
-0.15
G
d
o
t
0
0.05
0.1
G

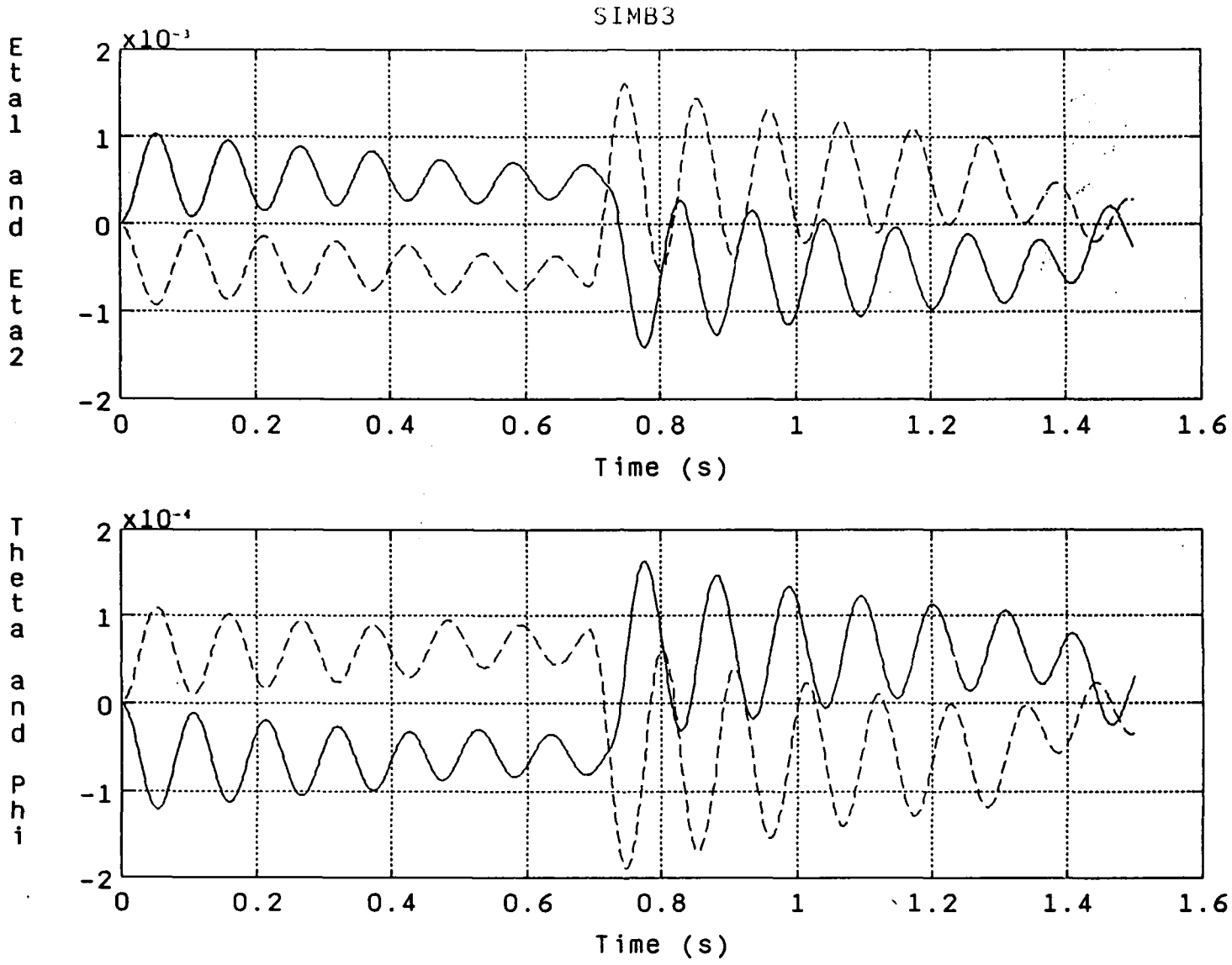
SIMB3
x10⁻³
Eta1 and Eta2
2
1
0
-1
-2
0
0.2
0.4
0.6
0.8
1
1.2
1.4
1.6
Time (s)
x10⁻⁴
Theta and Phi
2
1
0
-1
-2
0
0.2
0.4
0.6
0.8
1
1.2
1.4
1.6
Time (s)

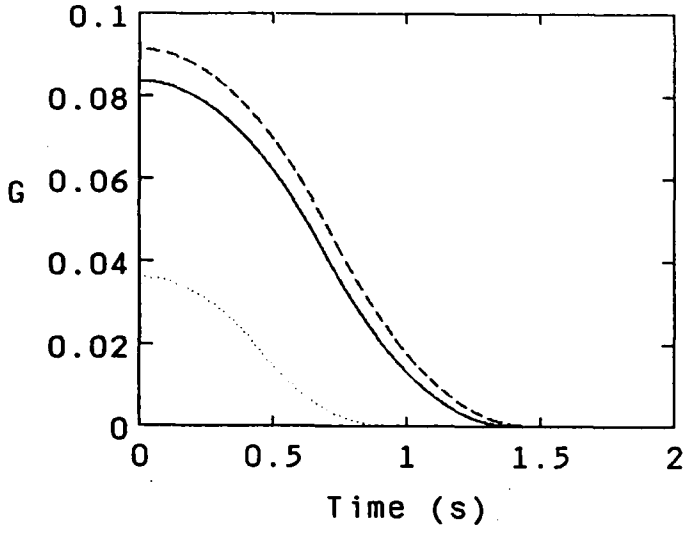
0.1
0.08
0.06
0.04
0.02
0
G
0
0.5
1
1.5
2
Time (s)

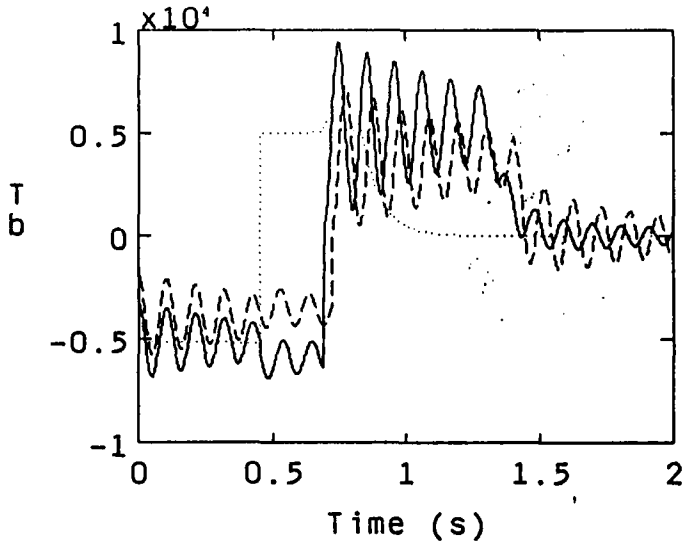
x10⁴
1
0.5
0
-0.5
-1
T
b
0
0.5
1
1.5
2
Time (s)

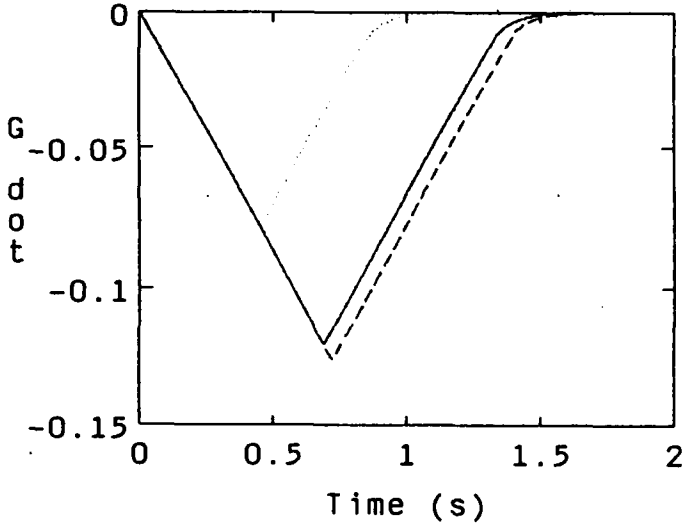
0
-0.05
-0.1
-0.15
G
d
o
t
0
0.5
1
1.5
2
Time (s)

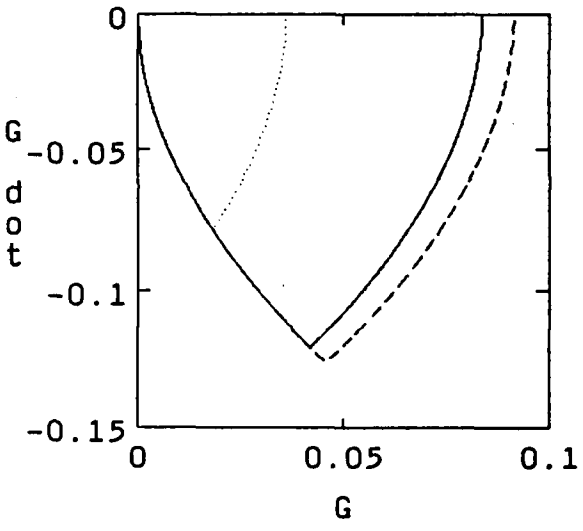
0
-0.05
-0.1
-0.15
G
d
o
t
0
0.05
0.1
G

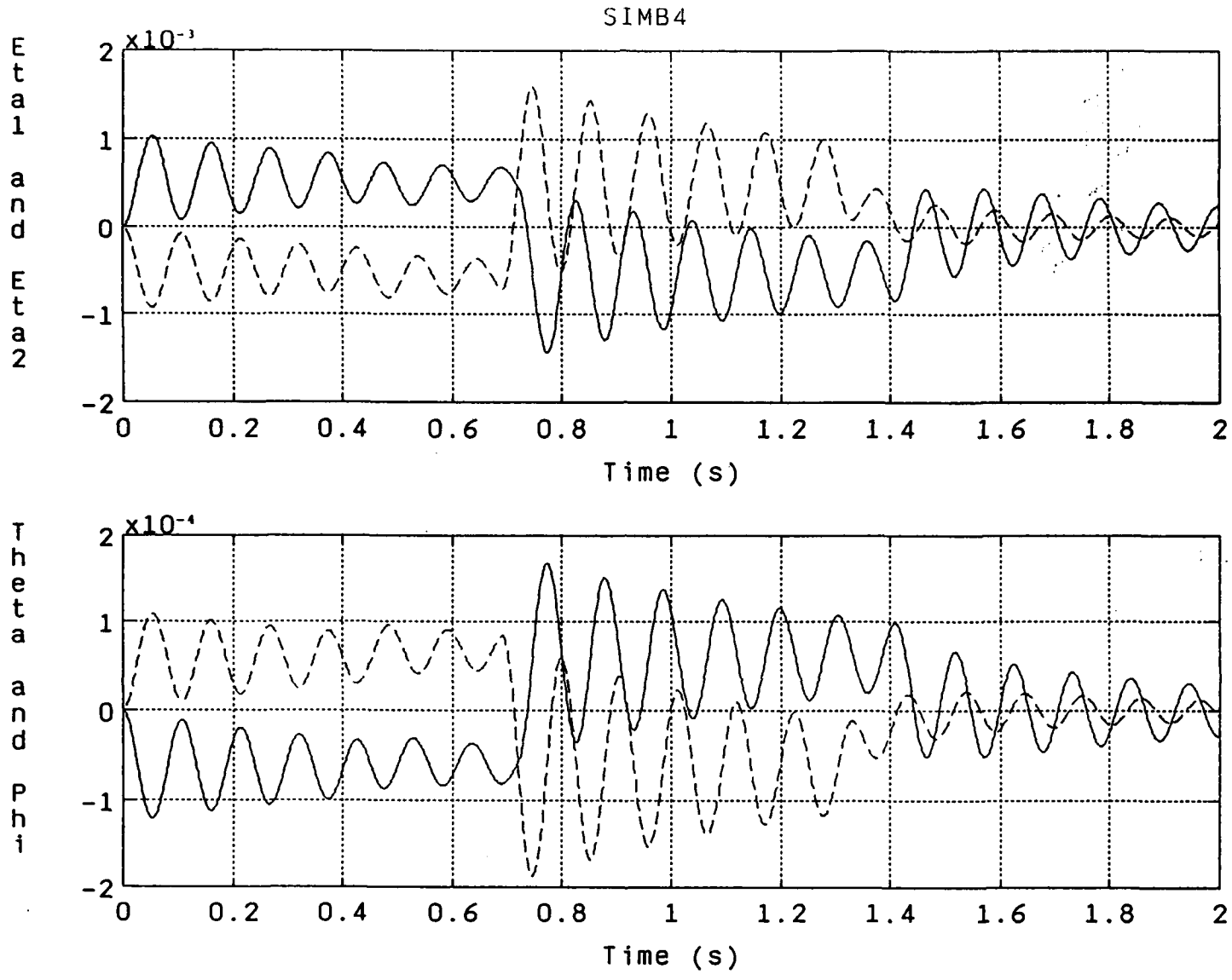
SIMB4
x10⁻³
Eta1 and Eta2
2
1
0
-1
-2
0
0.2
0.4
0.6
0.8
1
1.2
1.4
1.6
1.8
2
Time (s)
x10⁻⁴
Theta and Phi
2
1
0
-1
-2
0
0.2
0.4
0.6
0.8
1
1.2
1.4
1.6
1.8
2
Time (s)

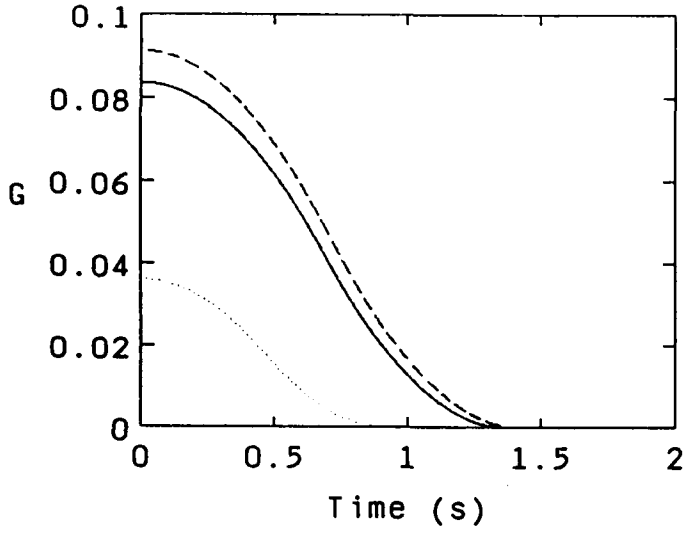
0.1
0.08
0.06
0.04
0.02
0
G
0
0.5
1
1.5
2
Time (s)

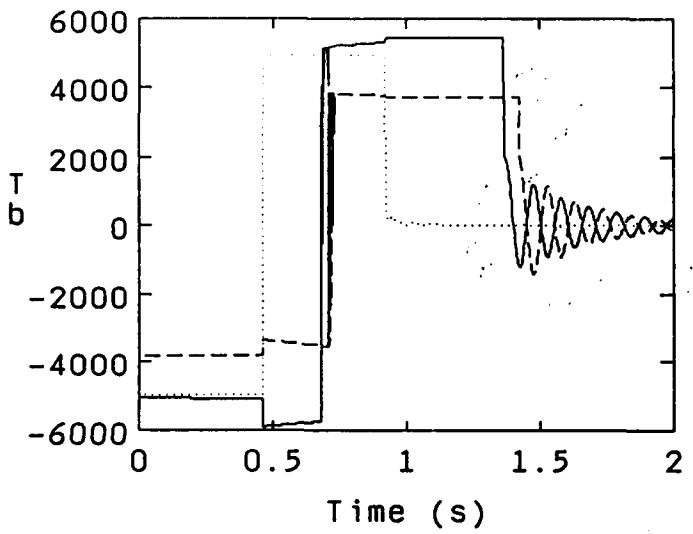
6000
4000
2000
0
-2000
-4000
-6000
T
b
0
0.5
1
1.5
2
Time (s)

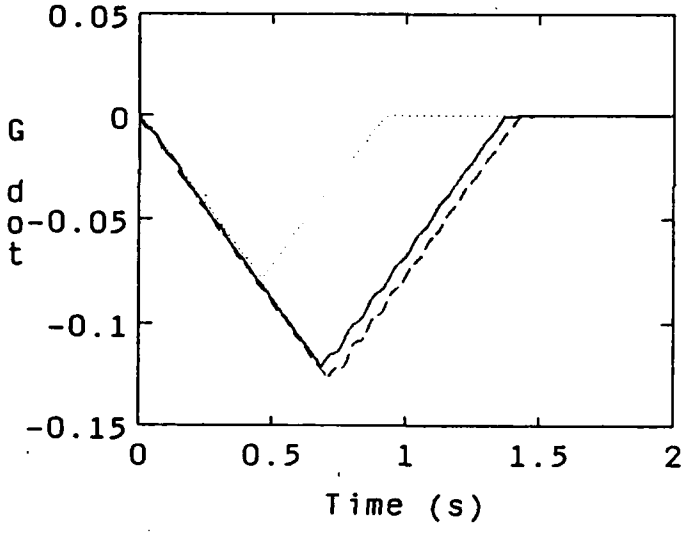
0.05
0
-0.05
-0.1
-0.15
G
d
o
t
0
0.5
1
1.5
2
Time (s)

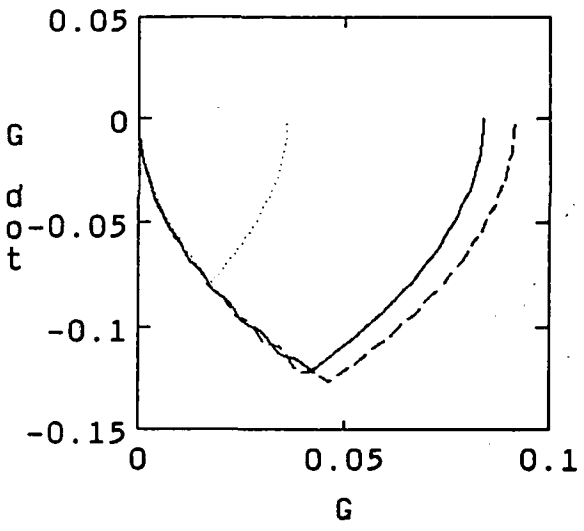
0.05
0
-0.05
-0.1
-0.15
G
d
o
t
0
0.05
0.1
G

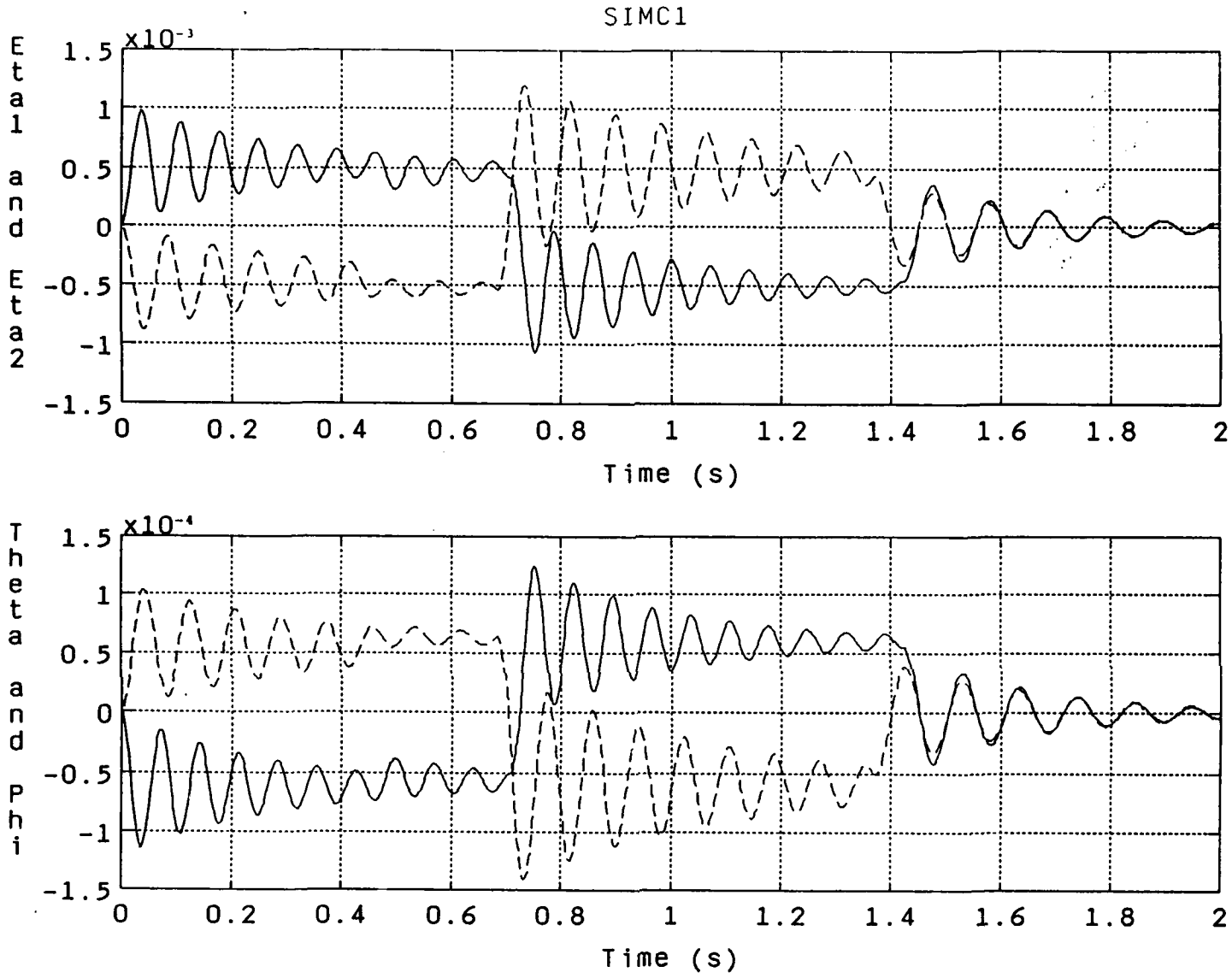
SIMC1
x10⁻³
Eta1 and Eta2
1.5
1
0.5
0
-0.5
-1
-1.5
0
0.2
0.4
0.6
0.8
1
1.2
1.4
1.6
1.8
2
Time (s)
x10⁻⁴
Theta and Phi
1.5
1
0.5
0
-0.5
-1
-1.5
0
0.2
0.4
0.6
0.8
1
1.2
1.4
1.6
1.8
2
Time (s)

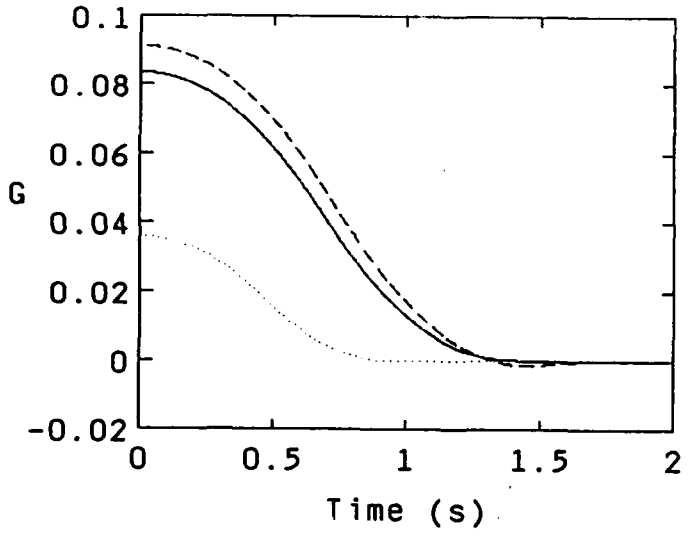
0.1
0.08
0.06
0.04
0.02
0
-0.02
G
0
0.5
1
1.5
2
Time (s)

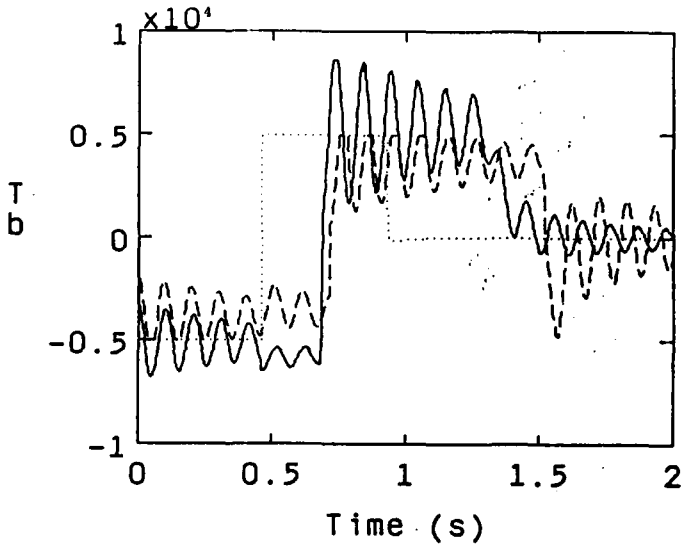
x10⁴
1
0.5
0
-0.5
-1
T
b
0
0.5
1
1.5
2
Time (s)

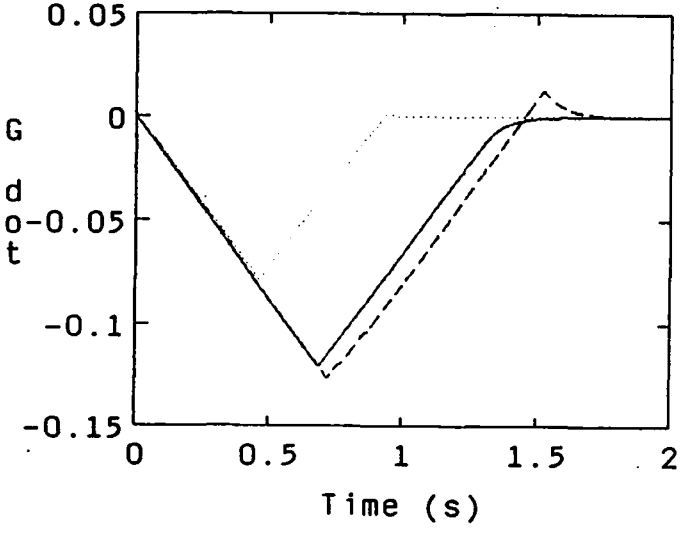
0.05
0
-0.05
-0.1
-0.15
G
d
o
t
0
0.5
1
1.5
2
Time (s)

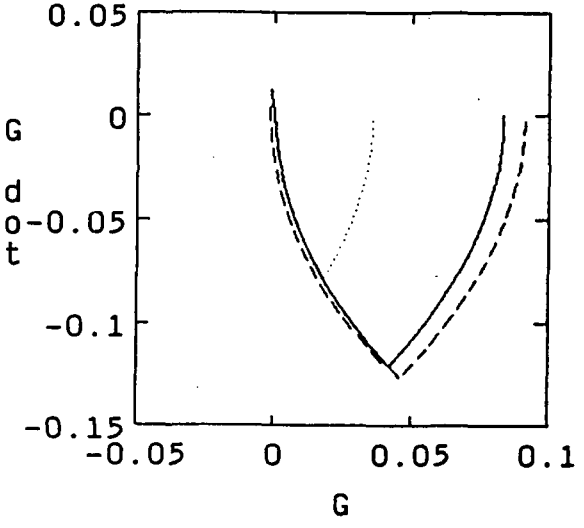
0.05
0
-0.05
-0.1
-0.15
G
d
o
t
-0.05
0
0.05
0.1
G

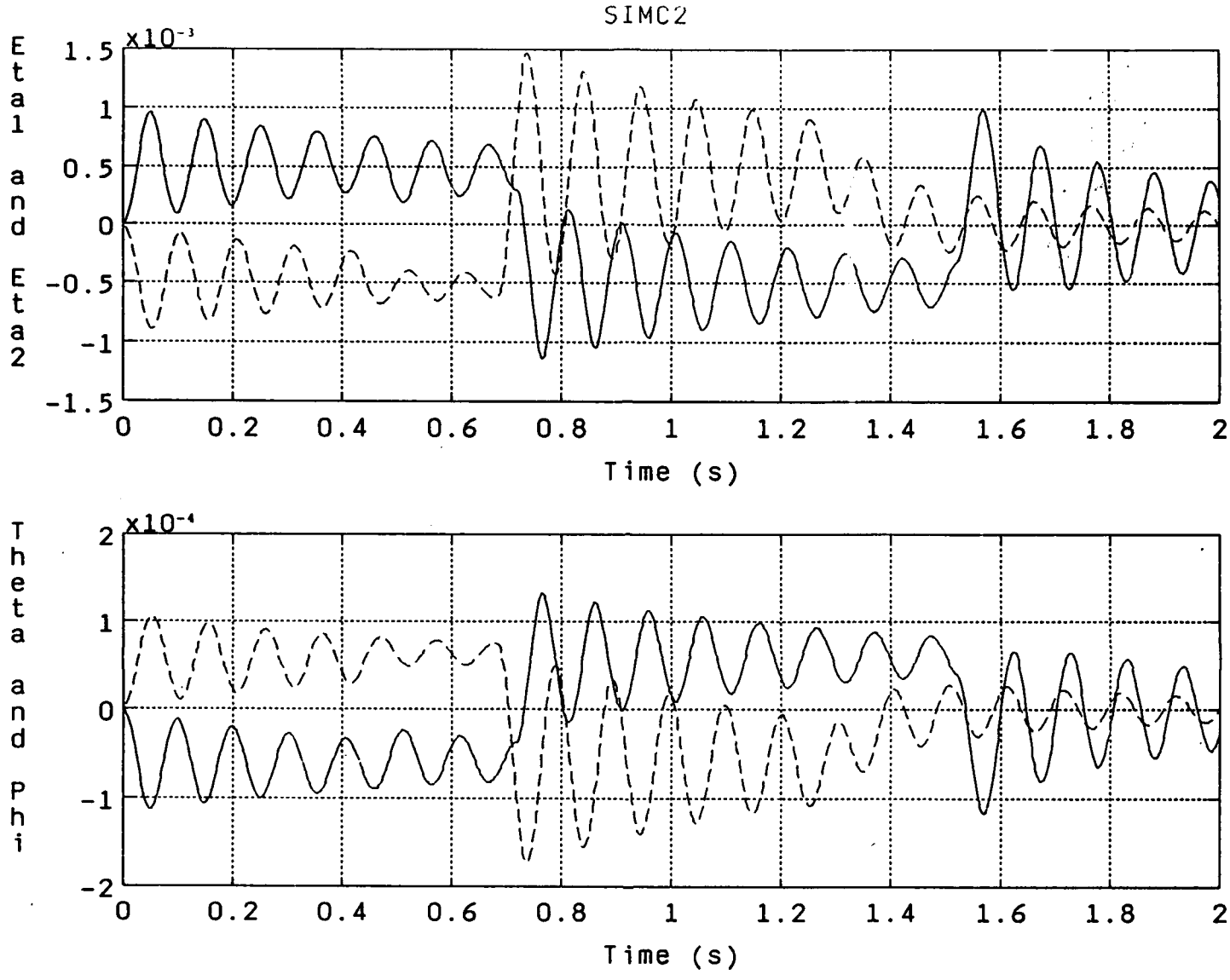
SIMC2
x10⁻³
Eta1 and Eta2
1.5
1
0.5
0
-0.5
-1
-1.5
0
0.2
0.4
0.6
0.8
1
1.2
1.4
1.6
1.8
2
Time (s)
x10⁻⁴
Theta and Phi
2
1
0
-1
-2
0
0.2
0.4
0.6
0.8
1
1.2
1.4
1.6
1.8
2
Time (s)

SIMC3

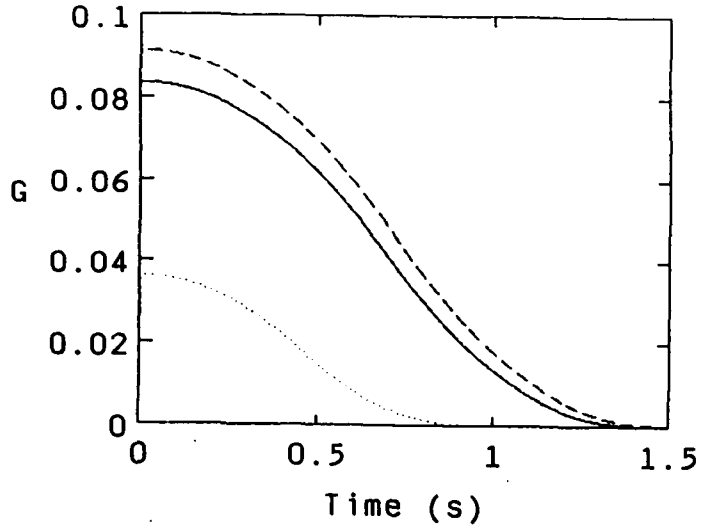
0.1
0.08
0.06
0.04
0.02
0
G
0
0.5
1
1.5
Time (s)

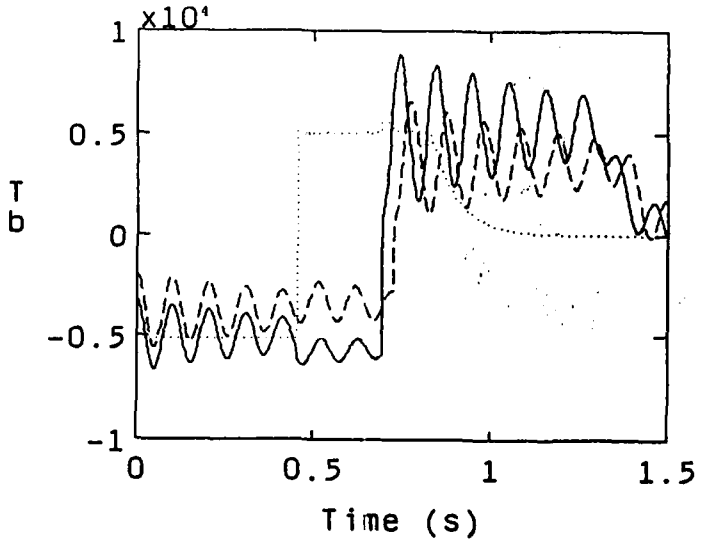
x10⁴
1
0.5
0
-0.5
-1
T
b
0
0.5
1
1.5
Time (s)

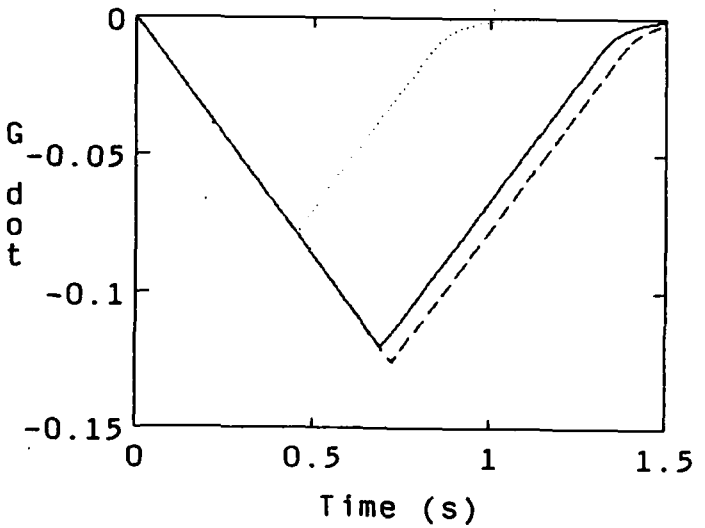
0
-0.05
-0.1
-0.15
G
d
o
t
0
0.5
1
1.5
Time (s)

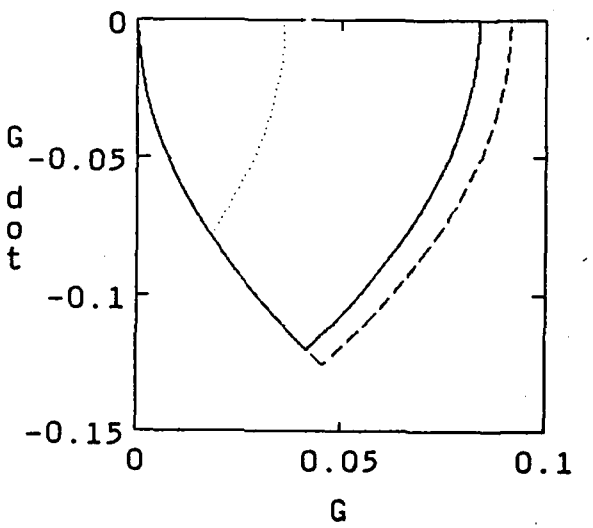
0
-0.05
-0.1
-0.15
G
d
o
t
0
0.05
0.1
G

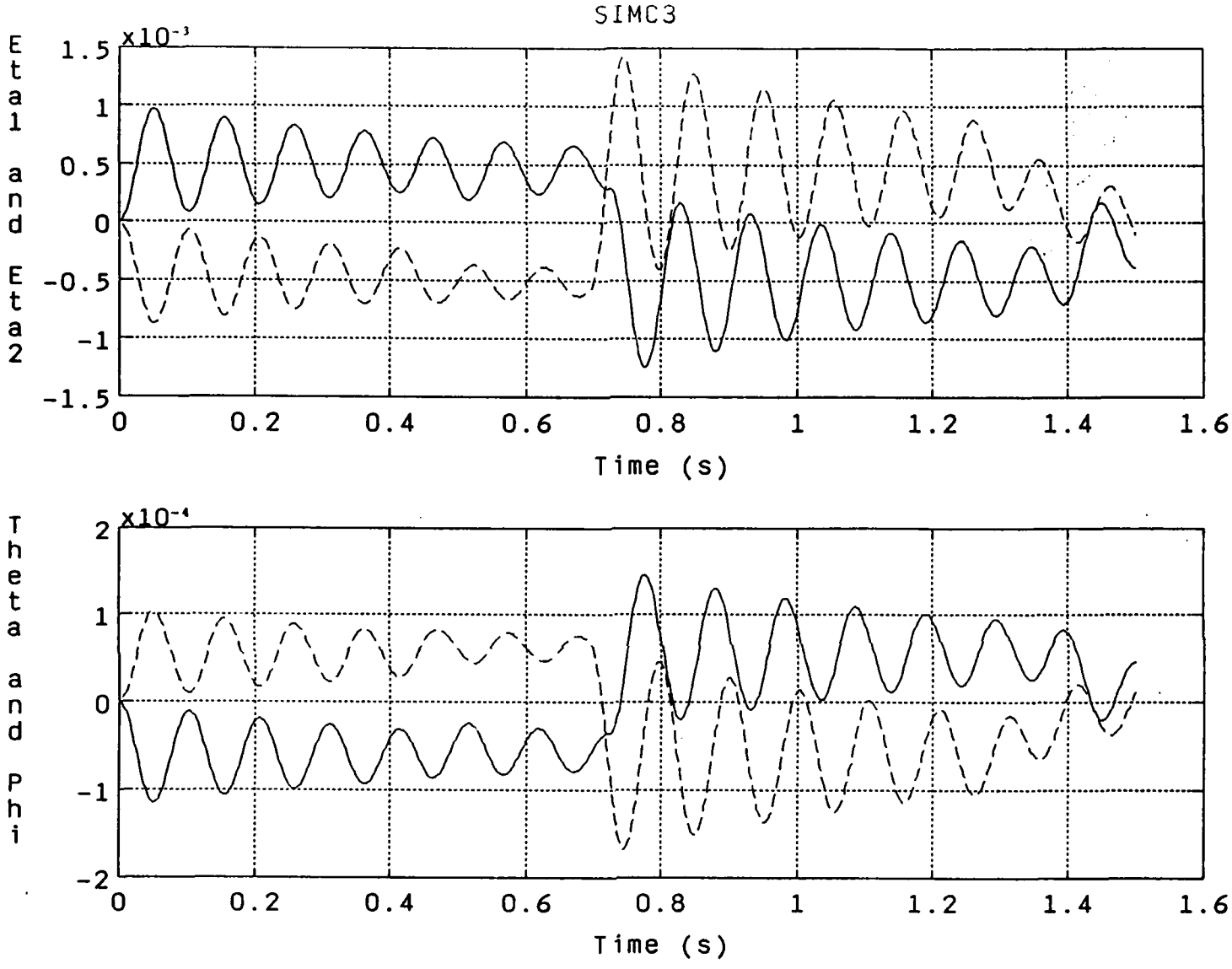
SIMC3
x10⁻³
Eta1 and Eta2
1.5
1
0.5
0
-0.5
-1
-1.5
0
0.2
0.4
0.6
0.8
1
1.2
1.4
1.6
Time (s)
x10⁻⁴
Theta and Phi
2
1
0
-1
-2
0
0.2
0.4
0.6
0.8
1
1.2
1.4
1.6
Time (s)

SIMD1

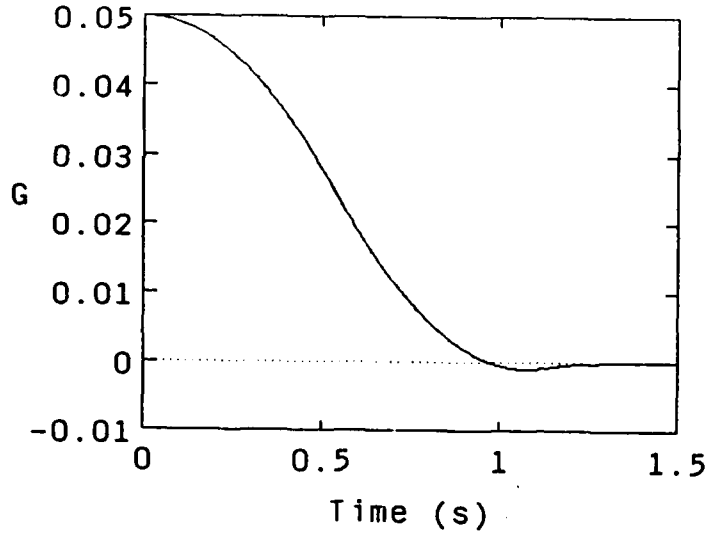
0.05
0.04
0.03
0.02
0.01
0
-0.01
G
0
0.5
1
1.5
Time (s)

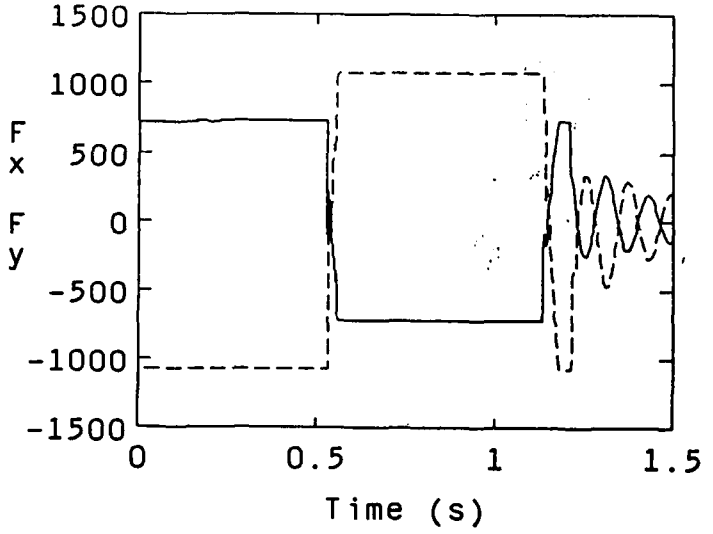
1500
1000
500
0
-500
-1000
-1500
F x
F y
0
0.5
1
1.5
Time (s)

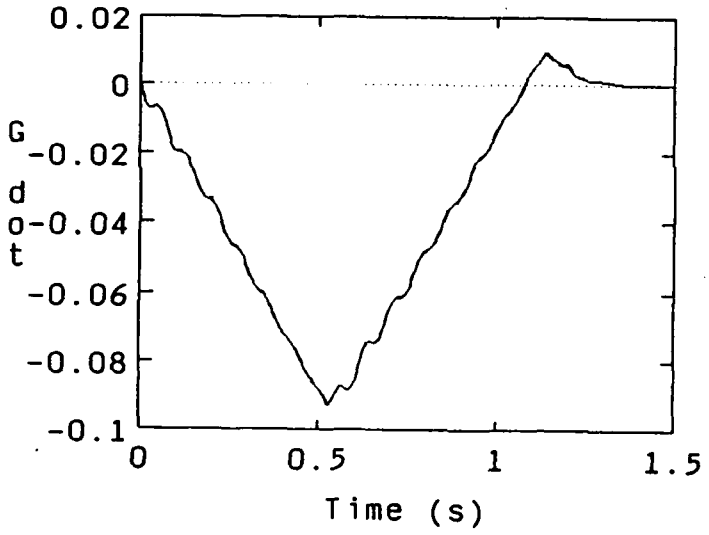
0.02
0
-0.02
-0.04
-0.06
-0.08
-0.1
G dot
0
0.5
1
1.5
Time (s)

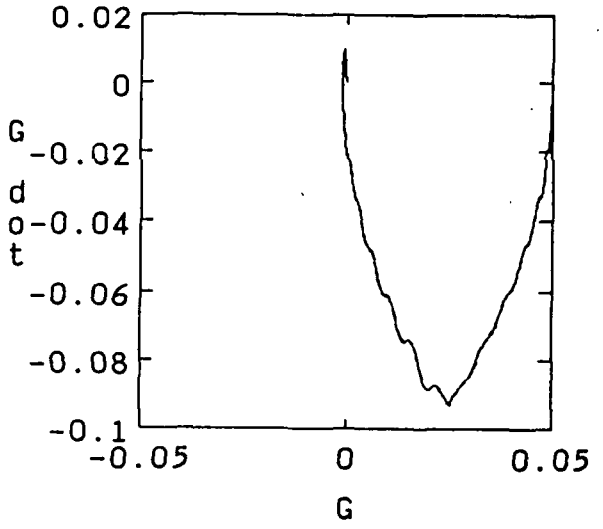
0.02
0
-0.02
-0.04
-0.06
-0.08
-0.1
G dot
-0.05
0
0.05
G

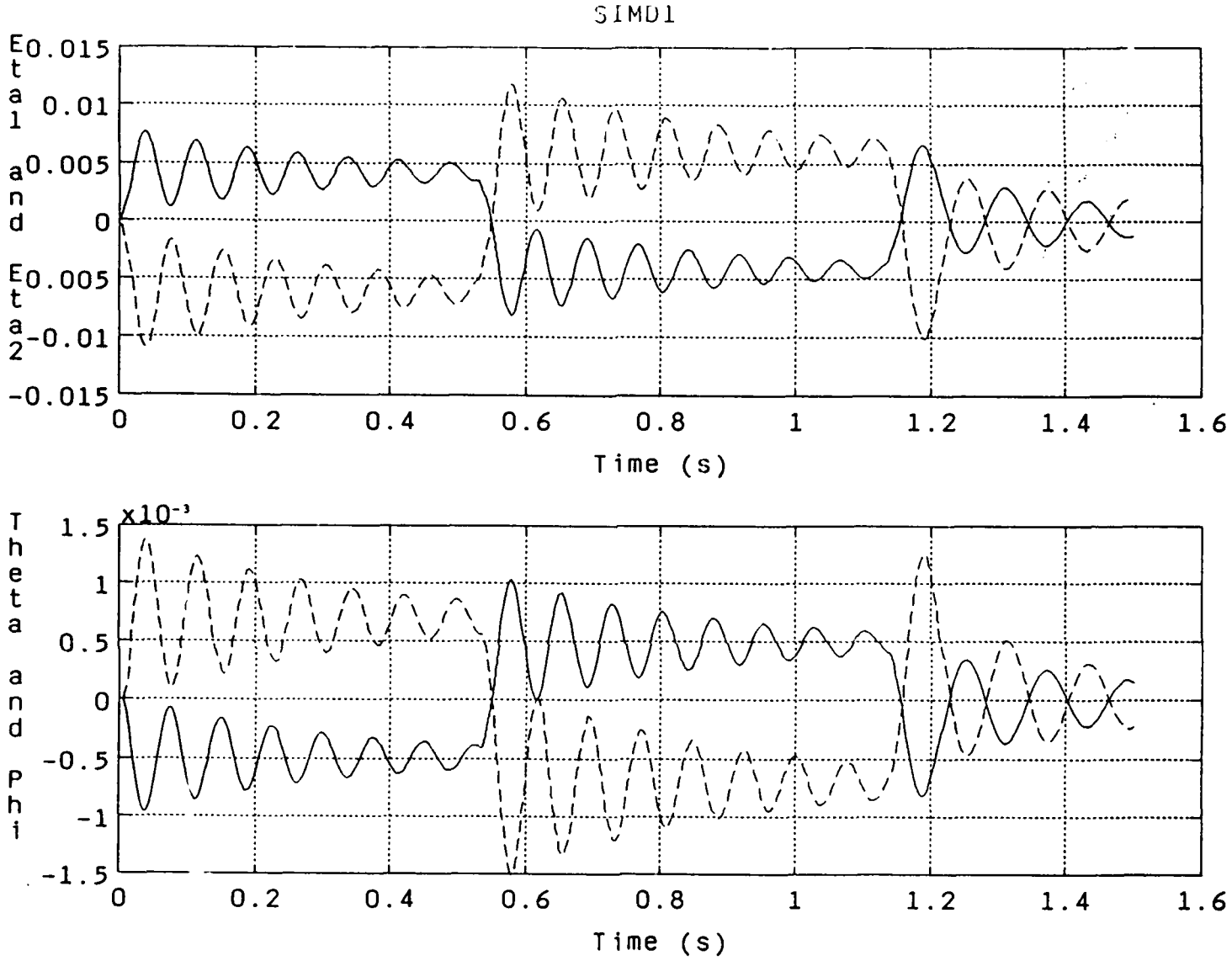
SIMD1
Eta1 and Eta2
0.015
0.01
0.005
0
-0.005
-0.01
-0.015
0
0.2
0.4
0.6
0.8
1
1.2
1.4
1.6
Time (s)
Theta and Phi
x10⁻³
1.5
1
0.5
0
-0.5
-1
-1.5
0
0.2
0.4
0.6
0.8
1
1.2
1.4
1.6
Time (s)

SIMD2

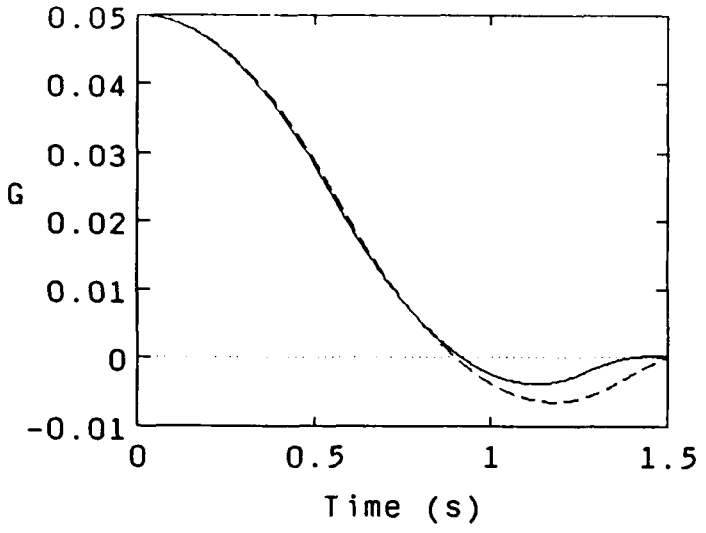
0.05
0.04
0.03
0.02
0.01
0
-0.01
G
0
0.5
1
1.5
Time (s)

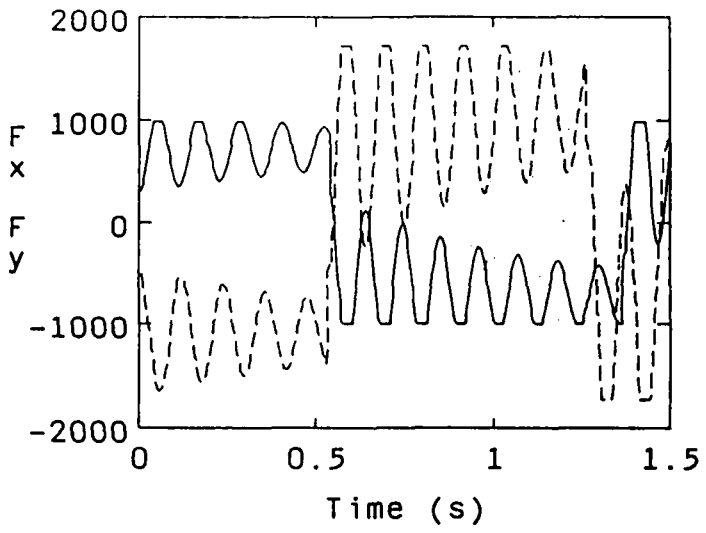
2000
1000
0
-1000
-2000
F x
F y
0
0.5
1
1.5
Time (s)

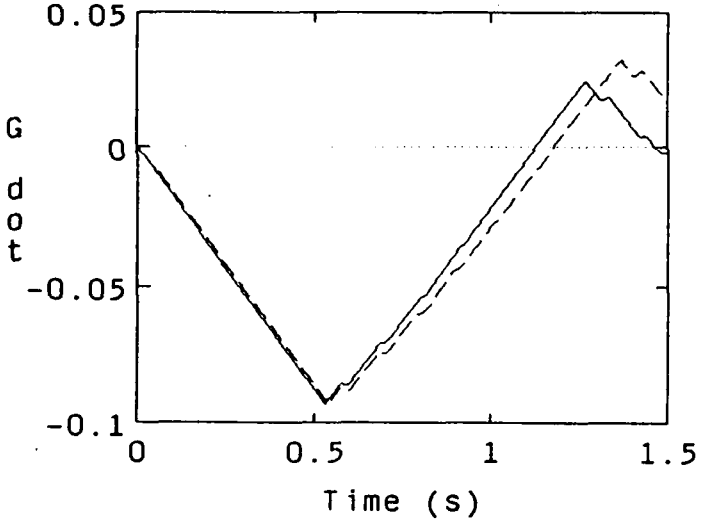
0.05
0
-0.05
-0.1
G dot
0
0.5
1
1.5
Time (s)

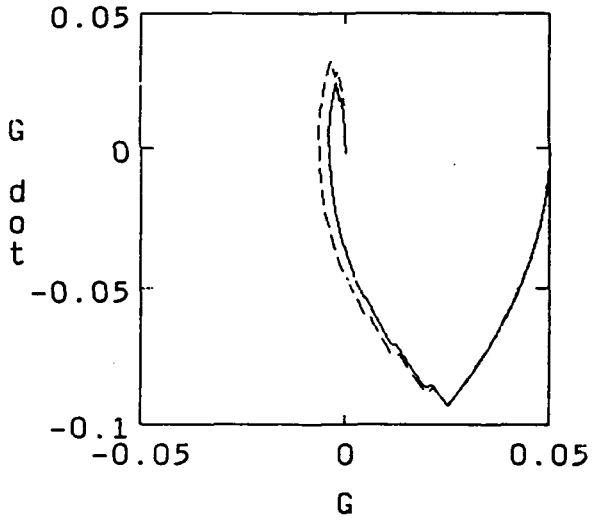
0.05
0
-0.05
-0.1
G dot
-0.05
0
0.05
G

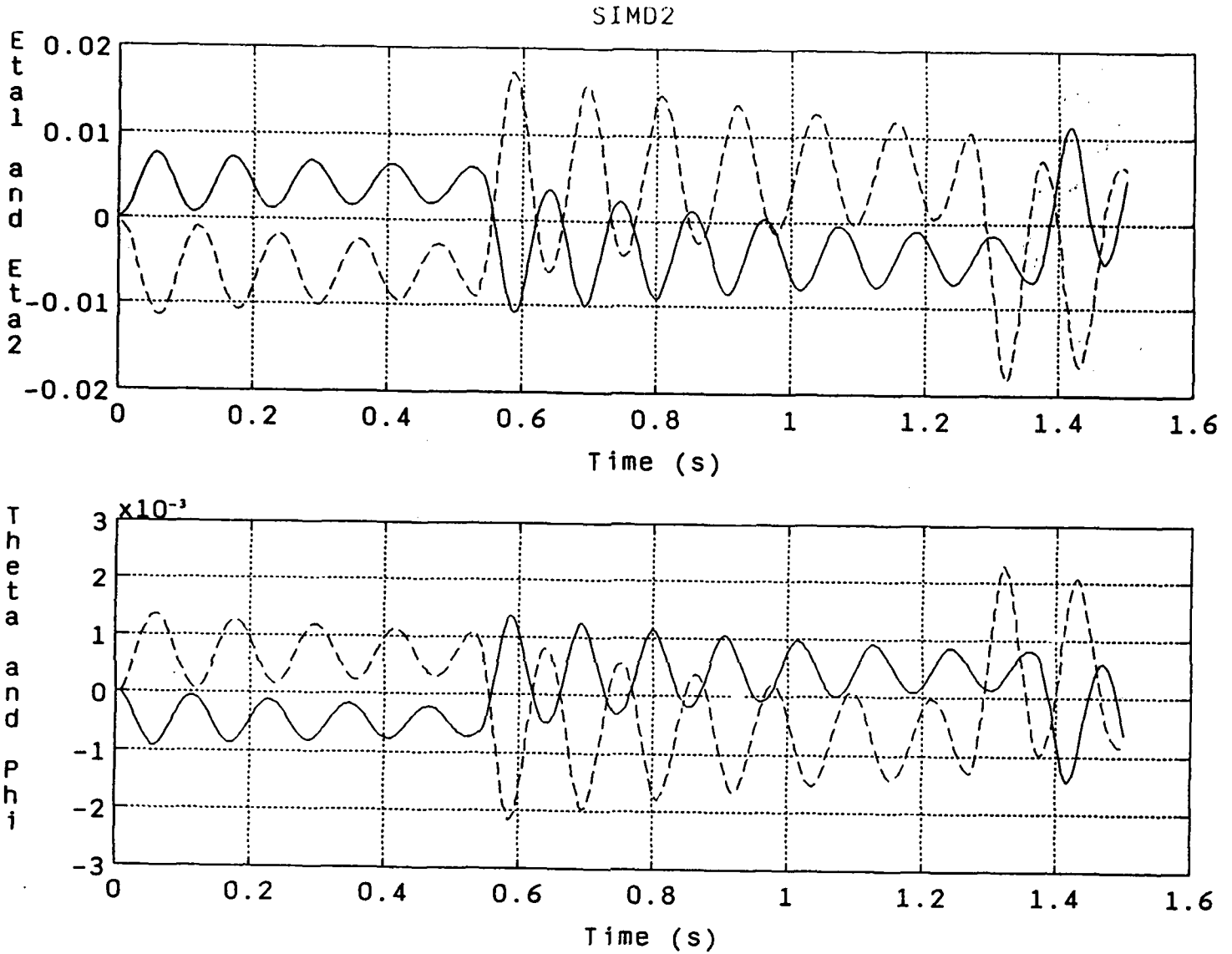
SIMD2
Eta1 and Eta2
0.02
0.01
0
-0.01
-0.02
0
0.2
0.4
0.6
0.8
1
1.2
1.4
1.6
Time (s)
Theta and Phi
x10⁻³
3
2
1
0
-1
-2
-3
0
0.2
0.4
0.6
0.8
1
1.2
1.4
1.6
Time (s)

SIMD3

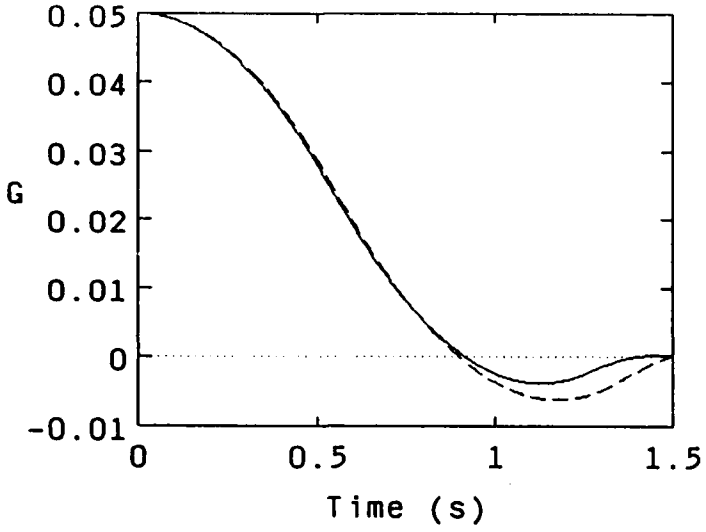
0.05
0.04
0.03
0.02
0.01
0
-0.01
G
0
0.5
1
1.5
Time (s)

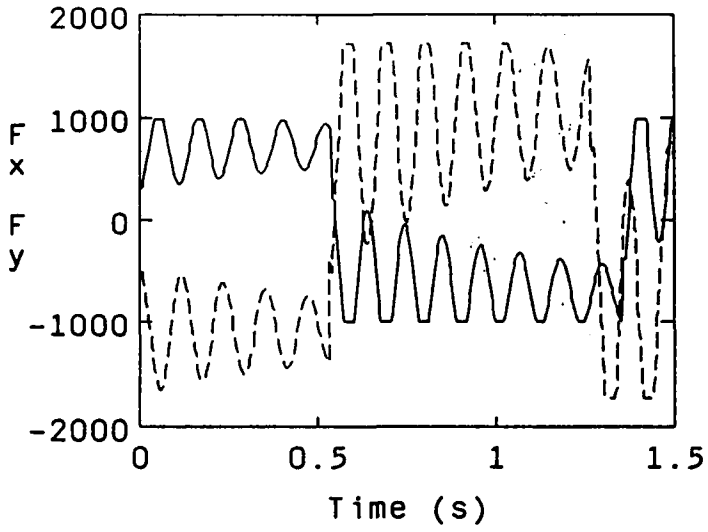
2000
1000
0
-1000
-2000
F x
F y
0
0.5
1
1.5
Time (s)

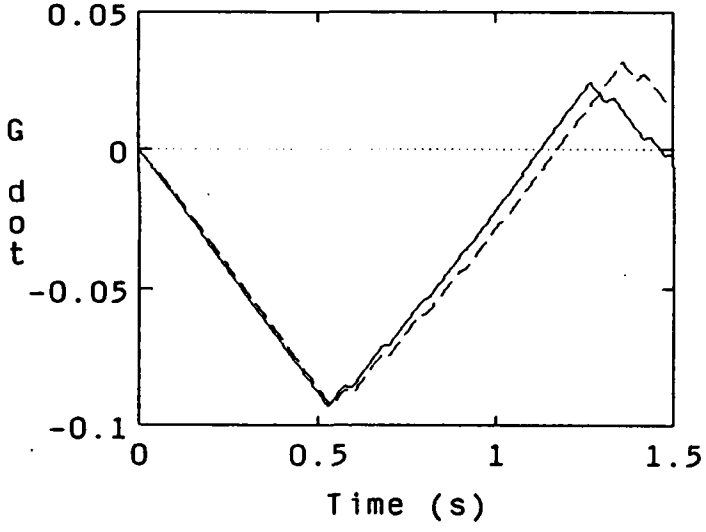
0.05
0
-0.05
-0.1
G dot
0
0.5
1
1.5
Time (s)

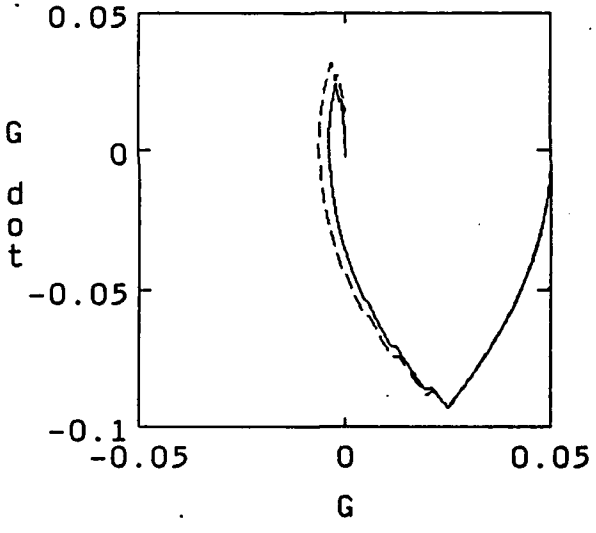
0.05
0
-0.05
-0.1
G dot
-0.05
0
0.05
G

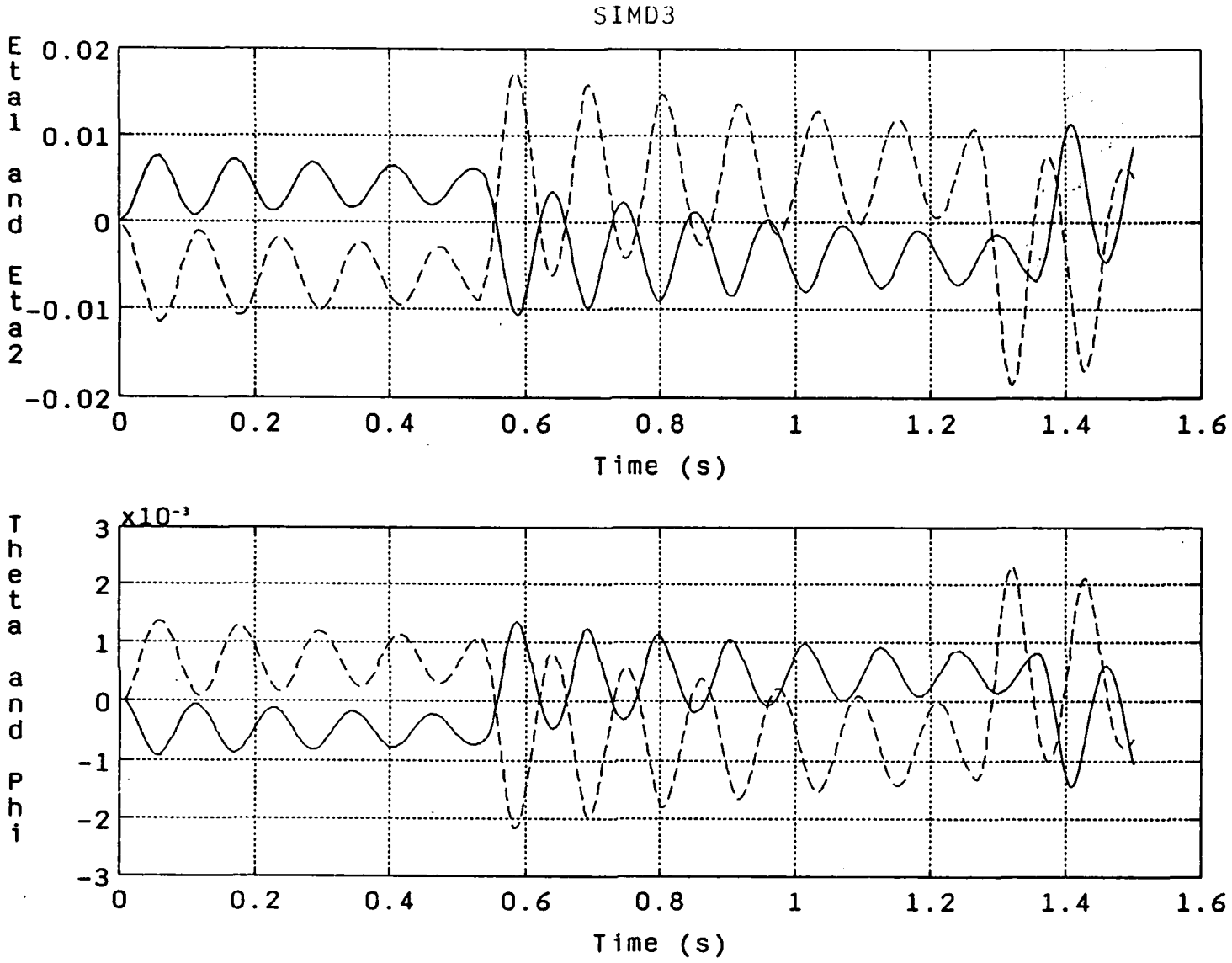
SIMD3
Eta1 and Eta2
0.02
0.01
0
-0.01
-0.02
0
0.2
0.4
0.6
0.8
1
1.2
1.4
1.6
Time (s)
Theta and Phi
x10⁻³
3
2
1
0
-1
-2
-3
0
0.2
0.4
0.6
0.8
1
1.2
1.4
1.6
Time (s)

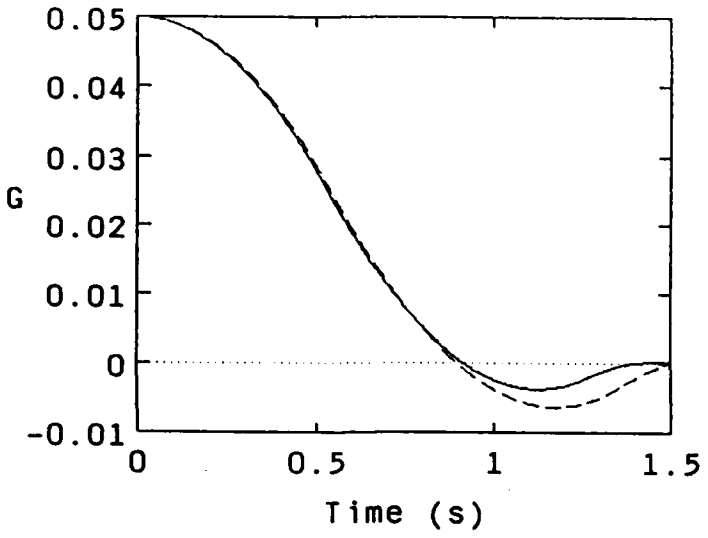
0.05
0.04
0.03
0.02
0.01
0
-0.01
G
0
0.5
1
1.5
Time (s)

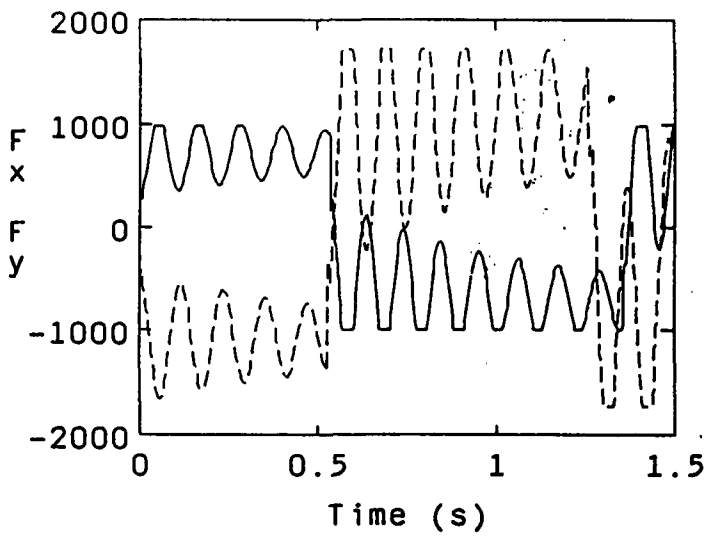
2000
1000
0
-1000
-2000
F x
F y
0
0.5
1
1.5
Time (s)

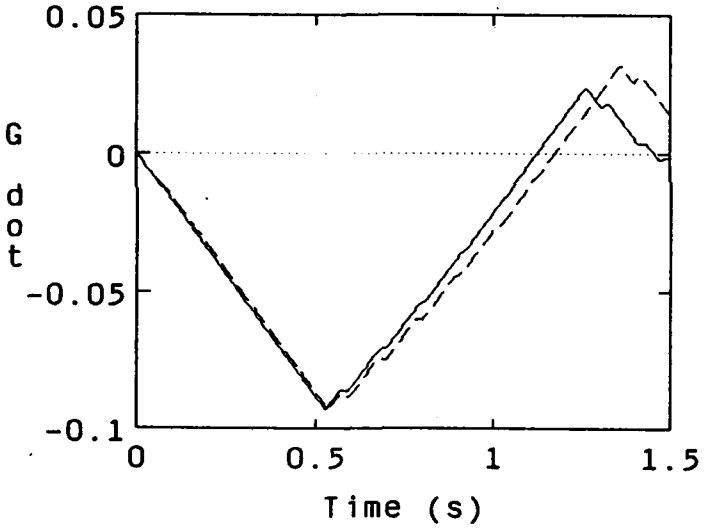
0.05
0
-0.05
-0.1
G dot
0
0.5
1
1.5
Time (s)

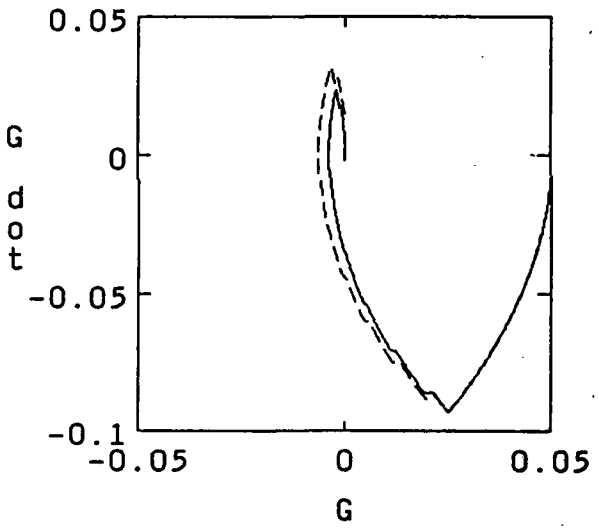
0.05
0
-0.05
-0.1
G dot
-0.05
0
0.05
G

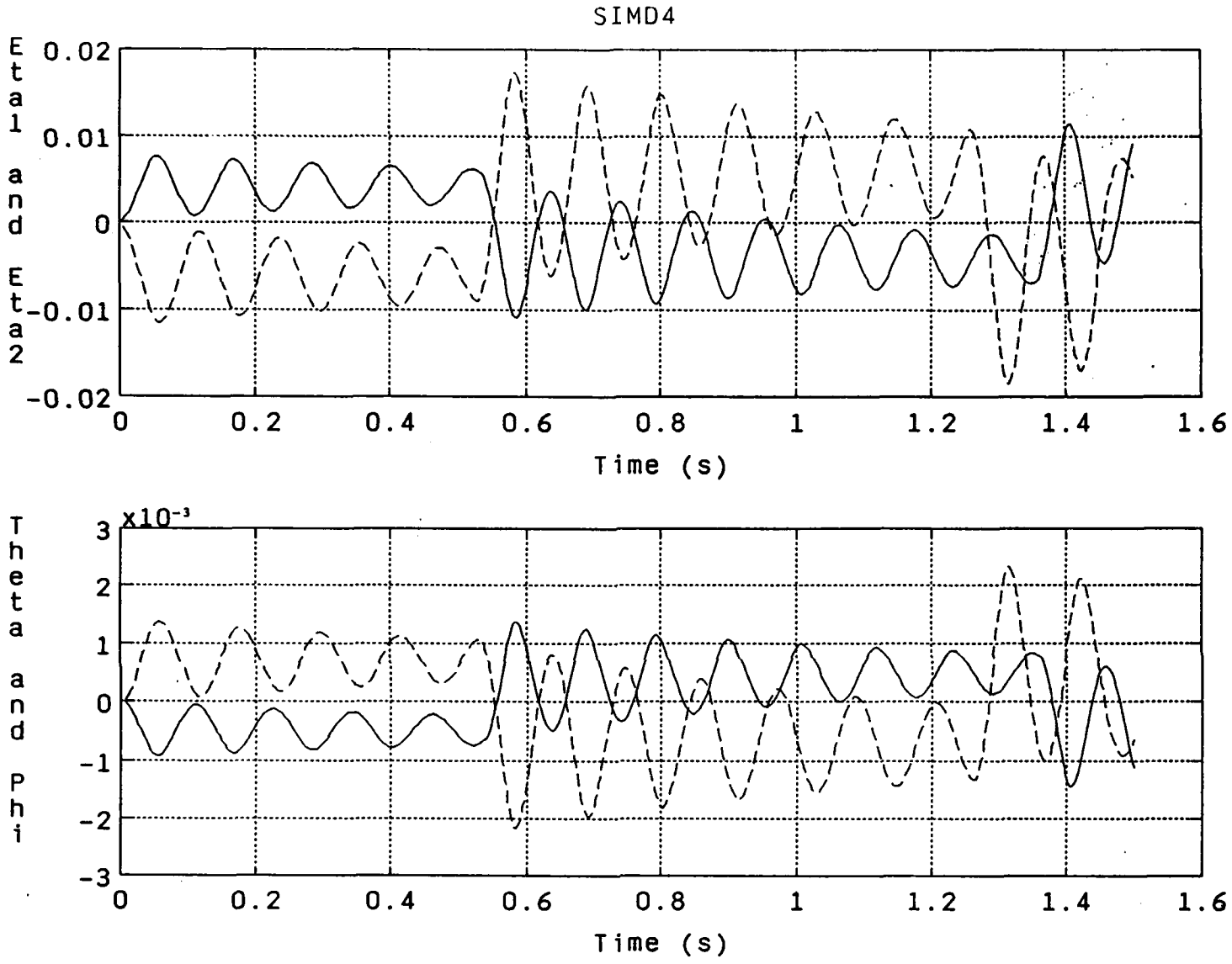
SIMD4
Eta1 and Eta2
0.02
0.01
0
-0.01
-0.02
0
0.2
0.4
0.6
0.8
1
1.2
1.4
1.6
Time (s)
Theta and Phi
x10⁻³
3
2
1
0
-1
-2
-3
0
0.2
0.4
0.6
0.8
1
1.2
1.4
1.6
Time (s)

SIME1

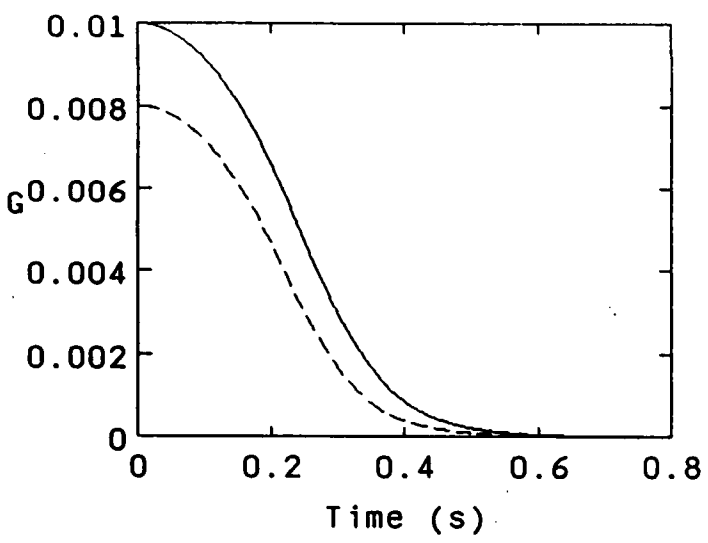
0.01
0.008
G 0.006
0.004
0.002
0
0
0.2
0.4
0.6
0.8
Time (s)

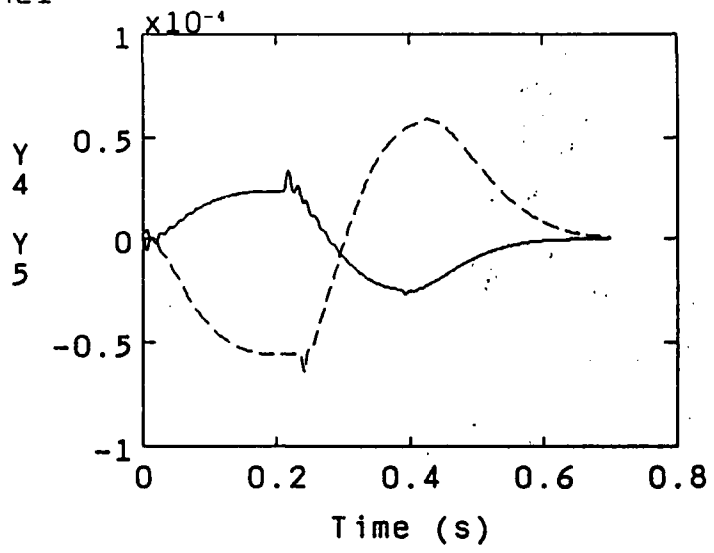
x10⁻⁴
1
0.5
Y 4 Y 5
0
-0.5
-1
0
0.2
0.4
0.6
0.8
Time (s)

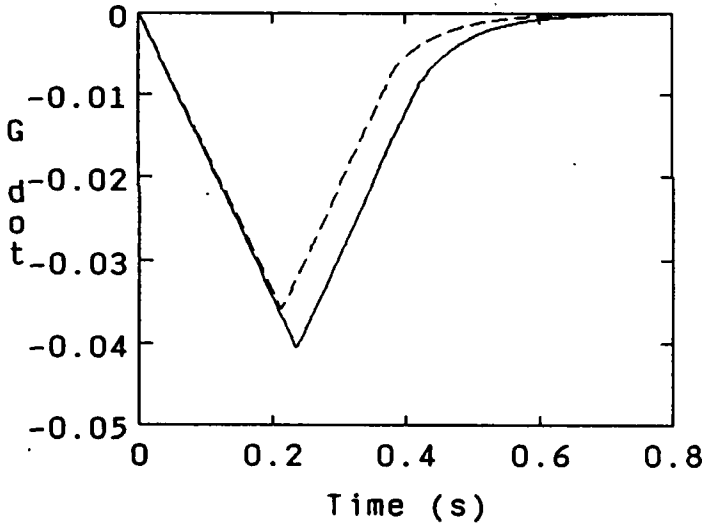
0
-0.01
G dot -0.02
-0.03
-0.04
-0.05
0
0.2
0.4
0.6
0.8
Time (s)

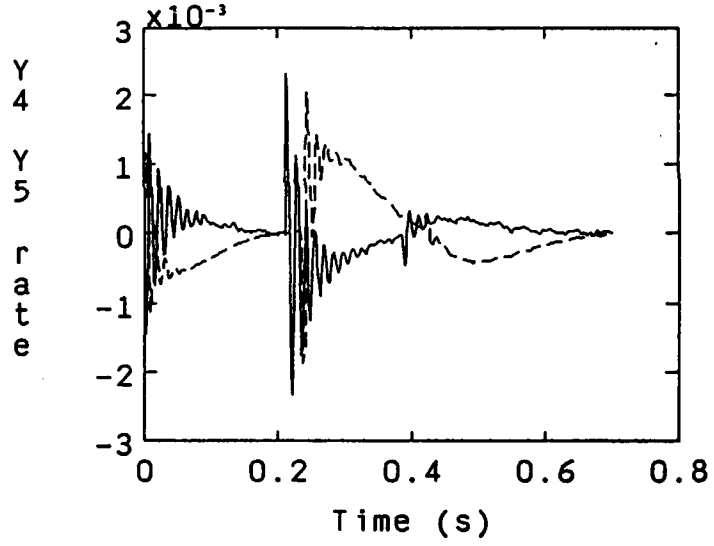
x10⁻³
3
2
Y 4 Y 5 rate
1
0
-1
-2
-3
0
0.2
0.4
0.6
0.8
Time (s)

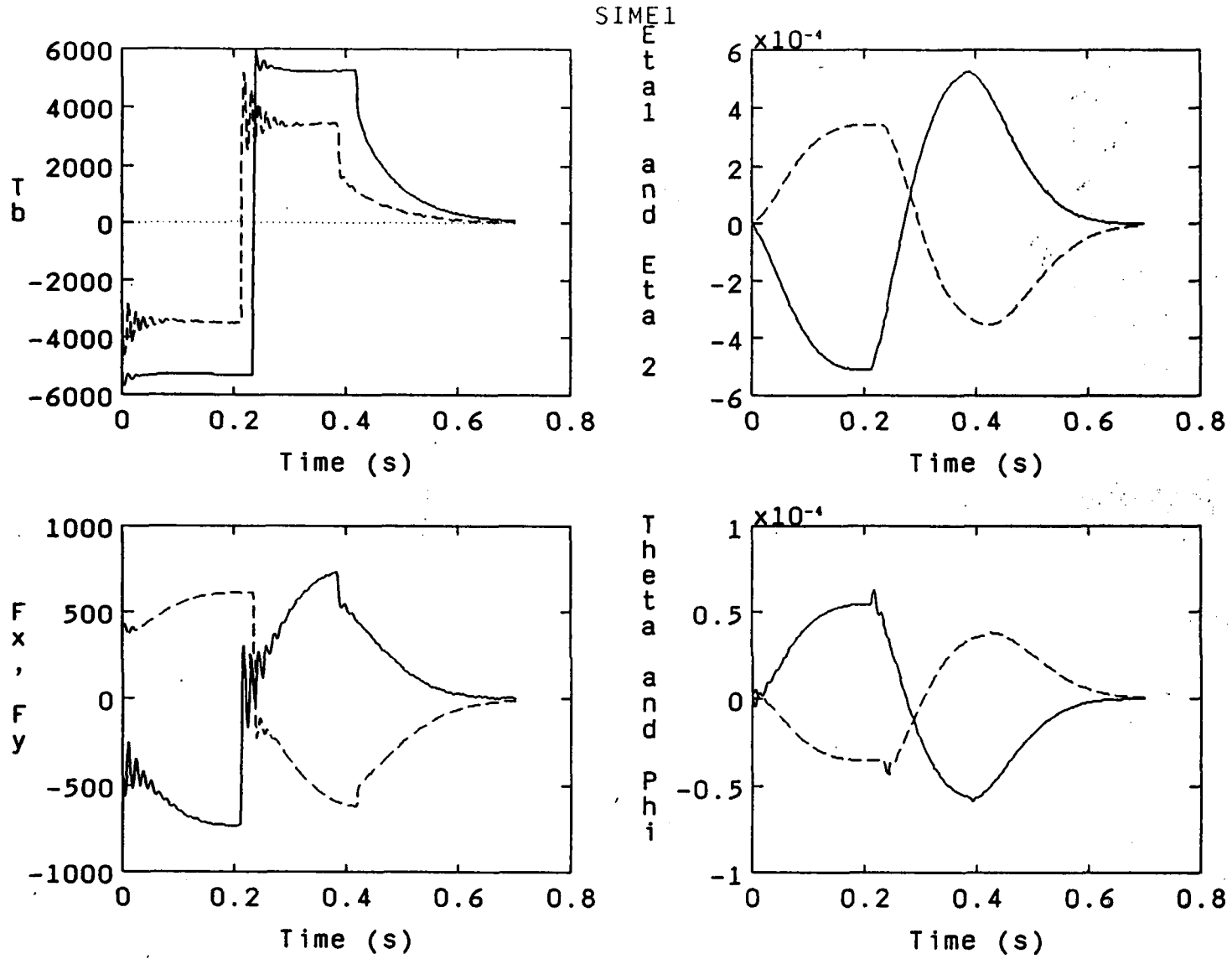
SIME1
Tb
Time (s)
Eta1 and Eta2
x10⁻⁴
Time (s)
Fx, Fy
Time (s)
Theta and Phi
x10⁻⁴
Time (s)

SIME2

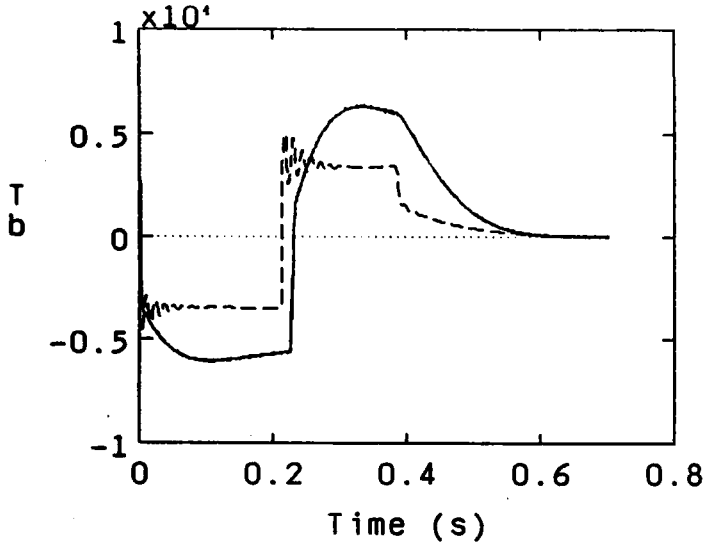
x10⁴
1
0.5
0
-0.5
-1
Tb
0
0.2
0.4
0.6
0.8
Time (s)

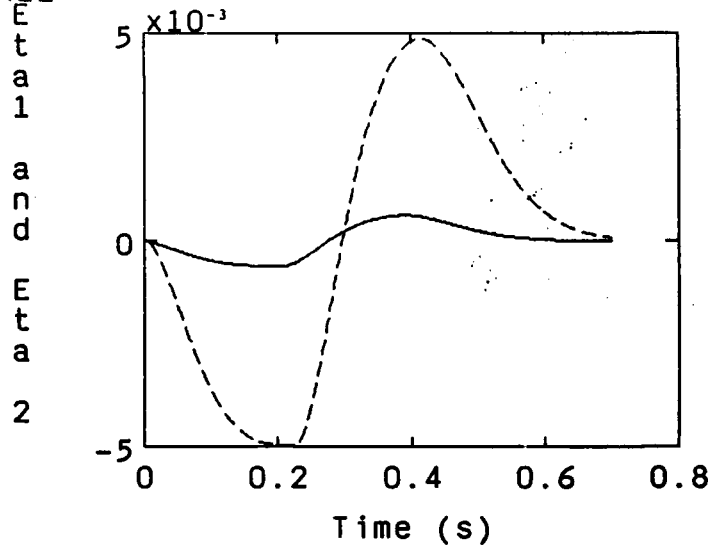
x10⁻³
5
0
-5
Eta1 and Eta2
0
0.2
0.4
0.6
0.8
Time (s)

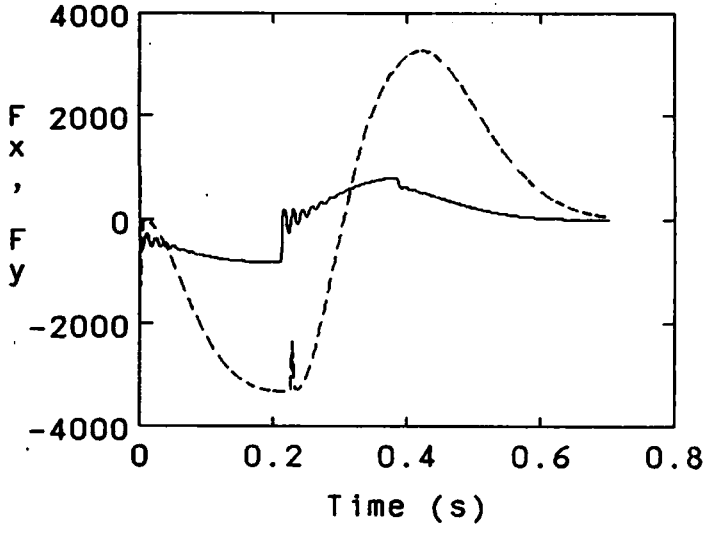
4000
2000
0
-2000
-4000
Fx, Fy
0
0.2
0.4
0.6
0.8
Time (s)

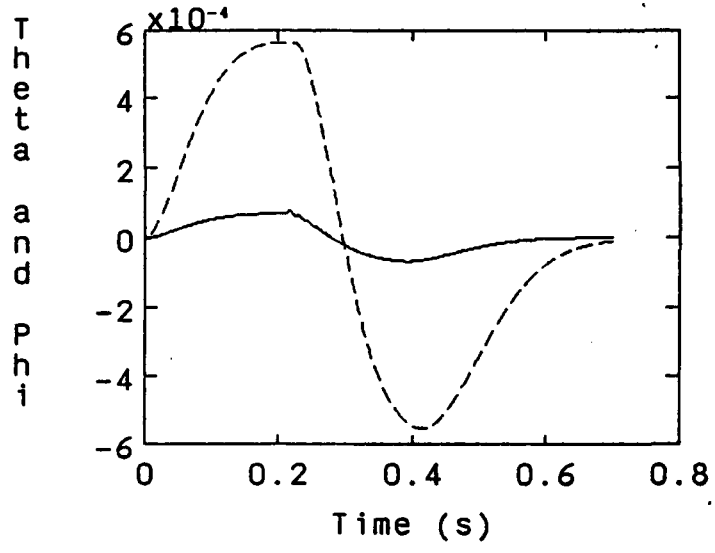
x10⁻⁴
6
4
2
0
-2
-4
-6
Theta and Phi
0
0.2
0.4
0.6
0.8
Time (s)

SIME2

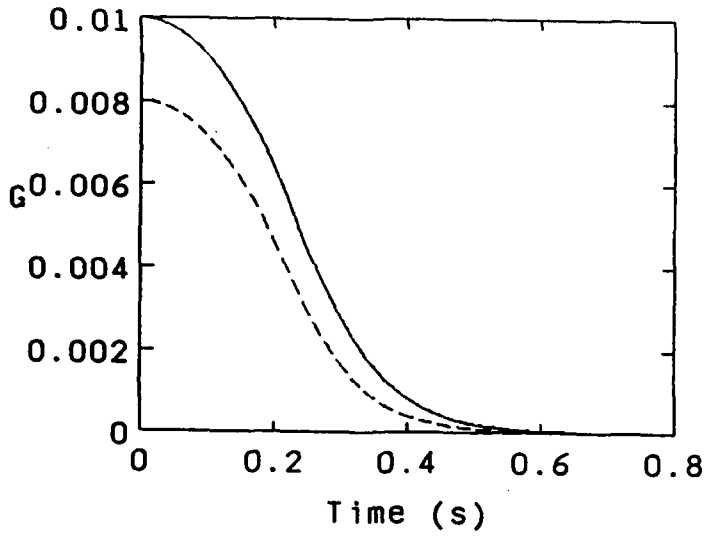
0.01
0.008
G 0.006
0.004
0.002
0
0
0.2
0.4
0.6
0.8
Time (s)

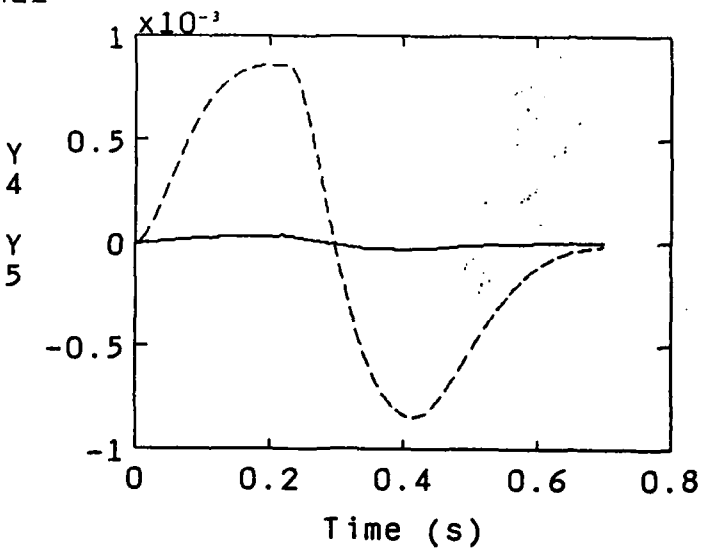
x10⁻³
1
0.5
Y 4
Y 5
0
-0.5
-1
0
0.2
0.4
0.6
0.8
Time (s)

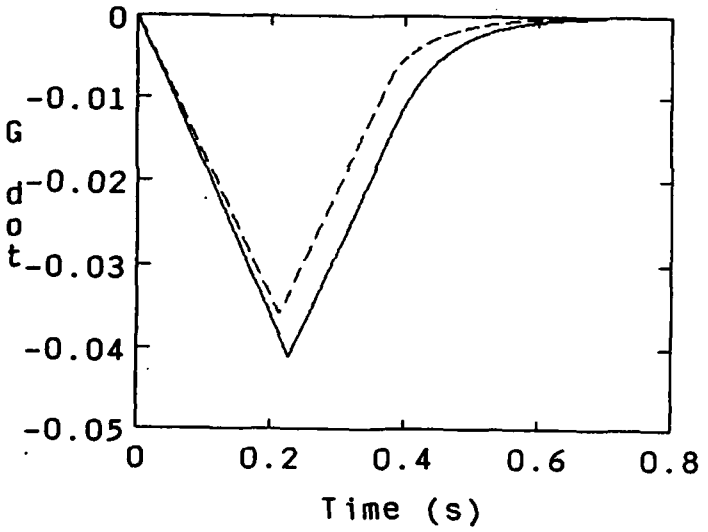
0
-0.01
G
d -0.02
o
t -0.03
-0.04
-0.05
0
0.2
0.4
0.6
0.8
Time (s)

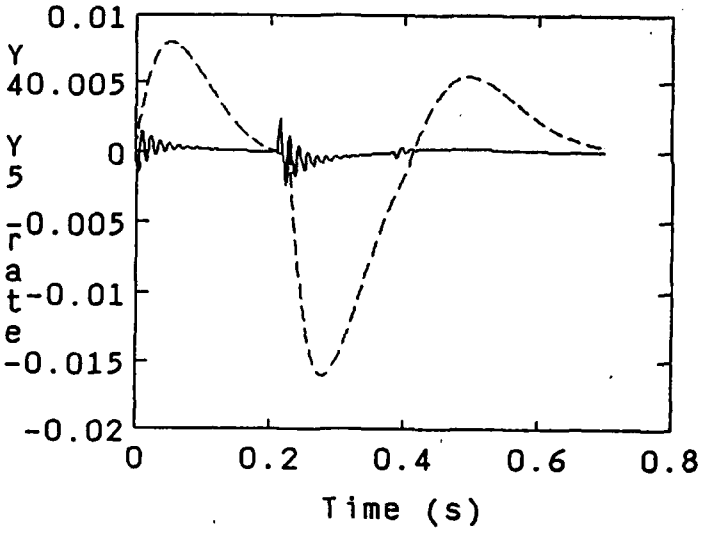
0.01
Y
40.005
Y
5
0
r -0.005
a
t -0.01
e
-0.015
-0.02
0
0.2
0.4
0.6
0.8
Time (s)

SIMF1

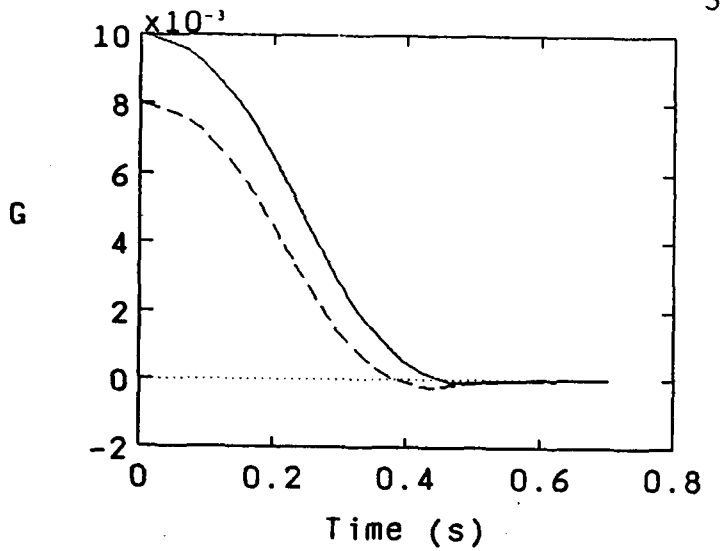
x10⁻³
10
8
6
4
2
0
-2
G
0
0.2
0.4
0.6
0.8
Time (s)

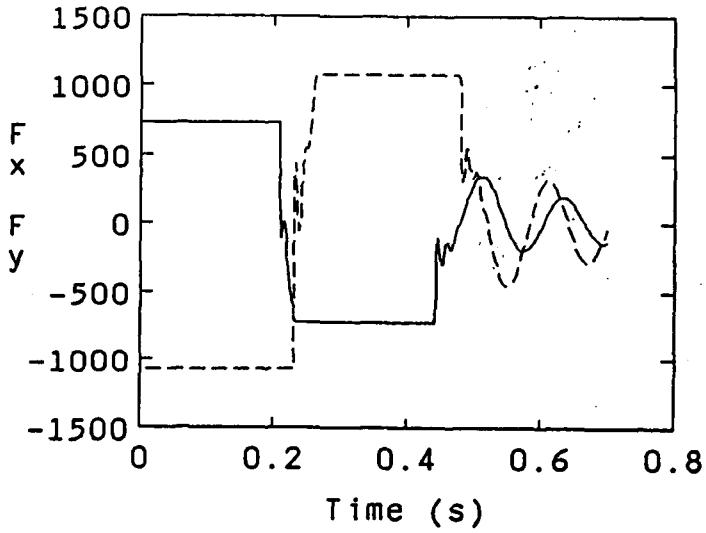
1500
1000
500
0
-500
-1000
-1500
F x
F y
0
0.2
0.4
0.6
0.8
Time (s)

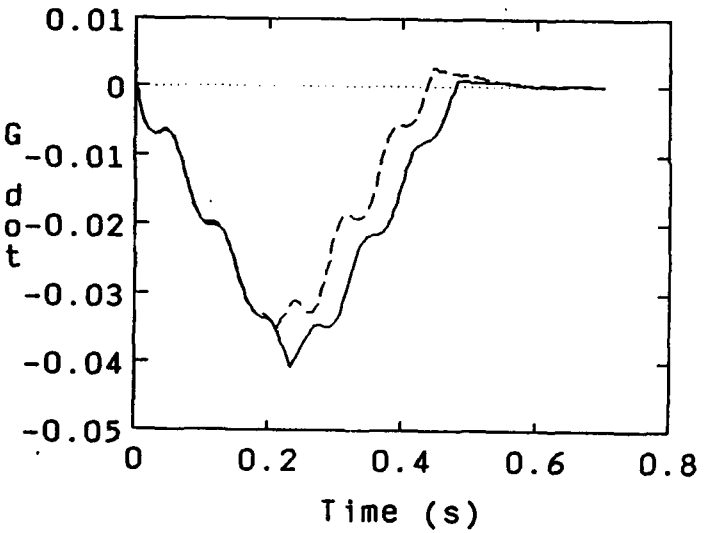
0.01
0
-0.01
-0.02
-0.03
-0.04
-0.05
G dot
0
0.2
0.4
0.6
0.8
Time (s)

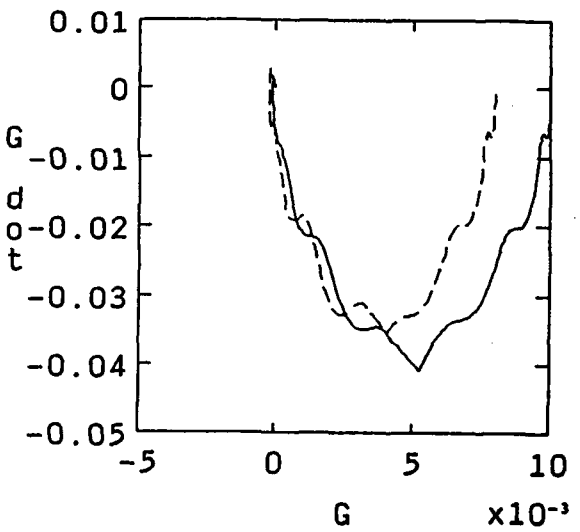
0.01
0
-0.01
-0.02
-0.03
-0.04
-0.05
G dot
-5
0
5
10
G
x10⁻³

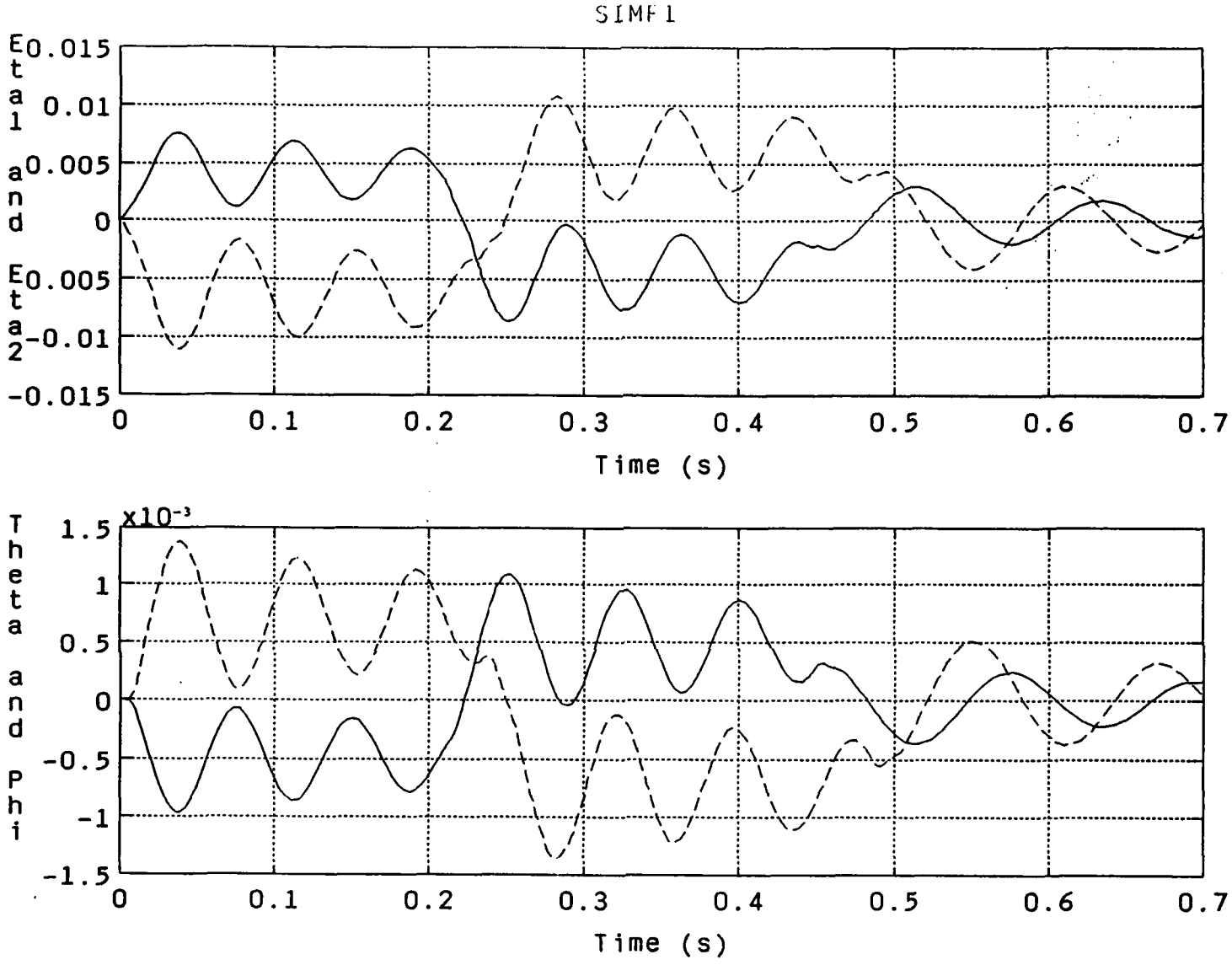
SIMF1
Eta1 and Eta2
0.015
0.01
0.005
0
-0.005
-0.01
-0.015
0
0.1
0.2
0.3
0.4
0.5
0.6
0.7
Time (s)
Theta and Phi
x10⁻³
1.5
1
0.5
0
-0.5
-1
-1.5
0
0.1
0.2
0.3
0.4
0.5
0.6
0.7
Time (s)

SIMF2

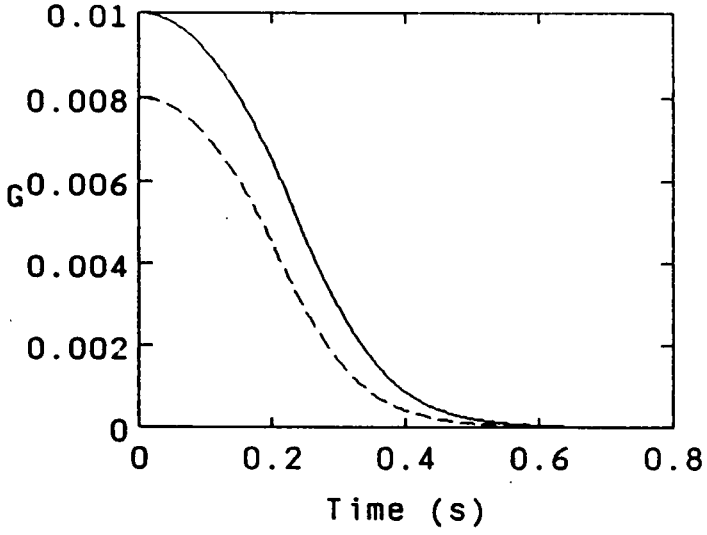
0.01
0.008
G 0.006
0.004
0.002
0
0
0.2
0.4
0.6
0.8
Time (s)

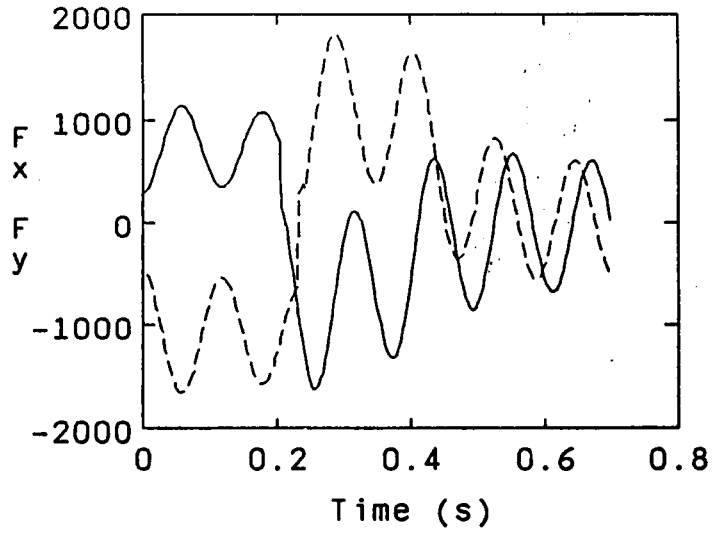
2000
1000
F x
F y
0
-1000
-2000
0
0.2
0.4
0.6
0.8
Time (s)

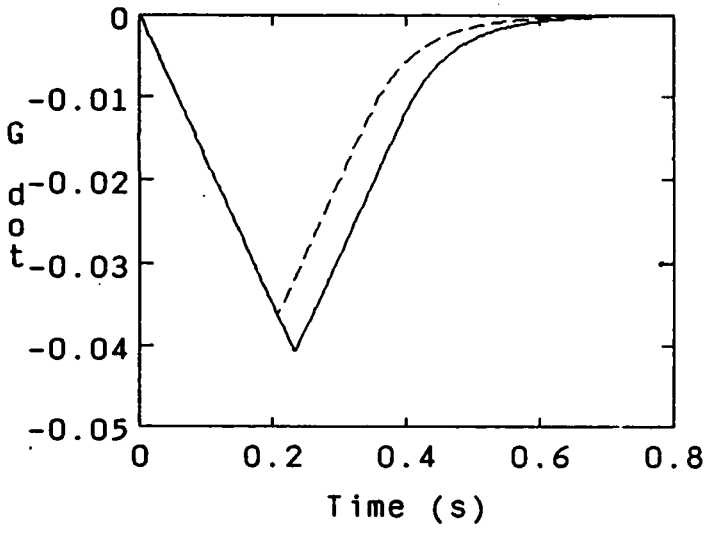
0
-0.01
G
d -0.02
o
t -0.03
-0.04
-0.05
0
0.2
0.4
0.6
0.8
Time (s)

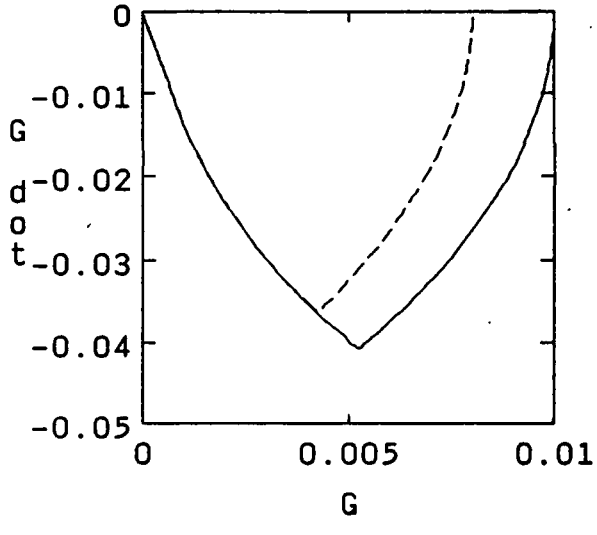
0
-0.01
G
d -0.02
o
t -0.03
-0.04
-0.05
0
0.005
0.01
G

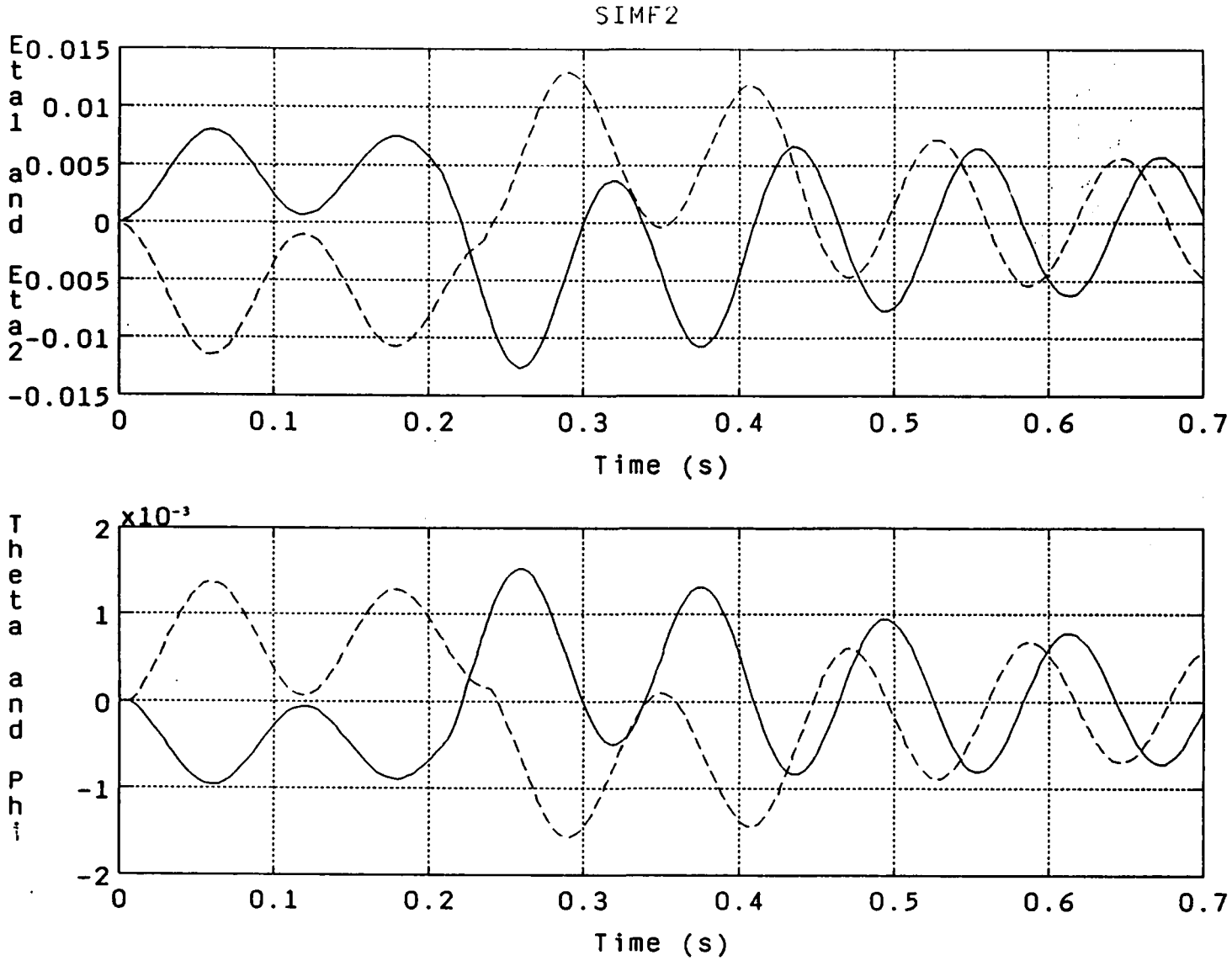
SIMF2
Eta1 and Eta2
0.015
0.01
0.005
0
-0.005
-0.01
-0.015
0
0.1
0.2
0.3
0.4
0.5
0.6
0.7
Time (s)
Theta and Phi
x10⁻³
2
1
0
-1
-2
0
0.1
0.2
0.3
0.4
0.5
0.6
0.7
Time (s)

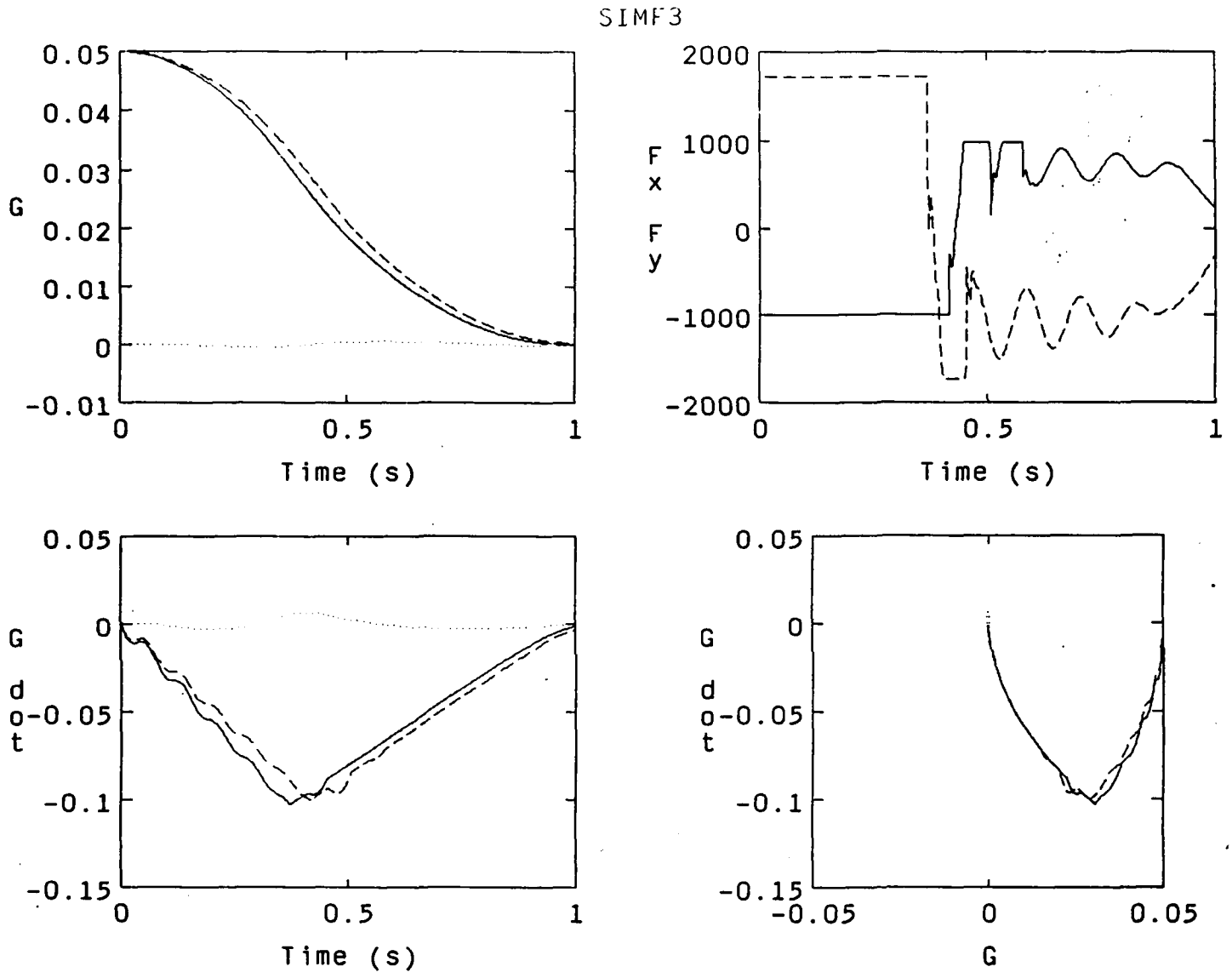
SIMF3
0.05
0.04
0.03
0.02
0.01
0
-0.01
G
0
0.5
1
Time (s)
2000
1000
0
-1000
-2000
F x
F y
0
0.5
1
Time (s)
0.05
0
-0.05
-0.1
-0.15
G dot
0
0.5
1
Time (s)
0.05
0
-0.05
-0.1
-0.15
G dot
-0.05
0
0.05
G

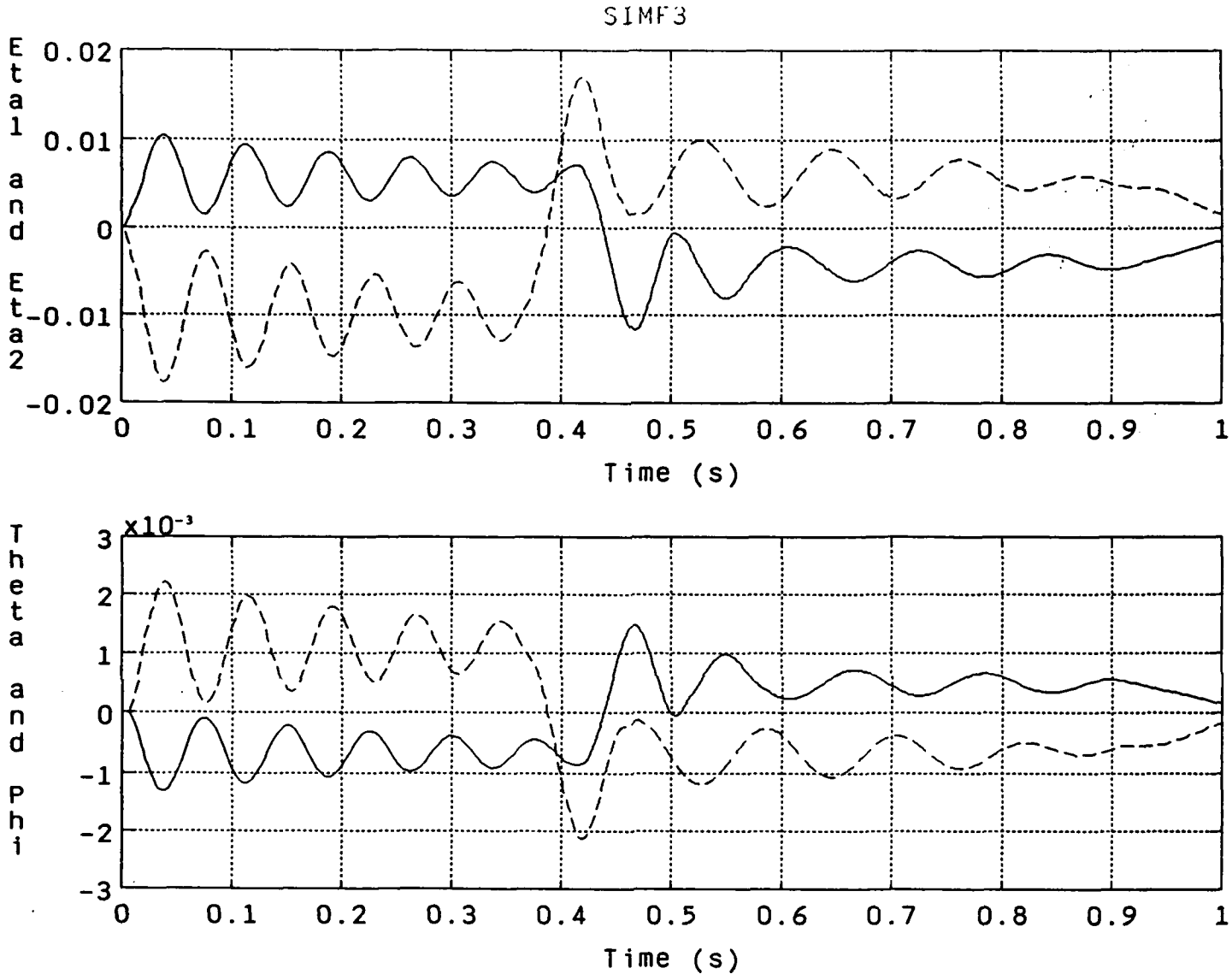
SIMF3
Eta1 and Eta2
0.02
0.01
0
-0.01
-0.02
0
0.1
0.2
0.3
0.4
0.5
0.6
0.7
0.8
0.9
1
Time (s)
Theta and Phi
x10⁻³
3
2
1
0
-1
-2
-3
0
0.1
0.2
0.3
0.4
0.5
0.6
0.7
0.8
0.9
1
Time (s)

SIMF3

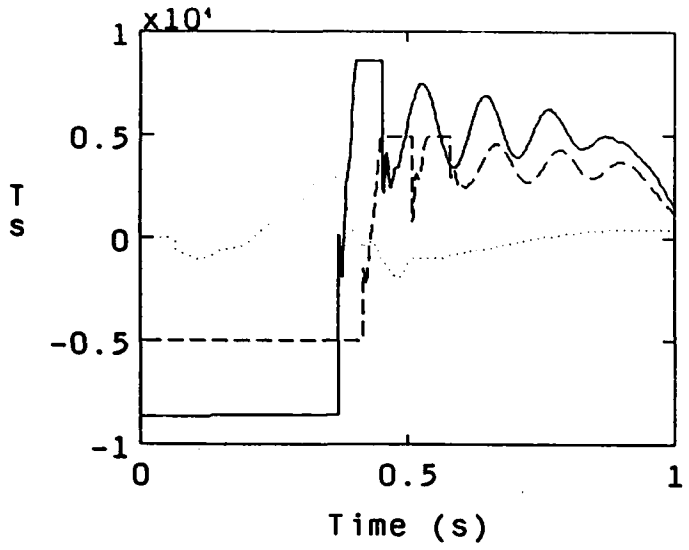

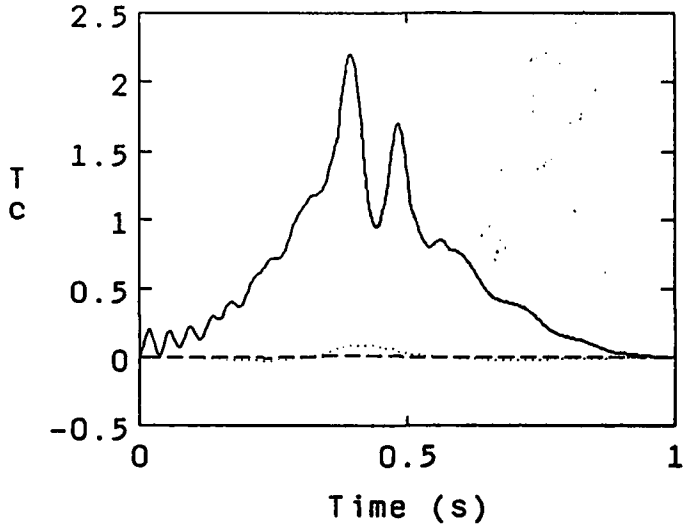

SIMF4

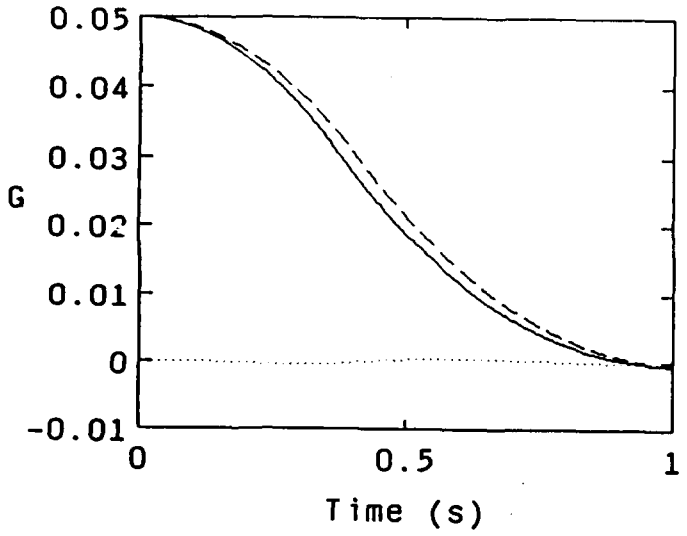
0.05
0.04
0.03
0.02
0.01
0
-0.01
G
0
0.5
1
Time (s)

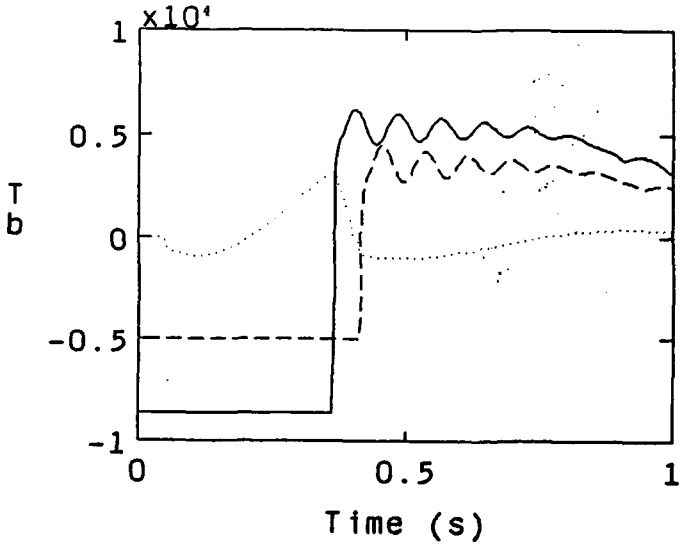
x10⁴
1
0.5
0
-0.5
-1
T
b
0
0.5
1
Time (s)

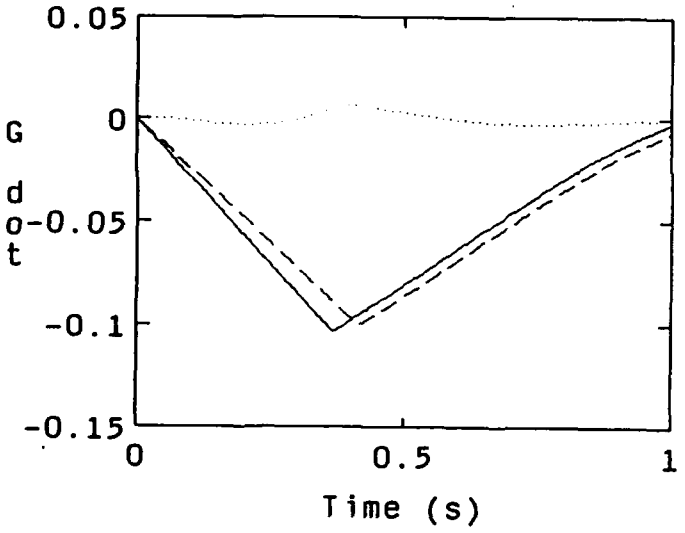
0.05
0
-0.05
-0.1
-0.15
G
d
o
t
0
0.5
1
Time (s)

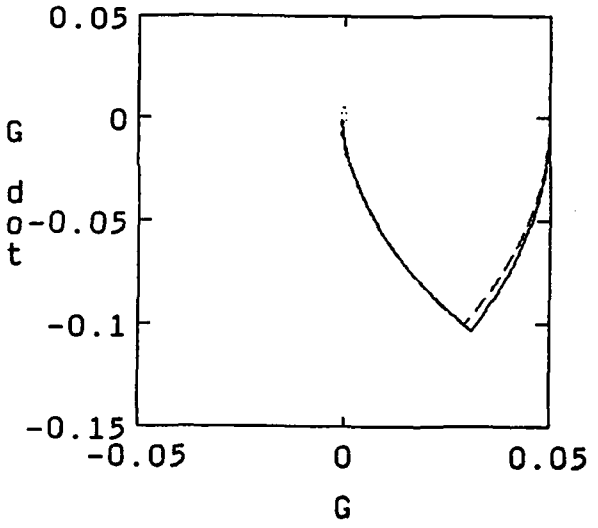
0.05
0
-0.05
-0.1
-0.15
G
d
o
t
-0.05
0
0.05
G

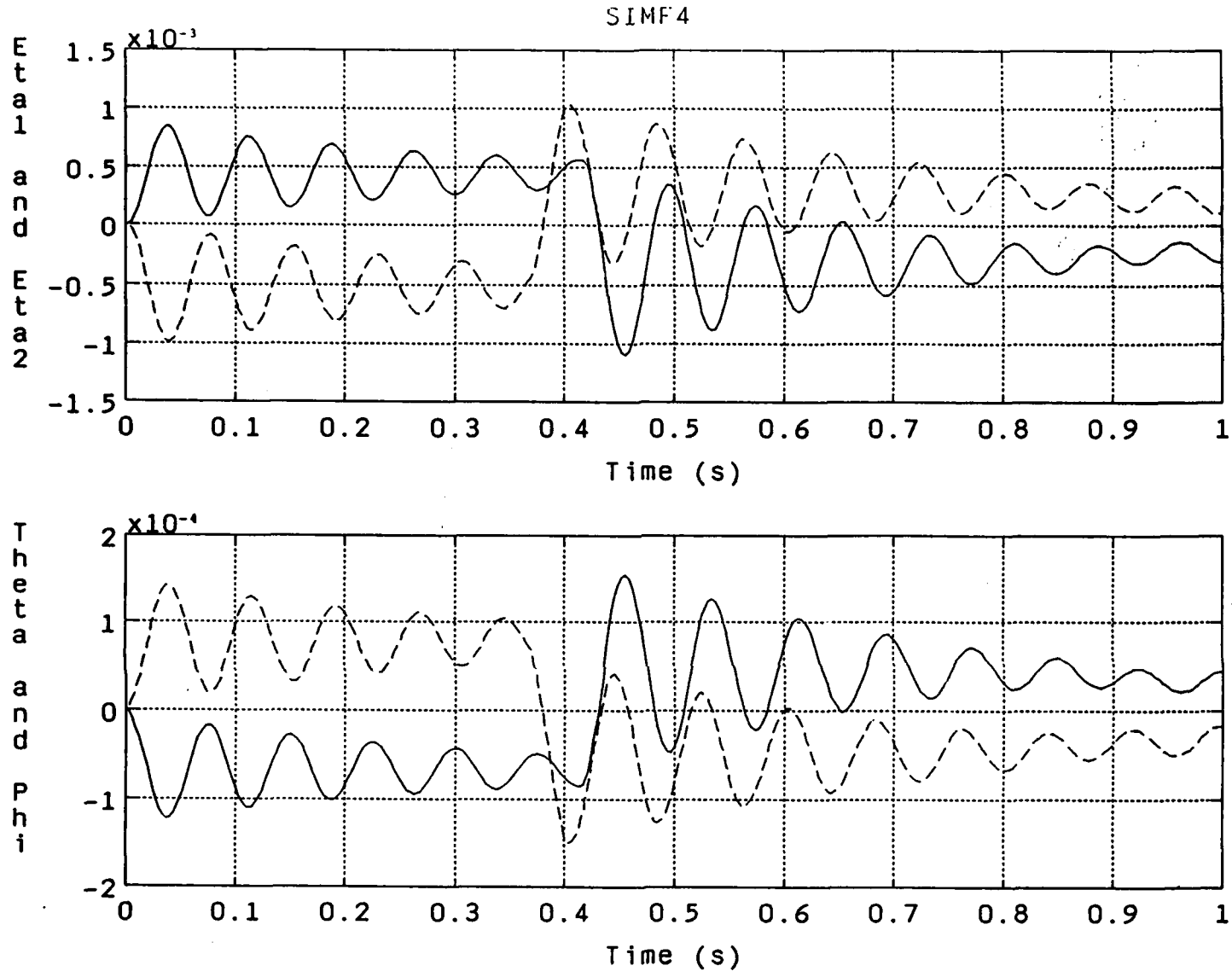
SIMF4
x10⁻³
Eta1 and Eta2
1.5
1
0.5
0
-0.5
-1
-1.5
0
0.1
0.2
0.3
0.4
0.5
0.6
0.7
0.8
0.9
1
Time (s)
x10⁻⁴
Theta and Phi
2
1
0
-1
-2
0
0.1
0.2
0.3
0.4
0.5
0.6
0.7
0.8
0.9
1
Time (s)

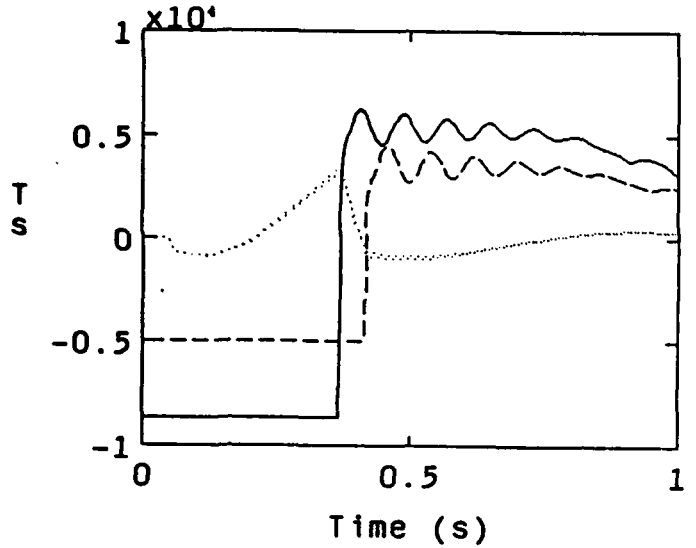
x10⁴
1
0.5
0
-0.5
-1
T
s
0
0.5
1
Time (s)

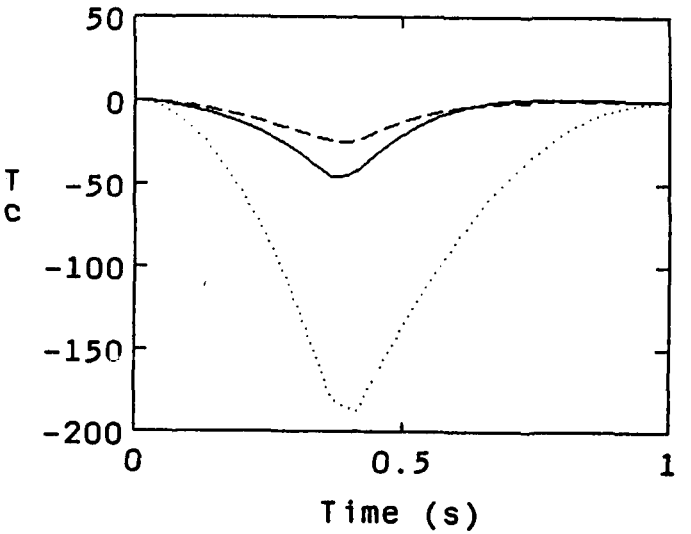
50
0
-50
-100
-150
-200
T
c
0
0.5
1
Time (s)